

IMAGING SERVICES NORTH

Boston Spa, Wetherby

West Yorkshire, LS23 7BQ

www.bl.uk

This PDF was created from the British Library's microfilm copy of the original thesis. As such the images are greyscale and no colour was captured.

Due to the scanning process, an area greater than the page area is recorded and extraneous details can be captured.

This is the best available copy

048198 / 84

Attention is drawn to the fact that the copyright of this thesis rests with its author.

This copy of the thesis has been supplied on condition that anyone who consults it is understood to recognise that its copyright rests with its author and that no quotation from the thesis and no information derived from it may be published without the author's prior written consent.

"An experimental investigation of the motion of flexible
molecules in the liquid state by light scattering."

John Martin Bagshaw B.A., M.Inst.P.

A thesis submitted in partial fulfillment of the require-

ments for the C.N.A.A. degree of

Doctor of Philosophy

Department of Physics

Sir John Cass School of Science and
Technology

City of London Polytechnic

LONDON EC3

September 1983

ABSTRACT

"An experimental investigation of the motion of flexible molecules in the liquid state by light scattering."

John M Bagshaw

Depolarised light scattering is used to investigate the motion of flexible molecules in the liquid state. The spectra obtained are separated into a high frequency component associated with collisional motion, and a low frequency component associated with reorientation.

The high frequency component is separated from spectra for the n-alkanes. The time scale and collision induced anisotropy is such that this component is interpreted as being due to interactions between chain ends.

The low frequency component is examined for n-alkanes, both pure liquids and solutions in CCl_4 , the n-alcohols, and the isomer, 224-trimethyl pentane. For the low viscosity liquids this component is Lorentzian. For the higher viscosity liquids the spectrum is modified by shear rotational coupling and exhibits a dip, the depth of which is related to the coupling parameter R. From spectral analysis one obtains molecular reorientation times and in addition for the higher viscosity liquids values of R.

The values of R are a weakly increasing function of chain length and almost independent of temperature. For pentadecane solutions in CCl_4 , R is almost linear with concentration, in agreement with theory and observations for rigid molecules.

The reorientation times are interpreted using the Stokes Einstein relation. The Stokes Einstein volumes are interpreted as the quantity $G\alpha pV$ where V is the molecular volume, α and p are associated with molecular shape and hydrodynamics and G with orientational correlation.

An attempt is made to separate $G\alpha p$ by solution measurements. The results indicate that a simple separation may not be possible for flexible molecules, G, α and p being independent functions of concentration and temperature.

For the shorter alkanes the results suggest that the more globular the molecule, the more it rotates within its cavity in the liquid, interacting less with surroundings, than hydrodynamics would suggest. This is substantially confirmed by the Stokes Einstein volume obtained for 224-trimethyl pentane.

Acknowledgements

I would like to make thanks to the City of London Polytechnic for providing a research assistantship and funding for the apparatus which made this work possible, also my supervisor Dr J V Champion for useful advice throughout the project. I would also like to thank Dr P Madden and Dr T Cox of Cambridge University (now both at RSRE) for the use of the monochromator and useful discussions especially at the start of the project.

I finally would like to thank Mr Arthur Dyer of the GEC Hirst Research Centre, for providing encouragement and the use of facilities for the completion of this thesis.

CONTENTS

	<u>Page</u>
Title	1
Abstract	2
Acknowledgements	3
Chapter 1 Introduction	
1.1 Introduction	8
1.2 Qualitative Description of Spectra	10
1.3 Chapter References	14
Chapter 2 Review of Theory	
2.1 Light Scattering - Intensity Measurements and Theory	15
2.2 Light Scattering - Spectral Measurements and Theory Collision Induced Scattering	18 29
2.3 Molecular Correlation Times - The Stokes Einstein Relation and Stick Slip Behaviour	35
2.4 Molecular Correlation Times - Models and Computer Simulations	44
2.5 Chapter References	54

	<u>Page</u>
Chapter 3 Experimental Work	
3.1 Introduction	60
3.2 Description of the Fabry Perot Spectrometer	60
Fitting Procedure for Spectral Shape	64
Results from Fitting Procedures	66
Calculations of the Relative Intensities of	67
the Collisional Background and the Intrinsic Scattering	69
Corrections	
3.3 Description of the Double Grating Monochromator	71
Form of Data	73
Analysis of Data	74
Fitting Procedure	75
Other Spectral Forms	77
3.4 Sample Preparation and Ancillary Measurements	79
3.4.1 Filtering Techniques	79
3.4.2 Density Measurements	82
3.4.3 Concentration Measurements	82
3.4.4 Viscosity Measurements	83
3.5 Chapter References	86

	<u>Page</u>
Chapter 4 Results and Analysis	
4.1 Monochromator Results	87
4.1.1 Introduction	87
4.1.2 Collisional Portion of the Spectrum	89
4.1.3 Problems with Simple Interpretation	94
4.2 Results from the Fabry Perot System	96
4.2.1 N-Alkanes: Neat Liquids	96
Results: R Parameters	112
Stokes Einstein Relation	113
Comparison of Effective Volumes obtained with Stokes Einstein Volumes	125
Note on Interpretation of Stokes Einstein Results for Neat Liquids	129
4.2.2 N-Alkanes: Solutions in Carbon Tetrachloride	130
Results: R Parameters for Pentadecane	138
Stokes Einstein Fits to Data	139
4.2.3 N-Alcohols: Neat Liquids	153
Results: R Parameters	160
Stokes Einstein Relation	161
4.2.4 Isooctane: 2, 2, 4 Trimethyl Pentane	174
Results: Stokes Einstein Relation	176
4.3 Chapter References	180

CHAPTER 1 INTRODUCTION

	<u>Page</u>
1.1 Introduction	181
Chapter 5 Summary of Conclusions and Suggestions for Future Work	181
5.1 Results from Spectral Fits - A Summary	181
5.2 The Stokes Einstein Relation - A Comparison of Results from Spectral Fits with Theoretical Modelling	186
5.3 Suggestions for Future Work	189
5.4 Chapter References	192

The technique which we have used to investigate these molecular motions is depolarised Rayleigh light scattering. In this technique a collimated beam of light from a laser source enters and passes through a sample of liquid. The incident light is vertically polarised. Light is scattered in all directions from the incident beam. The light scattered at right angles to the incident beam may be separated into two polarisation states, one vertically polarised, the other horizontally polarised. The horizontal polarised component is of much smaller intensity than the vertically polarised component and it is the horizontally polarised component in which we are interested.

A diagram is given of the scattering geometry in Fig 1.1. As depolarised scattered light carries information about anisotropic fluctuations in the polarisability tensor of the scattering medium, these fluctuations are thermally driven and on a microscopic scale result from the molecular motion within the scattering medium.

CHAPTER 1 INTRODUCTION

1.1 Introduction

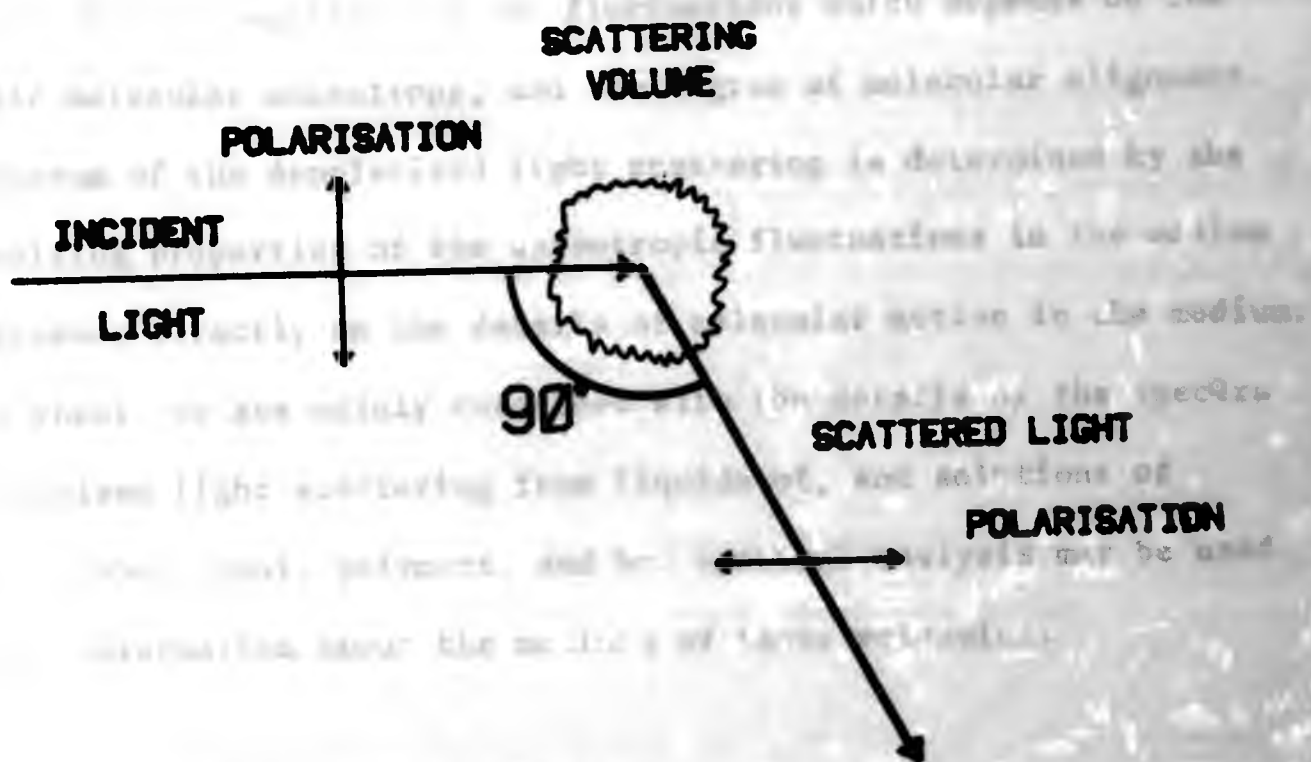
Recently, (1) there has been a great deal of interest in the molecular dynamics of short chain polymer molecules. Due to the complexity of the individual motions of the constituent atoms, an adequate description of the motions of these molecules has yet to be obtained. Early theoretical work, (2), (3) has covered the dynamics of both small rigid molecules, and large polymer molecules, whilst the intermediate region has always been difficult to describe. The purpose of this work has been to obtain some experimental evidence about the details of these molecular motions and to relate the data obtained to simple theory in such a way that useful information may be supplied to aid the development of further theory.

The technique which we have used to investigate these molecular motions is depolarised Rayleigh light scattering. In this technique a collimated beam of light from a laser source enters and passes through a sample of liquid. The incident light is vertically polarised. Light is scattered in all directions from the incident beam. The light scattered at right angles to the incident beam may be separated into two polarisation states, one vertically polarised, the other horizontally polarised. The horizontally polarised component is of much smaller intensity than the vertically polarised component and it is the horizontally polarised component in which we are interested.

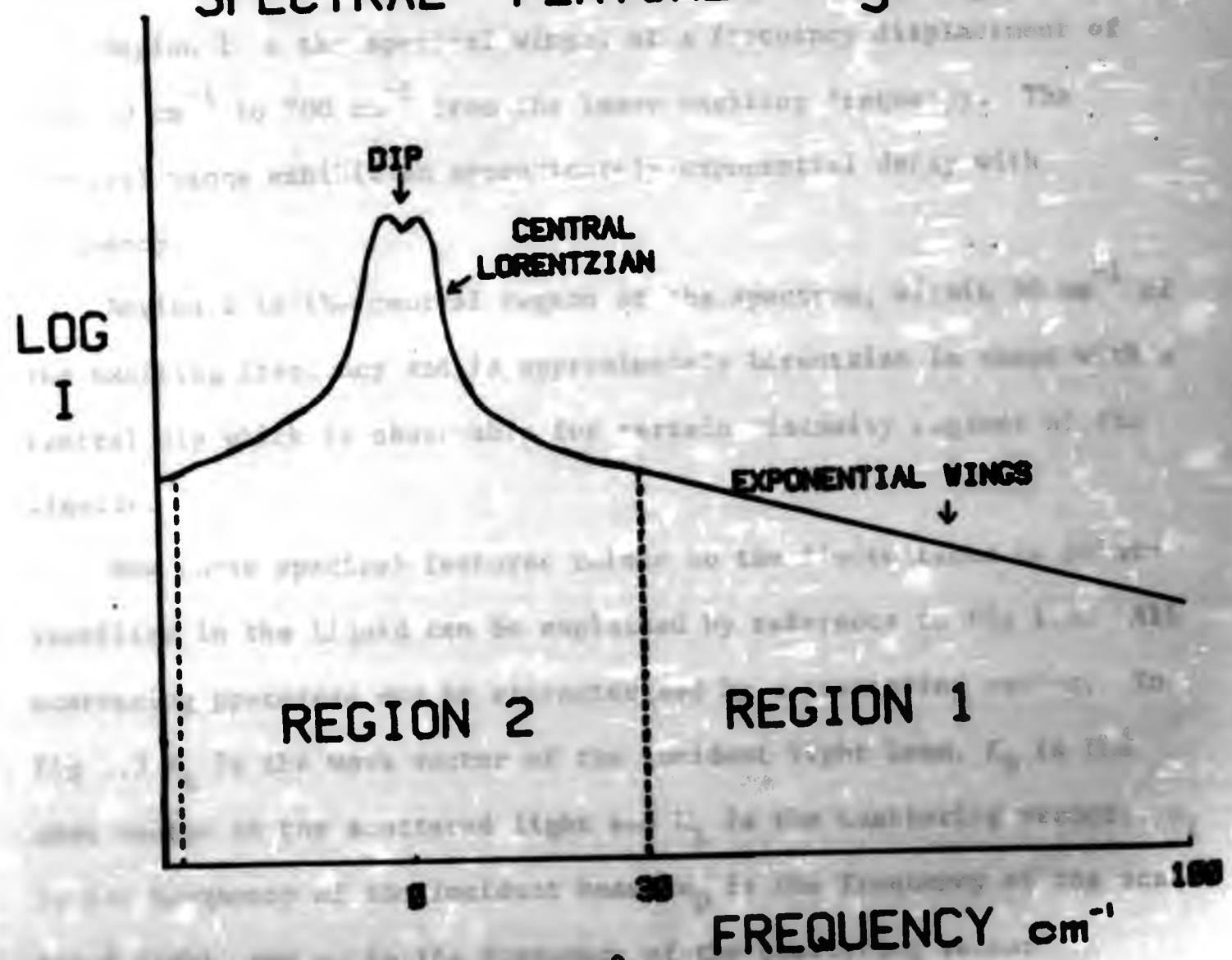
A diagram is given of the scattering geometry in Fig 1.1.

The depolarised scattered light carries information about anisotropic fluctuations in the polarisability tensor of the scattering medium. These fluctuations are thermally driven and on a microscopic scale result from the molecular motion within the scattering medium.

SCATTERING GEOMETRY fig 1



SPECTRAL FEATURES fig 1.2



The intensity of the depolarised light scattering from a medium is determined by the magnitude of the fluctuations which depends on the intrinsic molecular anisotropy, and the degree of molecular alignment. The spectrum of the depolarised light scattering is determined by the time evolving properties of the anisotropic fluctuations in the medium which depends directly on the details of molecular motion in the medium. In this thesis we are mainly concerned with the details of the spectra of depolarised light scattering from liquids of, and solutions of liquids of short chain polymers, and how spectral analysis may be used to obtain information about the motions of these molecules.

1.2 Qualitative Description of Spectra

For the n-alkanes the spectra observed may be conveniently separated into two main regions, with three main spectral features - see fig 1.2.

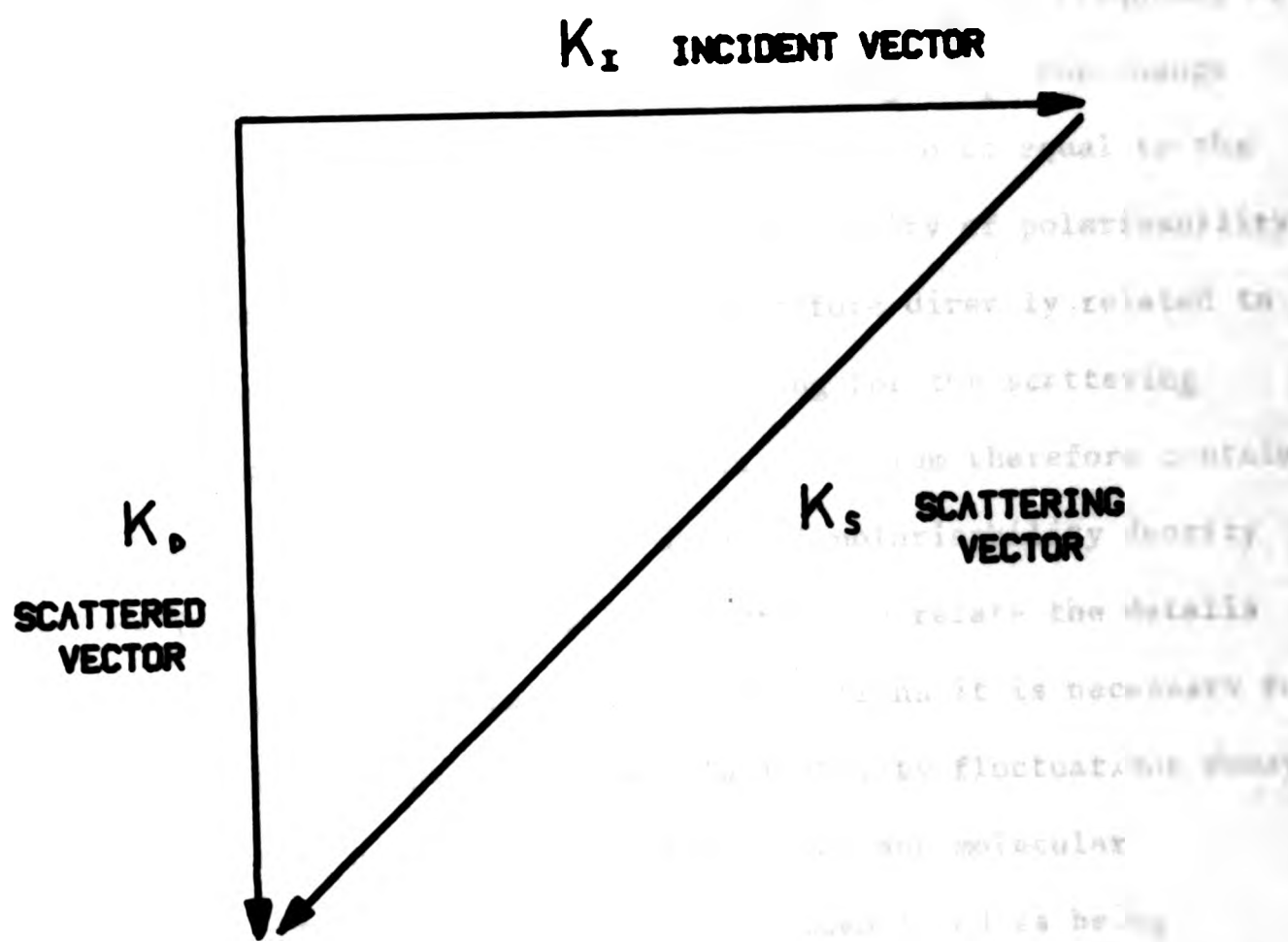
Region 1 is the spectral wings, at a frequency displacement of some 30 cm^{-1} to 200 cm^{-1} from the laser exciting frequency. The spectral wings exhibit an approximately exponential decay with frequency.

Region 2 is the central region of the spectrum, within 30 cm^{-1} of the exciting frequency and is approximately Lorentzian in shape with a central dip which is observable for certain viscosity regimes of the liquids.

How these spectral features relate to the fluctuations in polarisability in the liquid can be explained by reference to Fig 1.3. All scattering processes may be characterised by a scattering vector. In Fig 1.3 \mathbf{k}_I is the wave vector of the incident light beam, \mathbf{k}_D is the wave vector of the scattered light and \mathbf{k}_S is the scattering vector. ω_I is the frequency of the incident beam, ω_D is the frequency of the scattered light, and ω_S is the frequency of the scattering vector

SCATTERING: WAVE VECTOR REPRESENTATION

fig 1.3



By conservation of momentum

$$K_S = K_D - K_I \quad 1.1$$

and by conservation of energy

$$\omega_S = \omega_D - \omega_I \quad 1.2$$

$(\omega_D - \omega_I)$ is the frequency shift of the scattered light relative to the laser exciting line, and is seen to be equal to ω_S the frequency of the fluctuation giving rise to the scattering. $(K_D - K_I)$ the change in the wave vector of the scattered light, is seen to be equal to the wave vector of the fluctuation. The spectral density of polarisability tensor fluctuations at wave vector K_S is therefore directly related to the spectra of the depolarised light scattering for the scattering vector K_S . The depolarised light scattering spectrum therefore contains a great deal of information about the decay of polarisability density fluctuations in the scattering media. In order to relate the details of depolarised Rayleigh spectra to molecular motions it is necessary to have a theoretical description of how polarisability fluctuations decay and how they are related to the molecular motion and molecular polarisabilities. The central Lorentzian is identified as being associated with molecular reorientation, with the inverse half width being equal to a correlation time for molecular reorientation. (4). The dip, observed under certain viscosity conditions, is associated with coupling between rotational and translational motion in the liquid (5). The high frequency spectral wings have been identified as being associated with collisional motion (6), the optical anisotropy being generated by the electronic interaction between colliding molecules.

The theory of depolarised light scattering has been further developed, combining elements of the above and useful experimental and theoretical work has been performed on systems consisting of small symmetric top molecules (7), (8).

For non rigid molecules a limited amount of light scattering data is at present available (9). So far there are no theoretical studies of depolarised light scattering although there are simulations of reorientational, and conformational fluctuation behaviour for short chain n-alkane molecules (10).

The purpose of this thesis is the presentation of results obtained from depolarised light scattering experiments on short chain flexible molecules, and an evaluation of the results obtained in terms of a simple theoretical treatment, which may aid the development of the theory.

1.3 References for Chapter 1

- (1) G T Evans and D C Knauss, 1980, J Chem Phys 72, 3, 1504.
- (2) B J Alder, J J Weiss and H L Strauss, 1973, Phys Rev A 7, 281.
- (3) P J Flory, 1969, "Statistical Mechanics of Chain Molecules", Interscience, New York.
- (4) R Pecora, 1968, J Chem Phys 49, 1035.
- (5) M A Leontovich, 1941, Izv Akad Nauk SSR Ser Fiz 5, 148 (J Phys USSR, 1941, 4, 499).
- (6) J A Bucaro and T A Litovitz, 1971, J Chem Phys 54, 9, 3846.
- (7) T I Cox, M R Battaglia, P A Madden, 1979, Mol Phys 38, 1539.
- (8) D Frenkel and J P McTague, 1980, J Chem Phys 72, 4, 2801.
- (9) J V Champion and D A Jackson, 1976, Mol Phys 31, 1169.
- (10) J A Montgomery, S L Holmgren, D Chandler, 1980, J Chem Phys 73, 8, 3688.

CHAPTER 2 REVIEW OF THEORY

2.1 Light Scattering - Intensity Measurements and Theory

The first calculation of the intensity of light scattering from thermal fluctuations in simple liquids was performed by Einstein (8), this being an extension of Smoluchowski's (9) treatment of critical opalescence. Einstein's result indicates that the intensity of light scattered by a medium is directly related to the mean square fluctuations in dielectric constant. The fluctuations are thermally driven, and are fluctuations in a scattering volume of a number of isotropically polarisable scattering particles. The fluctuations in the dielectric tensor are therefore isotropic, and the polarisation of the scattered light should be identical to that of the incident beam. Later experimental work showed however the existence of a non negligible depolarised component. Cabannes (10) was the first to examine and derive relationships between the relative intensities of isotropic, and anisotropically scattered light and experimentally measured depolarisation ratios.

Initially work on the depolarised light scattering concentrated on measurement of the intensities of the light scattering, and the relation of the intensity to molecular quantities.

The anisotropic and isotropic Rayleigh ratios for a molecular liquid are given by

$$R_{AN} = \frac{8\pi^4}{\lambda^4} \left(\frac{n^2 + 2}{3} \right)^4 \times \frac{13}{45} \rho \gamma^{-2} \quad 2.1$$

$$R_{ISO} = \frac{8\pi^4}{\lambda^4} \left(\frac{n^2 + 2}{3} \right)^4 \times KT \beta_T \rho \alpha^{-2} \quad 2.2$$

(SI units)

γ^{-2} is the mean squared optical anisotropy

α^{-2} is the mean optical polarisability

ρ is the number of scatterers

The factor $\left(\frac{n^2 + 2}{3}\right)^4$ is known as the internal field factor and corrects for the effect of the field in surrounding molecules on the field in the scattering molecules.

There has been disagreement over the exponent of the internal field factor which should be used in the formulae for R_{ISO} and R_{AN} . Some authors use exponents of 2 in the internal field factor, others use factors of 4, depending on the manner and model from which the equations were derived.

Coumou et al (11), (12), (13) use $\left(\frac{n^2 + 2}{3}\right)^2$ for R_{AN} and $\left(\frac{n^2 + 2}{3}\right)^4$ for R_{ISO} , the difference coming from the fact that for R_{ISO} the effect of the internal field is approximately orientation independent, whereas for R_{AN} the effect is strongly dependent on the molecular orientation with respect to the field. Averaging over all possible molecular orientations gives the different internal field factors. Kielich in a set of papers (14), (15), (16) uses $\left(\frac{n^2 + 2}{3}\right)^2$ as the internal field factor for both R_{AN} and R_{ISO} . Dezelic (17) does not explicitly give an internal field factor although from his equations it is possible to derive an internal field factor of $\left(\frac{n^2 + 2}{3}\right)^4$ for R_{ISO} . Malmberg and Lippincott (18) use internal field factors of $\left(\frac{n^2 + 2}{3}\right)^4$ for both R_{AN} and R_{ISO} , and also identify a problem inherent in the interpretation of light scattering data obtained for solutions. In varying solution concentration one varies the effective cavity shape used in the calculation of the internal field factor using the Onsager (19) - Scholte (20) model. They comment on the fact that angular correlation is a problem in interpretation of the data, and deduce from their results evidence of non-random molecular orientation in the liquids investigated.

The effect of angular correlation on depolarised light scattering is to increase the intensity of the light scattering. This is

essentially due to the fact that as depolarised light scattering is a coherent process molecular angular correlation results in in-phase scattering from molecules which leads to an increased intensity.

Clement and Bothorel (21) studied the optical anisotropy of the n-alkanes, over a range of alkane chain numbers and in solution in a number of liquids. In a later paper (22) the same authors examine the optical anisotropy of the n-alkanes in solution in carbon tetrachloride and identify G the orientational correlation parameter which is approximately one for pentane to octane and increases with increasing alkane chain number. The effective mean squared optical anisotropy is given by $G \gamma^{-2}$, on dilution the scattering molecules are separated and the effective mean squared molecular optical anisotropy becomes γ^{-2} . Therefore dilution experiments provide a means to measure angular correlation in the n-alkanes. A large number of papers have been published on this subject, both experimental measurements on the n-alkanes (23), (24), (25), (26), and theoretical modelling of the local order in liquids consisting of chain molecules, and modelling of molecular polarisability depending on bond polarisability models, (27), (28), (29).

The important results from these are that to obtain valid values of G from light scattering experiments a correction must be applied for the collision induced contribution to the scattered intensity, corrections must be applied for the changing refractive index of the solution, and the correct internal field factor must be used. Also G has been shown experimentally and theoretically to have a temperature dependence such that

$$G \propto \frac{T}{T - T^*}$$

2.3

where T^* is a hypothetical ordering temperature, judged for the n-alkanes to be about thirty degrees below the melting point. Elements

of these results are used in the following papers, in studies of anisotropic molecules (30), (31) and of the n-alkanes (32), (33). One further point becomes apparent. For flexible molecules in solution there is the possibility that by varying solution concentrations one does not only vary angular correlation between the molecules. It is probable that molecular conformation also changes as solution concentration changes, and this results in a varying molecular anisotropy. The G parameters measured for the n-alkanes by solution measurements therefore consist of a component due to intermolecular orientational correlations, and a component due to intramolecular correlations down the molecular chain, dependent on molecular conformation.

2.2 Light Scattering - Spectral Measurements and Theory

With the advent of the laser, a spectrally pure high intensity narrow line width light source, and with the development of improved interferometric techniques it became possible to study the spectral details of depolarised light scattering. As a consequence of this there has been a great deal of interest both in spectral measurements of depolarised light scattering and in theoretical modelling of the spectra.

The spectrum of light scattered from a medium carries information about the time evolving properties of the polarisability fluctuations in the medium. Indeed the spectrum reproduces the spectral density of the polarisability fluctuations in the liquid, and therefore contains significant information on molecular motions.

Berne and Pecora (34) give a comprehensive analysis of light scattering from molecular liquids, relating polarisability fluctuations to the observed spectral distribution. From this approach it follows that to calculate the light scattering spectrum it is essential to have

a model for the decay in the polarisability fluctuations.

Kivelson and Madden (35) review recent advances in the analysis of depolarised Rayleigh and Raman spectra from liquids consisting of small rigid molecules, and also discuss the relevance of results from molecular dynamics simulations to the light scattering experiments. It is apparent that the contribution made by collision induced scattering to the depolarised Rayleigh spectra is very important. A recent review of this aspect by Tabisz (36) discusses techniques for observing collision induced spectra, and details of the possible mechanisms for production of the interaction induced component to depolarised spectra.

The fluctuations in polarisability which cause depolarised Rayleigh scattering result from the effect of molecular motion upon the intrinsic and interaction induced molecular optical anisotropies. The scattering volumes over which these fluctuations occur are large compared to the size of an individual molecule, but small compared to the probing optical wavelength. Ignoring initially the interaction induced contribution to the polarisability fluctuations, the shape of the depolarised Rayleigh spectrum is determined by the Fourier transform over both time and position of an autocorrelation function for a collective molecular orientation density. For symmetric top molecules the intensity is determined by the anisotropy in the molecular polarisability and a static orientational parameter g_2 which is given by

$$g_2 = 1 + \frac{1}{2} \sum_{j \neq i} (3 \cos^2 \theta_{ij} - 1)$$

2.4

where θ_{ij} is the angle between the molecular axes. In the rotational diffusion limit the decay of the fluctuations for symmetric tops is approximately exponential and therefore the spectrum is Lorentzian in form. Keyes and Kivelson (37) identified the fact that in depolarised light scattering the spectrum is due to the decay of a collective mole-

cular orientation density. If there is no coupling between orientation and momentum densities the correlation time τ_{LS} from the light scattering spectra may be related to the single particle correlation time by the relation

$$\tau_{LS} = \frac{1}{2\pi f_{\frac{1}{2}}} = (g_2/j_2) \tau_s \quad 2.5$$

where τ_{LS} = light scattering correlation time

$f_{\frac{1}{2}}$ = half width of Lorentzian

τ_s = single particle correlation time

g_2 = static orientational correlation parameter

j_2 = dynamic orientational correlation parameter.

The correlation times obtained may be related to simple models of molecular reorientation based on rotational diffusion behaviour. However the depolarised Rayleigh spectra are more complex than the above simple model would indicate. The presence of coupling between molecular orientation and shear modes adds an extra feature to the spectra and when the presence of interaction induced contributions to the polarisability fluctuations is considered, the spectra become yet more complex.

The existence of a dip in the central Lorentzian component of the depolarised Rayleigh spectra due to propagating but highly damped shear waves was first predicted by Leontovich (2). Rytov (38) presented a more general approach to the same analysis. These visco elastic theories assume that the light scattering arises from fluctuations in the stress tensor (which microscopically may be related to a collective reorientation of individual molecules). In the Rytov theory the stress tensor is coupled to the strain tensor by a frequency dependent shear modulus. The reorientational motion is characterised by a single relaxation time. The spectral form for the VH spectrum in this theory

is given by

$$I_{VH}(q, \omega) \propto \frac{\Gamma}{\Gamma^2 + \omega^2} \sin^2(\frac{\theta}{2}) + \frac{\omega^2 \Gamma}{\Gamma_w^2 + (\omega^2 - \omega_T^2)^2} \cos^2(\frac{\theta}{2}) \quad 2.6$$

$\omega_T = (\mu_\infty / \rho_0)^{1/2} q$ is the frequency of the shear wave

μ_∞ is the shear modulus in the high frequency limit

q is the wave vector of the fluctuation being studied

Γ is the reciprocal of the correlation time for shear mode

relaxation and ρ_0 is the liquid density.

The spectrum is therefore of the form of a Lorentzian (first term) plus a narrow dip of width ω_T^2 / Γ (second term) in the Lorentzian line. The simple viscoelastic approach to the theory of depolarised spectra has largely been superceded by approaches using "microscopic" theories based on the Mori formalism (39). Without understanding the underlying mechanisms giving rise to the fluctuations causing the light scattering, one can, by choosing a set of primary variables which are coupled to the local dielectric constant, which are in turn coupled to a set of secondary variables by a set of linear transport equations, produce a theoretical description of the depolarised Rayleigh spectra which may be used to analyse single particle relaxation. The number of variables in each set, and their exact definition differs from author to author.

Although the variables in the different theories have differing physical interpretations, in most cases the same general spectral form is predicted. Keyes and Kivelson (40) developed a two variable approach and argued, from the physical fact that the depolarised dip vanishes at low temperatures, that the primary variable is directly related to molecular reorientation and the secondary variable is related to the shear wave. In an earlier paper (41) they drew analogies between the reasonably well understood Brillouin splitting

observed in the polarised spectrum and the splitting or "dip" observed in the depolarised Rayleigh spectra. In the case of the Brillouin spectra the coupling is between molecular orientation and longitudinal waves. In both cases the waves to which the molecular orientation couples are not propagative but dissipative. In common with all "two variable" theories Keyes and Kivelson's theory predicts only the features of the spectra in the low frequency regime, and not the existence of the high frequency spectral background.

In the limit of small K , (where K is the scattering vector) the spectral form predicted by Keyes and Kivelson is

$$I_{VH}(\omega) \propto \frac{\Gamma}{\Gamma^2 + \omega^2} - R(\cos^2 \theta/2) \frac{K^2 \eta/\rho}{\Gamma} \frac{(K^2 \eta/\rho)}{(K^2 \eta/\rho)^2 + \omega^2} \quad 2.7$$

η is the viscosity of the liquid

ρ is the mass density

K is the scattering vector = $\frac{4\pi n}{\lambda} \sin (\theta/2)$

Γ is the reciprocal of the molecular reorientation time where

λ = optical wavelength

θ = scattering angle

n = liquid refractive index

R is the dimensionless coupling parameter. The spectrum has the form of a positive Lorentzian of half width Γ plus a negative Lorentzian with a dip half width of $K^2 \eta/\rho$. The depth of the dip observed is determined directly by the parameter R which has a significance depending on the specific model used in the calculations. The equation 2.7 is only valid in the limit $K^2 \eta/\rho \Gamma \ll 1$ 2.8

When the above simplifying assumption is removed the spectral form obtained by Keyes and Kivelson is given by

$$I_{VH}(\omega) \propto \frac{\Gamma}{\Gamma^2 + \omega^2} (\sin^2 \theta/2) + \frac{\Gamma(\cos^2 \theta/2)}{\left[\frac{K^2 n^2 / \rho^2 (1 - R) + \omega^2}{(\Gamma - \eta K^2 / \rho - \omega^2)^2 + \omega^2 (\Gamma + \eta K^2 / \rho - \eta K^2 / \rho R)^2} \right]} \quad 2.9$$

It is this equation which we use in our analysis of depolarised light scattering spectra from the n-alkanes, and from other chain molecules.

In the initial paper (41) Keyes and Kivelson predicted an inverse square temperature dependence of the coupling parameter R. It was later pointed out by Alms et al (42) that the manner in which R was defined meant that it was identically equal to zero. Andersen and Pecora (43) presented a more general formulation of Mori's theory of fluctuations and applied it to derive a two variable theory essentially equivalent to Keyes and Kivelson's, and also a three variable theory. In the two variable theory the R parameter is a constant, independent of temperature.

The various theories and their merits are examined in (44), a review of the early theories, and in (45) which summarized some of the theories and compared and contrasted results predicted by them under different physical circumstances.

The spectral form is characterised by the quantity R and by the value of the quantity $K^2 n / \rho \Gamma$, the ratio of the "dip half width" to the half width of the main Lorentzian feature. R represents a measure of the depth of the dip relative to the main Lorentzian feature. It is strictly incorrect to talk of a main Lorentzian feature and a dip half width as this implies that the spectra are of the form predicted by equation 2.7. Γ (the main Lorentzian half width) is identified as being the inverse of the orientational correlation time, while $K^2 n / \rho$ is the

inverse of the shear wave correlation time. In the limit in which $K^2 \eta / \rho \Gamma \ll 1$, the spectrum approximates to a positive (reorientational) Lorentzian and a negative (shear wave) Lorentzian one can talk of a main Lorentzian and a dip half width. Outside this region the spectra are more complex and the terminology is not strictly correct.

In (45) an examination is made of the spectral form predicted by equation 2.9 for various values of R, for four different regions of the quantity $K^2 \eta / \rho \Gamma$. These regions are

- (1) $K^2 \eta / \rho \Gamma \ll 1$
- (2) $K^2 \eta / \rho \Gamma < 1$
- (3) $K^2 \eta / \rho \Gamma > 1$
- (4) $K^2 \eta / \rho \Gamma \gg 1$

R values obtained from depolarised light scattering experiments on a number of liquids vary between 0.2 to 0.7.

For region 1, $K^2 \eta / \rho \Gamma \ll 1$ the spectral form is that of a central Lorentzian plus a very narrow dip. This regime is characteristic of liquids with small molecules, which have a fast reorientation time and a low viscosity. In this situation the spectrum observed approximates very well to a Lorentzian. The very narrow central dip is not observable being much narrower than the instrumental width.

For region 2, $K^2 \eta / \rho \Gamma < 1$ a dip is clearly observed in the spectrum. R parameters are readily obtained from fits to spectra in this region. The R values obtained lie as stated between values of 0.2 to 0.7.

For region 3, $K^2 \eta / \rho \Gamma > 1$, which is characteristic of viscous liquids, the dip half width is comparable with the half width of the main Lorentzian and the spectra observed are non Lorentzian, becoming more triangular in shape. As $K^2 \eta / \rho \Gamma$ increases a number of authors (46) have found increasingly poor fits. The liquids studied generally

consisted of highly anisotropic molecules, such as quinoline and benzyl alcohol, high quality spectra were obtained, with low noise levels, and with (relatively) low levels of parasitic scattering. For viscous liquids with low anisotropies a problem arises in that the noise level on the resultant spectra is much higher and the level of parasitic scattering is relatively much larger. This means that for liquids with a low molecular anisotropy, in the $K^2 n / \rho \Gamma > 1$ region it is very difficult to get good fits to the spectral data.

Region 4, $K^2 n / \rho \Gamma \gg 1$, is characteristic of supercooled liquids close to the glass transition temperature. In (45), Searby et al give a modification to equation 2.9 from Tsay and Kivelson's paper (44) retaining terms to higher order in K . Unfortunately the expression given is in the third term incorrect in the powers of frequency. Liquids in this region have been studied by Enright and Stoicheff (47). At the lowest temperature the spectra exhibited sharp and well separated doublets, centred about a sharp depolarized, unshifted component indicating that the shear waves responsible for the shear-rotational coupling, have become propagative.

These early two variable theories explain the spectra fairly well in liquids of low and moderate viscosity liquids. Chappell et al (48) have recently derived a "three variable" theory of depolarised light scattering which describes the observed spectra over the entire viscosity range. Having examined the depolarized spectra of tri-phenyl phosphite in the high viscosity range ($K^2 n / \rho \Gamma \gg 1$) and detected the two side peaks (which are characteristic of shear reorientational coupling) the measured intensity was far below that predicted by the two variable theory. Chappell et al concluded that the large discrepancy between the observed and predicted intensity of the side peaks (~ two orders of magnitude) indicates that a two variable theory is inadequate to account for the spectral features observed over the

whole viscosity range. The spectra observed were analysed in terms of three features - a dip, sharp line, and a broad line. At high temperatures when the dip feature is very narrow and not observable, it is perhaps surprising that to fit the spectra adequately a two Lorentzian fit with comparable half widths was required. To obtain these fits however, a simultaneous fit had to be performed to two separate spectra, recorded with the liquid under identical physical conditions, but using different instrumental free spectral ranges. In all cases the value of R obtained decreases uniformly with increasing temperature falling from 0.79 at -27.7 °C to 0.42 at 87.5 °C.

In another paper published at the same time, (49) the same authors apply the "three variable" theory to the phenomenon of flow birefringence and its relationship to depolarized light scattering. This represents an extension of the earlier work of Kivelson et al (50) in which it was shown that the R parameter, which may be obtained from fits to VH depolarised spectra may also be obtained by combining the stress optical coefficient measured by flow birefringence, with information obtained from HH depolarised spectra, specifically the integrated intensity and the spectral linewidths. In (50), a measured value of R for triphenyl phosphite was used to calculate a value of the stress optical coefficient which was found to be in good agreement with measured values. The "three variable" theory was used for an identical comparison in (49), again for triphenyl phosphite. The theoretical values were in good agreement with the experimental values, but only at temperatures of 35 °C to 40 °C. For lower temperatures the disagreement between the theoretical and experimental results increased, the theoretical result being approximately 40% greater than the experimental at 10 °C.

We conclude that the "three variable" theory of Kivelson, Chappell, Allen and Hallem represents the best model at present for shear-

rotationally aligned molecules. In addition to rotational coupling in the depolarised Rayleigh spectra. However to fit data to this spectral model it is necessary to "double" fit simultaneously spectra obtained at different free spectral ranges, and to have good quality spectra such that in the high viscosity case, the low intensity satellite shear mode peaks can be fitted. The "three variable" theory however does not completely explain the variation of the stress optical coefficient with temperature for triphenyl phosphite.

The R parameter as discussed, is a measure of coupling between molecular reorientation and the hydrodynamic shear modes. It has been measured spectrally and can be obtained from flow birefringence. There are also a number of theoretical modellings of the parameter. We now examine specifically the R parameter.

Champion and Jackson (51) calculated values of the R parameter for the n-alkanes from measured values of the stress optical coefficient. The values obtained are well below values which have subsequently been obtained from spectral fits to the VH spectra. The model which was used in this calculation was derived in (50) and related R to ratios of functions of dynamic variables which were obtained from flow birefringence and HH depolarised light scattering.

Kivelson and Hallem (52) extend the model for the calculation of R, and by a selective set of approximations express the ratio of dynamic factors by static quantities. R is derived by two methods, one in which it is expressed in terms of correlations over molecular quantities, and the other in which a hydrodynamic model is used. From these it follows that if R_o is the parameter for the neat liquid, the R observed for a solution is given by

2.10

where R = solution parameter

x = mole fraction

R_o = neat liquid parameter

In the hydrodynamic model the calculation depends upon Peterlin and Stuart's (53) classical hydrodynamic theory based upon Jeffreys (54) hydrodynamic results for stick boundary conditions.

The expression derived for R is a function of the geometric quantities describing molecular shape and hydrodynamic properties and is as below

$$R = \left\{ \frac{3}{5} P \left[\frac{1 - (b/a)^2}{1 + (b/a)^2} \right] \right\} \cdot v N_o^\alpha \quad 2.11$$

p is the Perrin factor (see 2.28 and 2.29)

b/a is ratio minor to major axis for a prolate ellipsoid

v is the molecular volume

α is the stick slip coefficient

N_o is the molecular number density

This hydrodynamic model is only valid for approximately spheroidal particles, which are undergoing rotational diffusion processes and are therefore large compared to molecular size. It is also only valid in the $\alpha = 1$ stick limit. Equation 2.11 is therefore of doubtful value for liquids consisting of small molecules. The corresponding equation obtained for R from the molecular theory is a ratio of zero frequency correlation functions which should have similar dynamical properties. This implies that if R is a function of temperature it should only have a weak temperature dependence.

There have been a large number of determinations of R by VH depolarised light scattering for different liquids. In most cases R is nearly independent of temperature and the temperature variation if observed is weak. Alms and Patterson (55) determined R values for isotropic MBBA and for the n-alkanes hexadecane, and docosane. The values

were respectively 0.36, 0.33 and 0.38. The values for the alkanes are in accordance with values obtained for other liquids and considerably larger than those obtained from calculations by Champion and Jackson (51) based on flow birefringence measurements.

Lempert and Wang (56) determined the R parameters for solutions of nitrobenzene in carbon tetrachloride, by fitting the observed low frequency spectra to a form resulting from a "two variable" theory. R was found to be independent of temperature, and to be strongly dependent on concentration. The R parameter was approximately linear in solution concentration, however the lowest solution concentration at which it was measured was 78%. At lower solution concentrations the contribution to the depolarised intensity is low and it is difficult to resolve the dip due to the spectral noise. The value of the R parameter obtained for the neat liquid (0.55 ± 0.03) is in fair agreement with the value obtained by Stegeman and Stoicheff (57) (0.5). Lucas and Jackson (58) earlier had also examined the depolarised dip in nitrobenzene, but had not obtained values of the R parameter.

Other determinations of R in which the R parameter is approximately constant with temperature are those of Tsay and Kivelson (44) for triphenyl phosphite, Rouch et al (60) for quinoline, Alms et al (42) for anisaldehyde and Enright and Stoicheff (61) for CS_2 . A large systematic decrease in R with temperature has only been observed in (48) where depolarised Rayleigh spectra for triphenyl phosphite were fitted to a "three variable" theory over a large temperature range.

Collision Induced Scattering

For atomic liquids and liquids composed of isotropic molecules the depolarised light scattering is due exclusively to interaction induced

polarisability fluctuations in the liquid. For anisotropic liquids the interaction introduced phenomena also contribute to the depolarised light scattering, along with the polarisability fluctuations associated with the intrinsic molecular anisotropy. Keyes et al (62) developed a theory relating depolarised Rayleigh spectra to two separate processes, one being molecular reorientation, a relatively slow process, the other being a fast intermolecular interaction. The time scale separation of the two processes leads to a two component spectrum, one component being a narrow Lorentzian associated with molecular reorientation, the other broad Lorentzian being associated with the interaction induced phenomena. If there is no time scale separation, then there are contributions in the spectrum due to cross correlations between the intrinsic and interaction induced polarisability fluctuations. The simple spectral form, in which interaction induced and intrinsic features are separable is invalid.

The first study of integrated depolarised light scattering, in which an account was taken of collision induced scattering was that of Patterson and Flory (63). The collision induced scattered intensity was estimated by determining the decrease in intensity when a narrow-band filter was used. Champion et al (32) fitted spectra obtained for the n-alkanes using a Fabry Perot spectrometer to a single Lorentzian, and a high frequency exponential. From this they obtained values of the contributions to the molecular optical anisotropy due to the fast collisional contribution and due to the slow reorientational contribution. Champion et al defined the ν parameter, the ratio of the slow intensity to the total depolarised scattered intensity.

$$\nu = \frac{I_{SLOW}}{I_{SLOW} + I_{COLLISIONAL}}$$

2.12

The total amount of depolarised light scattered by collisional processes may be related to a collision induced mean squared optical anisotropy. R_{AN} is the anisotropic Rayleigh ratio, and the total intensity of depolarised light scattering is directly proportional to this ratio. The proportion of the intensity of the depolarised light scattering due to collisional processes is given by $(1 - v)$. Therefore by reference to equation 2.1 the relationship between R_{AN} , v and $\gamma_{COLLISIONAL}^{-2}$ may be given by

$$(1 - v)R_{AN} = \frac{8\pi^4}{\lambda^4} \left[\left(\frac{n^2 + 2}{3} \right)^4 \times \frac{13}{45} \circ \gamma_{COLLISIONAL}^{-2} \right] \quad 2.13$$

Brown et al (31) obtained depolarised spectra of a number of binary mixtures of cylindrically symmetric anisotropic molecules. The spectra were recorded using a double grating monochromator and a separation of the collision induced contribution to the spectra was obtained by fitting the far wings to a spectral form derived from the isolated binary collision model of Bucaro and Litovitz (3).

There have been a large number of theoretical and experimental studies of collision induced depolarised light scattering. These have been extensively reviewed in an article by Gelbart (64) and an article by Tabisz (36).

There are basically two types of models from which the time evolving properties of the polarisability fluctuations which give rise to the collision induced scattering can be calculated. These are the dipole induced dipole (DID) model and the electron overlap (EO) model. In the DID case two atoms or molecules approach each other in a collisional process. The field of the randomly fluctuating dipole in one molecule (or atom) induces a dipole in the other molecule (or atom). For the colliding pair there is an induced anisotropy in the

polarisabilities which gives rise to the collisional induced contribution to the depolarised Rayleigh spectrum. The time evolving properties of the anisotropy, which are determined by the manner in which dipole strength varies with particle separation, and with collision geometry and approach velocity, determines the form of the collision induced spectrum.

In the EO model the collision induced anisotropy has different time evolving properties to the DID case. The anisotropy in the DID case is relatively a long range property of the collisional process. In the EO case the two molecules approach each other and are relatively isotropic until the moment of collision when their electronic shells overlap and distort.

For both EO (65) and DID (66) models, the dependence of the collision induced intensity with density is given by

$$I_{\text{COLLISIONAL}} \propto \rho^2$$

2.14

This is valid at low densities and is due to the fact that the interaction is between pairs of particles. At higher densities the dependence breaks down as the probability of collisions is no longer directly dependent on the density of liquid or gas. As DID is a longer range interaction than EO equation 2.14 breaks down at lower densities for the DID case than for the EO case. At higher densities multiparticle interactions become important and reduce the scattered intensity, (in a perfect cubic lattice, DID contributions would cancel out exactly) the contributions to the scattered amplitude from interactions between odd numbers of particles being negative, and reducing the total scattered intensity.

The separation of interaction induced spectra into two, three and four body terms has been performed by a number of authors. Gelbart (64) derived quantum mechanical expressions for the two and three body contributions to the scattered intensity. Others (67) working on simple atomic liquids have fitted spectra to a sum of separate exponential wings describing the two, three and four body spectra. The systems for which such a separation has been performed are very simple compared to the n-alkanes.

In the dense state it may be impossible to distinguish between DID and EO effects, however it seems likely that the high frequency part of the collisional spectrum for molecular liquids is due to the short range intermolecular interaction and hence is determined mainly by EO processes.

Bucaro and Litovitz (3) perform calculations on the shape and intensity of the Rayleigh wings of the spectrum based upon a binary collision, EO model. The calculation used a Lennard Jones potential and assumes zero impact parameter for collisions. Assuming that for two particles the polarisability difference is given by an expression of the form

$$\Delta\alpha(r) \propto r^{-m}$$

2.15

Bucaro and Litovitz obtained the following form for the spectrum by a numerical integration

$$I(\omega) = I_0 \omega^{2[(m-7)/7]} \exp(-\omega/\omega_0)$$

2.16

For molecular liquids Bucaro and Litovitz argue that the polarisability anisotropy is due to frame distortion, that is, it is due to the repulsive part of the Lennard Jones potential. $m = 13$

$$\text{Therefore } I(\omega) = I_0 \omega^{12/7} \exp(-\omega/\omega_0) \quad 2.17$$

ω_0 is related to the mean frequency of collision and is shown to be given by the relation

$$\frac{1}{\omega_0} = \frac{1}{6} \pi r_0 (\mu/KT)^{\frac{1}{2}} \left[1 - \left(\frac{2\epsilon_0}{KT} \right)^{\frac{1}{2}} \right] \quad 2.18$$

ϵ_0 and r_0 are the constants used in the standard expressions of the Lennard Jones potential and μ is the reduced mass.

Later calculations show that taking account of the non zero collision parameters and an appropriate distribution of molecular velocities the preexponential part of the spectrum reduce to ω^0 .

Therefore

$$I(\omega) = I_0 \exp(-\omega/\omega_0) \quad 2.19$$

Kyu Shin (68) extended the binary collision model of Bucaro and Litovitz. Performing a direct integration he considers all possible encounters between molecules and finds that his formula fits the spectra observed over a greater frequency range.

Levine and Birnbaum (65) also performed a calculation of the spectral form of the interaction induced spectrum assuming EO effects.

In this model it is shown that

$$I(\omega) = \omega^{\frac{1}{2}} \exp(-\omega/\omega_0) \quad 2.20$$

$$\text{and } \frac{1}{\omega_0} = \frac{2\pi}{\gamma} \left[\frac{m}{KT} \right]^{\frac{1}{2}} \quad 2.21$$

$\frac{1}{\gamma}$ is effectively the average intermolecular distance, $1/\omega_0$ is the average time between molecular collisions and $(m/KT)^{\frac{1}{2}}$ is related to the average molecular velocity. The factor 2π comes from the averaging

process over the particular velocity distribution used.

All the above calculations use binary collision models, which are unlikely to be correct in the case of molecular liquids. The calculations also assume that the molecules have aspherical symmetry. For anisotropic molecules $\Delta\alpha$ depends not only on molecular separation, but varies in a complex manner with molecular orientation. To adequately model the interaction induced spectrum for anisotropic molecules, taking into account contributions from two, three and four particle correlation functions and to relate the model to experimentally observed spectra is a daunting task. Such modellings have been carried out by Madden and Cox (69), (4) for CS_2 using a multipole expansion for the interaction induced moments. So far this approach has not been extended to flexible molecules.

2.3 Molecular Correlation Times - The Stokes Einstein Relation and Stick Slip Behaviour

For many liquids there is a linear relationship between single particle reorientational correlation times and the macroscopic viscosity of the liquid divided by the absolute temperature.

$$\tau_s = \left(\frac{\eta}{T}\right) C + \tau_0 \quad 2.22$$

τ_s is a single particle correlation time

τ_0 is the finite intercept on the τ_s axis and the suggestion has been made (72) that it is associated with inertial rotation, that is, it is the classical free rotor time of the molecule.

$$\tau_0 (\text{RIGID ROTOR}) = \left(\frac{2\pi}{9}\right) \left(\frac{KT}{I}\right)^{\frac{1}{2}} \quad 2.23$$

$\left(\frac{\eta}{T}\right) C$ may be related to $(\frac{1}{6\theta})$, (1), where θ is the molecular rotational diffusion coefficient. The rotational diffusion

coefficient θ for a spherical hydrodynamic particle is given by the Stokes Einstein equation, in terms of the viscosity η of the fluid, and the radius a of the particle.

$$\theta = KT/8\pi\eta a^3 \quad 2.24$$

2.24 in 2.22 leads to the relationship for a spherical hydrodynamic particle.

$$\tau_s = \frac{4\pi\eta a^3}{3KT} + \tau_0 \quad 2.25$$

This may be written as

$$\tau_s = \frac{V\eta}{KT} + \tau_0 \quad 2.26$$

where V = particle volume

This applies only to spherical particles. For ellipsoidal particles Perrin (70) derived expressions for translational and rotational diffusion coefficients in terms of the liquid viscosity and particle dimensions. For a non spherical particle the rotational and translational diffusion coefficients are smaller than for a spherical particle with the same volume. The effect on the correlation times is that they are longer for a non spherical particle than for the equivalent spherical particle. For the reorientational correlation times for an ellipsoidal particle (prolate ellipsoid)

$$\tau_s = \frac{pV\eta}{KT} + \tau_0 \quad 2.27$$

where p = Perrin factor, which for a prolate ellipsoid is given by

$$p = \frac{2[1 - (b/a)^4]}{3(b/a)^2 [\{2 - (b/a)^2\} s - 1]} \quad 2.28$$

$$\text{where } S = \frac{1}{\sqrt{(1 - (b/a)^2)}} \log_e \frac{1 + [1 - (b/a)^2]^{\frac{1}{2}}}{b/a} \quad 2.29$$

b/a is the ratio of the minor axis to the major axis of the ellipsoid.

Equation 2.27 results from a hydrodynamic model of molecular reorientation. In applying this to molecules other considerations come into force. The hydrodynamic model assumes that a rotating particle is surrounded by a continuum. For a molecule undergoing rotational diffusion in a fluid composed of other molecules this is not a valid approximation. The more globular a molecule, the more likely it will undergo reorientation within its own volume in the medium, interacting less with its surroundings than predicted by the macroscopic viscosity of the liquid. This leads to a concept of "stick" and "slip" coefficients. The molecule sees an effective viscosity which is less than the macroscopic viscosity of the liquid. The Stokes Einstein relation becomes

$$\tau_s = \frac{\alpha p V n}{K T} + \tau_0 \quad 2.30$$

where α = stick slip coefficient.

"Stick" and "slip" refer to the two possible classes of boundary conditions at the surface of a particle undergoing translational and rotational diffusion processes in a liquid. These boundary conditions may be summarised as follows (91).

For "stick" boundary conditions the fluid velocity at the particle's surface is continuous with the surface velocity of the particle.

For "slip" boundary conditions the tangential component of the normal stress on the surface of the particle is identically equal to zero.

The parameter α , the stick slip coefficient is a function both of particle geometry and of boundary conditions. For a spherical particle, for the "slip" condition, $\alpha = 0$. As this is manifestly not the case for macroscopic particles, in the macroscopic limit "stick" boundary conditions are appropriate. For molecular reorientation processes "slip" boundary conditions appear to be more appropriate.

α has been calculated by a number of authors for ellipsoids using the slip boundary condition. Hu and Zwanzig (91) obtained values of the frictional coefficient α for "slip" boundary conditions and the ratio $\alpha_{\text{SLIP}}/\alpha_{\text{STICK}}$ for both prolate and oblate ellipsoids. In the disc limit (oblate ellipsoid) and the needle limit (prolate ellipsoid) the ratio $\alpha_{\text{SLIP}}/\alpha_{\text{STICK}}$ is equal to one. Hu and Zwanzig's results are useful, however the formulation used is strictly inapplicable to molecular shapes other than spheroids. Youngren and Acrivos (92), using a curvilinear coordinate system, and dividing the surface of the particle up into individual elements obtain values for the friction coefficients of both prolate and oblate ellipsoids which agree well with those of Hu and Zwanzig. Youngren and Acrivos were also able to obtain a value of the frictional coefficient for benzene, using a molecular shape based on six hemispheres (hydrogen atoms) symmetrically attached to the side of an oblate ellipsoid.

The question has arisen as to why "stick" boundary conditions should be appropriate to the reorientation of macroscopic particles, while "slip" boundary conditions appear to be appropriate to molecular orientation. This question has been substantially answered by Zwanzig (93) in a study of rotational friction coefficients of a "bumpy cylinder" with both slip and stick boundary conditions. The effect of "bumps" or cusps in the surface of a particle are such that, in the neighbourhood of a cusp, very large fluid velocity gradients

occur, which cause a dissipation of energy, and the tangential flow along the surface is slowed down. In the limit of a large particle with a rough surface, stick and slip boundary conditions give the same result. Therefore the reason why a macroscopic particle appears to exhibit "stick" boundary conditions is because the surface of the particle is on a microscopic scale molecularly rough which through energy dissipation causes the slip boundary conditions to appear identical to stick conditions.

Energy dissipation therefore plays an important part in whether stick or slip boundary conditions are appropriate to particle orientation. For a molecule, the intermolecular potential as well as molecular shape plays a part in the determination of the frictional coefficients due to the fact that molecules neither have a well defined surface, nor are they rigid bodies. There is therefore a difficulty in assigning boundary conditions to a molecular surface. In the first paper to use a microscopic level approach Peralta-Fabi and Zwanzig (94) have attempted to overcome this difficulty. The interaction of the molecule with the fluid is described by an intermolecular potential rather than by imposing boundary conditions at a defined surface. Two simple interaction potentials were used, one being a ramp potential, the other a step potential. Only translational motion was investigated in this study, and the results showed that the hydrodynamic drag on the molecule resulted essentially from energy dissipation in the moving force field around the molecule, and that this drag could be calculated without imposing boundary conditions. The friction coefficient was a strong function of the strength of the potential used, approaching one as the potential approached infinity. This type of calculation of the friction coefficient probably represents the best method of obtaining

theoretical values of the molecular friction coefficients as it involves no assumptions about boundary conditions. However the models which were used are very simple, molecules being described by a spherical, either ramp or step, potential. Until this approach is further developed, the method of Youngren and Acrivos using slip boundary condition provides the best method of calculating the frictional constant α .

Equation 2.30 may be applied to correlation times from Raman scattering and NMR relaxation. τ_s is a single particle correlation time. The above equation has been applied to NMR relaxation times of some aromatic compounds in solution (71). Depolarised light scattering is however a coherent process, if there is angular correlation between adjacent molecules in the liquid, one measures a collective particle orientation (37). Recalling equation 2.5

$$\tau_{LS} = (g_2/j_2) \tau_s \quad 2.5$$

one obtains the Stokes Einstein relationship for depolarised light scattering

$$\tau_{LS} = (g_2/j_2) \left[\frac{\alpha p V n}{V T} + \tau_o \right] \quad 2.31$$

The factor (g_2/j_2) the orientational correlation parameter is often written as $\frac{1+fN}{1+gN}$ or simply as G or g. This equation and equations related to it have often been used as the basis for interpretation of correlation times obtained from depolarised light scattering.

Alms et al (72), (73), (74), (75) in a series of papers applied the Stokes Einstein relationship to light scattering data from molecules

in solution. In all cases the experiments were performed at a fixed temperature and so the T dependence in equation 2.31 was not investigated. A comparison was made of the correlation times obtained from depolarised light scattering with relaxation times obtained from NMR. The liquids examined generally were composed of small rigid molecules. In the first paper of the series Alms et al examined the liquids benzene, toluene and para xylene, in a variety of solvents. The reorientational times obtained versus solution viscosity fitted well to straight lines with non zero intercept. In all cases the values of the intercepts were positive, approximating to the free rotor time. The volumes obtained from the slope of the Stokes Einstein data plots were compared with molecular volumes and were found to be less than the molecular volumes. Alms et al noted that while for dilute solutions the reorientation times obtained were dependent only on solution viscosity, for concentrations close to the neat liquid, the reorientation times depended on solution concentration also. In (78) this was further investigated for the liquids chloroform and nitrobenzene. These liquids are examined in a range of solvents such that viscosity is kept constant, while solution concentration varies. The NMR times change, increasing by a small amount with increasing solution concentration, while the light scattering times increase by much more. This is interpreted in terms of orientational correlation in the neat liquid. Alms et al obtain values for $(1 + fN)$ and $(1 + gN)$, the static and dynamic orientation correlation parameters.

It is perhaps important to note the circumstances in which Alms et al were able to effect a separation of the static and dynamic correlation factors. Referring to equation 2.31 - in Alms et al experiments the temperature T was constant, the viscosity was varied by

varying solution concentration. The quantities unknown in 2.31 are

$$(g_2/j_2) \text{ or } \frac{1 + fN}{1 + gN}$$

α

pV

g_2/j_2 is a function of concentration

α is a function of the molecular "hydrodynamic" environment

and pV is a function of molecular shape.

pV is constant for small rigid molecules, α is variable with the liquid structure, and g_2/j_2 is the quantity which Alms et al are able to separate. This is due to the fact that with the reorientation times from the NMR one can independently evaluate α and pV .

In the case of flexible molecules pV is also dependent on solution concentration, the extra variable makes a separation of (g_2/j_2) for flexible molecules extremely unlikely without independent measurements of molecular correlation times.

Kivelson and Madden (35) in a review of depolarised light scattering discuss results obtained by Schroeder et al (75). Kivelson and Madden note the ratio τ_{LS}/τ_S varies slightly with (n/T) . The possible implication of this is that equation 2.5 is not valid for those parts of τ_{LS} and τ_S which are due to inertial contributions. This would mean that equation 2.31 is incorrect. A corrected form for this would be

$$\tau_{LS} = (g_2/j_2) \left(\frac{\alpha p V n}{K T} \right) + \tau_o$$

2.32

In most circumstances the differences between equation 2.31 and 2.32 are not important. τ_o is usually much smaller than the measured values of τ_{LS} , values of (g_2/j_2) are of the order of one. However for

systems in which τ_0 is comparable with the measured values of τ_{LS} the differences between the two equations can cause significant inconsistencies in the interpretation of the data.

Similar inconsistencies occur in the work of Lund, Whittenburg et al (77), (78), on solutions of pyridine in carbon tetrachloride, and pyridine in cyclohexane. These mixtures are of interest because of the strong intermolecular interaction which in both cases causes a strongly non linear viscosity concentration relation. Lund et al use a "viscosity scaling" technique to correct the reorientation time observed to the viscosity of the neat liquid. Briefly the viscosity scaling technique may be described by the relation

2.33

$$\tau_{LS} = \tau_{OBS} \eta_{PL} / \eta_{SOL}$$

τ_{LS} is the corrected light scattering time

τ_{OBS} is the experimentally observed scattering time

η_{PL} is the viscosity of the pure liquid

η_{SOL} is the viscosity of the solution

We believe that viscosity scaling should only be applied to the viscosity dependent part of τ_{LS} . If τ_0 is small compared to τ_{LS} then the inconsistencies introduced should be small. If τ_0 is comparable to τ_{LS} then the inconsistencies introduced are significant. This is perhaps born out by the same group's work on solutions of CS_2 in CCl_4 (79). For pyridine in carbon tetrachloride and in cyclohexane the values of τ_{LS} are linear in (η/T) . The lowest value of τ_{LS} in both cases was approximately 2.0 ps and τ_0 was approximately 0.68 ps. Whittenburg et al concluded that for pyridine $(g_2/j_2) = 1$.

For CS_2 in CCl_4 the lowest value of τ_{LS} obtained was approximately 1.4 ps and the value of τ_0 obtained was 0.9 ps. In this worst case of

the viscosity scaling technique Whittenburg et al find that (g_2/j_2) increases far more markedly with concentration than in the measurements of Cox et al (4) on CS_2 , in which Cox et al examine the behaviour of τ over a far larger range of value of n/T . In Cox's measurement the intercept τ_0 is found to be zero within the limits of experimental error, and we would suggest that the work of Cox et al on CS_2 represents the better measurement.

We conclude that the Stokes Einstein equation represents a compact method of relating correlation times obtained from light scattering experiments to the macroscopic viscosity of the liquid and that from Stokes Einstein fits to the data one can obtain useful information about the dynamics of molecular motion in the liquid state.

2.4 Molecular Correlation Times - Models and Computer Simulations

In the previous section the molecular reorientational correlation time was related to the linewidth of the Lorentzian component of the depolarised Rayleigh spectrum via a rotational diffusion coefficient.

Simply the relation outlined may be expressed

$$\frac{1}{2\pi f_{\frac{1}{2}}} \equiv \tau_{LS} = (g_2/j_2) \tau_S = (g_2/j_2) \frac{1}{60} \quad 2.34$$

All the symbols are as defined previously. The above relation ignores the question of whether (g_2/j_2) the orientational correlation parameter should be only a multiplier for the viscosity dependent part of τ_S .

The relationship between the single particle reorientational correlation time τ_S and the rotational diffusion coefficient is given by (ignoring inertial effects)

$$\tau_S = (1/60) \quad 2.35$$

This is only valid in limit of small rigid particles with a high symmetry.

Pecora's (1) original calculation of the spectral form of I_{VH} was for identical molecules of cylindrical symmetry undergoing independent rotational and translational diffusion with respective diffusion coefficients θ and D . For this case

$$\tau_s = 1/(K^2 D + 6\theta) \quad 2.36$$

K is the scattering vector

For small molecules $6\theta \gg DK^2$ and so the linewidth observed is independent of translational diffusion processes. The above equation is only valid for diffusion processes involving molecules of cylindrical symmetry. In the case of molecules with a lower symmetry the molecule undergoes diffusion processes about the different molecular axes each of which is characterised by a different rotational diffusion coefficient. The spectrum observed is a combination of a number of Lorentzians corresponding to the diffusion coefficients about the different axes, and the intensity of each Lorentzian is weighted according to the optical anisotropy about the appropriate reorientational axis. For an asymmetric molecule the spectrum decomposes into the sum of five Lorentzians (72). In most cases the linewidths of these are comparable and the individual components are not separable in the spectra. Alms et al (74) discuss the circumstances in which the various components are separable, the conclusion being that this is not possible unless the Lorentzian linewidths are significantly different, their intensities are comparable, and the signal to noise ratio is very high. There have been no light scattering measurements in which the individual Lorentzian components due to reorientation/translation about the different molecular axes have been separated. There have however

been a number of NMR relaxation experiments in which a successful separation of the individual reorientational components has been achieved (71).

Strictly speaking for asymmetric molecules an analysis of the light scattering data in which the reorientational part of the spectrum is assumed to be a single Lorentzian is inappropriate. For flexible asymmetric molecules the situation is yet more complicated.

Flexible molecules such as the n-alkanes may exist in a number of possible conformations. These are not individually stable and molecules constantly undergo transitions between the various conformations. The effect of this on the observed spectra is two-fold.

Each conformation has a characteristic reorientation time about its separate axes. The observed reorientational spectrum will be the sum of the (up to five) separate Lorentzians for each conformation each weighted according to the polarisability differences of each conformation about the rotational axis concerned. The optical anisotropy of the n-alkanes is a strong function of chain conformation, the observed spectrum is therefore strongly weighted to the conformation with the largest optical anisotropy, essentially that of the all trans chain.

This picture is further complicated by the fact that separate molecular conformations are not individually stable, and molecules constantly undergo transitions between them. If the transition time between the conformational states is longer than the characteristic reorientational time, one could theoretically at least analyse the spectra observed in terms of contributions from individual conformations. If the transition time is of the order of, or less than the reorientational time one could analyse the spectra observed in terms of the reorientation of a molecule in an average conformational state.

The transition rate between conformations is of great importance to the spectra observed. A conformational change is equivalent to a partial reorientation of the molecule. Also conformational changes are related to collisional processes in the liquid.

If the time scale of the conformational changes is comparable to molecular reorientation times one introduces problems into the spectral analysis. Extra features would appear essentially as a result of coupling between reorientation, and conformational changes. Also due to the relationship between conformational changes, and collisional processes one would expect features to appear in the spectra associated with coupling between rotational and collisional processes.

Therefore a knowledge of the dynamics of chain molecules is required before one can obtain a complete understanding of the depolarised light scattering spectra of the n-alkanes.

There have been a large number of simulations of the n-alkanes. These molecules have been simulated by Monte Carlo methods (MC), molecular dynamics simulations (MD) and Brownian dynamics simulations (BD). The first simulations were using Monte Carlo techniques, however the only information obtained are static properties although some dynamic information may be derived from the static properties.

Molecular dynamics simulations represent a more direct method of obtaining information about the dynamic properties of chain molecules. Generally molecules are described as consisting of a number of individual masses connected by bonds of a fixed length and with a bond-bond angle of $109^{\circ} 28'$ (the tetrahedral bond angle). Individual bonds are free to rotate, however there is a potential energy function associated with the dihedral angle which describes the bond angle with respect to adjacent bonds. In most cases the hydrogen atoms are not included explicitly. In the simulations, a number of molecules of the

order of one hundred are set in a volume (such that the number density is equal to that in the thermodynamic state being simulated). The boundary conditions of the box are periodic such that a molecule leaving the top of the box is replaced by one, entering at the bottom of the box, having an identical conformation and velocity. The interactions between individual molecules, and individual mass points in adjacent molecules are described by Lennard Jones potentials. To save computer time these potentials are generally truncated. This limits the number of molecules which a single molecule is interacting with at any time.

From molecular dynamics experiments one obtains a variety of thermodynamic information such as pair distribution functions, trans gauche ratios, and internal chain relaxation times. In molecular dynamics simulations one can also study the effect of introducing a solvent into an n-alkane liquid, by replacing some of the n-alkane molecules in the simulation with appropriately modelled solvent molecules.

There are a number of problems associated with molecular dynamics simulations, perhaps not the least being that in order to perform the simulation one makes a large number of simplifications concerning molecular structure and intermolecular and interatomic forces. Even with these simplifications the computer time used presents limitations to the work.

Brownian dynamics has been used to circumvent the latter limitation. In Brownian dynamics one considers a single molecule in vacuo. The influence of neighbouring molecules is simulated by describing analytically a potential of mean force which gives the average molecular interaction with its surroundings. A further approximation is to introduce into the simulation a randomly

fluctuating force having stochastic properties which mimics the fluctuating molecular environment.

These are the basic simulation techniques which have been used for the n-alkanes. We now discuss results from a number of simulations and the limitations of those results.

Chandler et al (80), (81) examine using a statistical mechanical theory the effects of liquid structure on molecular conformation of n-butane in solution in carbon tetrachloride and in neat n-butane. These calculations are essentially Monte Carlo calculations. The results indicate that in going from the gaseous state to the liquid state there is a displacement in the trans gauche equilibrium constant towards an increased concentration of gauche states. Chandler et al also analyse n-butane dissolved in n-hexane. It is of interest to note that the number density of n-hexane molecules given as being used in the calculation is approximately one order of magnitude greater than that for the liquid state at room temperature. No dynamic information was given in these papers.

Chandler and other co-workers (82) examined essentially the same problem using molecular dynamics simulations. There is qualitative agreement between the "exact" molecular dynamics results and the statistical mechanical results, however the solvent shift (in the trans gauche ratio) appears to be overestimated in the "approximate" theory.

Ryckaert and Bellemans (83) performed molecular dynamics simulations of the liquid alkanes n-butane, and n-decane. The simulations cover time periods of between ten and twenty picoseconds. Again the trans gauche ratio decreases in going from the gas to the neat liquid. Of importance for interpretation of spectra is that for n-decane (at 480 °K) the average time between conformational changes is approximately 2 ps, (for a single bond). The average time between

conformational changes in the n-decane molecule (nine bonds) is therefore ~ 0.3 ps.

Weber (84) performed molecular dynamics calculations on a n-octane fluid using a realistic model potential incorporating bond stretch, bend and rotation terms and Lennard Jones fluid interactions. Weber obtains rotational diffusion coefficients for the middle bond vector of 0.28 p sec^{-1} at 300°K and 0.57 p sec^{-1} at 600°K . This implies reorientational frequencies (of the middle bond vector) of 270 GHz and 545 GHz at 300°K and 600°K respectively. However Weber does not discuss how the rotational diffusion coefficient obtained for the middle bond vector relates to that for the whole molecule.

Evans and Knauss in a series of papers (85), (86), (87) simulated n-alkane chains using a variety of techniques. Two of the papers deal with a torsional dynamics simulation using models for the torsional characteristics of the chain which are extensions of the rotational isomeric model of Flory. The results obtained from these simulations are compared with results from a Brownian dynamics simulation. The n-alkanes examined were liquids from n-butane to n-undecane and the results obtained were orientational correlation times for first and second rank harmonics for the different possible modes of molecular motion.

A significant point about the results is that in changing from one model of torsional motion to another, the values of the correlation times obtained change significantly. Also changing the values of the torsional potentials significantly changes the correlation times. When the results obtained are so sensitive to the form and detail of so many of the parameters involved in the simulations, one has to be confident that the input data selected for the simulation is of a sufficiently high quality, before one can have any faith in the results of the simulation.

Evans and Knauss identify the $Q = 1$ mode, first harmonic correlation time as that closest to the overall molecular orientation time. The calculation of this was performed for a number of potentials, for a number of molecules. They choose the $\beta U = 5$ potential as being most appropriate, and obtain values for this by interpolation between results obtained for $\beta U = 0, 4, 8$ and ∞ (rigid body) and compare correlation times calculated with those obtained experimentally for the 1-bromoalkanes and find reasonable agreement.

In Section 5.2 Evans and Knauss's results are discussed in more detail and a comparison is made with our experimental results from depolarised light scattering.

Chandler et al (7) in a stochastic dynamics study examine how conformational transition rates depend on the intermolecular collisional frequency. The range of intermolecular collisional rates studied vary from $0.1 \times 10^{13} \text{ sec}^{-1}$ to $32 \times 10^{13} \text{ sec}^{-1}$. A comparison of results obtained for different collisional rates, with results from molecular dynamics calculations gives best agreement with a collisional rate of $0.2 \times 10^{13} \text{ sec}^{-1}$. The average time between trans gauche transitions for butane is calculated to be 23 ps, a time approximately ten times longer than that obtained for decane by Ryckaert and Bellemans.

Gunsteren et al (88) review the technique of Brownian dynamics simulation and show how constraints can be incorporated into the simulation producing a variety of stochastic dynamics models. Gunsteren et al compare the results of their Brownian dynamics simulations with the molecular dynamics simulations of Ryckaert and Bellemans. Exactly the same model is used in both cases for the description of the n-alkane chain. The Brownian dynamics simulation essentially gives the same results as the molecular dynamics

simulation. For butane the average time in a trans or gauche state is calculated to be of the order of 15 ps, while for decane the time is calculated to be of the order of 3 ps. In analysing the conformational transitions a correlation between successive transitions is observed which Gunsteren et al interpret as being due to persistence of angular momentum after a transition.

The various simulations may be summarised in the following manner. If the simulation is carried out with well conditioned algorithms and good quality starting data then useful dynamic information can be obtained. However in reviewing a large number of papers on simulations one can not help but feel that the various "simulators" perform "experiments" for different models and potentials and then select a posteriori as the best model that which produces models which are as consistent as possible with results of previous simulations. My personal view is that there is a disinclination on the behalf of the "simulators" to relate events in the physical world outside the computer to the simulated events inside the computer. One cannot help but doubt the validity of the results of some of the simulations in which the "simulators" have not attempted a comparison of the results with physical reality.

From the simulations a value of the average collisional rate for the n-alkane would be $\omega_{COLL} = 0.2 \times 10^{13} \text{ sec}^{-1}$ and an average time between conformational changes would be

for n-decane $\tau_{t-g} = 1 - 4 \text{ ps}$

and for n-butane $\tau_{t-g} = 10 - 30 \text{ ps}$.

The relationship between these time scales and frequencies, and the observed reorientational times has some bearing on the interpretation of the spectra in that if there is no time scale separation between collisional and rotational motion, one may observe extra

features in the spectra due to rotational-collisional coupling.

For anisotropic molecules one observes the Lorentzian feature due to overall molecular reorientation. For isotropic molecules Madden (89) calculated the depolarised Rayleigh spectrum. Scattering is by pairs of density fluctuations and the central region of the spectrum is Lorentzian with a linewidth given by

$$f_{\frac{1}{2}} \propto 2DK_{\sigma}^2$$

2.37

D is the translational self diffusion coefficient

K_{σ} is the magnitude of the scattering vector at the maximum in the centre of the mass structure factor.

This translational diffusion central Lorentzian is present in spectra for all liquids, however for most liquids it is masked out by the reorientational diffusion component due to the intrinsic molecular anisotropy. Patterson and Carroll (90) reasoned that for small alkanes, that as the intrinsic molecular anisotropy decreases with decreasing molecular size, and increasing branching, the Lorentzian component of the spectra may be due to interaction induced effects and the characteristic time determined by translational diffusion.

The translational self diffusion coefficients were determined by the NMR spin echo method, K_{σ} was determined by X-ray scattering. Patterson and Carroll's results indicate that for the n-alkanes the spectra are due to rotational diffusion, and the source of the scattering is the intrinsic molecular anisotropy. For the highly branched alkanes the results are more open to interpretation but translational diffusion and scattering from intermolecular pair anisotropy is a distinct possibility.

2.5 References for Chapter 2

- (1) R Pecora, 1968, J Chem Phys 49, 1036.
- (2) M A Leontovich, 1941, Izv Akad Nauk SSR Ser Fiz 5, 148, (J Phys USSR, 1941, 4, 499).
- (3) J A Bucaro and T A Litovitz, 1971, J Chem Phys 54, 9, 3846.
- (4) T I Cox, M R Battaglia, P A Madden, 1979, Mol Phys 38: 1539.
- (5) B Frenkel and J P McTague, 1980, J Chem Phys 72, 4, 2801.
- (6) J V Champion and D A Jackson, 1976, Mol Phys 31: 1169.
- (7) J A Montgomery, S L Holmgren, D Chandler, 1980, J Chem Phys 73, 8, 3688.
- (8) A Einstein, 1910, Ann Physik 33, 1275.
- (9) Smoluchowski, 1908, Ann Physik 25, 205.
- (10) Cabannes, 1929, La Diffusion Moléculaire de la Lumière, Les Presses Universitaires de France.
- (11) Coumou, Mackor, Hilmans, 1964, Trans Far Soc 60, 1539.
- (12) Coumou, Hilmans, Mackor, 1964, Trans Far Soc 60, 2, 2244.
- (13) Coumou, 1969, Trans Far Soc 65, 10, 562.
- (14) Kielich, 1960, Acta Physica Polonica, XIX FASC 2, 149.
- (15) Kielich, 1967, J Chem Phys, 46, 10, 4090.
- (16) Kielich, 1968, Acta Physica Polonica, XXXIII FASC 1, 63.

- (17) Dezelic, 1966, J Chem Phys 45, 1, 185.
- (18) Malmberg and Lippincott, 1968, J Coll Interf Science 27, 8, 591.
- (19) L Onsager, 1936, J Am Chem Soc 58, 1486.
- (20) T Scholte, 1949, Physica 15, 437.
- (21) C Clement and P Bothorel, 1964, J Chimie Phys 61, 877.
- (22) P Bothorel, Such, Clement, 1972, J Chimie Phys 10, 1453.
- (23) Bothorel, Fourche, 1973, JCS, Faraday II 69, 441.
- (24) Patterson, Flory, 1972, JCS Faraday II 68, 1098.
- (25) J V Champion, Meeten, Southwell, 1975, JCS Faraday II 71, 225.
- (26) Patterson, Kennedy, Latham, 1977, Macromolecules 10, 667.
- (27) Fourche, Lemaire, 1971, J Chimie Phys 68, 7-8, 1170.
- (28) J T Bendler, 1977, Macromolecules 10, 162.
- (29) Jernigan, Flory, 1967, J Chem Phys 47, 6, 1999.
- (30) Clement, 1978, J Chimie Phys 75, 7-8, 747.
- (31) Brown, Maguire, Swinton, 1979, Far Disc 66/18.
- (32) Champion, Dandridge, Meeten, 1978, Far Disc 66, 266.
- (33) Fischer, Stroble, Dettenmaier, Stamm, Steidle, 1979, JCS Faraday II 295.
- (34) B J Berne and R Pecora, 1976, "Dynamic Light Scattering", Wiley, New York.

- (35) D Kivelson and P A Madden, 1980, Ann Review Phys Chem 523.
- (36) G C Tabisz, 1979, Mol Spectroscopy 6, Chem Soc 136.
- (37) T Keyes and D Kivelson, 1972, J Chem Phys 56, 1057.
- (38) S M Rytov, 1958, Zh Eksp Teor Fiz (Sov Phys JETP) 6, 401.
- (39) H Mori, 1965, Prog Theor Phys, Kyoto 33, 423.
- (40) T Keyes and D Kivelson, 1972, J Chem Phys 56, 1876.
- (41) T Keyes and D Kivelson, 1971, J Chem Phys 54, 1786.
- (42) Alms, Bauer, Brauman, Pecora, 1973, J Chem Phys 59, 5304.
- (43) H C Anderson and R Pecora, 1971, J Chem Phys 54, 2584.
- (44) Shyr-Jin Tsay and D Kivelson, 1975, Mol Phys 29, 1-27.
- (45) G Searby, P Bezot and P Sixou, 1977, Faraday Symposium II, 63.
- (46) P Bezot, G M Searby and P Sixou, 1975, J Chem Phys 30, 1149.
- (47) G D Enright and B P Stoicheff, 1976, J Chem Phys 64, 9, 3658.
- (48) P J Chappell, M P Allen, R I Hallem and D Kivelson, 1981, J Chem Phys 74, 11, 5929.
- (49) M P Allen, P J Chappell and D Kivelson, 1981, J Chem Phys 74, 11, 5942.
- (50) D Kivelson, T Keyes and J Champion, 1976, Mol Phys 31, 1, 221.
- (51) J V Champion and D A Jackson, 1976, Mol Phys 31, 4, 1169.
- (52) D Kivelson and R Hallem, 1979, Mol Phys 38, 5, 1411.

- (53) A Peterlin and H Stuart, 1939, Z Phys 112, 1.
- (54) G B Jeffrey, 1922, Proc R Soc A 102, 161.
- (55) G R Alms and G D Patterson, 1978, J Coll Interf Sci 63, 2, 184.
- (56) W Lempert and C H Wang, 1980, J Chem Phys 72, 6, 3490.
- (57) G L A Stegemann and B P Stoicheff, 1973, Phys Rev A 7, 3, 1160.
- (58) H C Lucas and D A Jackson, 1971, Mol Phys 20, 801.
- (60) J Rouch, J P Chabrat, L Letamendia and C Vaucamps, 1975, J Chem Phys 63, 4, 1383.
- (61) G Enright and B P Stoicheff, 1974, J Chem Phys 60, 6, 2536.
- (62) T Keyes, D Kivelson and J P McTague, 1971, J Chem Phys 55, 8, 4096.
- (63) G D Patterson and P J Flory, 1972, JCS Faraday II 68, 1098.
- (64) W M Gelbart, 1974, Advances Chem Phys XXVI 1.
- (65) H B Levine and G Birnbaum, 1968, Phys Rev Lett 20, 439.
- (66) M Thibeau and B Oksengorn, 1968, Mol Phys 15, 6, 579.
- (67) M Berard and P Lallemand, 1977, Mol Phys 34, 251.
- (68) Hyung Kyu Shin, 1972, J Chem Phys 56, 6, 2617.
- (69) P A Madden and T I Cox, 1981, Mol Phys 43, 2, 287.
- (70) F Perrin, 1934, J Phys Radium 5, 33; 1936 J Phys Radium 7, 1.
- (71) D R Bauer, G R Alms, J I Brauman and R Pecora, 1974, J Chem Phys 61, 6, 2255.

- (72) G R Alms, D R Bauer, J I Brauman and R Pecora, 1973, J Chem Phys 58, 12, 5570.
- (73) G R Alms, D R Bauer, J I Brauman and R Pecora, 1973, J Chem Phys 59, 10, 5310.
- (74) G R Alms, D R Bauer, J I Brauman and R Pecora, 1973, J Chem Phys 59, 10, 5321.
- (75) D R Bauer, J I Brauman and R Pecora, 1975, J Chem Phys 63, 1, 53.
- (76) J Schroeder, V H Schiemann and J Jonas, 1978, J Chem Phys 69, 5479.
- (77) P A Lund, S L Whittenburg, C H Wang, D H Christensen, 1979, Mol Phys 37, 3, 749.
- (78) S L Whittenburg, D R Jones, D H Christensen, C H Wang, 1979, J Chem Phys 70, 4, 2035.
- (79) Y Higashigaki, S L Whittenburg, C H Wang, 1978, J Chem Phys 69, 7, 3297.
- (80) L R Pratt, C S Hsu and D Chandler, 1978, J Chem Phys 68, 9, 4202.
- (81) C S Hsu, L R Pratt and D Chandler, 1978, J Chem Phys 68, 9, 4213.
- (82) D W Rebertus, B J Berne and D Chandler, 1979, J Chem Phys 70, 7, 3395.
- (83) J P Ryckaert and A Bellemans, 1978, Faraday Disc 66/5.
- (84) T A Weber, 1979, J Chem Phys 70, 9, 4277.
- (85) G T Evans and D C Knauss, 1979, J Chem Phys 71, 5, 2255.

- (86) D C Knauss and G T Evans, 1980, J Chem Phys 72, 3, 1499.
- (87) G T Evans and D C Knauss, 1980, J Chem Phys 72, 3, 1504.
- (88) W F van Gunsteren, H J C Berendsen and J A C Rullman, 1981,
Mol Phys 44, 1, 69.
- (89) P A Madden, 1978, Mol Phys 36, 365.
- (90) G D Patterson and P J Carroll, 1982, J Chem Phys 76, 9, 4356.
- (91) C M Hu and R Zwanzig, 1974, J Chem Phys 60, 11, 4354.
- (92) G K Youngren and A Acrivos, 1975, J Chem Phys 63, 9, 3846.
- (93) R Zwanzig, 1978, J Chem Phys 68, 9, 4327.
- (94) R Peralta-Fabi and R Zwanzig, 1979, J Chem Phys 70, 1, 504.

CHAPTER 3 EXPERIMENTAL WORK

3.1 Introduction

The experimental work presented in this chapter was performed at two separate laboratories. At Cambridge in the University Chemistry laboratories the depolarised Rayleigh spectra of several n-alkanes were recorded out to 200 cm^{-1} (6000 GHz) using a Coderg double grating monochromator and subsequently computer analysed.

The Fabry Perot spectrometer at the City of London Polytechnic was used to examine the fine structure of the central, approximately Lorentzian component of the depolarised Rayleigh spectrum and for determining the linewidth of spectra which have a half width of less than 0.2 cm^{-1} (6 GHz). The double grating monochromator was used to determine linewidths of spectra which are greater than about 2 cm^{-1} (60 GHz) and to determine the collision induced contribution to the depolarised light scattering.

In the monochromator spectra the collision induced contribution is seen as an exponential background. In the Fabry Perot spectra it is seen as a flat background the value of which is made uncertain by the contribution of overlapping spectra. The tails of all the Lorentzians also make a contribution to the spectral background as well as the overlapping exponential for wings. The accuracy for determining an appropriate correction for this is limited.

3.2 Description of the Fabry Perot Spectrometer

Measurements were made of the depolarised (VH) spectra using a piezoelectrically scanned Fabry Perot etalon. The spectra were recorded using a photon counting system and the first three digits from the output of the photon counting system were passed in an analogue form into a transient recorder with a resolution of one part in 256. The transient recorder has a store of 1024 channels in which

the spectra are recorded as the Fabry Perot is scanned using a staircase voltage ramp applied to the scanning pads. At the end of the Fabry Perot scan the transient recorder is triggered and the information is retained in the recorder. The spectrum so obtained is displayed on an oscilloscope and then punched out onto paper tape. The data on the paper tape is subsequently computer analysed using a fitting procedure.

The liquids which were examined were the n-alkanes from pentane to pentadecane, solutions of the n-alkanes, octane, decane and pentadecane in CCl_4 and several of the n-alcohols from n-propan-1-ol to n-undecan-1-ol.

The optical anisotropy of the alkanes and alcohols is very low compared to other liquids commonly examined (eg. benzene = $43.6 \times 10^{-48} \text{ cm}^6$ compared to octane = $3.68 \times 10^{-48} \text{ cm}^6$). The intensity of the depolarised scattering is proportional to the mean squared optical anisotropy and hence the low optical anisotropy of the n-alkanes leads to a poor signal to noise ratio.

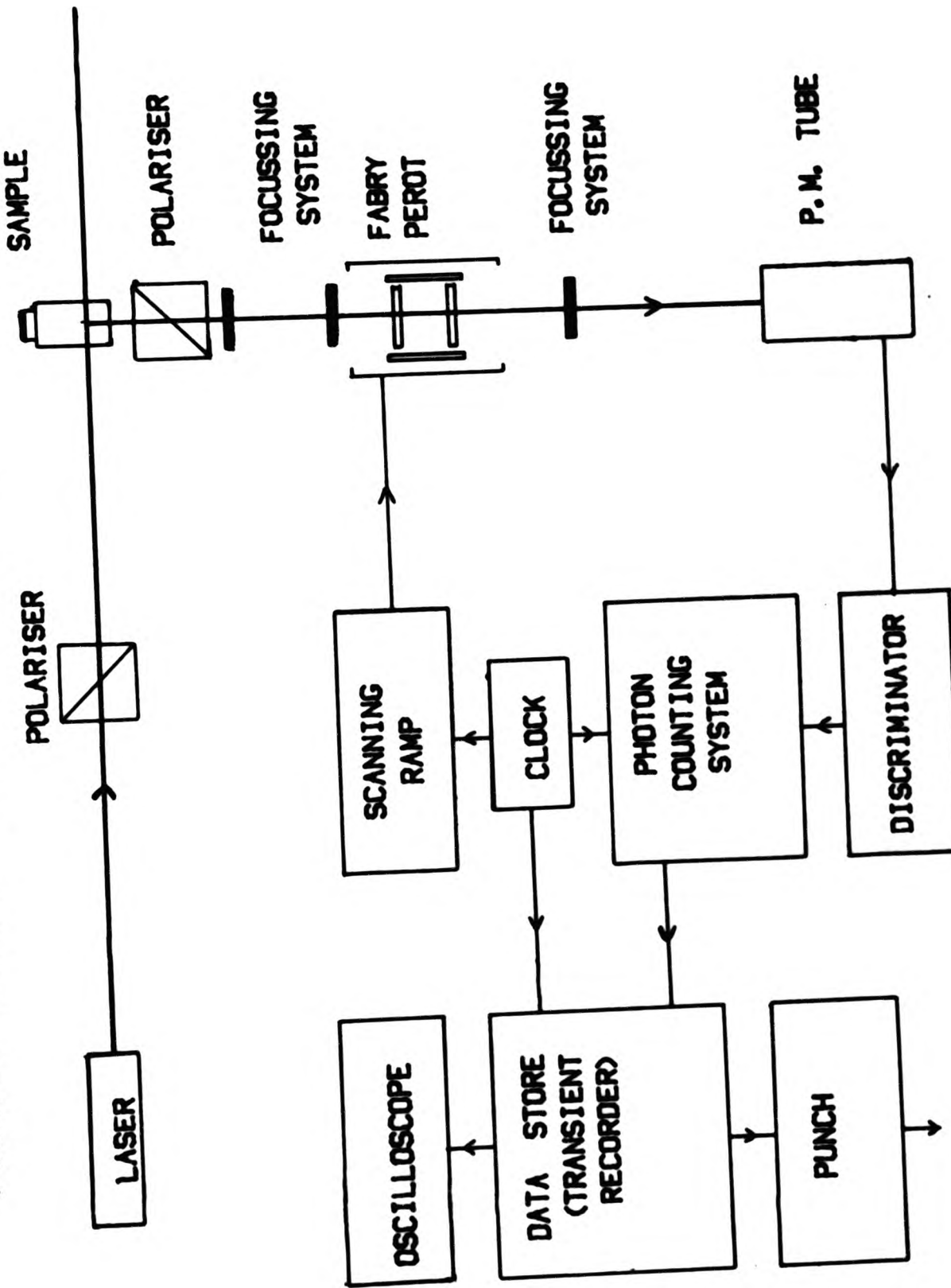
To obtain good quality spectra we use plates in the Fabry Perot with coatings of 93.5% reflectivity. This allows a considerable light throughput whilst limiting the maximum finesse to 47. The choice is made so as to obtain spectra in which the statistical noise is kept as low as possible, and the scanning time is shorter than the time it takes the etalon to go out of adjustment due to thermal fluctuations and random vibrations (typically 30 minutes). Scanning times varied between three and thirty minutes.

The sample cells are held in a thermostated metal block in which the temperature is stable to about 0.2°C in the range 20°C to 100°C .

The light source was a Spectra Physics 165 Argon Ion laser operating in single mode at a wavelength of 514.5 nm. The power of the

FABRY PEROT SPECTROMETER

fig 3.1



collimated beam passing through the sample was < 300 mW for the work on the n-alkanes.

For the measurements on solutions and on the n-alcohols laser powers up to 500 mW were used. All measurements were made at a fixed scattering angle of 90°.

The 9789 B photomultiplier tube used had an extremely low dark count of about 1 sec^{-1} at a voltage of 1140 V. The Fabry Perot etalon was adjusted so that its free spectral range was between five and twelve times the half width of the depolarised spectrum being examined. Before a spectrum is recorded the liquid sample was replaced with a sample of a colloid which relative to the n-alkanes and alcohols has a very narrow depolarised Rayleigh spectrum.

With the Fabry Perot scanning continuously the etalon adjusting pads are used to obtain a narrow as possible peak corresponding to the depolarised Rayleigh spectrum of the colloid. From this the etalon finesse may be measured.

The colloid is removed and the depolarised spectrum of the liquid is then recorded.

The etalon finesse is remeasured using the colloid sample and the finesse during the scan is assumed to be the average of the two finesses measured (provided the etalon finesse has not dropped as low as 25 during the scan when the spectrum is rejected).

A diagram is given of the experimental arrangement, Fig 3.1.

For the liquids which scattered the least light (the lower n-alcohols and the lowest concentration alkane solutions) extra care was taken to minimise the parasitic scattered light (from cell walls and optics) entering the spectrometer by introducing and placing baffles.

Fitting Procedure for Spectral Shape

The data output is a set of 1024 numbers corresponding to the channels in the store of the transient recorder. To scale the width of the peaks observed to the free spectral range of the etalon it is necessary to have two orders in the spectrum. The scanning of the etalon is generally non-linear and so the scanning voltage is set to cover between two and three orders so that the fitting routine can adequately take account of the non-linearity of the scan from the peak shape.

The program first locates the peak positions as a function of channel number. The program is given starting guesses for the peak half width in terms of the number of channels, the separation of the peaks, the linearity of the scan, the shift of the central peak from the edge of the data file, the height of the peaks and the height of the background observed. The program then produces a spectrum from the starting guesses which it compares to the experimentally observed spectrum and generates an error function which corresponds to the sum of the squared differences between the observed spectrum and that calculated from the starting guesses. The program then uses a minimisation routine to adjust the parameters to the fit selectively so as to minimise the error function.

Initially the program assumes that the peaks are Lorentzian in form (which is a good approximation in the low viscosity case when the shear wave dip is narrow compared to the main structure). The parameters obtained from this fit are the peak half width, background, peak height, separation, linearity and shift.

For liquids with higher viscosities it is necessary to fit the data to a more complicated spectral form. The form chosen is that of the second equation of Keyes and Kivelson, (1) and an approximation often used to describe it is that the spectrum is of the form of a

positive Lorenzian which is accompanied by a dip which is a negative Lorenzian. The depth of the dip is related to a coupling parameter R which gives a measure of coupling between molecular orientation and shear waves in the body of the liquid. The half width of the dip is given by $K^2 n/p$ where K is the scattering vector. The fitting procedure gives fits to Keyes and Kivelson's equation, not to the approximation.

For the fit to "Lorentzian with dip" or "Double Lorenzian" the program is adjusted so as to perform initially a single Lorenzian fit and then holding the obtained parameters of separation, shift and linearity (which are characteristics of the scan and not of the spectrum) constant the program performs a fit to Lorentzian with dip in which the parameters peak half width, background, peak height, dip half width and coupling parameter R are adjusted and obtained from the best fit.

A third option is also available in the fitting procedure. As well as fitting the spectra to the Lorentzian with dip and obtaining from the fit values of $K^2 n/p$ and R it is also possible to input into the program the measured values of $K^2 n/p$. A comparison of the R values obtained by the two separate methods may be made.

For the n-alcohols the spectra have a low signal to noise ratio compared with the spectra for the corresponding n-alkane. A n-alcohol has about the same optical anisotropy as the corresponding n-alkane and so scatters approximately the same amount of light but because of the higher viscosity the n-alcohol molecules move more slowly in the liquid than the n-alkane. The n-alcohol spectra are much narrower and an appropriate free spectral range for the etalon is much smaller.

Hence in the collection optics used for the alcohols the final pinhole at the photomultiplier tube is smaller than that for the n-alkanes and generally the noise level on the data obtained is greater

than that for alkanes.

Results from Fitting Procedures

The computed observed values of peak and dip half width and separation are given in terms of number of channels. They can be converted into frequency units by scaling them to the peak separation and multiplying the result by the etalon free spectral range.

These widths obtained are not the actual widths of the spectra, as the observed spectrum is the convolution of the true spectrum with the instrumental function. In using the double grating spectrometer a deconvolution of the spectrum may readily be performed as the shape of the instrumental function is constant and determinable over the complete spectrum. With the Fabry Perot system this is not the case.

The form of the instrumental function of Fabry Perot interferometers is a Voigt function (2) (a mixture of Gaussian and Lorentzian forms) for a fixed spacing interferometer, pressure scanned and once adjusted, stable for time periods of the order of a month.

Our Fabry Perot system has an adjustable spacing, is piezo-electrically scanned and is stable for periods of the order of an hour, hence a variable instrument function exists in practice.

For simplicity in the deconvolution procedure we assume an instrumental function which is Lorentzian. The width of this Lorentzian may be measured by determining the width of the spectrum of the depolarised light scattered by a colloid solution. The ratio of the free spectral range to this instrumental width is called the finesse of the etalon.

$$\text{FINESSE} = \frac{\text{FREE SPECTRAL RANGE}}{\text{INSTRUMENTAL WIDTH}}$$

Convoluting the real spectrum (Lorentzian) with the instrumental function (Lorentzian) produces an observed spectrum (Lorentzian). The

relationship between the half widths is given by (3).

$$\text{Real PKHW} + \frac{1}{2}\text{IW} = \text{PKHW}_{\text{OBSERVED}}$$

$$\therefore \text{Real PKHW} = \text{PKHW}_{\text{OBSERVED}} - \frac{1}{2}\text{IW}$$

3.1

where $\frac{1}{2}\text{IW}$ is the instrumental half width.

This simple deconvolution procedure is valid for Lorentzian spectra and Lorentzian instrumental functions, only when the half widths are not comparable. The same simple deconvolution procedure is applied to the dip half width, as it approximates to a negative Lorentzian form. The real dip half width is given by the observed half width minus the instrumental half width.

The value of the R parameter which is obtained in the spectral fit is also deconvoluted by making the assumption that with the negative Lorentzian approximation the intensity observed in the dip with the spectrum undeconvoluted is equal to the intensity observed in the dip with the spectrum deconvoluted. As the depth of the dip is proportional to the R parameter this simple approach leads to the conclusion that

$$R = R_{\text{MEASURED}} \times \frac{\text{DIPH}_{\text{OBSERVED}}}{(\text{DIPH}_{\text{OBSERVED}} - \frac{1}{2}\text{IW})}$$

3.2

Calculations of the Relative Intensities of the Collisional Background
and the Intrinsic Scattering

The depolarised light scattering results from an optical anisotropy which results from at least two separate sources. One depends on intrinsic molecular anisotropy which is related to the molecular structure. The time dependent behaviour of this anisotropy is dependent on fairly slow molecular rotation processes and so the

spectrum of the light scattered is the low frequency part of the spectrum and is the central Lorentzian component.

The other molecular anisotropy is produced by Dipole Induced Dipole (DID) processes and its time evolving properties are governed by fast collisional processes in the liquids. The light scattered appears as an approximately exponential high frequency wing. In the spectra from the Fabry Perot this appears as a flat background.

An attempt is made to make a separation of these two components in the data from the Fabry Perot.

Each spectrum consists of a single Lorentzian sitting on broad exponential wings. In the Fabry Perot system these spectra overlap and the broad exponential background is smeared out to give a flat background. As the number of central Lorentzians and backgrounds are the same the integrated intensity of the exponential background is simply given by the intensity of the observed flat background which sits under a single Lorentzian. In terms of the output from the computer

$$I_{BACKGROUND} = I_{COLLISIONAL} = SEPN \times BASE \quad 3.3$$

The intensity of the slow contribution which is given by the central Lorentzian is an easy matter to calculate. The intensity of a Lorentzian is given by $\pi \times \text{amplitude} \times \text{half width}$. Thus

$$I_{LOR} = I_{SLOW} = \pi \times FHT \times PKHW \quad 3.4$$

Using these values it is possible to estimate the ν parameter defined as the fraction of the total light scattered which is due to the intrinsic molecular anisotropy.

In terms of I_{SLOW} and $I_{COLLISIONAL}$ it is given by

$$\nu = \frac{I_{SLOW}}{I_{SLOW} + I_{COLLISIONAL}}$$

2.12

The ν parameters obtained for various liquids were not reproducible to better than 20% or more, mainly due to the problems of overlapping spectra and fluorescence in the samples. One possible reason for the inconsistencies in the results lies in the fitting procedure. The program makes allowance for the contribution to the background from the tails of two Lorentzians on either side of the central peak observed. As the program does not take into account the much larger number of Lorentzians the background calculated by the fitting procedure is larger than the real background by an amount determined by the tails of these Lorentzians. The larger the ratio peak half width/peak separation the greater the correction required to the background.

CORRECTIONS

The correction to the background may be calculated in two ways. We can sum up the contributions at the central Lorentzian of the third, fourth and fifth Lorentzians and so on out to a point where the contributions from the Lorentzians become negligible. As there are orders on both sides of the central Lorentzian the total contribution is twice the sum of contributions from Lorentzians from three outwards.

If the peak half width is represented by p , separation by S and the full height is represented by F the magnitude of the intensity contribution at the central Lorentzian due to the n^{th} order away is given by

$$A_n = \frac{F}{1 + \left(\frac{nS}{p}\right)^2}$$

The total contribution to the intensity is given by twice the sum of this quantity for Lorentzians from three out to infinity.

This can be written as

$$A_{\text{TOTAL (LORENTZIAN)}} = \frac{2}{\text{BACKGROUND}} \sum_{n=3}^{\infty} \frac{F}{1 + \left(\frac{nS}{p}\right)^2}$$

Hence we calculate A_{TOTAL}/F , the ratio of the height of the contribution to the background from the Lorentzians to the full height of the Lorentzian for different values of the ratio S/p (the ratio of the separation of the orders to the peak half width). Using tables of these values gives a correction to the value of the baseline background obtained by the fitting procedure. For the particular value of p/S obtained by the fitting procedure the value of A_{TOTAL}/F is found from tables. As F is also obtained from the fit A_{TOTAL} , the amount of background which corresponds to the tails of far Lorentzians is calculated and a correction is obtained for the base.

An alternative method of calculating the correction may be performed. The fitting program takes into account contributions from the neighbouring four orders (two orders either side) which is equivalent to ignoring the intensity contribution to the background from the Lorentzian component at two orders out. This may be expressed as

$$I_{\text{BACK(CORRECTION)}} = \frac{2}{2S} \int_{-\infty}^{\infty} \frac{F}{1 + \left(\frac{\omega}{p}\right)^2} d\omega$$

$$\therefore I_{\text{BACK(CORRECTION)}} = Fp\left(\pi - 2 \tan^{-1}\left(\frac{2S}{p}\right)\right)$$

The two methods give different values for the correction factor A_{TOTAL} . The relationship between $I_{\text{BACK(CORRECTION)}}$ and A_{TOTAL} is simply

$$I_{\text{BC}} = S A_{\text{TOTAL}}$$

The correction factor for the second method is 20% higher than that given by the first method at S/p = 2 and at S/p = 20 the correction for the second method is 40% higher.

Even with these corrections the values of the ν parameter obtained are subject to a large scatter and appear to vary from sample to sample of the same liquid. A possible reason is a contribution to the background from fluorescence in the sample, the magnitude of which varies from sample to sample. It is not possible to separate the fluorescence contribution from the collisional contribution to the spectra in the Fabry Perot.

In experiments using the double grating monochromator it is possible to make a separation of the fluorescence induced background and the interaction induced background because of the functional form of the different backgrounds and the different frequencies at which they occur.

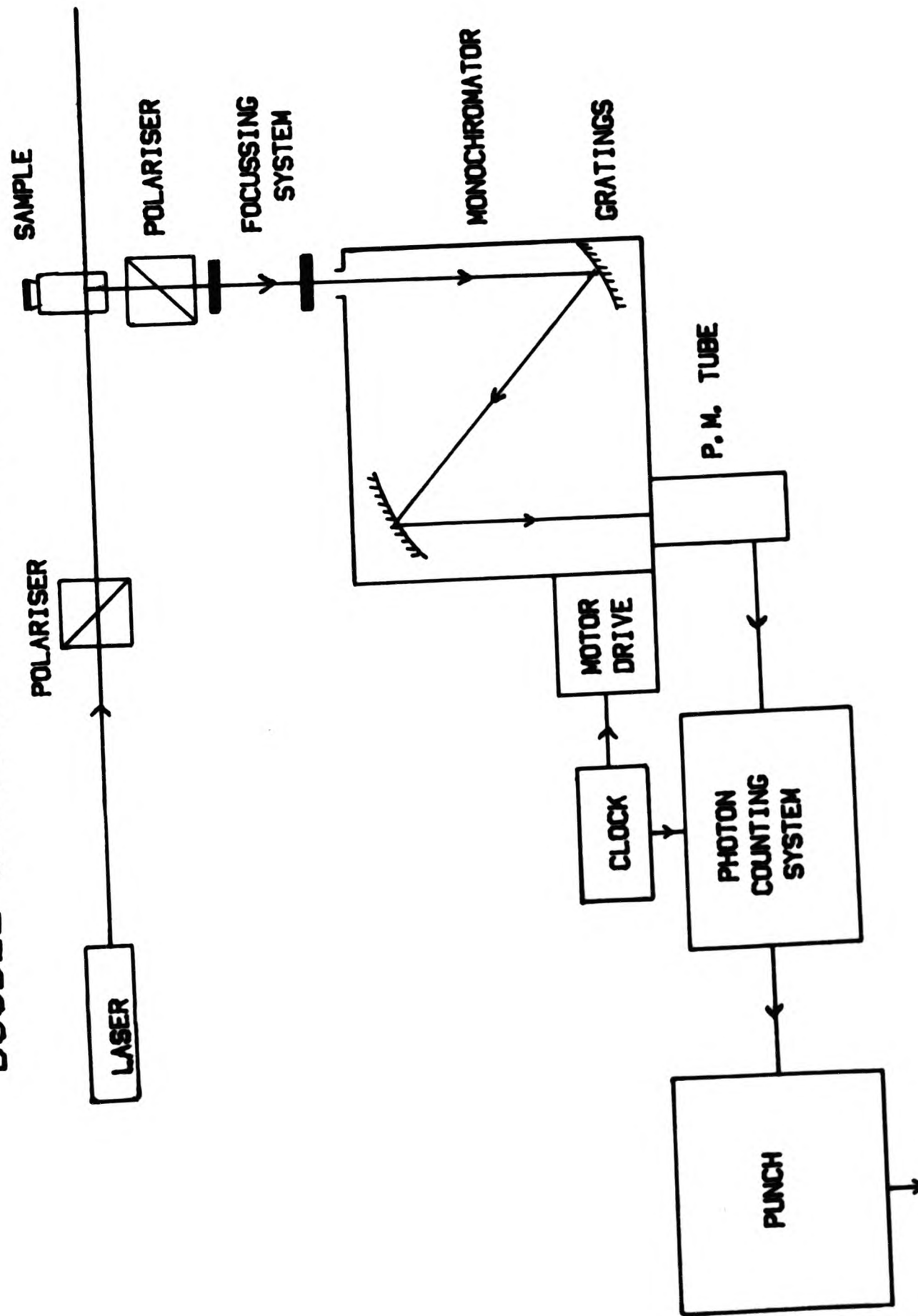
3.3 Description of the Double Grating Monochromator

Measurements were made of the depolarised (VH) spectra of some of the n-alkanes using a Coderg double grating monochromator at the Physical Chemistry Laboratories, Cambridge. The n-alkanes investigated were the even n-alkanes from hexane to hexadecane, and the odd n-alkanes pentane, heptane and nonane. All the materials apart from pentane were obtained from either Aldrich Chemicals Ltd or Koch Light Laboratories and the lowest purity quoted was 99%. Pentane was obtained from the stores of the Cambridge Laboratories.

The liquid samples were filtered as described into stoppered rectangular cells. The cells were held in a block in which the temperature was stable to about 1 °C.

The temperatures at which measurements were made were in the region 20 ° - 24 °C, an extra measurement was taken for C₁₆ H₃₄ at about 70 °C

DOUBLE GRATING MONOCHROMATOR fig 3.2



to obtain information about the relative intensities of the fast and slow contributions to the depolarised Rayleigh scattering in the temperature region in which the dip occurs in the depolarised Rayleigh spectrum for $C_{16}H_{34}$.

The light source was a Coherent Radiation argon ion laser operating in multiple modes at a wavelength of 514.5 nm. The power of the collimated beam passing through the sample was in all cases about 150 mW, all spectra were obtained at a fixed scattering angle of 90° .

The detector was a cooled gallium arsenide photomultiplier. Gallium arsenide has a very low work function and hence produces a very flat spectral response over the visible range. However the low work function causes the tube to produce a large number of thermal electrons at room temperature. This dark current is reduced by cooling the tube to about $-30^\circ C$ by thermostatically controlled boil-off of liquid nitrogen. This reduces the dark count from $5000 \text{ counts sec}^{-1}$ at room temperature to about $4 \text{ counts sec}^{-1}$.

Statistical noise in a counting experiment is proportional to $N^{\frac{1}{2}}$ where N is the total number of counts. By increasing the counting time N is increased and hence increases the signal to noise ratio. The slit widths are chosen so as not to distort the spectrum but to give as large a count rate as possible.

The accumulation time of 10 seconds is chosen to give as noise free a spectrum as possible without increasing the time of recording a single spectrum to too long a period.

The experimental arrangement is shown in Fig 3.2.

Form of Data

The data is output onto paper tape starting at one side of the central peak. The instrument has already been adjusted so that at the central peak the count rate does not exceed the maximum safe counting

rate of the photomultiplier tube ($50,000$ counts sec^{-1}). For the low frequency region of the spectrum the maximum resolution of the instrument is used (smallest slit widths 0.25 cm^{-1}) and counting at points $\frac{1}{16} \text{ cm}^{-1}$ apart. Corrections are made for the finite slit width in a computer deconvolution procedure.

Moving further out along the wings the counting rate decreased. To reduce statistical error in the counts the machine is stopped and a note is made of the position at which it has been stopped. The slits and aperture are opened so that the counting rate goes up to a level at which the statistical error is much lower. Two normalising counts are made - both 100 second counts - one before the machine is adjusted, the other after the machine adjustment. These are used to match up the two regions of the spectrum. The wider slit width makes no significant distortion to the final line shape as in the wings the intensity changes less rapidly with frequency than in the central region. Moving further out along the wings this process of changing the instrumental parameters is repeated to maintain a good signal to noise ratio.

The resulting data on the paper tape is reconstituted into a full spectrum by matching up the various portions of the spectrum. The spectrum is then plotted on a linear intensity scale and a logarithmic intensity scale.

Analysis of Data

The observed spectrum is a convolution of the true spectrum with the instrumental function. When the instrumental function has a width of the same order as the true spectrum the instrumental function must be well characterised.

The Cambridge group achieved this by using Rayleigh scattering from a dilute suspension of polystyrene latex spheres in water contained

in a cell of the same geometry as the cell containing the liquid samples. The slit functions are found to be almost triangular and are reproducible. These are used in the deconvolution of the spectrum particularly of the central region of the spectrum. The half width of the triangular slit function is about 0.2 cm^{-1} .

The depolarised Rayleigh spectrum consists of two main parts - a central Lorentzian and a collision induced scattering which takes the form of a roughly exponential background.

Fitting Procedure (4)

An exponential background is determined from the region beyond ten half widths of the central Lorentzian to represent the interaction induced background. This exponential is then subtracted from the data and then this residual spectrum is fitted out to six half widths to a single Lorentzian convoluted with the slit function determined as described previously where the width, position and intensity of the Lorentzian are allowed to vary. The residuals of the first fit are then added to the original exponential and a new exponential background determined from the resultant. The procedure is repeated until a consistent fit results, the final residuals of such a fit being small.

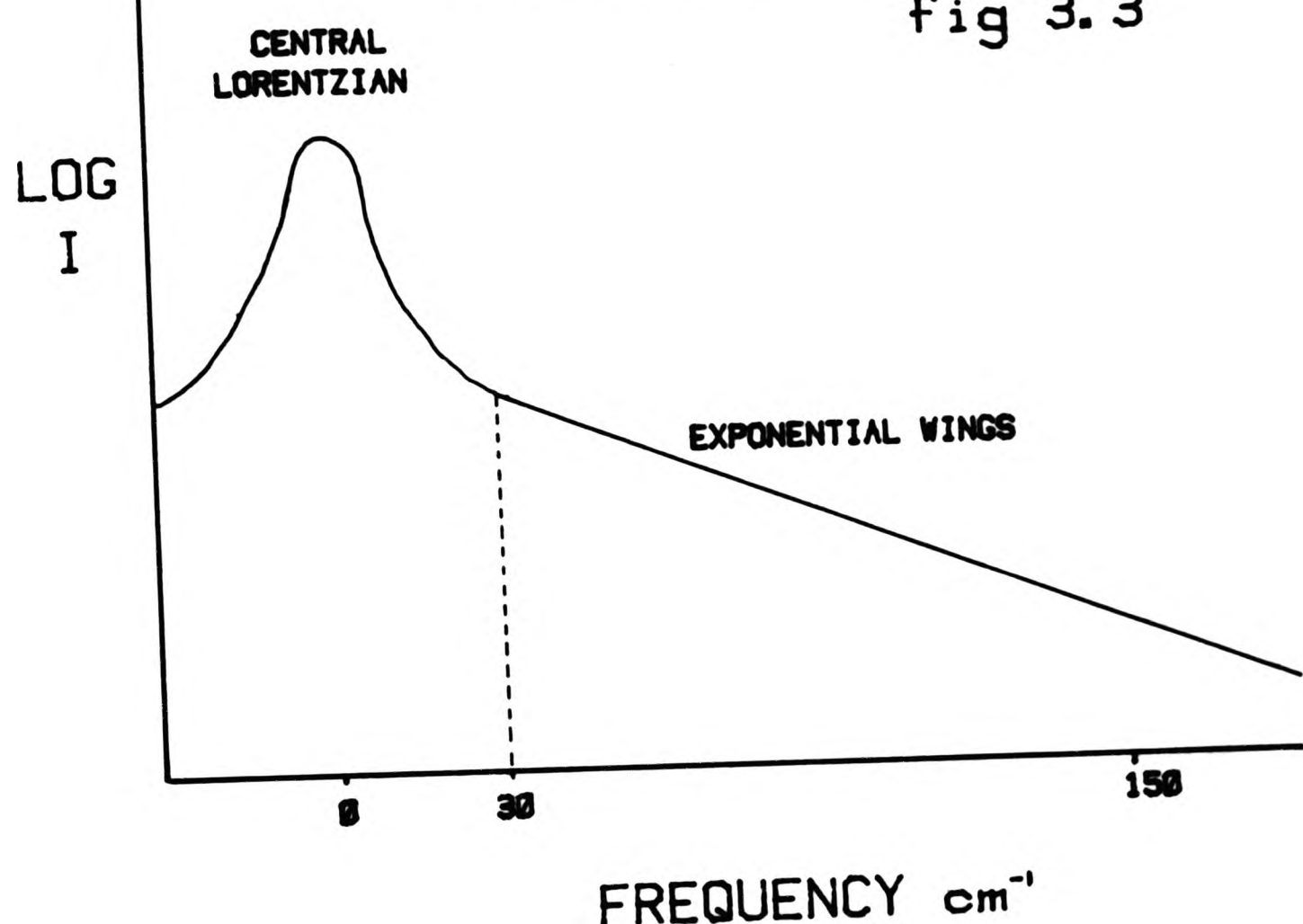
This fitting procedure assumes that the spectrum is of the form indicated in Fig 3.3.

The exponential part represents a fast collisional process, the Lorentzian represents the average reorientational motion.

Values of the half width of the central Lorentzian are obtained from the computer fitting procedure. Values of the intensity of this Lorentzian which can be labelled I_{SLOW} are obtained from the computer fit, assuming that the wings are given by the form $I = I_0 \exp \left(\frac{-\omega}{\omega_0} \right)$.

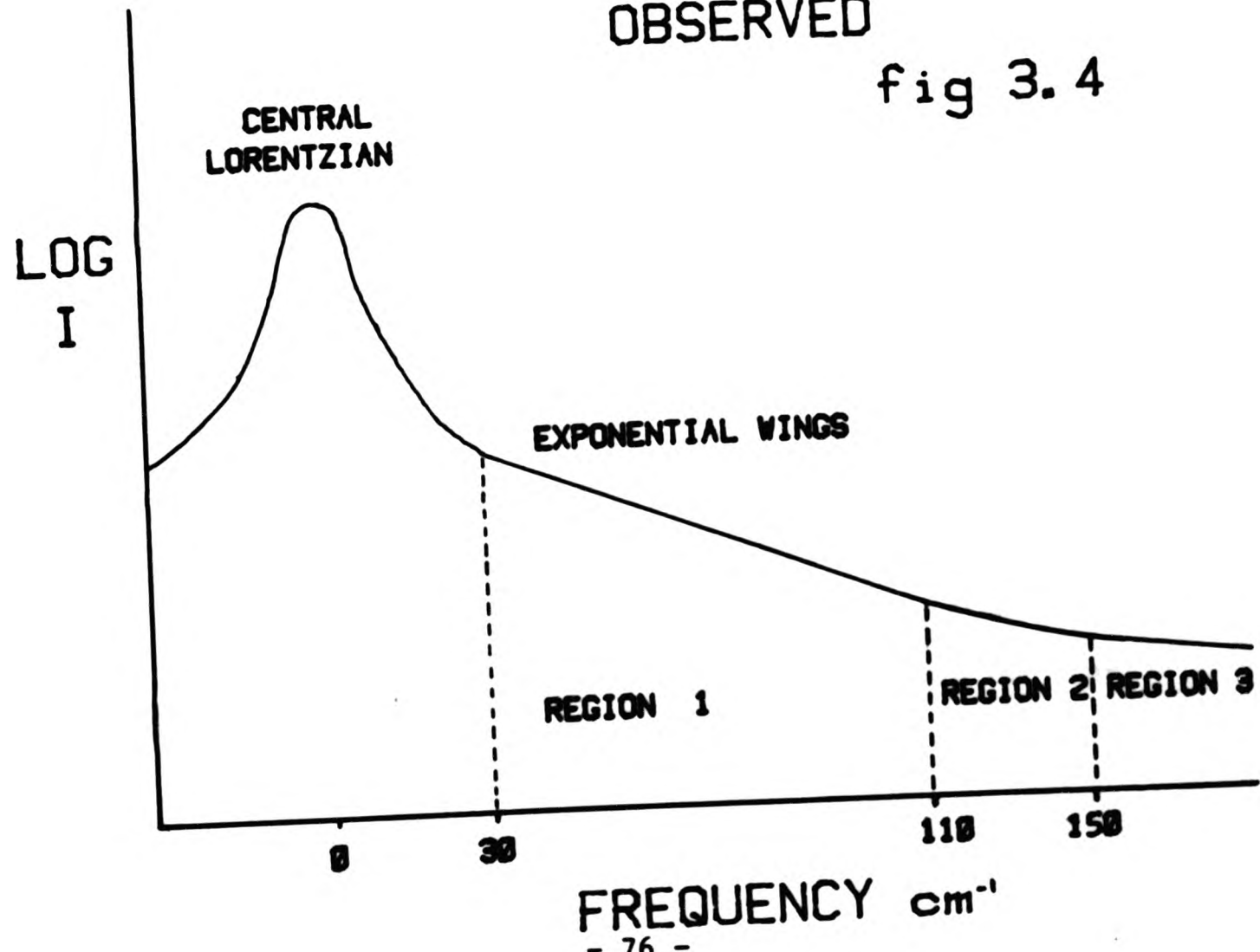
SPECTRAL FORM ASSUMED
BY FITTING PROCEDURE

fig 3.3



SPECTRAL FORM GENERALLY
OBSERVED

fig 3.4



FREQUENCY cm^{-1}

The computer output also contains details of the parameter A which is related to I_o , ($I_o = \exp A$) and the value of the slope of the logarithmic representation of the collision induced wings ($\frac{-1}{\omega_0}$). ω_0 is found to be within 10% of 30 cm^{-1} for all the n-alkanes concerned. It is a simple matter to calculate values for the total collisional intensity I_{FAST} .

$$I_{FAST} = 2 \int_0^{\infty} I_o \exp \left(\frac{-\omega}{\omega_0} \right) d\omega$$

$$I_{FAST} = 2 I_o \omega_0$$

From these results values of the ν parameter may be calculated. Because the instrumental width is of the order of 0.2 cm^{-1} the credibility of results for the half width of the central Lorentzian when the value given is below 0.2 cm^{-1} must be seriously questioned. However it is interesting to note that the value obtained for hexadecane at room temperature (0.019 cm^{-1}) is within 20% of a value which we have obtained using the Fabry Perot etalon. This is an indication that the fitting procedures used are fully adequate.

Other Spectral Forms

It was noticed that rather than fitting the spectra to a form described by a Lorentzian and a single exponential that the wings of the spectrum on a logarithmic intensity scale could perhaps be better described by three separate regions, each of a different slope, the slope decreasing moving further out from the centre of the spectrum. In Fig 3.4 the general appearance of the spectra is detailed. Region 1 appears to be a straight line and the slope seems to be more or less independent of the n-alkane studied. Region 2 for the lower n-alkanes is a straight line, the higher the n-alkane the more this

region becomes curved. The length of region 2 appears to decrease the higher the alkane. The slope of region 3 appears to take any value at all.

We attempted to make fits of the collision induced wings to the binary collision model of Bucaro and Litovitz (5), $I = \omega \frac{12}{7} \exp - (\omega/\omega_0)$ and found these fits very unsatisfactory in that any fitted parameters obtained depend very strongly on exactly which region of the spectrum the fitting procedure is applied to. This may be expected for on a logarithmic scale the form of $\omega \frac{12}{7} \exp (-\omega/\omega_0)$ is a convex shape. In all the spectra on a logarithmic scale we observed a concave shape. Moreover as discussed in chapter 2 the Bucaro and Litovitz formula is strictly incorrect for liquids due to the inapplicability of the binary collision model, and the fact that pair anisotropy is also a function of molecular orientation.

In all of the liquids examined at high frequencies the spectra observed on the logarithmic scale flatten out. The question arises whether this is a real effect or an instrumental effect. We investigated the possibility of there being a contribution to the far wings of the spectrum from scattering from the cell wall. The spectrum of light scattered from an empty cell was observed and all that appeared was the sum of the rotational spectra of oxygen and nitrogen. In between these rotational peaks the signal falls to the dark count indicating that in the spectra of the n-alkanes recorded there is little or no contribution to the far wings from stray light scattered from the cell walls.

The flattening out in the spectra is therefore a real effect. If the binary collision model is valid and describes the spectra of the light scattered for the low frequency wings an explanation of the higher frequency wings is that they are due to multi particle inter-

actions in the liquid. There is also a possibility that the flattening out is due to contributions to the intensity from the Raman lines which are $\sim 180 \text{ cm}^{-1}$ further out in the spectrum.

3.4 Sample Preparation and Ancillary Measurements

3.4.1 Filtering Techniques

Filtering was carried out using Millipore filtration units, with Millipore filters. The liquid is forced through the filtration unit using a syringe. The filtration unit and syringe are thoroughly cleaned before use, first being immersed in a hot recycling choroform bath and then are washed, first with filtered carbon tetrachloride and are blown dry in a filtered air stream or allowed to dry in an oven at approximately 60°C . This washing process is repeated with filtered chloroform and after drying repeated again with filtered propanol.

The filtering unit is assembled under strong illumination in a dust free cabinet and great care is taken to ensure that there are no particles of dust inside the unit. Any particles of dust which are seen on the unit are blown away by directing a stream of dust free air. Once the unit is assembled the unit is washed out by first passing a few mls of carbon tetrachloride through it, as particles of the filter may break away in the filtering process. This process is repeated using chloroform, then propanol, in each case allowing the unit to dry out before continuing with the washing process.

Initially the liquids investigated were the members of the n-alkanes from pentane to pentadecane and were filtered twice, once with a 0.2μ filter and again with a 0.025μ filter. However this was found to be unnecessary in that a single 0.025μ filtering sufficed except in cases where the liquid to be filtered had large quantities of

dust present which would damage the 0.025μ filter because of the extra pressure required to force the liquid through the clogged up filter. For dusty liquids a 0.2μ prefiltering was found to be necessary.

For the n-alcohols which are approximately ten times more viscous than the n-alkanes this procedure was found to be ineffective. These liquids are so viscous that they tear material from the filter and deposit it into the filtered sample. However examination of the used filters shows that they removed a large amount of dust from the unfiltered sample despite introducing fine fragments of disintegrated filter into the filtered sample.

A modified filtering procedure was evolved for these n-alcohols. This involved prefiltering the n-alcohols using the cellulose Millipore filters to remove the fine dust present in these samples. This filtering introduced larger particles, which were fragments of the filter. These were then removed by a second filtering using teflon Millipore filters. As these filters were not obtainable in a very small pore size a stack of three or four individual filters was used as a single filter. A more rigorous cleaning procedure was applied for these filters, the combined filter stack was first cleaned by passing several mls of di-methyl formamide (DMF) through the filter. This filter is entirely dried out and then the normal cleaning process is gone through, carbon tetrachloride, chloroform and then propanol being used.

The resulting samples are examined and, if the procedure has been carried out carefully, are found to be dust free. However in the most viscous liquid examined (n-undecanol) several large particles were observed in the sample. It seemed likely that the cause of this was that the backing of the teflon filters which is made of polythene was

breaking off. We found it impossible to prepare a particle free undecanol sample.

The solutions examined were of the form alkane plus carbon tetrachloride. A large amount of the particular alkane to be used was filtered into a clean stoppered flask using a 0.025μ filter. The flask had previously been cleaned using filtered carbon tetrachloride and filtered propanol. In each case the flask is blown dry.

A large amount of carbon tetrachloride was filtered into a clean stoppered flask using a 0.025μ filter.

The solutions were then prepared by weighing measured amounts of each liquid into a single vial. Once this process was completed, each vial was stoppered and the solutions were shaken to ensure thorough mixing.

The sample of the solution is then filtered through a 0.22μ filter. This minimises concentration changes which may occur during the filtering process.

At the final filtering the liquid is placed in a clean stoppered square Helma glass light scattering cell. The cell had been cleaned previously by immersion in a hot chloroform bath, and then by repeated washings with filtered carbon tetrachloride, chloroform and propanol, each time the cell is blown dry using filtered air.

The prepared sample is examined in a laser beam for particles of dust. If the sample appears clean its depolarised Rayleigh spectrum is examined for spikes in the central Lorentzian which would be indicative of dust in the sample. The samples which are prepared in this way are, if due care is taken, of a very high quality.

3.4.2 Density Measurements

Density measurements throughout are made using a Paar DMA 40 digital density meter.

The instrument is calibrated over a temperature range of 20 °C to 60 °C, the temperature being regulated by water circulating around a thin glass tube containing the sample tube. The temperature of the water bath is controlled at the required temperature to ±0.02 °C.

In all the situations in this thesis when a density value is used it has been calculated from linear fits to the data obtained using the digital density meter.

Density measurements were also used for measuring the concentration of solutions.

3.4.3 Concentration Measurements

Measurements of concentration were made using the density meter. We chose the density meter as a method of measuring concentrations rather than refractive index measurement mainly because for the alkane/carbon tetrachloride mixtures concerned there is a large change of density with concentration, and also because with the density meter as the sample volume is of the order of 1 cm³ and may be sealed, there is less chance of differential evaporation changing the solution concentration during the time scale of the measurement. With a refractometer problems associated with differential evaporation are much more marked.

Assuming that there is no change of volume on mixing the density of the mixture should be linear with volume fraction of the individual components of the liquid before mixings. For all the solutions investigated the relationship was linear, the deviation from linearity being less than 0.3%

When the solution samples are prepared, after the solution had been filtered directly into the sample cells, some of the filtrate was filtered into a syringe and injected into a density meter, the density obtained being used to calculate the volume concentration.

In all cases the volume concentration changed on filtering.

The sample is examined in the spectrometer for a period of several hours during which time, due to differential evaporation the solution concentration changes. After this period of time the volume concentration of the solution is measured again and the concentration for the experimental run is taken to be the average of the observed values. In the worst case the concentration change measured was $\sim 0.4\%$.

3.4.4 Viscosity Measurements

For all the liquids examined viscosity measurements are made using Ubbeholde viscometers.

Readings were made in the temperature range 10°C to 96°C with the viscometer immersed in a water bath thermostatically controlled to 0.1°C for temperatures below 60°C and to 0.3°C for temperatures above 60°C .

The viscometers were calibrated using liquids of known viscosities and the accuracy of the calibration was $\sim 1\%$.

Interpolation and extrapolation of data points was made using the Arrhenius expression $\eta = \eta_0 \exp(-B/T)$ a maximum extrapolation being 5°C .

For solution measurements a different technique was adopted due to the fact that differential evaporation changes the solution concentration during viscosity measurements.

A number of solutions (about 12) are made up of the mixture being investigated, varying in volume concentration of alkane from 100% to

0%, the concentrations being reasonably equally spaced.

The density meter is set at the temperature of the viscometer bath and the density of the particular sample about to be placed into the viscometer is measured. A number of viscosity determinations were made. The fall times varied showing that the concentration of the sample changed during the course of the measurement. The sample is then removed and the density remeasured. A concentration change is found. The sample is assumed during the run to have had an average density from which we obtain the average volume concentration.

Because of the averaging procedures, errors are introduced into the value of both viscosity and the concentration measurements. The extra error introduced is approximately 1%. The total error in viscosity measurements for the solutions was therefore estimated to be about 2%, whereas for the pure liquids it was about 1%.

In a single viscosity determination, for an approximately 50% volume concentration solution the volume concentration changes by about 1%. The data obtained is tabulated in the form of isotherms of viscosity over the total range of volume concentrations.

To obtain viscosity data for the solutions for which we have obtained light scattering information we use these isotherms in the following manner.

The volume concentration of a solution is obtained before and after the light scattering measurement, and so an average value of concentration during the light scattering measurement may be obtained.

The viscosity/concentration isotherms are then used to obtain a set of viscosity data over a range of temperature points for the volume concentration for which light scattering data has been obtained. (The volume concentration is corrected at each temperature point to

take account of temperature changes.) As the viscosity data for the solutions against temperature has a larger error than that for the pure liquids the method of calculation of viscosities used differs from that used for the pure liquid (interpolation between adjacent data points). The viscosity data for the solution is fitted to the straight line relationship obtained from the equation $\eta = \eta_0 \exp(-B/T)$. The standard deviation between the line and the data points is about 0.7% in the cases examined. We believe that this gives the best measurement method for viscosities of solutions in light scattering although the time involved in making such measurements is considerable (of the order of a week for each liquid).

3.5 References for Chapter 3

- (1) T Keyes and D Kivelson, 1972, J Chem Phys 56, 1057.
- (2) H W Leidecker and J T LaMacchia, 1967, J Acoust Soc Am 43, 143.
- (3) G R Alms, D R Bauer, J I Brauman and R Pecora, 1973, J Chem Phys 58, 12, 5570.
- (4) T I Cox, 1978, "Light Scattering Studies of the Structure and Dynamics of Molecular Liquids", PhD Thesis, Cambridge University.
- (5) J A Bucaro and T A Litovitz, 1971, J Chem Phys 54, 9, 3846.

CHAPTER 4 RESULTS AND ANALYSIS

In this chapter the terms "Lorentzian plus dip" and "Double Lorentzian" are interchangeable and refer to spectral fits to equation 2.9.

4.1 Monochromator Results

4.1.1 Introduction

The results from the monochromator were analysed as is detailed in the section on the experimental work. The fitting procedure employed fits the spectra to a central Lorentzian plus an exponential wing convoluted with the instrumental function and results are as shown in table 4.1.

Table 4.1

LIQUID	TEMP °C	A	$\frac{1}{\omega_0}$	I _{FAST}	I _{SLOW}	HALF WIDTH cm ⁻¹ LORENTZIAN	v
C ₅ H ₁₂	22.7	-2.04	.035	7.3	4.037	2.085	0.356
C ₆ H ₁₄	23.8	-3.36	.03	2.32	2.82	0.995	0.549
C ₇ H ₁₆	22.0	-4.24	.029	0.9936	1.8968	0.5994	0.656
C ₈ H ₁₈	22.7	-4.92	.027	0.541	1.316	0.373	0.709
C ₉ H ₂₀	21.0	-5.4	.034	0.2657	0.9598	0.2394	0.783
C ₁₀ H ₂₂	20.7	-6.0	.032	0.155	0.723	0.143	0.823
C ₁₂ H ₂₆	22.3	-6.6	.032	0.083	0.467	0.0444	0.848
C ₁₄ H ₃₀	23.3	-7.08	.031	0.0543	0.431	0.036	0.888
C ₁₆ H ₃₄	22.3	-7.32	.028	0.0473	0.349	0.019	0.881
C ₁₆ H ₃₄	70.1	-6.63		0.08	0.46		0.85

A is the intensity of the exponential wing relative to the central

Lorentzian at zero frequency on a logarithmic scale, $1/\omega_0$ is the rate at which the exponential wing falls off in inverse wave numbers.

I_{FAST} and I_{SLOW} are expressed simply in terms of the relative area under the curve for the fast and slow components of each spectrum.

The half width of the Lorentzian component of the spectrum is as shown - these results may be compared with results obtained from the Fabry Perot with single Lorentzian fits to the data (which are not properly valid for the alkanes $C_{12}H_{26}$, $C_{14}H_{30}$, $C_{16}H_{34}$, but are used here for the purpose of comparison as the fits to the data from the monochromator are to single Lorentzian plus background).

Table 4.2

A Comparison of Half Widths from Two Separate Instruments

LIQUID	MONOCHROMATOR (Instrumental Width = 6 GHz)	FABRY PEROT	% DIFFERENCE
$C_5 H_{12}$.62.6	59.4	+5.2
$C_6 H_{14}$	29.9	31.5	-5.2
$C_7 H_{16}$	18.0	18.5	-5.4
$C_8 H_{18}$	11.2	9.7	+14.6
$C_9 H_{20}$	7.2	5.8	+8.9
$C_{10} H_{22}$	4.3	3.8	+12.5
$C_{12} H_{26}$	1.33	1.56	-15.9
$C_{14} H_{30}$	1.08	0.92	+16.0
	GHz	GHz	

The difference between the readings increases as the half width of the Lorentzian component becomes equal to and less than the instrumental width of the monochromator. For $C_{14}H_{30}$ the narrowest

line, the width of the spectrum is one sixth of the instrumental width and the results agree to within 20%. Hence the fitting procedure used appears to be satisfactory. Our main interest in the monochromator data is in the collision induced portion of the spectra.

The other information in table 4.1 is the ν parameter. This represents the proportion of the total depolarised spectrum which is due to the intrinsic optical anisotropy of the molecule.

4.1.2 Collisional Portion of the Spectrum

We have obtained data from the spectral fits which give information about the collisional part of the spectrum. This may be related to the anisotropic Rayleigh ratio which for a molecular liquid is given by equation 2.1.

$$R_{AN} = \frac{8 \frac{\pi^4}{\lambda^4}}{\left[\left(\frac{n^2 + 2}{3} \right)^4 \times \frac{13}{45} \times \rho_N \bar{\gamma}^2 \right]} \quad \text{CGS}$$

$$R_{AN} = \frac{\frac{\pi^2}{2\epsilon_0^2 \lambda^4}}{\left[\left(\frac{n^2 + 2}{3} \right)^4 \times \frac{13}{45} \times \rho_N \bar{\gamma}^2 \right]} \quad \text{SI}$$

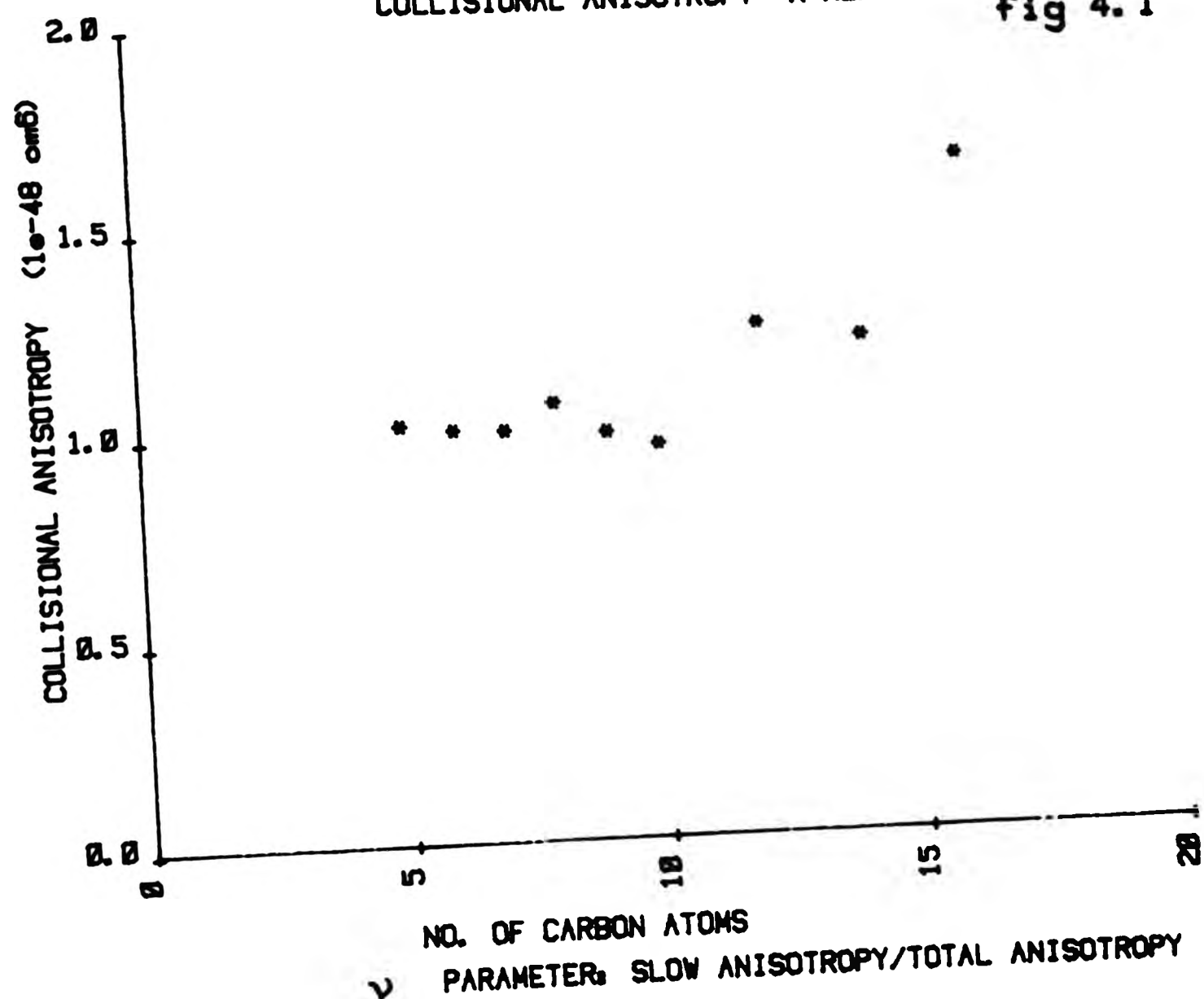
The intensity of the depolarised light scattered is directly proportional to R_{AN} . The total amount of depolarised light scattered by collisional processes is related to a collision induced mean squared optical anisotropy by equation 2.13.

$$(1 - \nu) R_{AN} = \frac{8 \frac{\pi^4}{\lambda^4}}{\left[\left(\frac{n^2 + 2}{3} \right)^4 \times \frac{13}{45} \times \rho_N \bar{\gamma}^2 \right]} \quad \text{COLLISIONAL}$$

Using R_{AN} values from Dandridge (1), and ρ_N number densities from the densities of the individual liquids we obtain the following results for $\bar{\gamma}^2$ collisional.

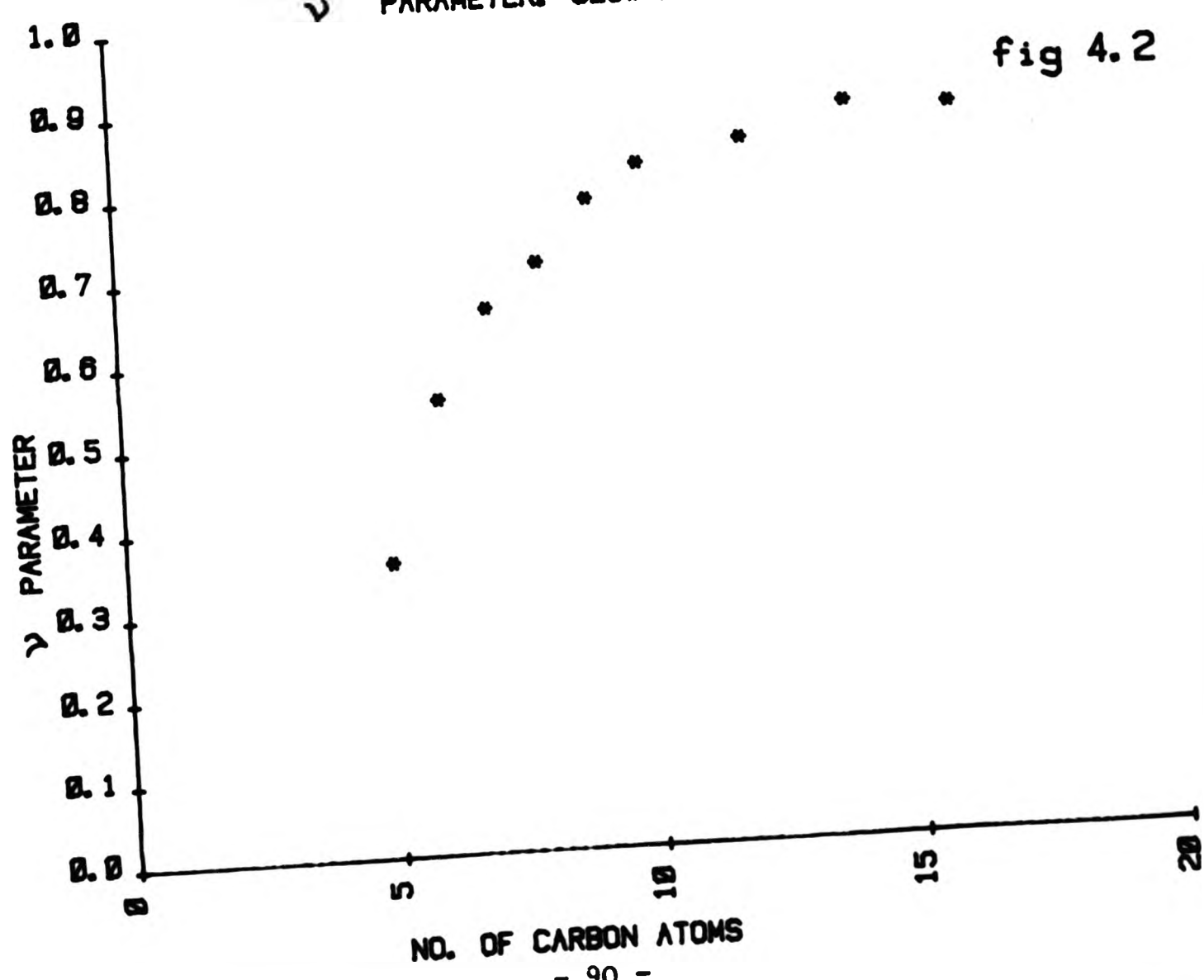
COLLISIONAL ANISOTROPY N ALKANES

fig 4.1



NO. OF CARBON ATOMS
PARAMETER: SLOW ANISOTROPY/TOTAL ANISOTROPY

fig 4.2



NO. OF CARBON ATOMS

Table 4.3
Collision Induced Anisotropies at 22 - 24 °C

LIQUID	γ^2	COLLISIONAL
C ₅ H ₁₂	1.02	x 10^{-48} cm ⁶
C ₆ H ₁₄	1.01	x 10^{-48} cm ⁶
C ₇ H ₁₆	1.01	x 10^{-48} cm ⁶
C ₈ H ₁₈	1.07	x 10^{-48} cm ⁶
C ₉ H ₂₀	1.00	x 10^{-48} cm ⁶
C ₁₀ H ₂₂	0.97	x 10^{-48} cm ⁶
C ₁₂ H ₂₆	1.25	x 10^{-48} cm ⁶
C ₁₄ H ₃₀	1.21	x 10^{-48} cm ⁶
C ₁₆ H ₃₄	1.65	x 10^{-48} cm ⁶

A graph is included of these results, Fig 4.1. Their possible relevance to collisional motion will be discussed later.

The values of ω_0 are calculated from the slope of the exponential part of the spectrum, ω_0 is related to the time between collisions by the way in which the induced anisotropy varies as the colliding entities approach each other.

The reasons behind using the equation $I = I_0 \exp(-\omega/\omega_0)$ implied are discussed in the theory section (Chapter 2). To summarise - Bucaro and Litovitz perform calculations on the shape and intensity of the Rayleigh wings of the spectrum based on a binary collision model (2). For molecular liquids they obtained the relation

$$I(\omega) = I_0 \omega^{12/7} \exp(-\omega/\omega_0)$$

ω_0 is shown to be given by the relation

$$\frac{1}{\omega_0} = \frac{1}{6} \pi r_0 (\mu/KT)^{\frac{1}{2}} \left[1 - (2/\pi) (2\epsilon_0/KT)^{\frac{1}{2}} \right]$$

ϵ_0 and r_0 are the constants used in the standard expressions of the Lennard Jones potential and μ is the reduced mass.

Later calculations show that taking account of the non zero collision parameters and an appropriate distribution of molecular velocities the preexponential part of the formula reduces to ω^0 . Therefore $I(\omega) = I_0 \exp(-\omega/\omega_0)$ which is the form used in the fitting procedure. As discussed in Chapter 2, Bucaro and Litovitz's formula is not applicable to anisotropic molecules as the Lennard Jones approximation is not valid, and $\Delta\alpha$ depends both on molecular orientation and separation.

Another possible form to describe the collisional spectrum is that due to Levine and Birnbaum (3) for which it is shown

$$I(\omega) = \omega^{\frac{1}{2}} \exp(-\omega/\omega_0) \quad 2.20$$

$$\text{and } 1/\omega_0 = \frac{2\pi}{\gamma} \left[\frac{m}{KT} \right]^{\frac{1}{2}} \quad 2.21$$

$\frac{1}{\gamma}$ is effectively the average intermolecular distance.

All these equations assume a binary collision model. We discuss the relevance of the results to this model despite its inadequacies as a description of collisional processes in the n-alkanes.

In all the n-alkanes investigated (pentane-to hexadecane) ω_0 is found to be within 15% of 30 cm^{-1} . If we examine Levine and Birnbaum's equation the significance of this may be seen. In all molecular liquids the molecular separation is the same - approximately 0.6 \AA . From this we get that m - the mass of the colliding entity in all the n-alkanes

examined is about 19 amu which is approximately the mass of a CH_3 group, a chain end, or a CH_2 group which is an independent group in the chain.

The value of $\omega_0 \sim 30 \text{ cm}^{-1}$ or 900 GHz is close to the frequency of conformational transitions in the computer simulations of Ryckaert and Bellemans (4) (see Chapter 2), that is the frequency of independent movement of elements of the alkane chain.

Perhaps a further indication of the significance of this may be seen from an estimation of a collision time from an expression due to Nikitin (5).

$$\frac{1}{\omega_0} = \frac{2\pi C^2}{\sigma} \left(\frac{M'}{KT} \right)^{\frac{1}{2}} \left[1 - \frac{2}{\pi} \arctan \left(\frac{2\varepsilon}{KT} \right)^{\frac{1}{2}} \right]$$

This according to Tabisz leads to an ω_0 value for CH_4 of about 30 cm^{-1} at room temperature (although that observed for CH_4 is about 138 cm^{-1}).

We believe that the value of ω_0 is an indication that collisional motion in the n-alkanes takes place between elements of individual alkane chains which are adjacent to each other, and that these elements contain a single carbon atom. As far as collisional motion is concerned alkane liquids behave as though they consist of individual CH_2 and CH_3 units.

Examining how the magnitude of the collision induced anisotropy varies with the number of carbon atoms in the chain the following points become apparent. One is that the collision induced anisotropy remains approximately constant for the alkanes from pentane to decane, and then increases sharply. As we would expect (if our assumption of individual elements of the chain being involved in collisional motion is correct) that $\bar{Y}^2_{\text{COLLISIONAL}}$ would be proportional to the number of

elements being involved in collisional motion we are led to the conclusion that for $C_5 H_{12}$ to $C_{10} H_{22}$ it is probably the chain ends alone that are involved in collisional motion and that moving up from $C_{10} H_{22}$ there is a tendency for the chains to bend back on themselves. This increases the anisotropy from a simple interaction with another molecule to an interaction with another molecule plus a self interaction.

4.1.3 Problems with Simple Interpretation

There are problems with this simple interpretation of the data. The experimental work with the monochromator was undertaken as a confirmation of the half widths obtained with the Fabry Perot and not as a full scale investigation of the collisional spectra. The interpretation presented of the collisional data is appropriate, bearing in mind the limited amount of data available.

One of the difficulties is that the simple binary collisional model is strictly inapplicable to systems as complicated as the n-alkanes. We conclude that as far as collisional motion is concerned there is an indication that the n-alkanes behave as liquids consisting of separate CH_2 and CH_3 groups and a number of corroborating pieces of evidence have been cited.

By using an analysis relying on the binary collision model we have obtained results which appear to validate that model. This may be an invalid approach.

In fitting the wings to the equation $I(\omega) = I_0 \exp(-\omega/\omega_0)$ we fit the wings from 30 cm^{-1} from the exciting line to about 100 cm^{-1} . Beyond 100 cm^{-1} the plots of intensity against frequency on a logarithmic scale flatten out. An argument which is often cited to explain this is that the very high frequency tail is due to multi particle

collisions. The time scale of these interactions is considerably faster than that for the two body interactions, and hence this contributes extra intensity to the high frequency portion of the spectrum.

An attempt to examine the possibility of three and four body interactions contributing to the high frequency portion was made. However we found it difficult to get consistent results, due to the fact that in the high frequency wing (from 100 cm^{-1} to 200 cm^{-1}) there are components due to Raman scattering and this is not separable in the small amount of data available.

The separation of interaction induced spectra into two, three and four body terms has been performed by a number of authors. This is discussed in detail in Chapter 2.

However all these measurements have been performed on systems which compared to the alkanes are very simple. Another problem in interpretation of the data arises from the flexibility of the alkane molecule and the fact that the time scale of collisional motion from the spectra ($1 \text{ ps} \sim 30 \text{ cm}^{-1}$) is the same as the time scale of conformational changes in the molecule (from simulations). The problem which arises is this. Implicit in the spectral analysis is that the spectrum is separated into two components I_{ROT} - which is the intrinsic scattering (and has a spectrum approximating to a Lorentzian) and $I_{\text{COLLISIONAL}}$ which is the collisional induced scattering (and has a spectrum approximating to an exponential). The first assumption which is made is that these two processes have widely different time scales and can be frequency separated. This is true in the case of the n-alkanes for in the "worst" case investigated (pentane) the rotational part has a half width of 2 cm^{-1} and the collisional part has a decay constant of $1/30 \text{ cm}^{-1}$ which gives a time scale separation by a factor of 15.

Another assumption implicit in the spectral analysis is that $I_{ROT-COLLISIONAL}$ (light scattering occurring as a result of coupled rotational and collisional motion) is negligible. When this assumption has been made before the experiments have been made on rigid molecules and there is some justification for this assumption. In the n-alkanes this may not be the case. It appears from the results that collisional motion is probably linked with conformational changes and as a conformational change in an n-alkane is essentially a reorientation of part of the molecule there is a coupling process between collisional motion and reorientational motion in the n-alkanes.

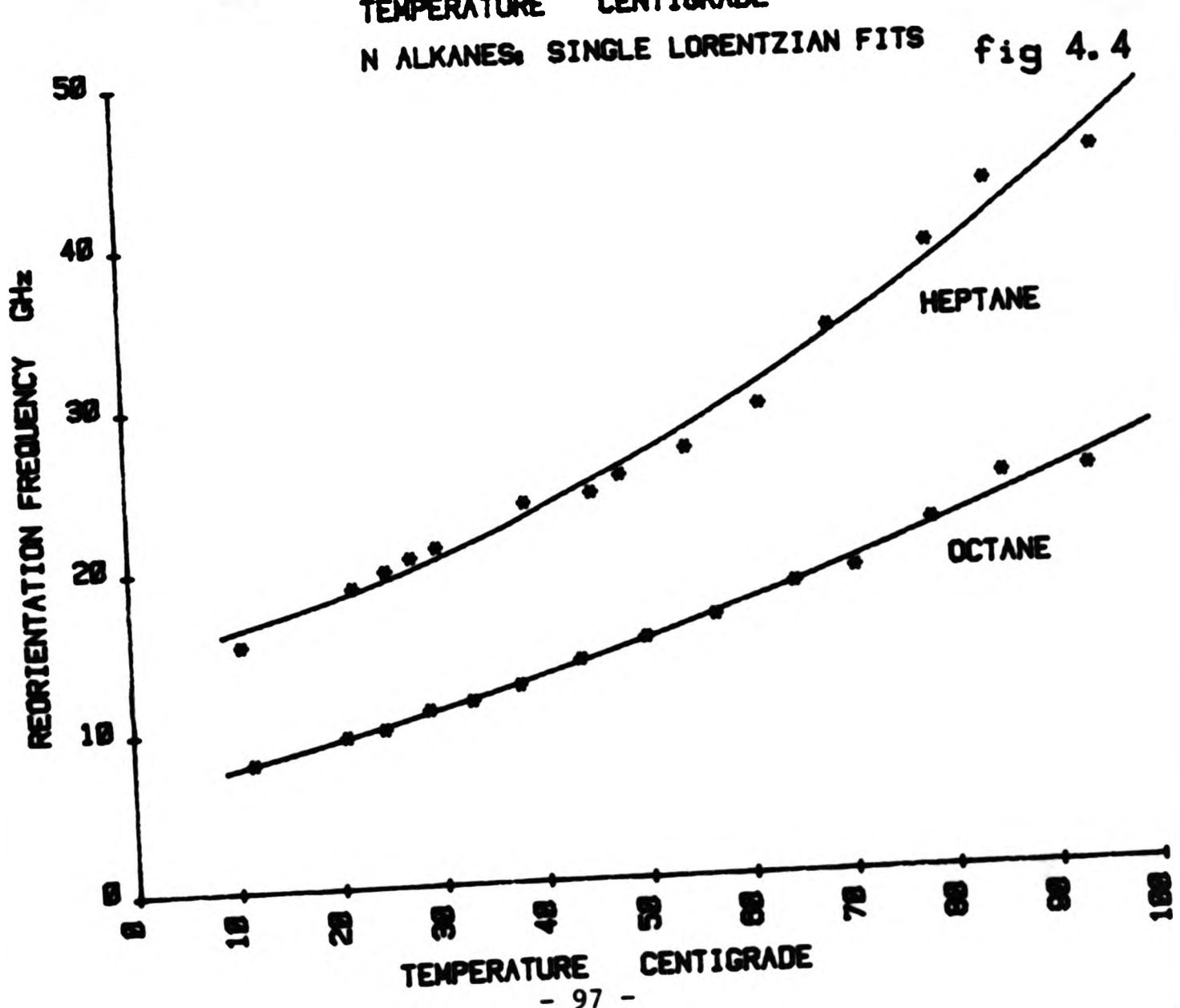
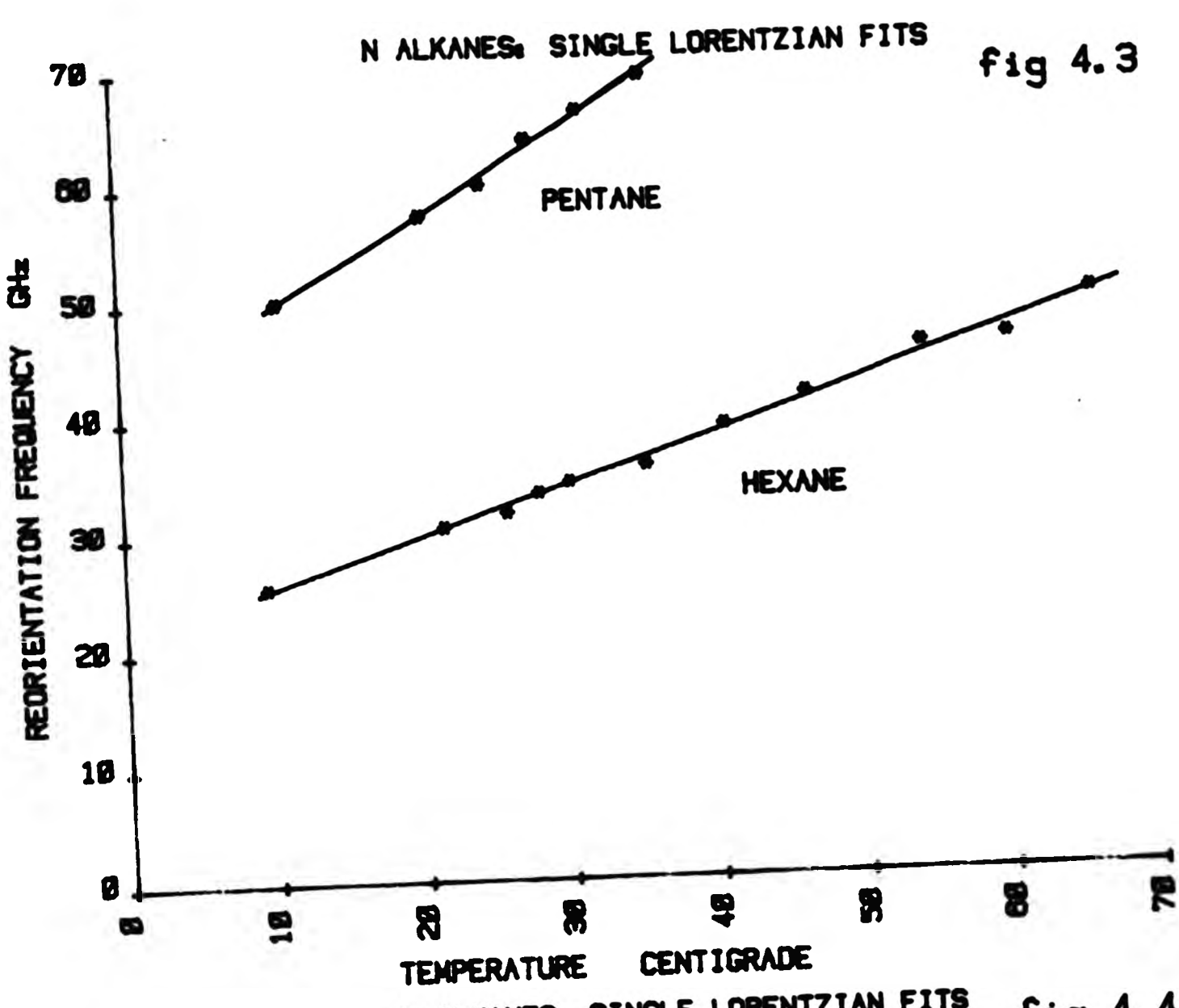
Calculation of $I_{ROT-COLLISIONAL}$ in magnitude and spectral form is difficult, in this work we make the perhaps unjustified assumption that it is negligible and does not contribute significantly to the depolarised Rayleigh spectrum.

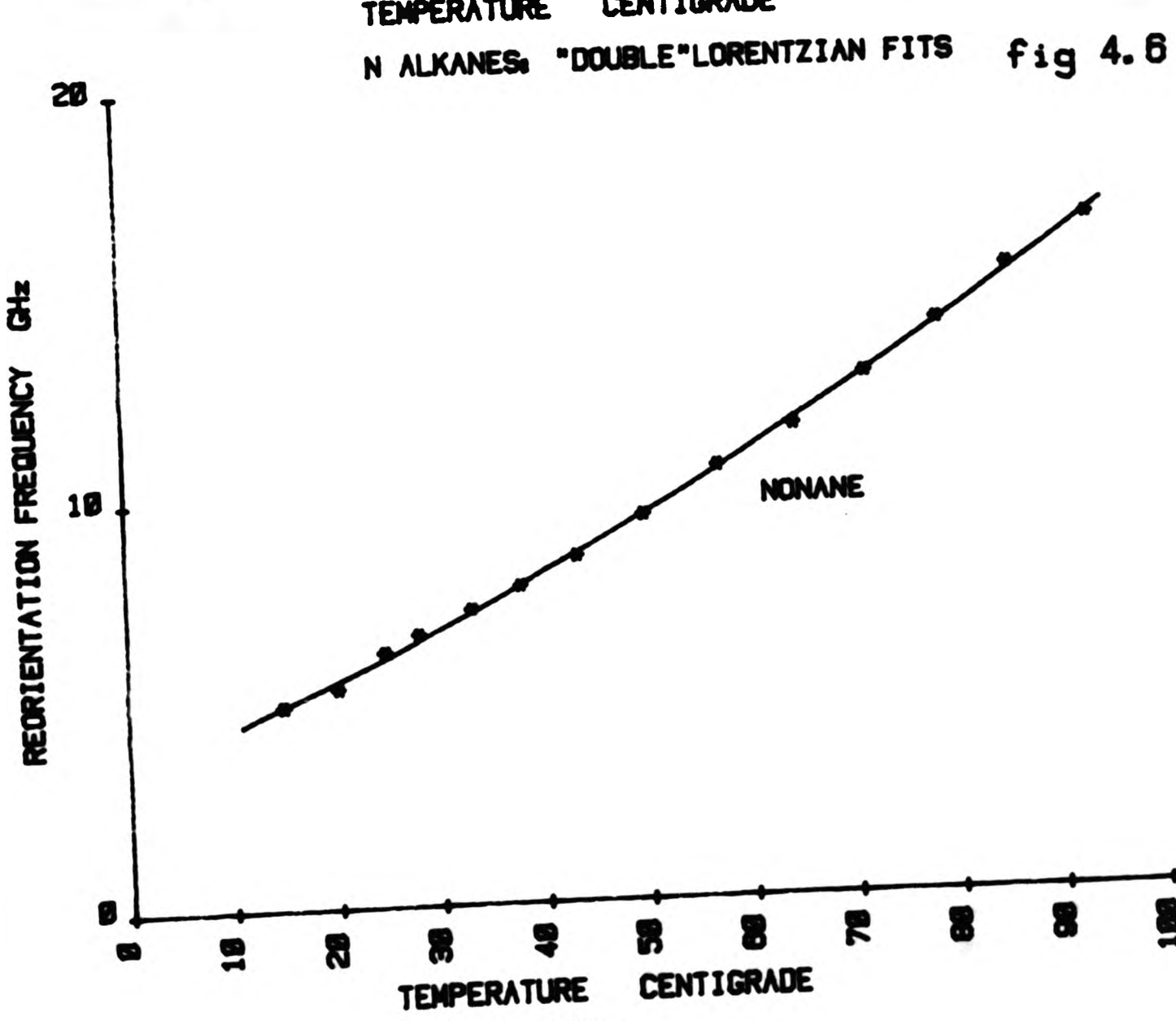
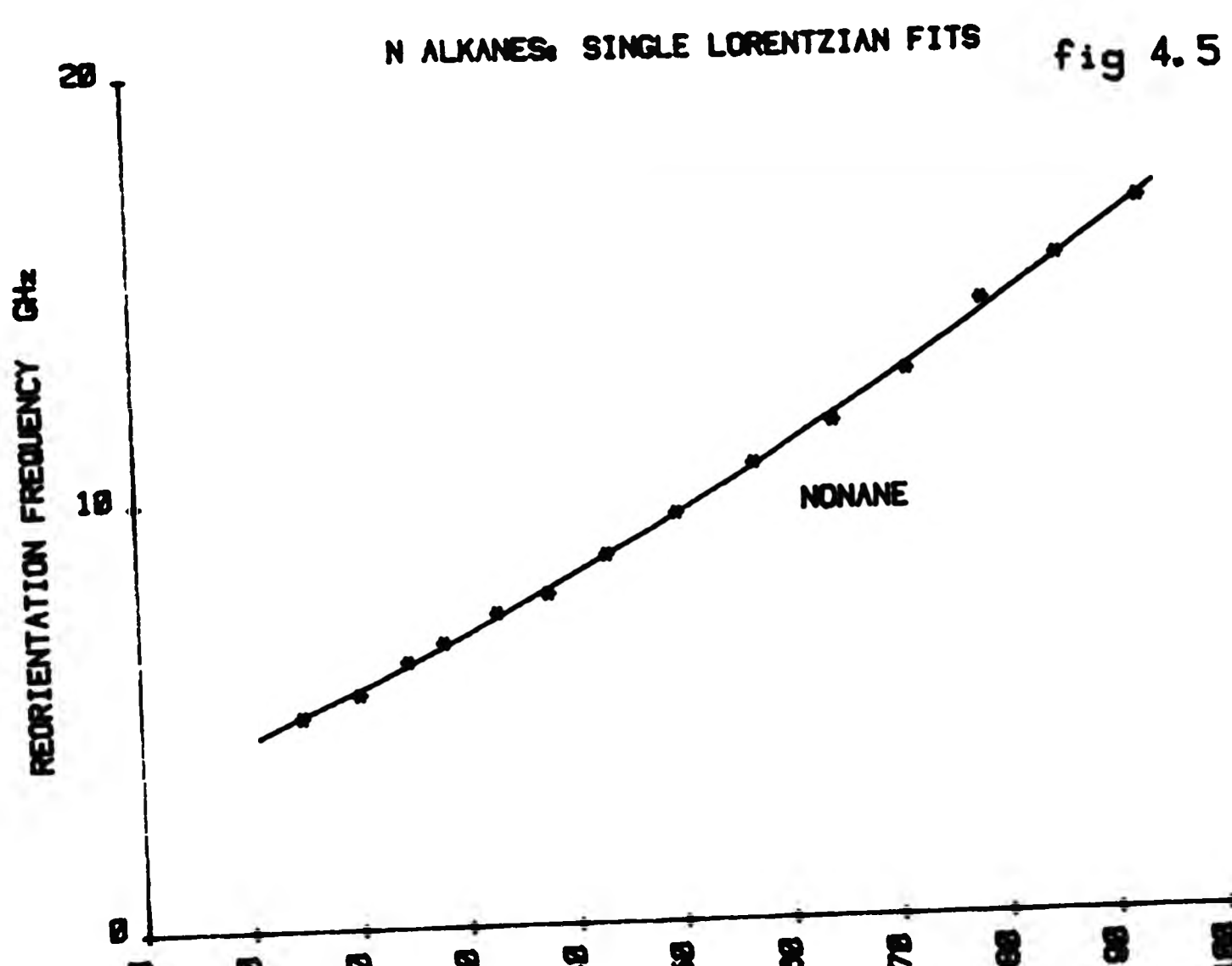
4.2 Results from the Fabry Perot System

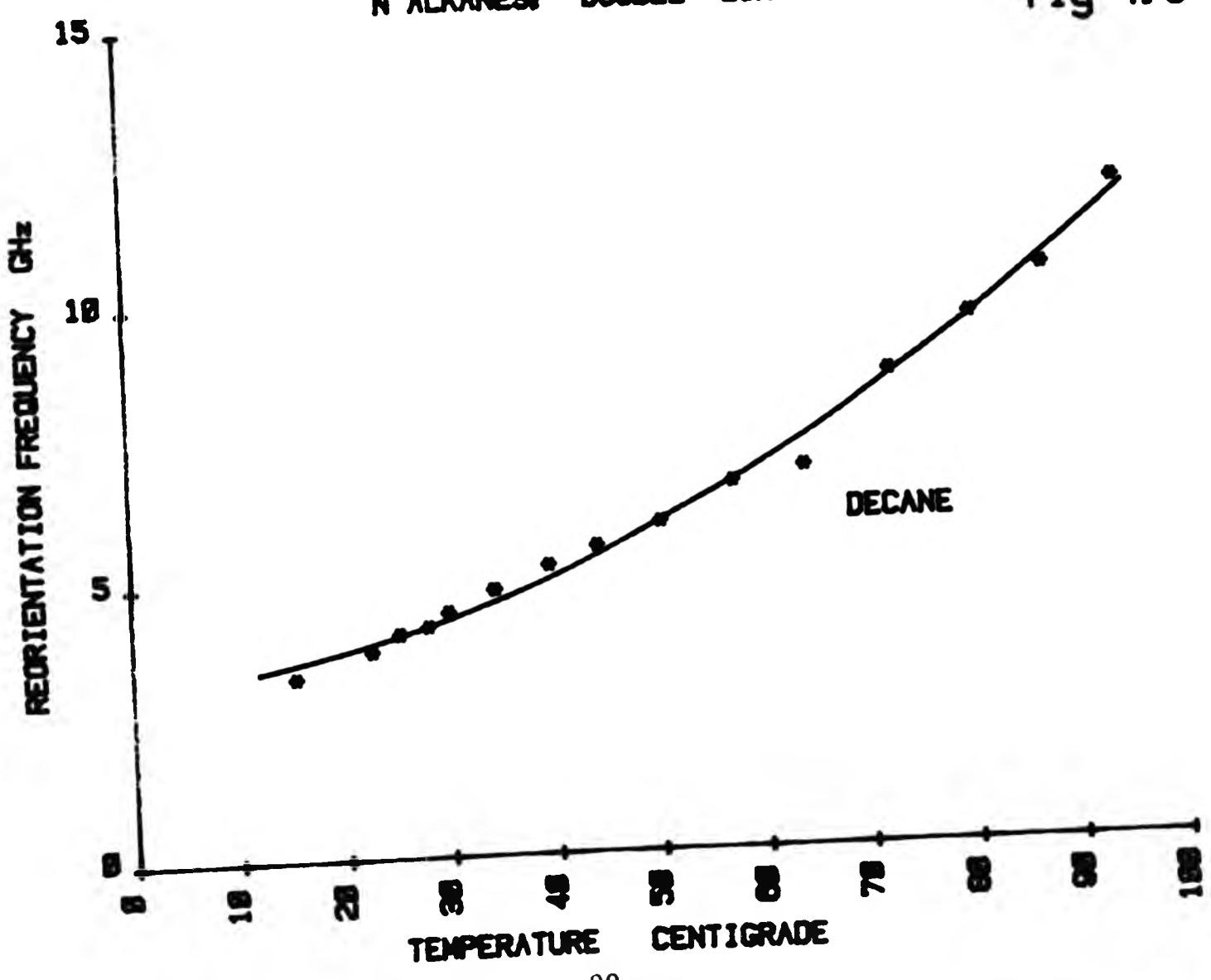
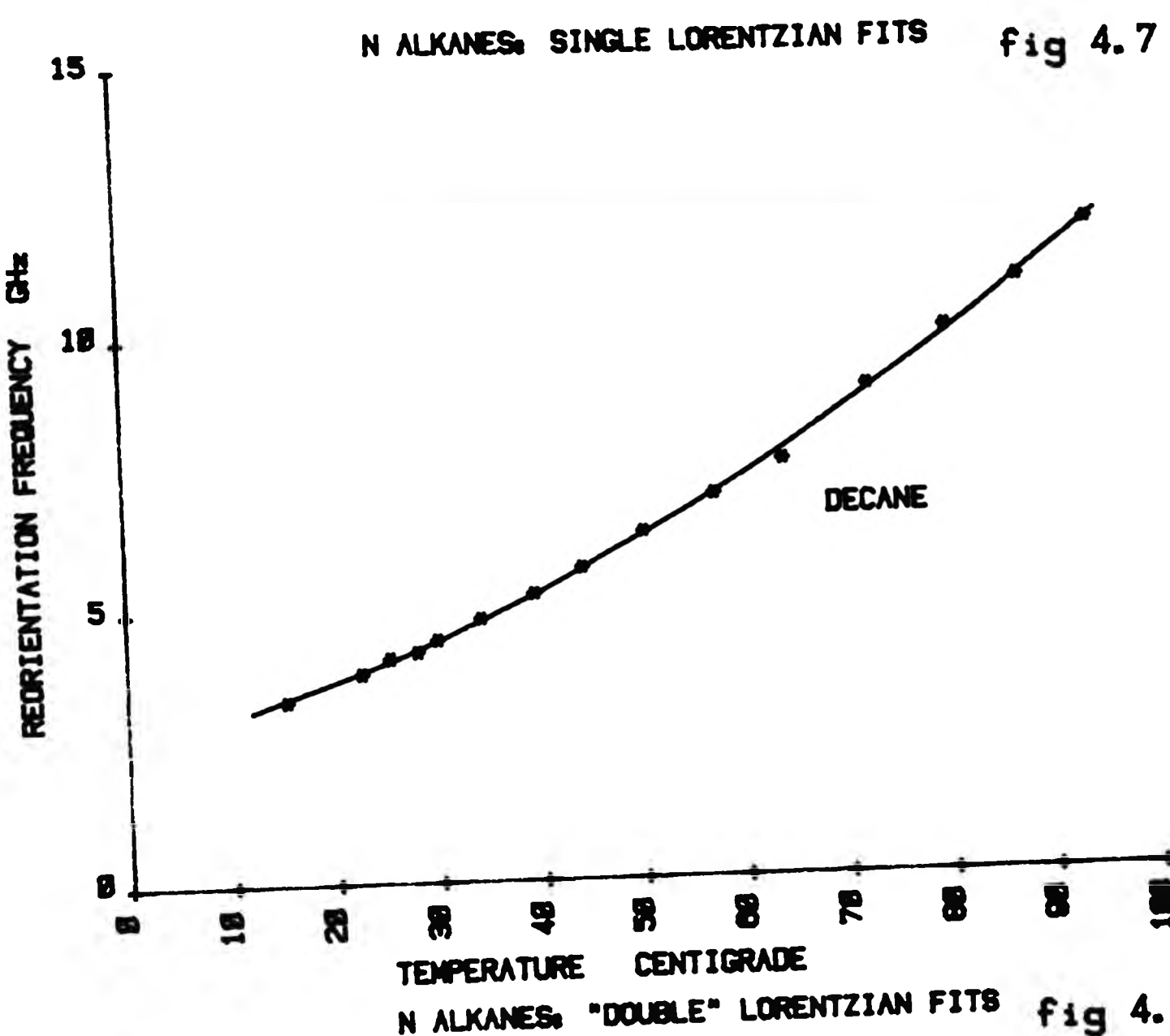
The method of analysis of the spectra obtained from the Fabry Perot system is detailed in the section on the experimental procedure. The fitting procedure fits the spectra to a central Lorentzian plus what the Fabry Perot sees as a flat background and where appropriate the fitting procedure continues to give a fit to what approximates to a Lorentzian with a dip plus a flat background. We present graphically the result of these fitting procedures and then continue with a simple analysis and a discussion of this data. Initially we examine the results from the depolarised Rayleigh spectra of the n-alkanes.

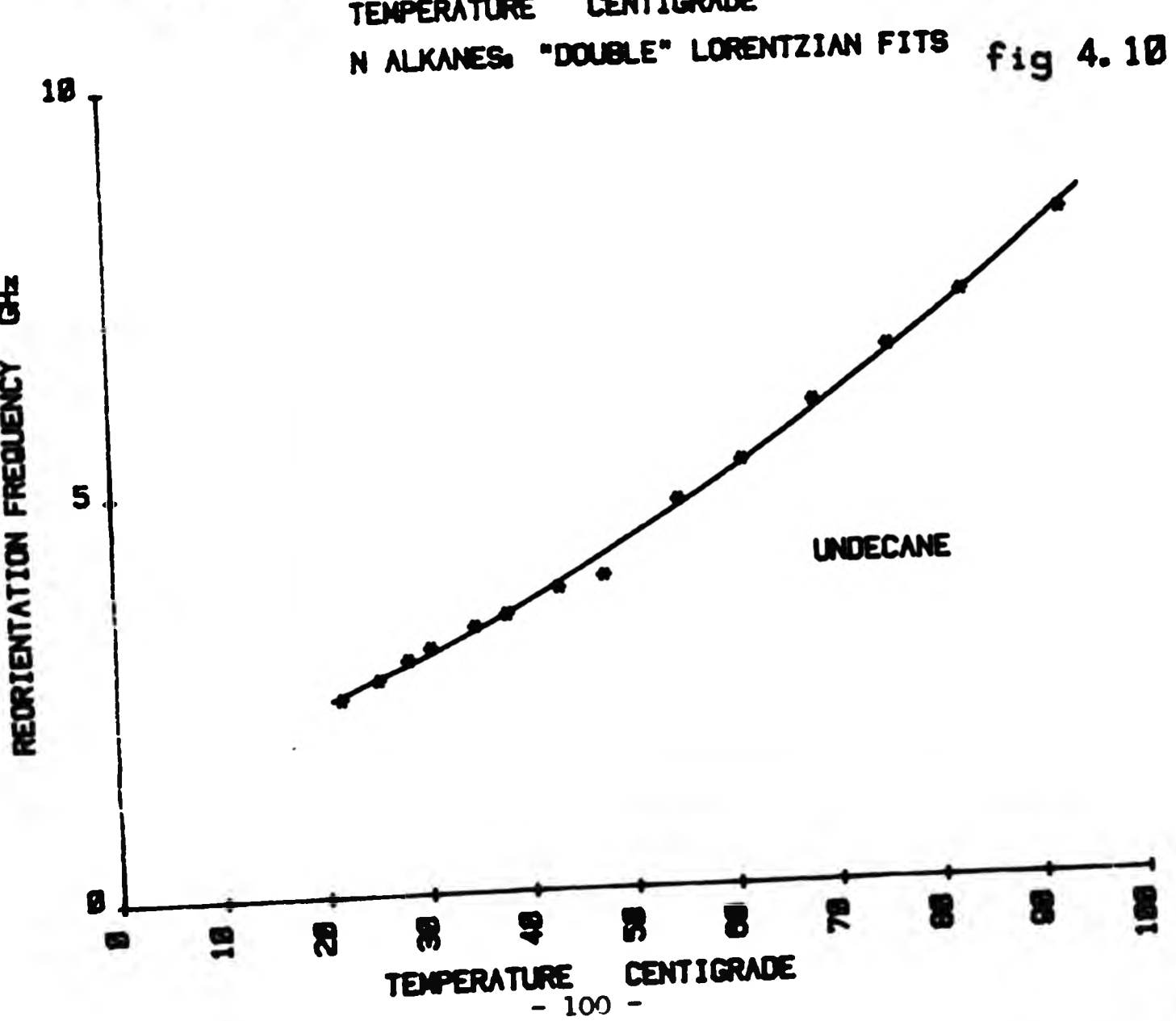
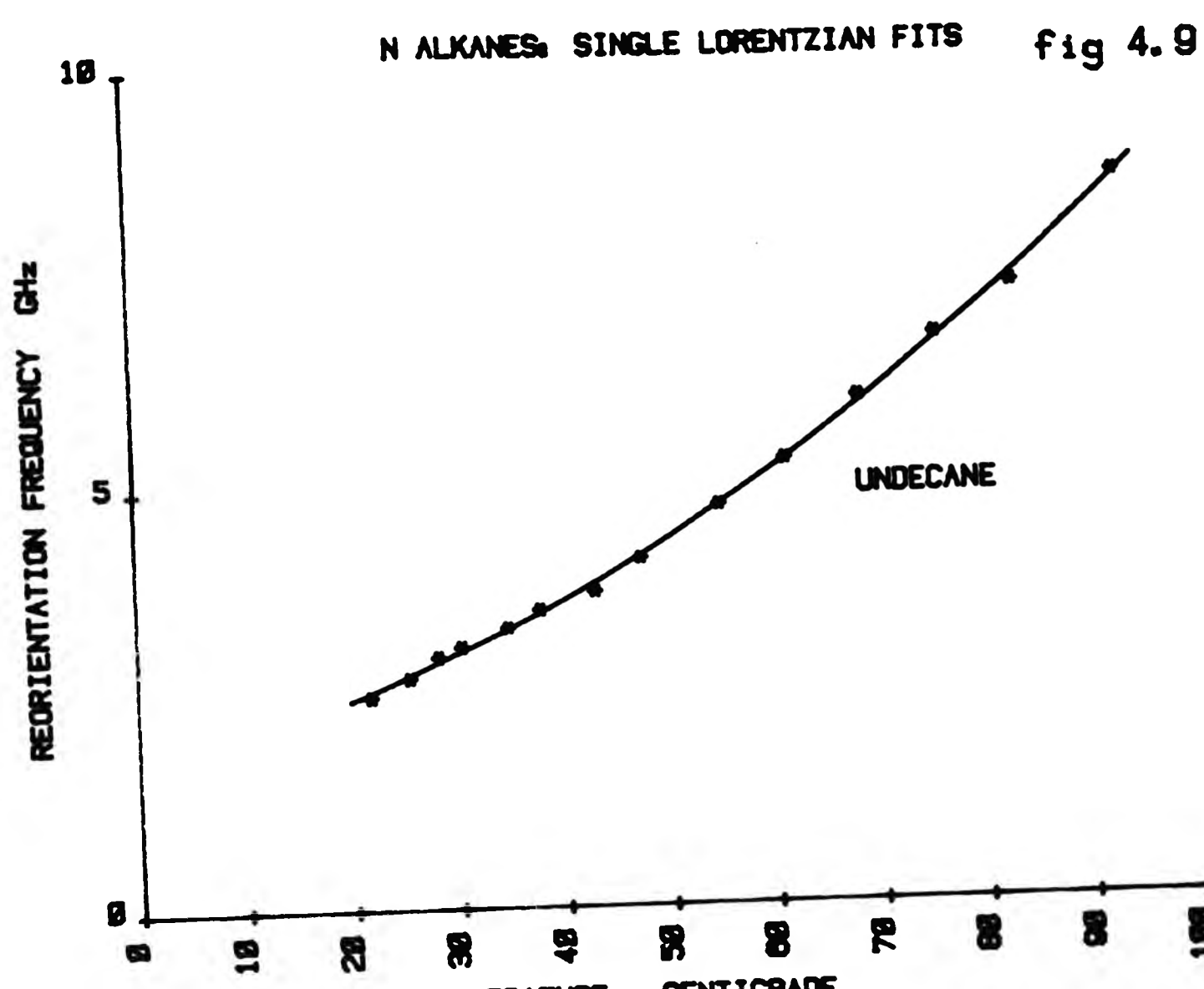
4.2.1 N-Alkanes: Neat Liquids

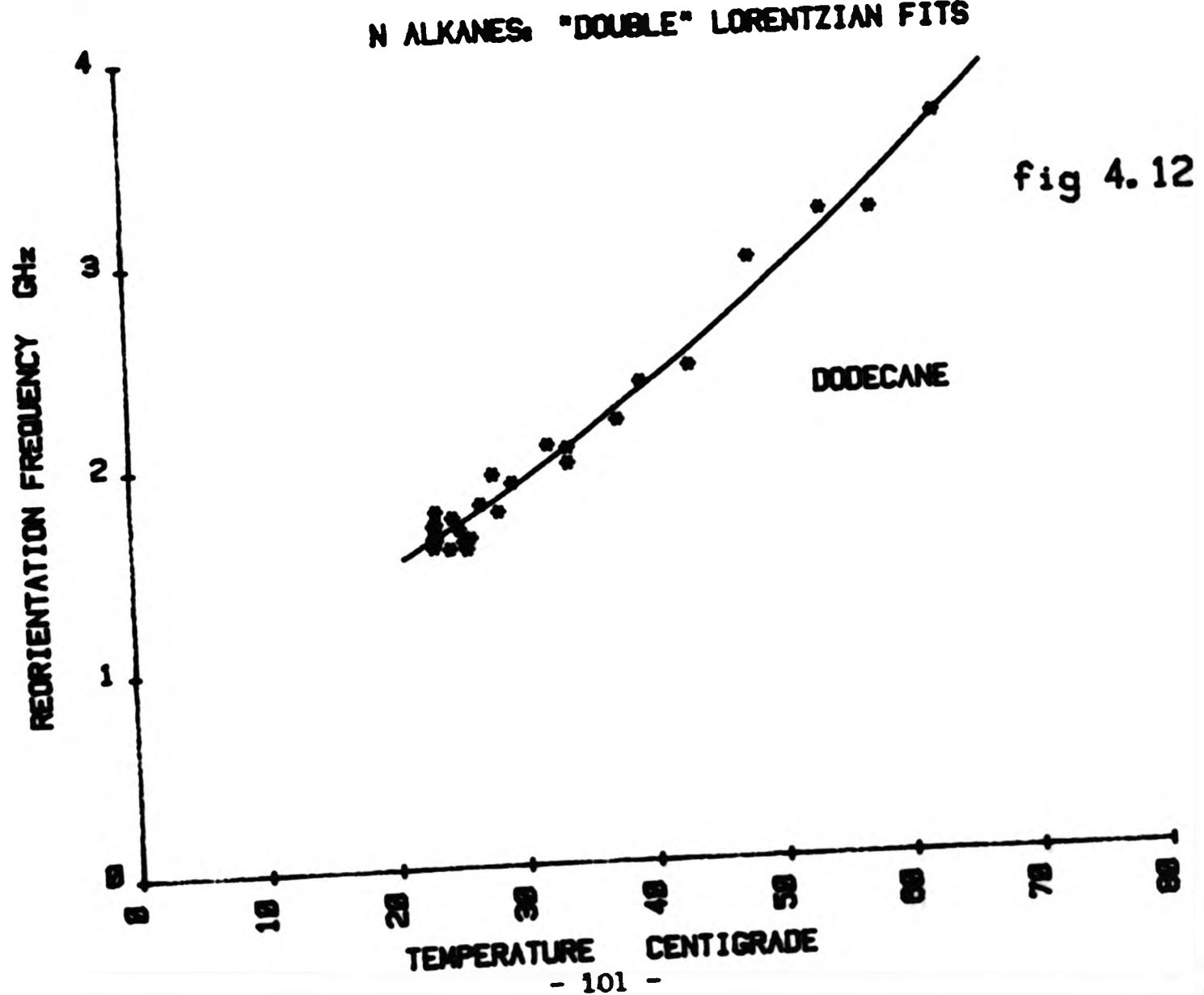
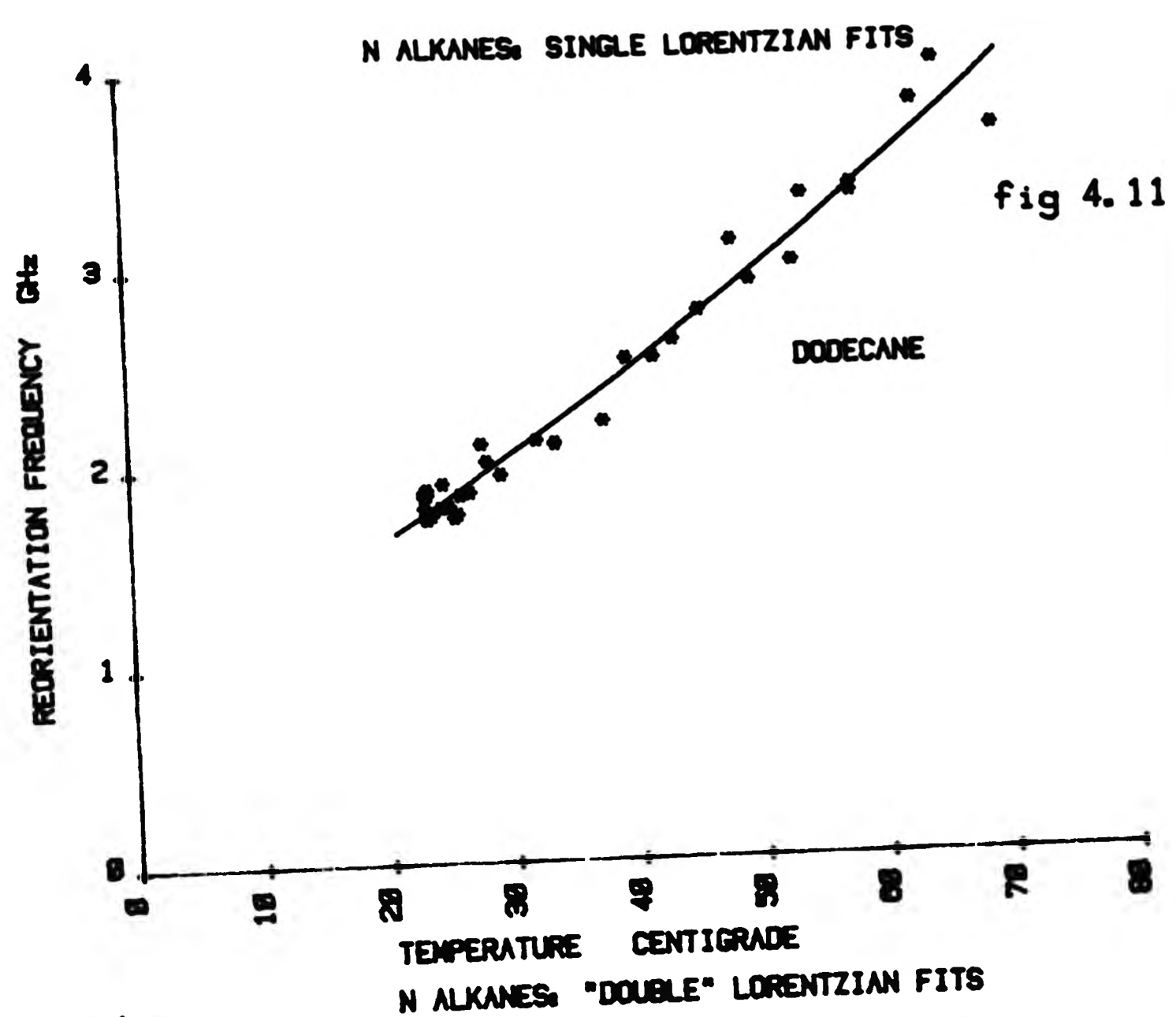
In this section we examine the results from fits to spectra of the n-alkanes. The liquids investigated were n-eicosane ($C_{20} H_{42}$) and the alkanes n-pentadecane to n-pentane ($C_{15} H_{32}$ to $C_5 H_{12}$) over temperature ranges which were easily available without the use of a

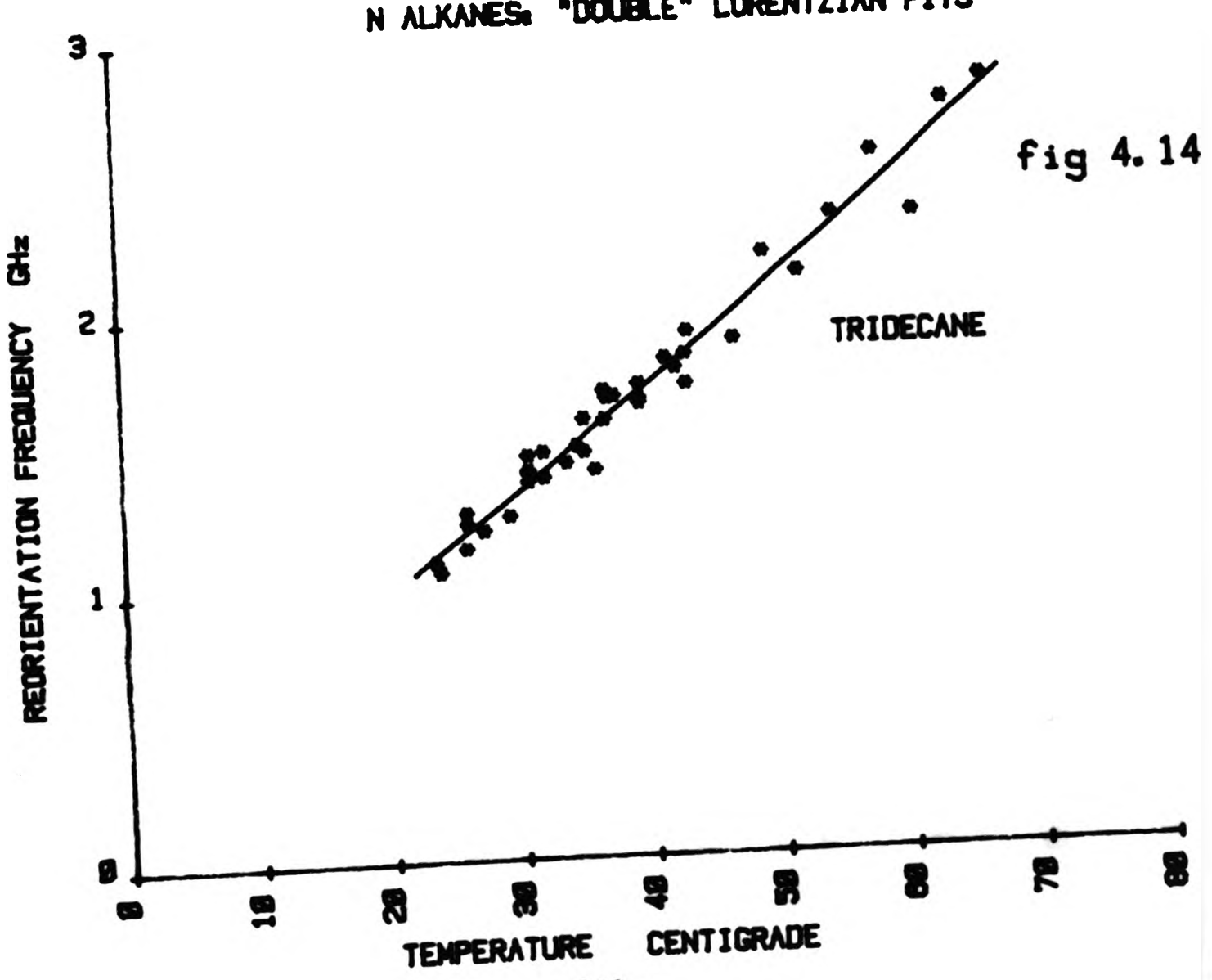
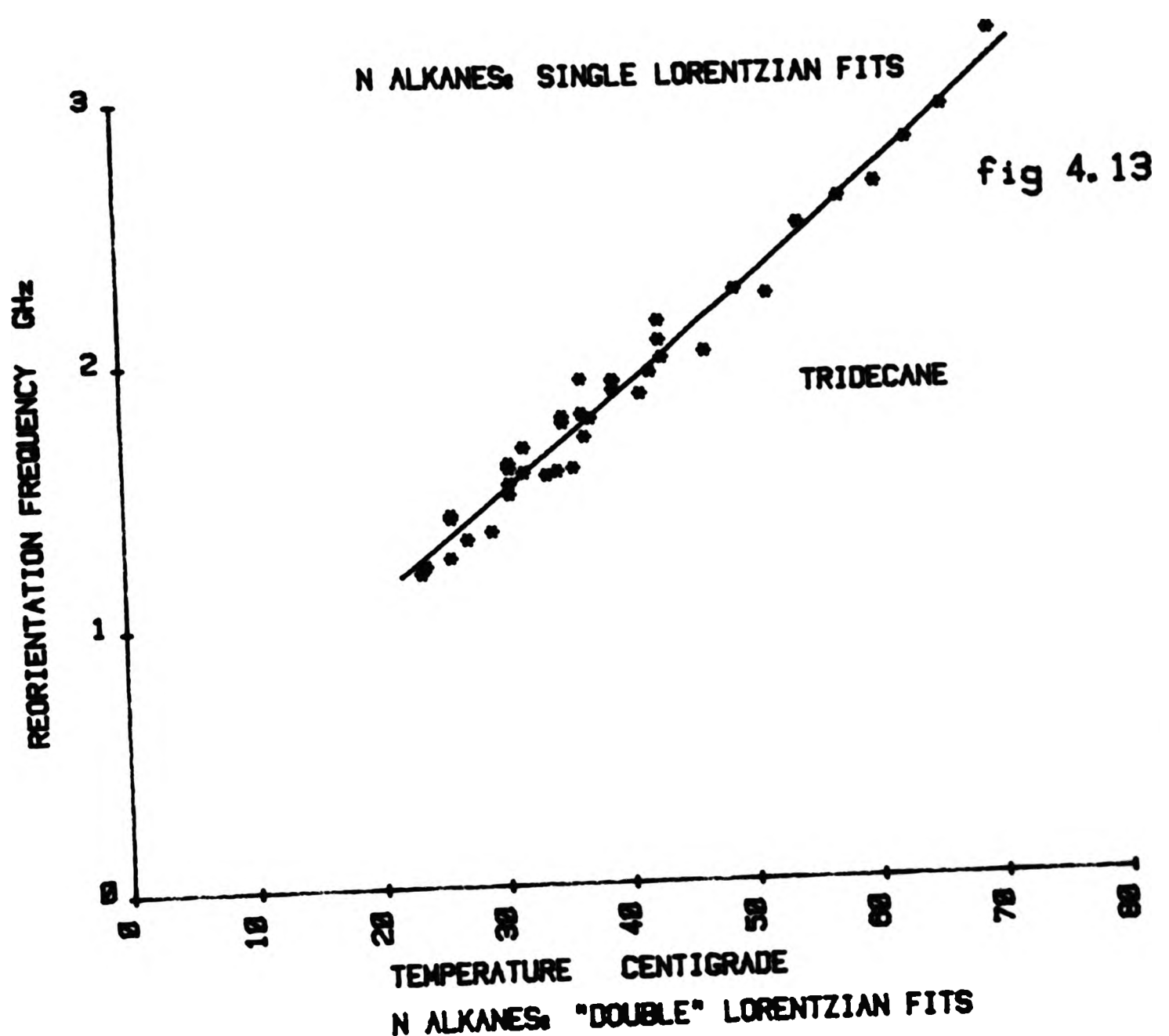




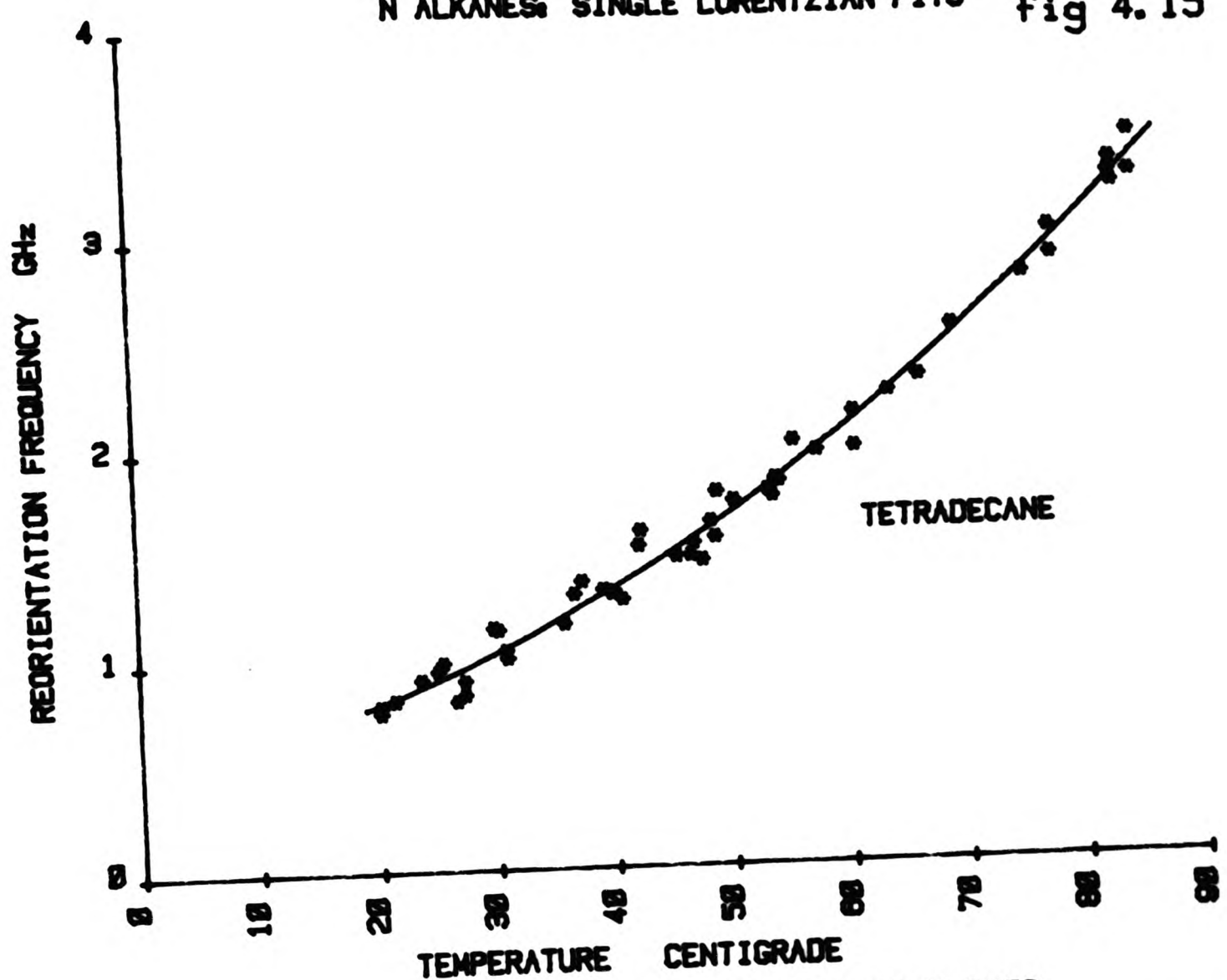




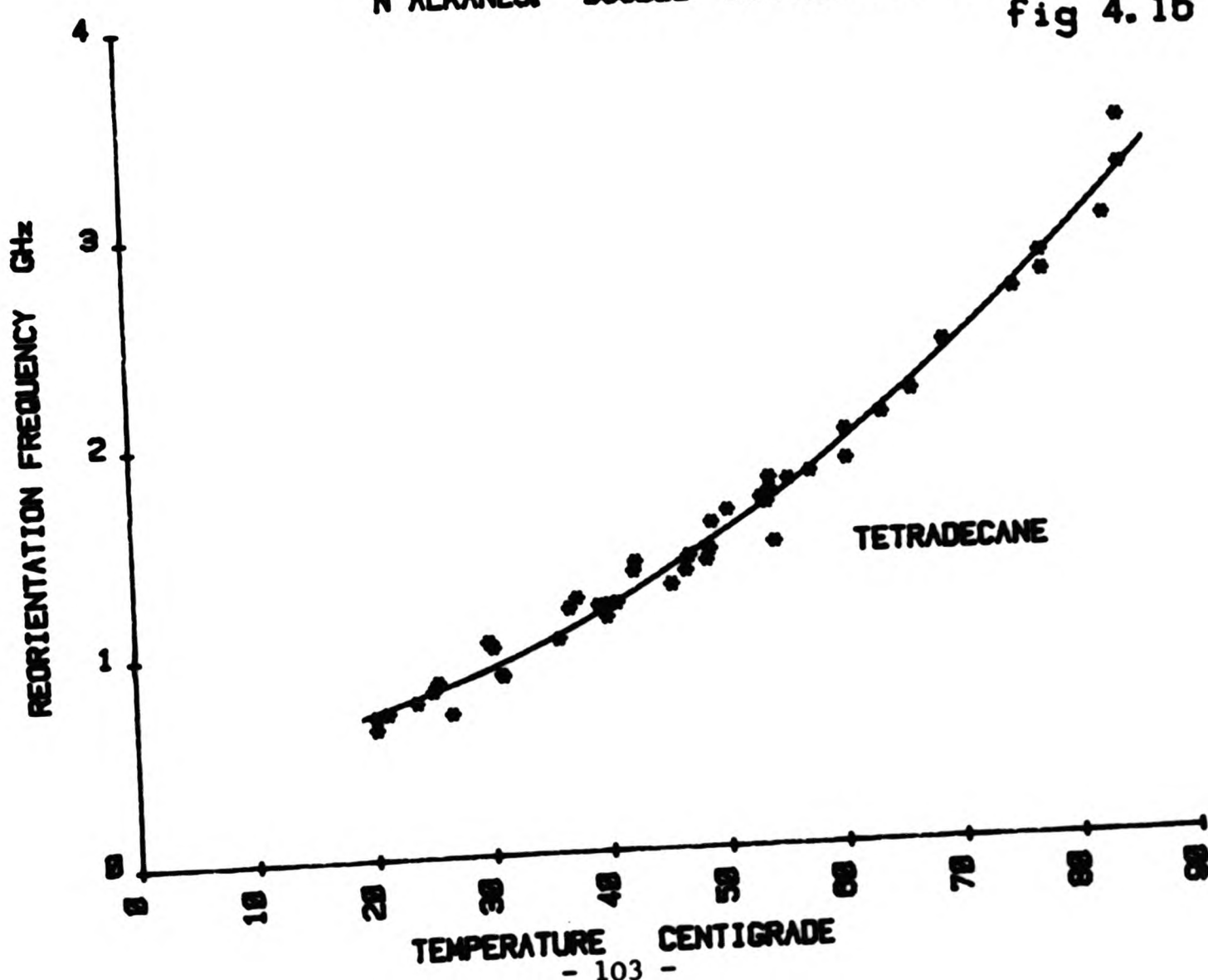


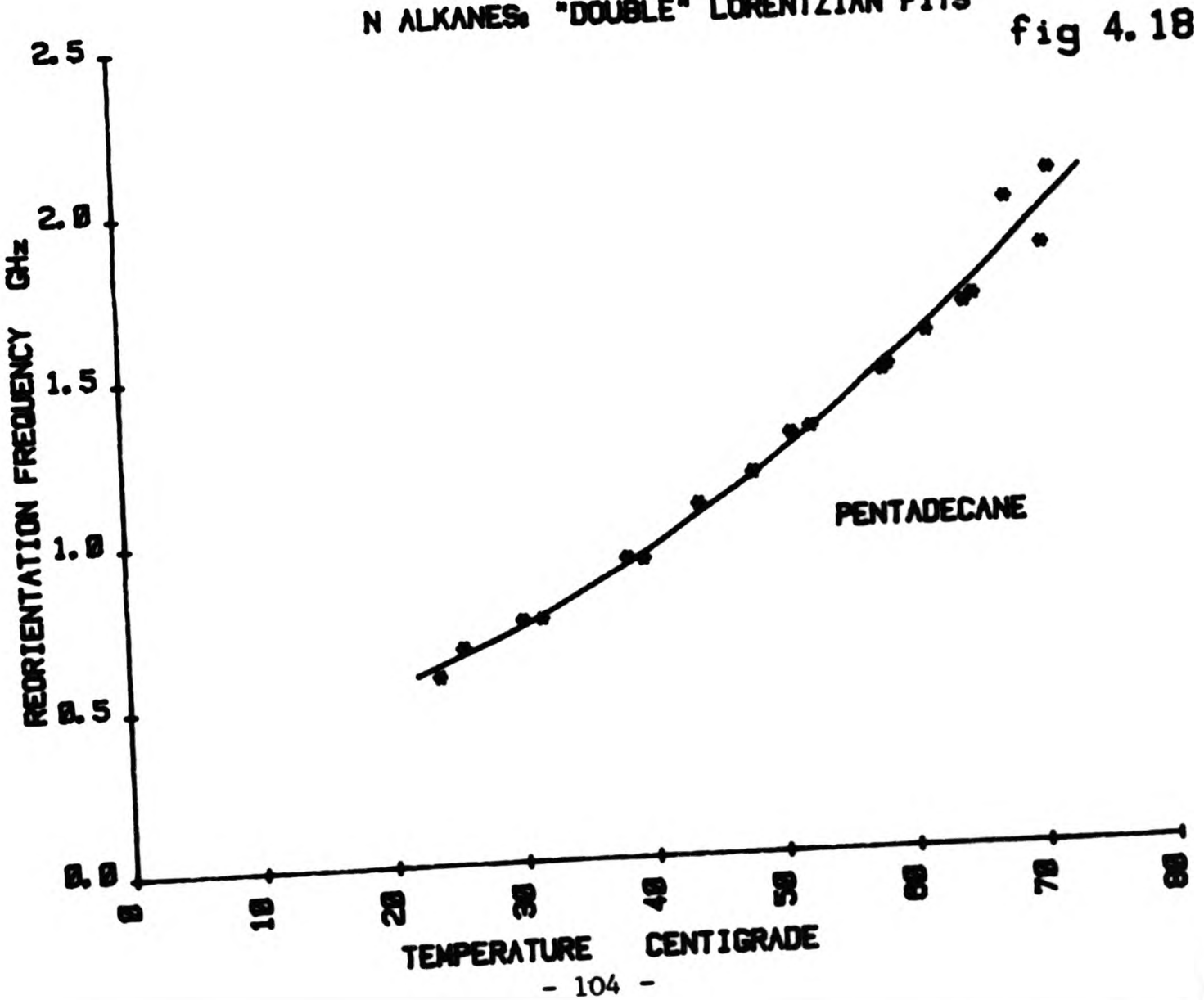
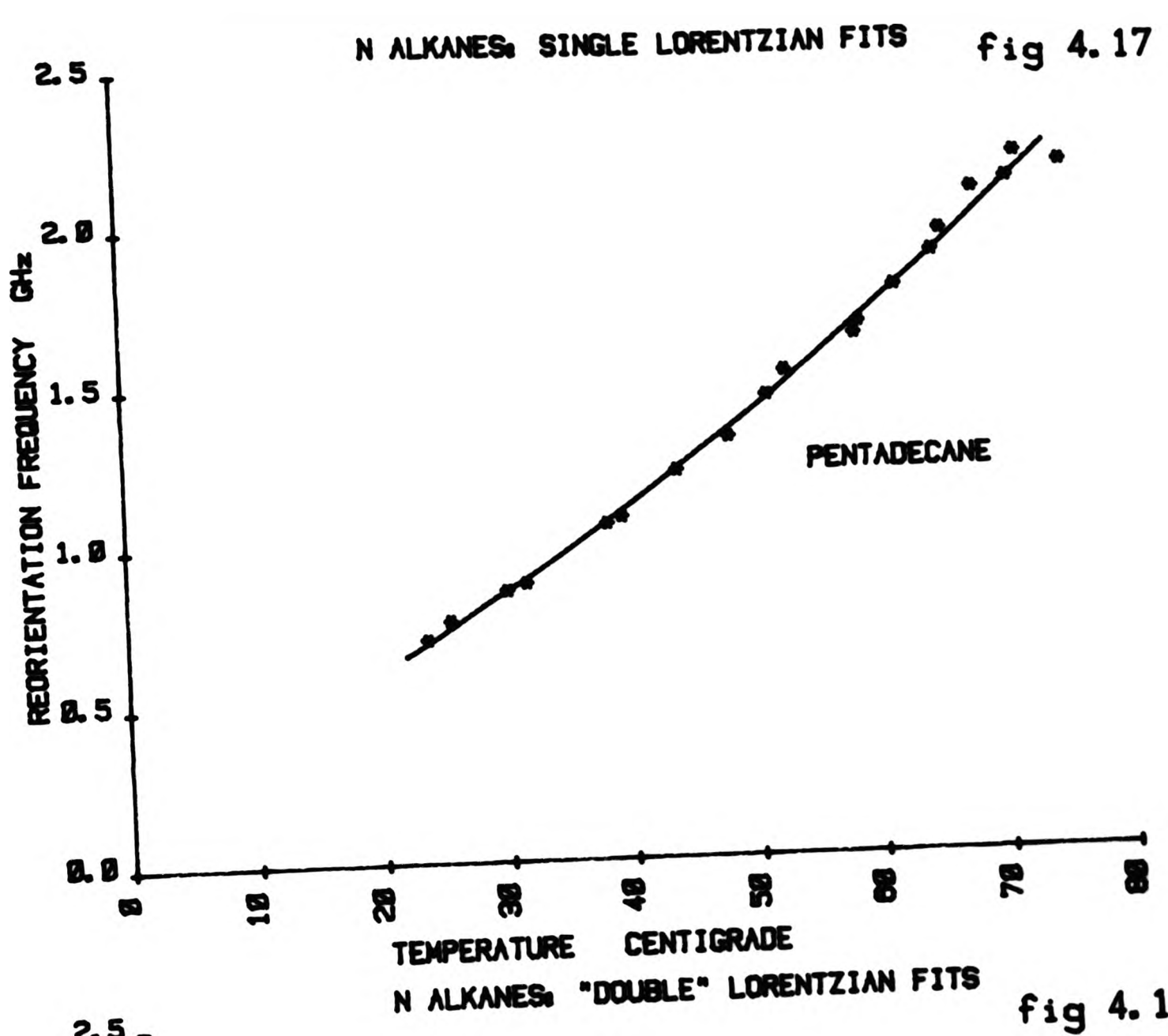


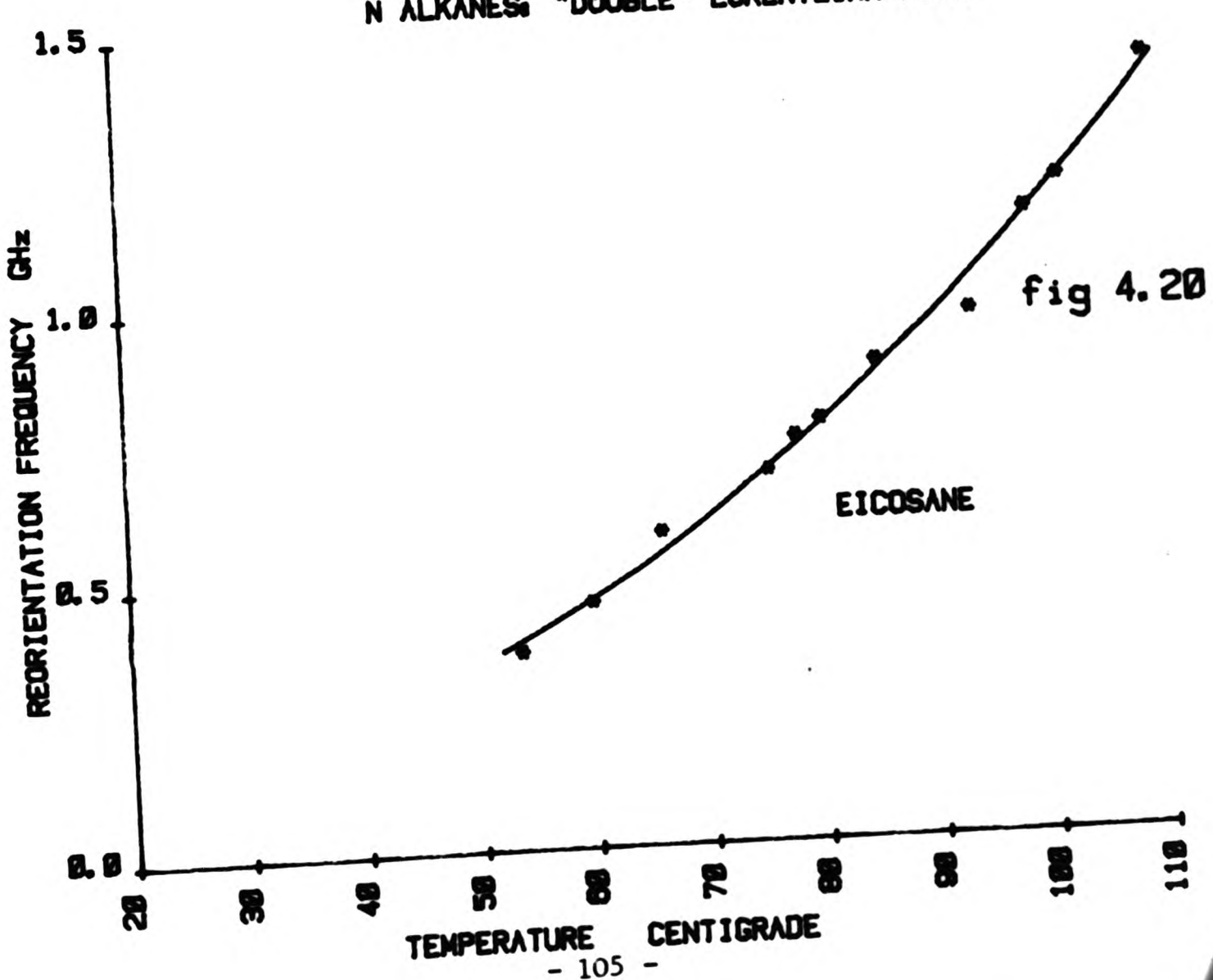
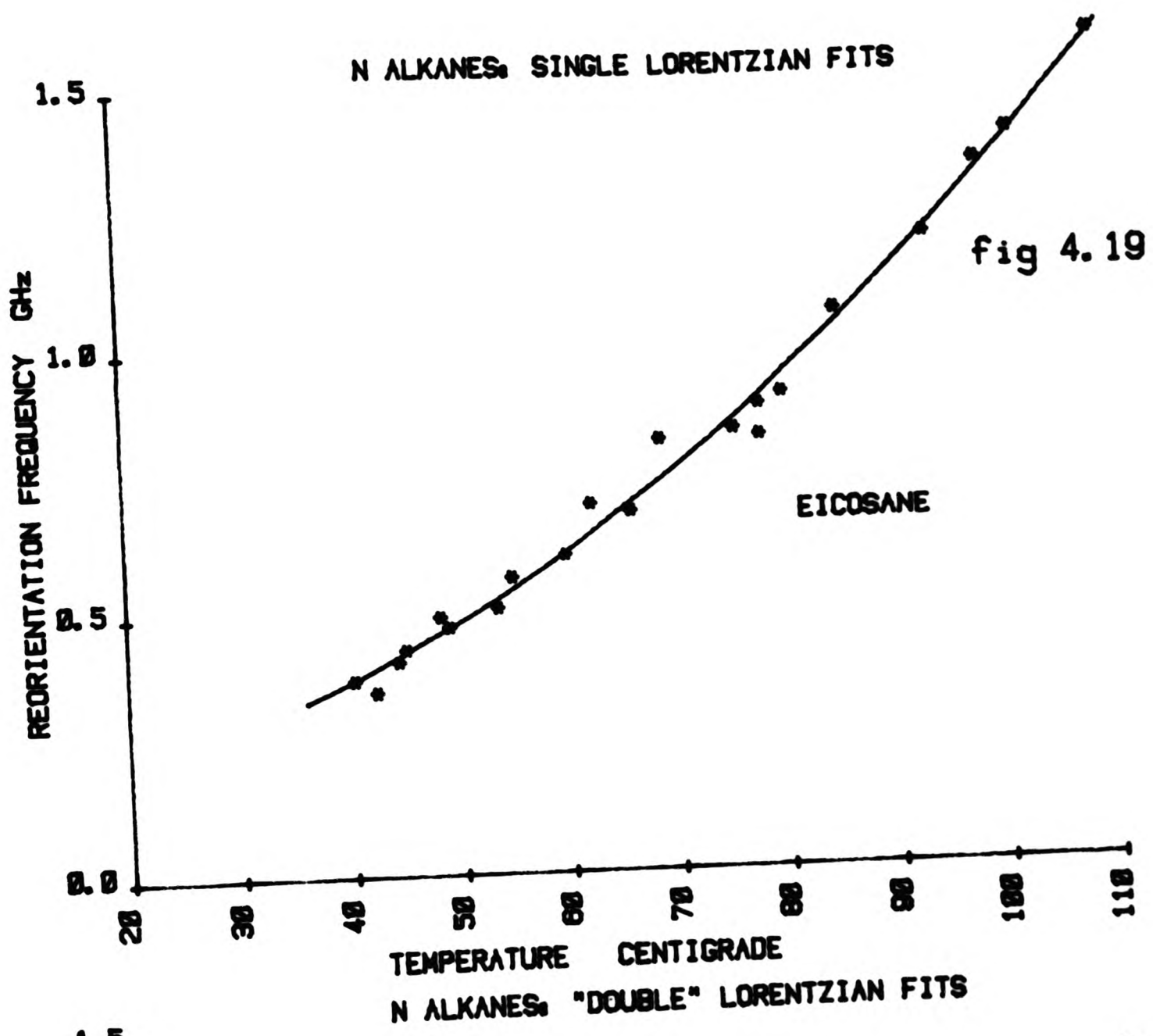
N ALKANES: SINGLE LORENTZIAN FITS fig 4.15



N ALKANES: "DOUBLE" LORENTZIAN FITS fig 4.16







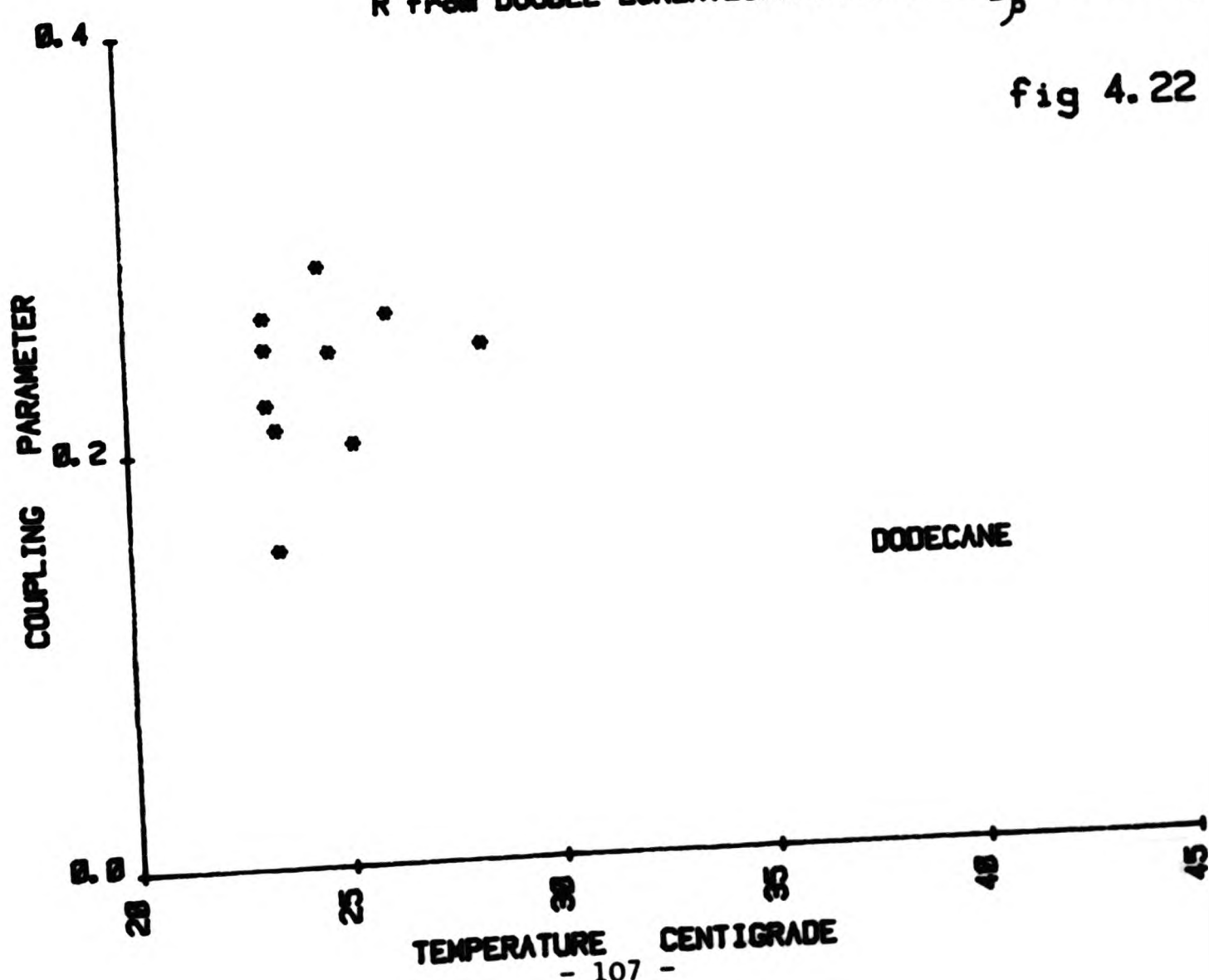
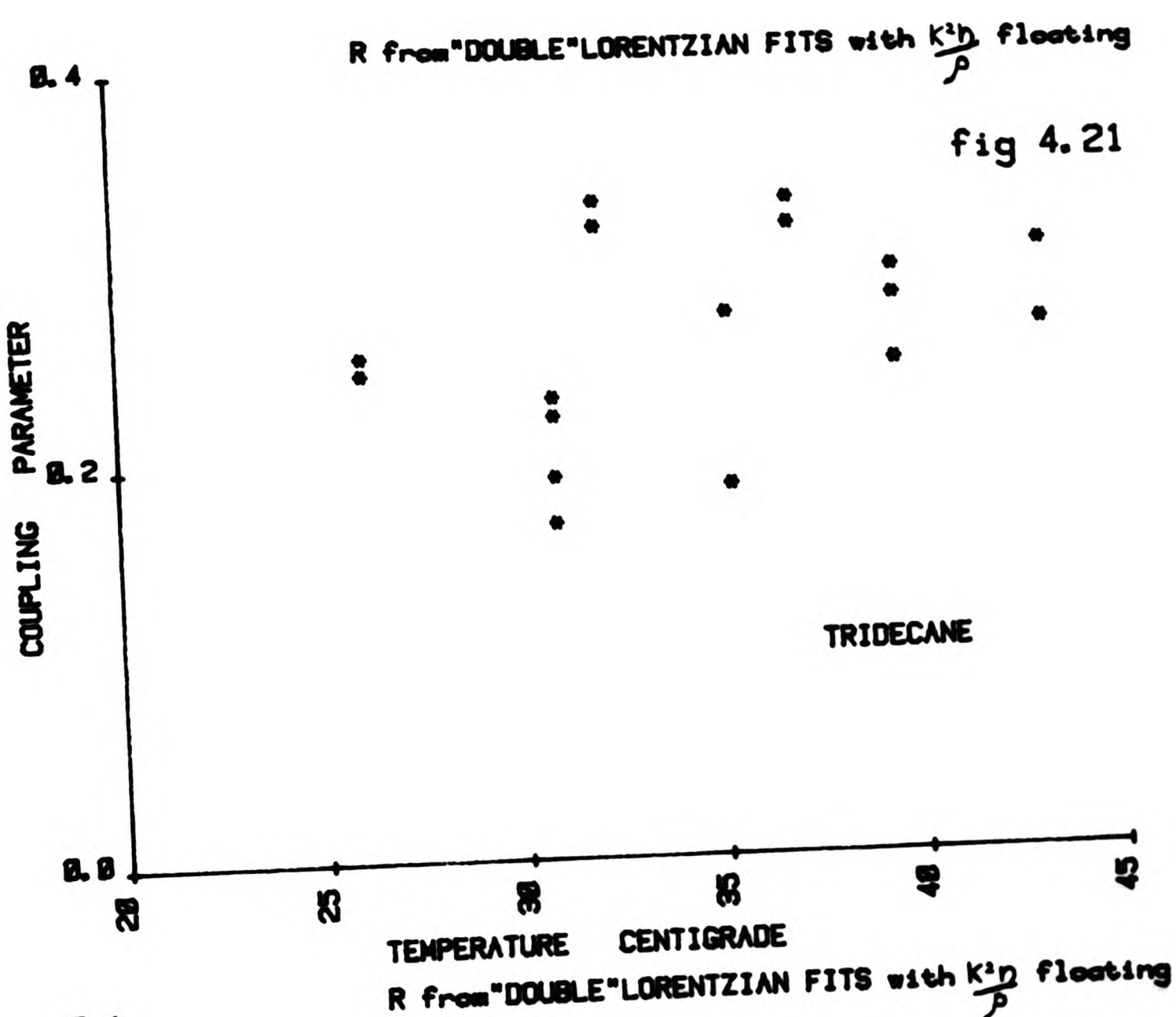
cryostat. The error on each individual peak half width measured was of the order of 6%. For the liquids which were first examined (n-eicosane, tetradecane, tridecane and dodecane) the procedure was simply to take one spectrum at each temperature investigated. There is therefore a fairly large scatter on the results given. For the other n-alkanes which were investigated at a later stage in the course of the work the procedure evolved was to take spectra at a fewer number of temperatures but to take three or four spectra at each and then to average the results. In this way the data obtained had less scatter on the final results.

Where appropriate a fit to Lorentzian plus dip or Double Lorentzian was performed as well as the fit to the single Lorentzian. In these cases the half width obtained from the more complicated fitting procedure is the correct one but we display the data from the simple fitting procedure to enable a comparison of the two sets of half widths to be made. (Figs 4.3 to 4.20).

We also present values for the R parameter obtained from the fit to Lorentzian plus dip, and values of the dip half width compared to the theoretical values of $K^2 n/\rho$. (Figs 4.21 to 4.29).

The graphs presented here provide a reasonably comprehensive set of light scattering data for the n-alkanes. The peak half widths obtained may be interpreted using the Stokes Einstein relation discussed in Chapter 2.

τ_{LS} the light scattering correlation time is given by $\frac{1}{2\pi f_1}$. τ_{LS} is related to the macroscopic viscosity of the liquid by equation 2.31.



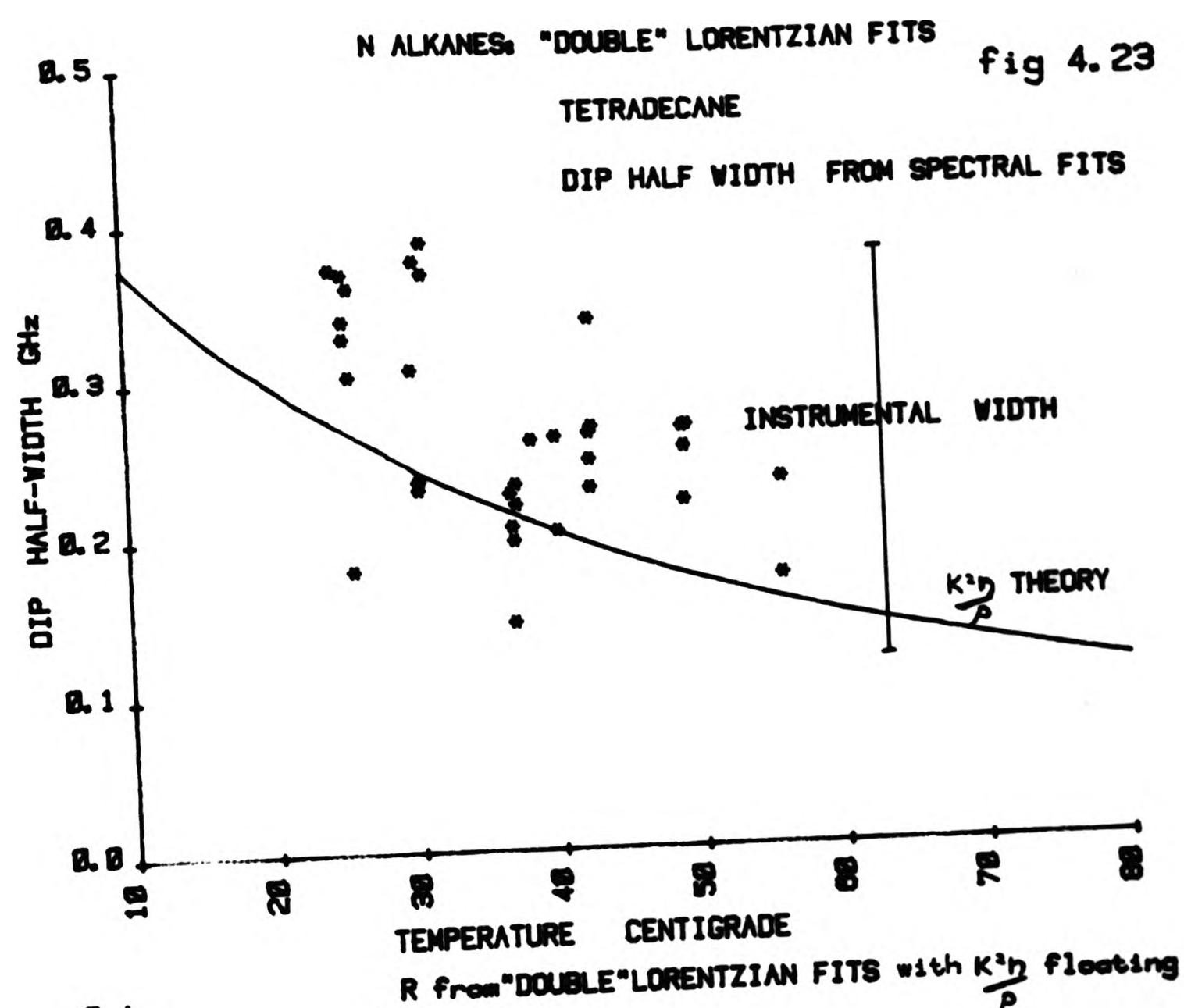


fig 4.23

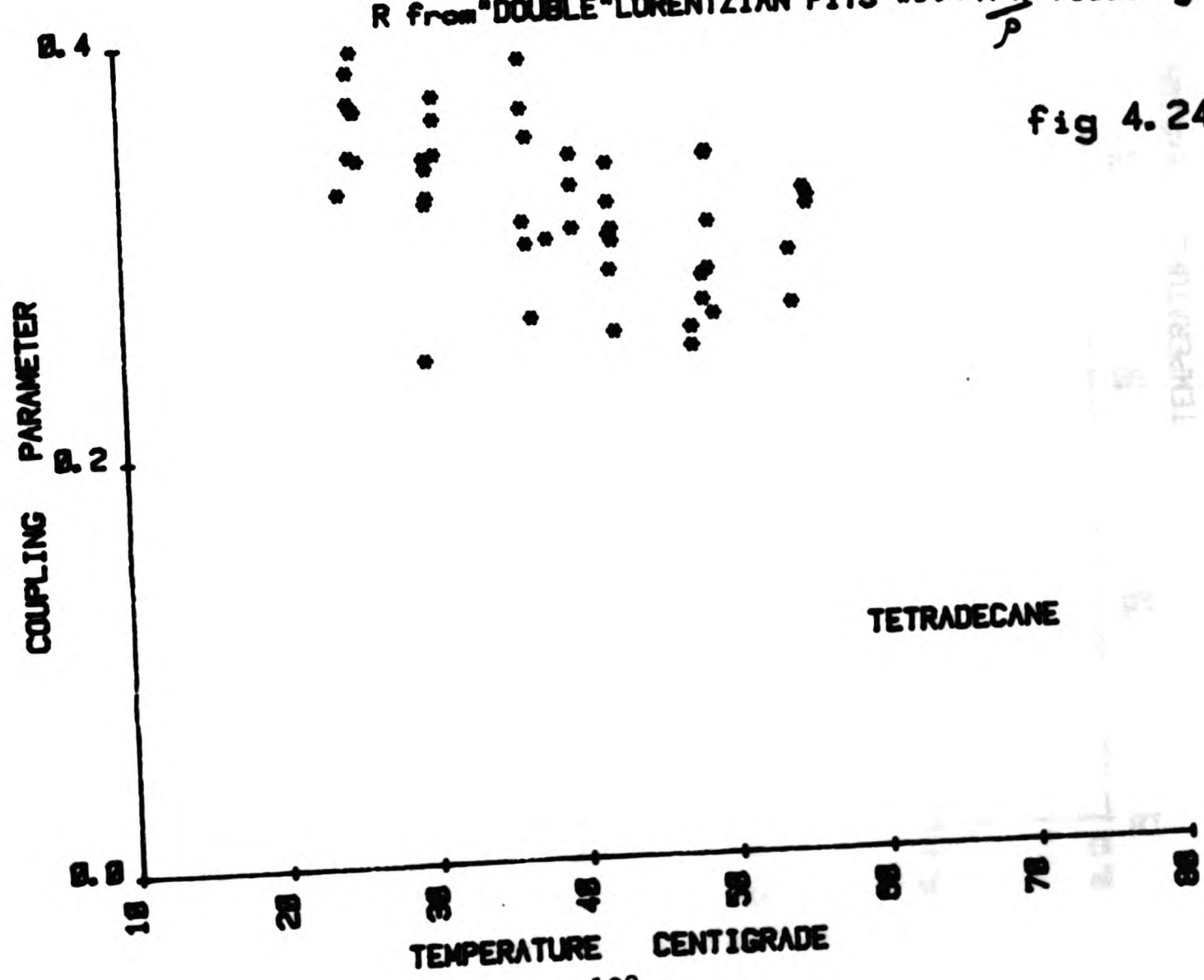


fig 4.24

fig 4.25

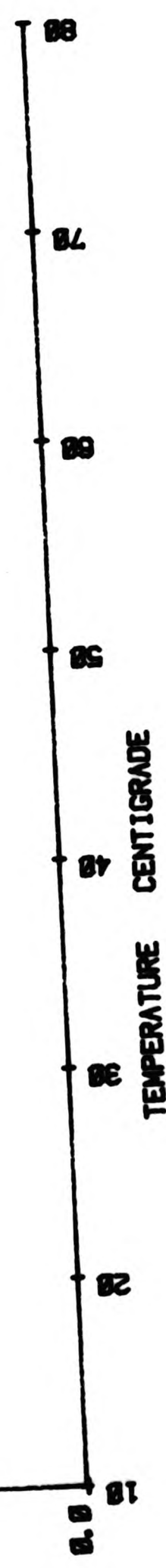
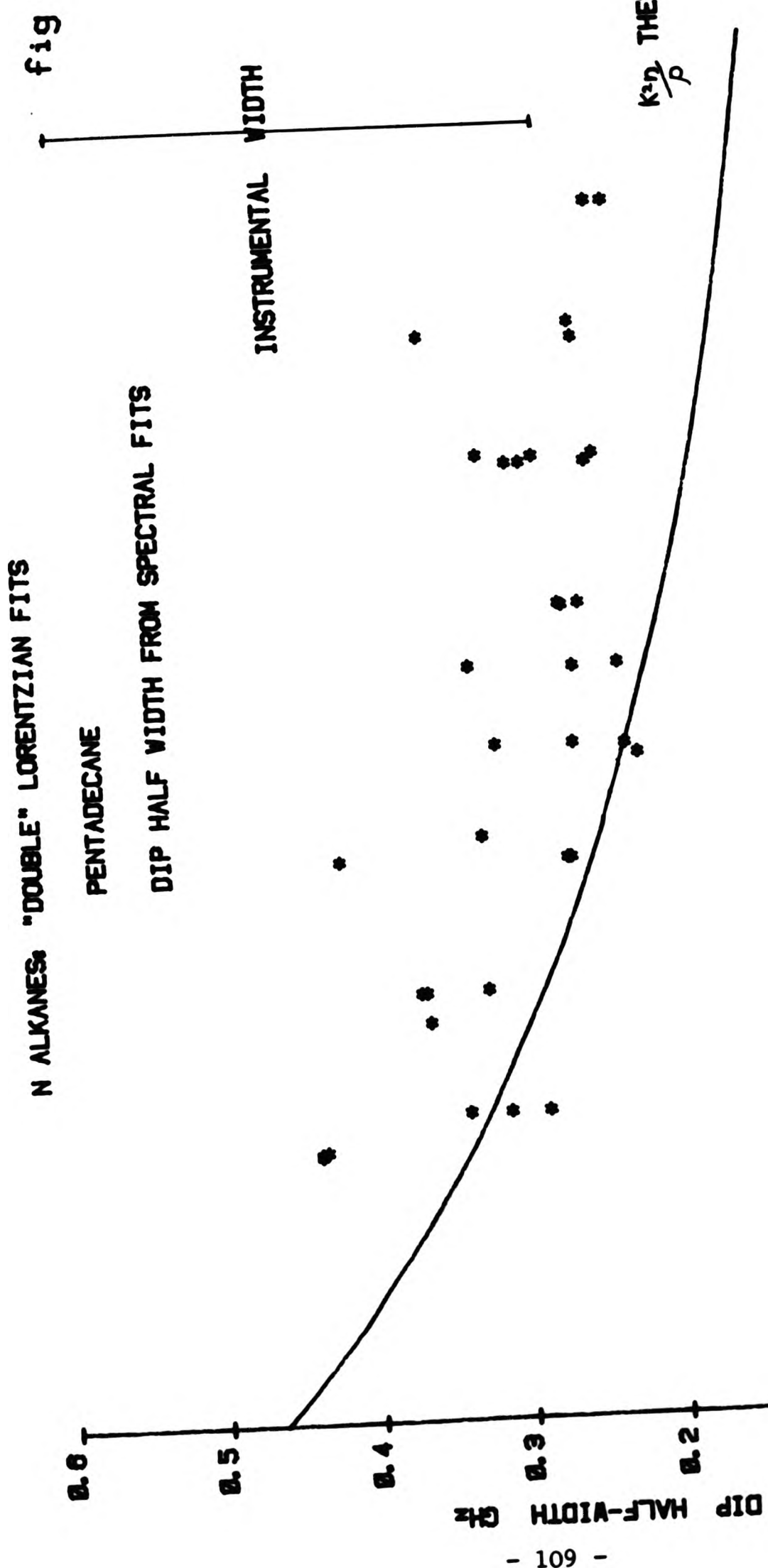
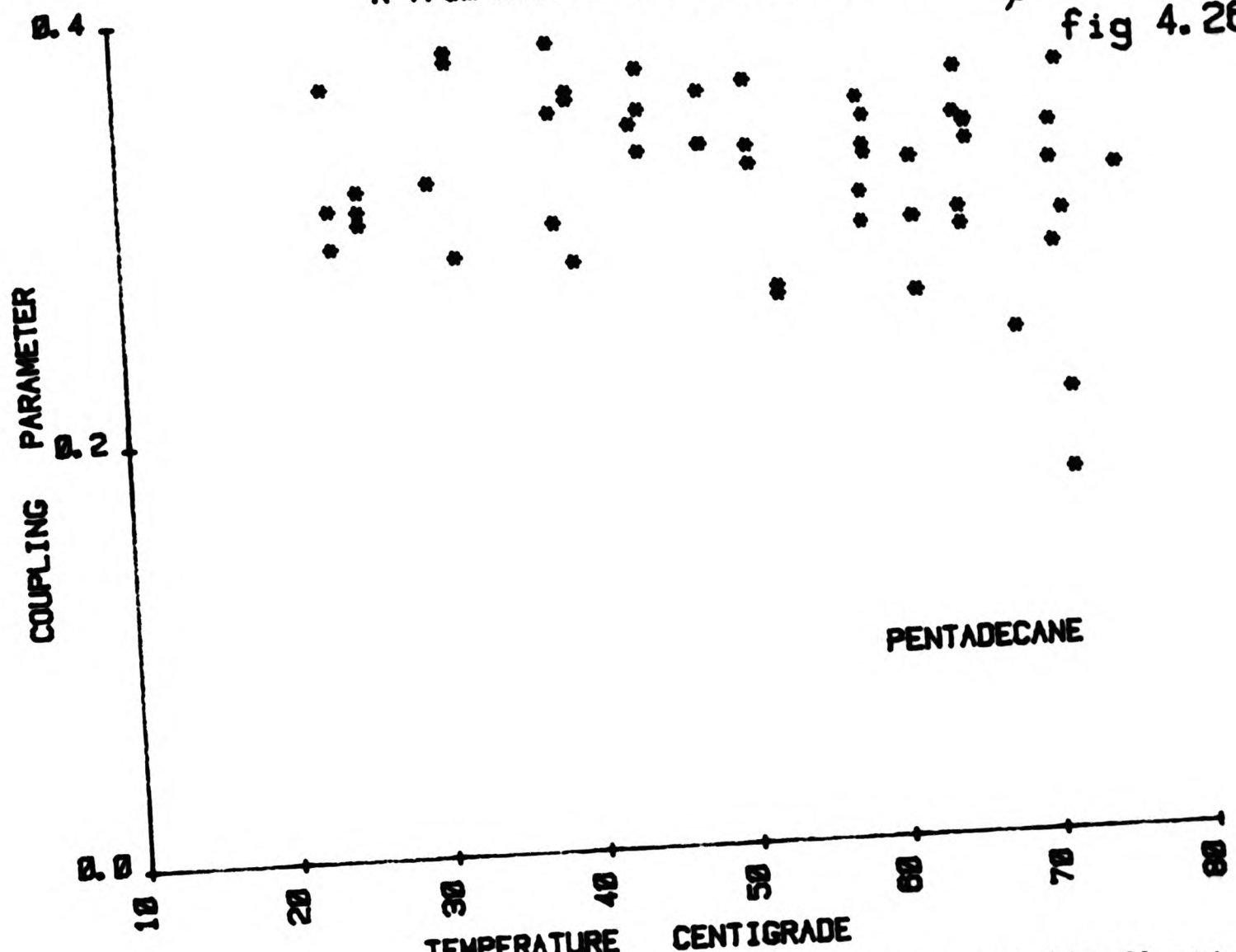


fig 4.25



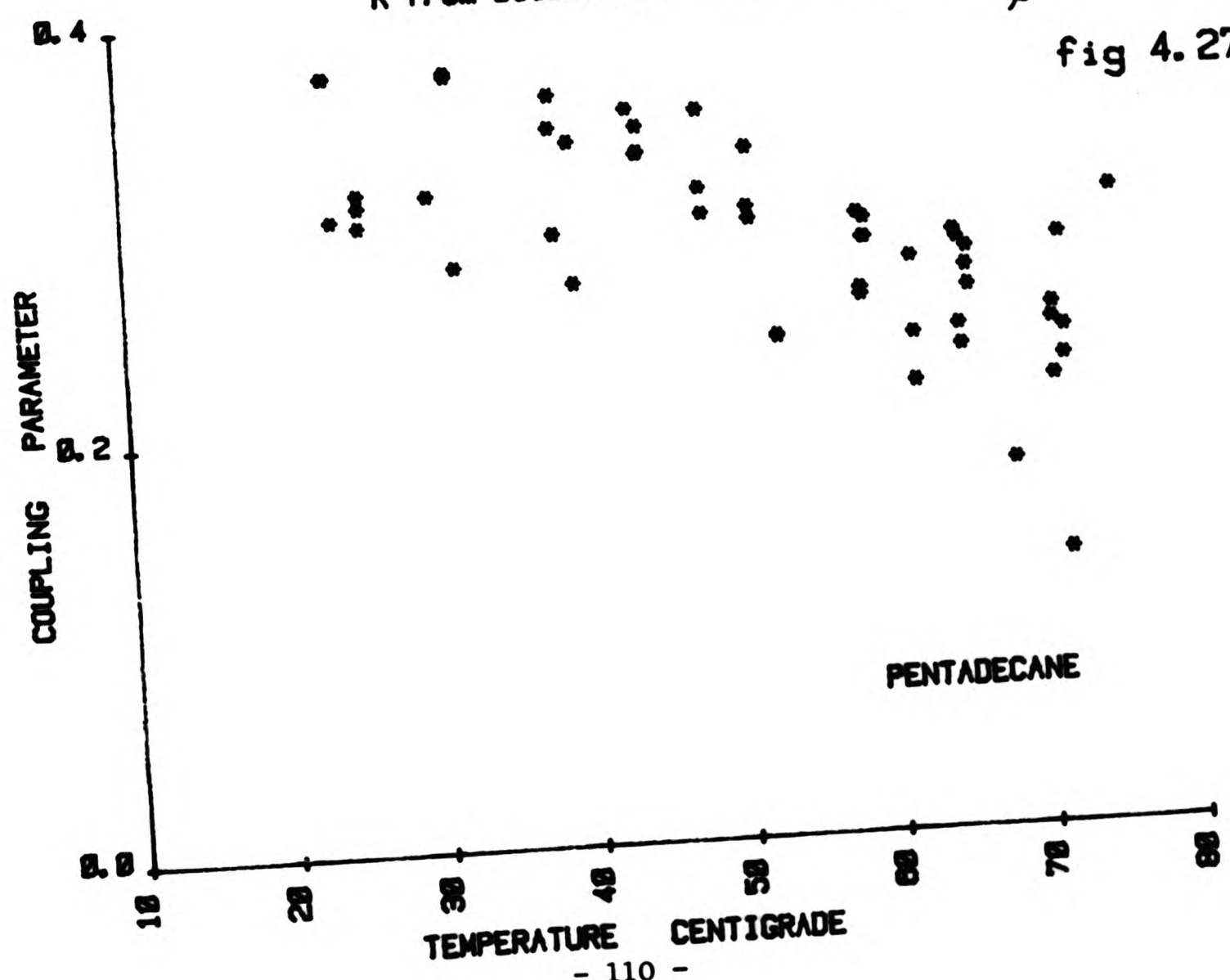
R from "DOUBLE" LORENTZIAN FITS with $\frac{K^2 n}{P}$ fixed

fig 4.26



R from "DOUBLE" LORENTZIAN FITS with $\frac{K^2 n}{P}$ floating

fig 4.27



N ALKANES: "DOUBLE" LORENTZIAN FITS

fig 4.28

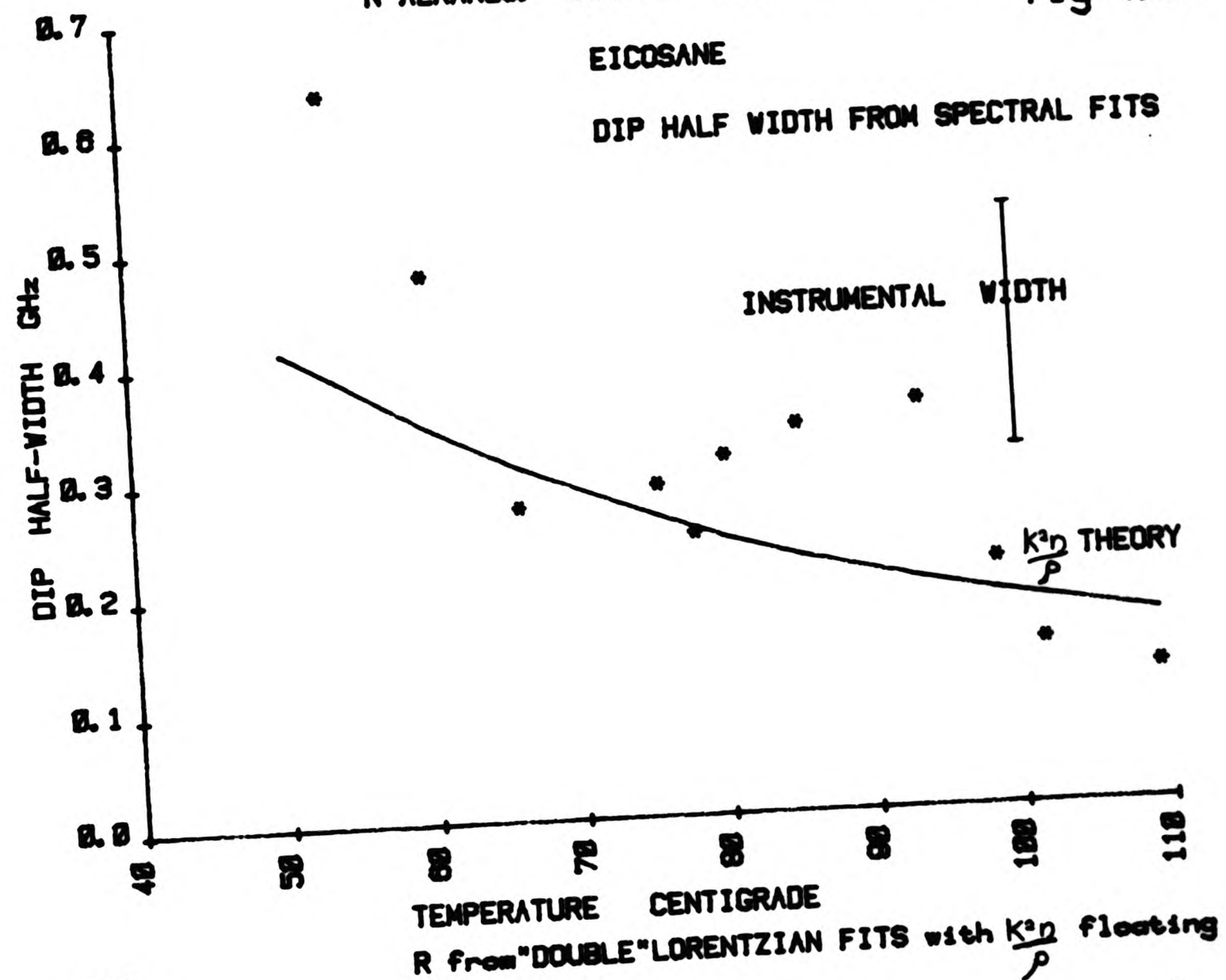
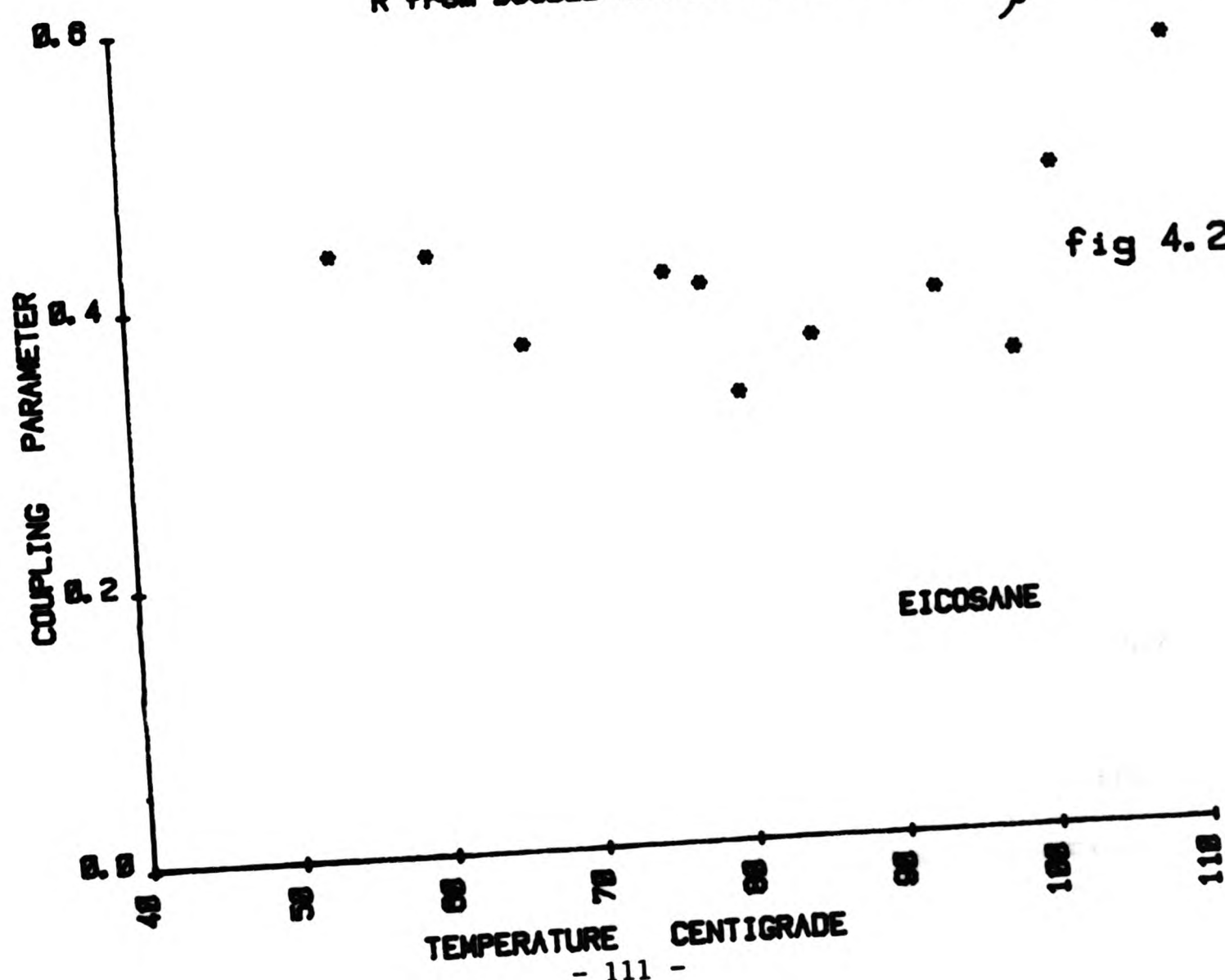


fig 4.29



$$\tau_{LS} = (g_2/j_2) \left| \frac{\alpha p V \eta}{K T} + \tau_0 \right|$$

2.31

(g_2/j_2) is the orientational correlation parameter

p is the Perrin factor given by equation 2.28

α is the stick slip coefficient discussed in Chapter 2

V is the molecular volume

η is the macroscopic viscosity of the liquid

T is the absolute temperature.

This equation is used as the basis of our interpretations of the light scattering data obtained for the n-alkanes and also for the n-alcohols.

Results

R PARAMETERS

Table 4.4

R Parameter

LIQUID	FITS TO LORENTZIAN + DIP	FITS WITH $\frac{K^2 \eta}{\rho}$ FIXED
C ₂₀ H ₄₂	0.41 ± 0.07	
C ₁₅ H ₃₂	0.30 ± 0.04	0.33 ± 0.03
C ₁₄ H ₃₀	0.33 ± 0.03	
C ₁₃ H ₂₈	0.27 ± 0.05 *	
C ₁₂ H ₂₆	0.24 ± 0.04 *	

* only over restricted temperature range.

These R values are in agreement with R values obtained for other molecular liquids. Referring to the graphs of R values against temperature (Figs 4.21, 4.22, 4.24, 4.27, 4.29) it is seen that the parameter remains approximately constant over the temperature ranges

investigated in which the dip is readily observable, except in the case of the R values obtained for fits to Lorentzian plus dip for pentadecane. In this case there appears to be a slight decrease with increasing temperature. This is likely to be an artefact due to errors in the deconvolution procedure. The higher temperatures correspond to the narrowest dip half width and from the graphs which compare the theoretical values of $\frac{K^2 n}{\rho}$ with the observed values of dip half width (Figs 4.23, 4.25, 4.28) it is apparent that deconvolution does not work as well as it could - however this is due to the fact that the instrumental width is comparable to size due to the dip half width.

The general trend in the R parameters obtained for the alkane chains is that the mean values obtained decrease as chain length decreases. The values obtained for C₁₂H₂₆ and C₁₃H₂₈ were obtained only over a restricted temperature range, due to the fact that at the higher temperatures at which the dip is still visible in other liquids, in these liquids the viscosity is such that the dip half width is much narrower than the main structure and is therefore not resolved.

STOKES EINSTEIN RELATION

The Stokes Einstein relation is given by

$$\tau_{LS} = G \left(\frac{\alpha p V}{K} \frac{n}{T} + \tau_0 \right)$$

2.31

In all cases τ_{LS} from fits to a Lorentzian and Lorentzian plus dip is plotted against the quantity n/T . (Figs 4.30 to 4.47).

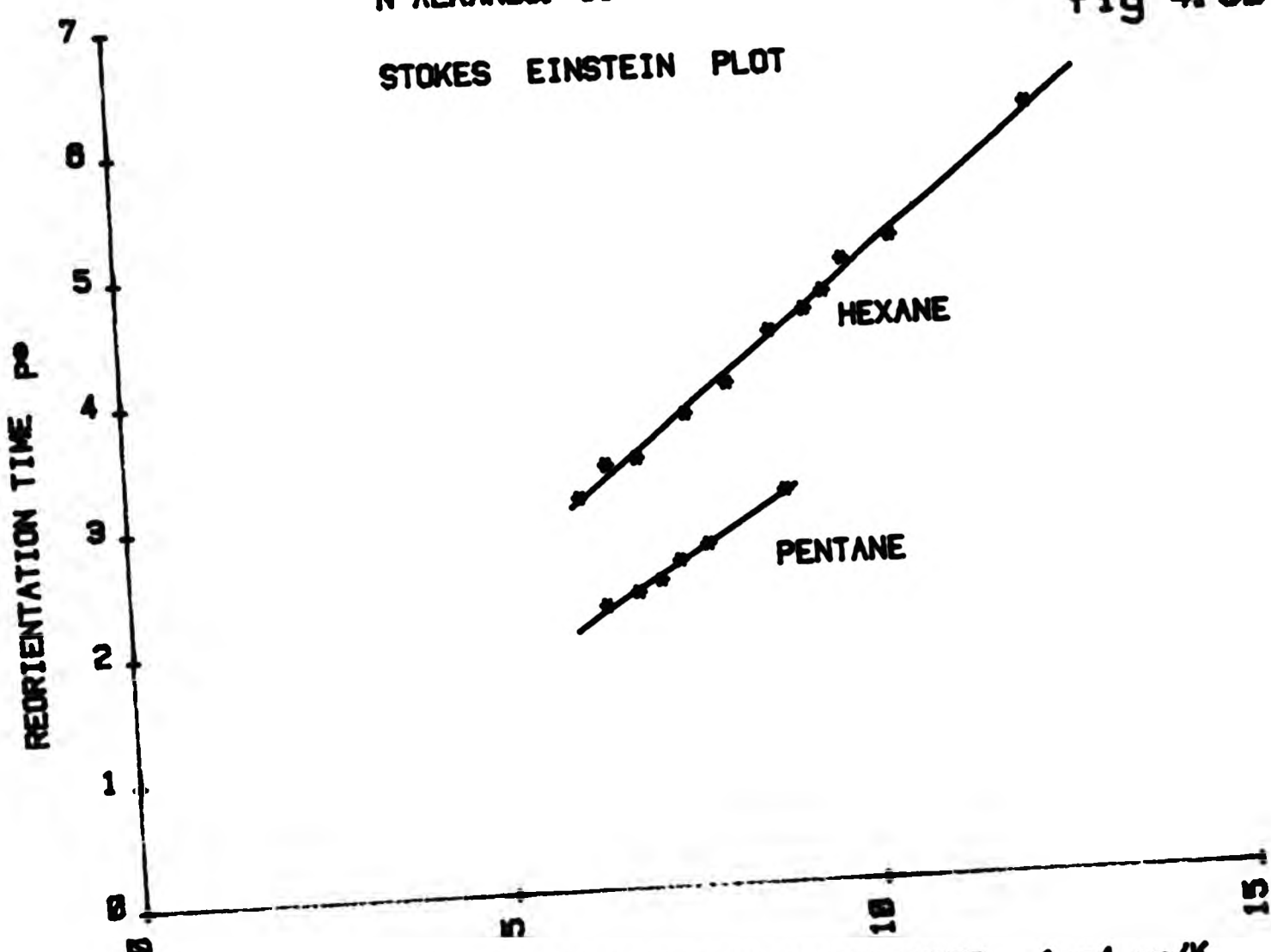
The following points are noted -

- (i) In all cases the graphs approximated (within the limits of experimental error) to straight lines. Values of the gradient of these graphs may be related to a molecular volume.

N ALKANES: SINGLE LORENTZIAN FITS

STOKES EINSTEIN PLOT

fig 4.30

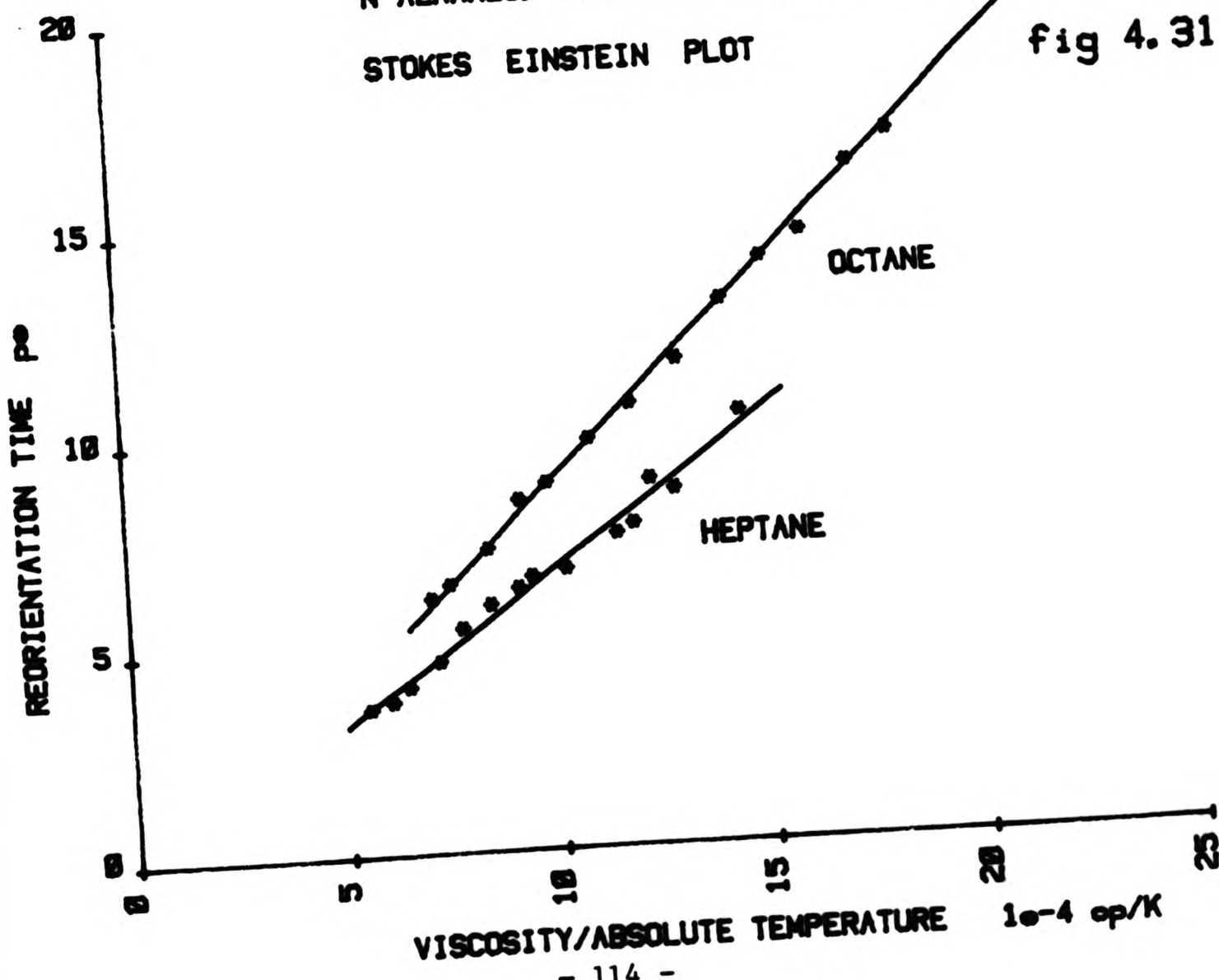


VISCOSITY/ABSOLUTE TEMPERATURE 10^{-4} cP/K

N ALKANES: SINGLE LORENTZIAN FITS

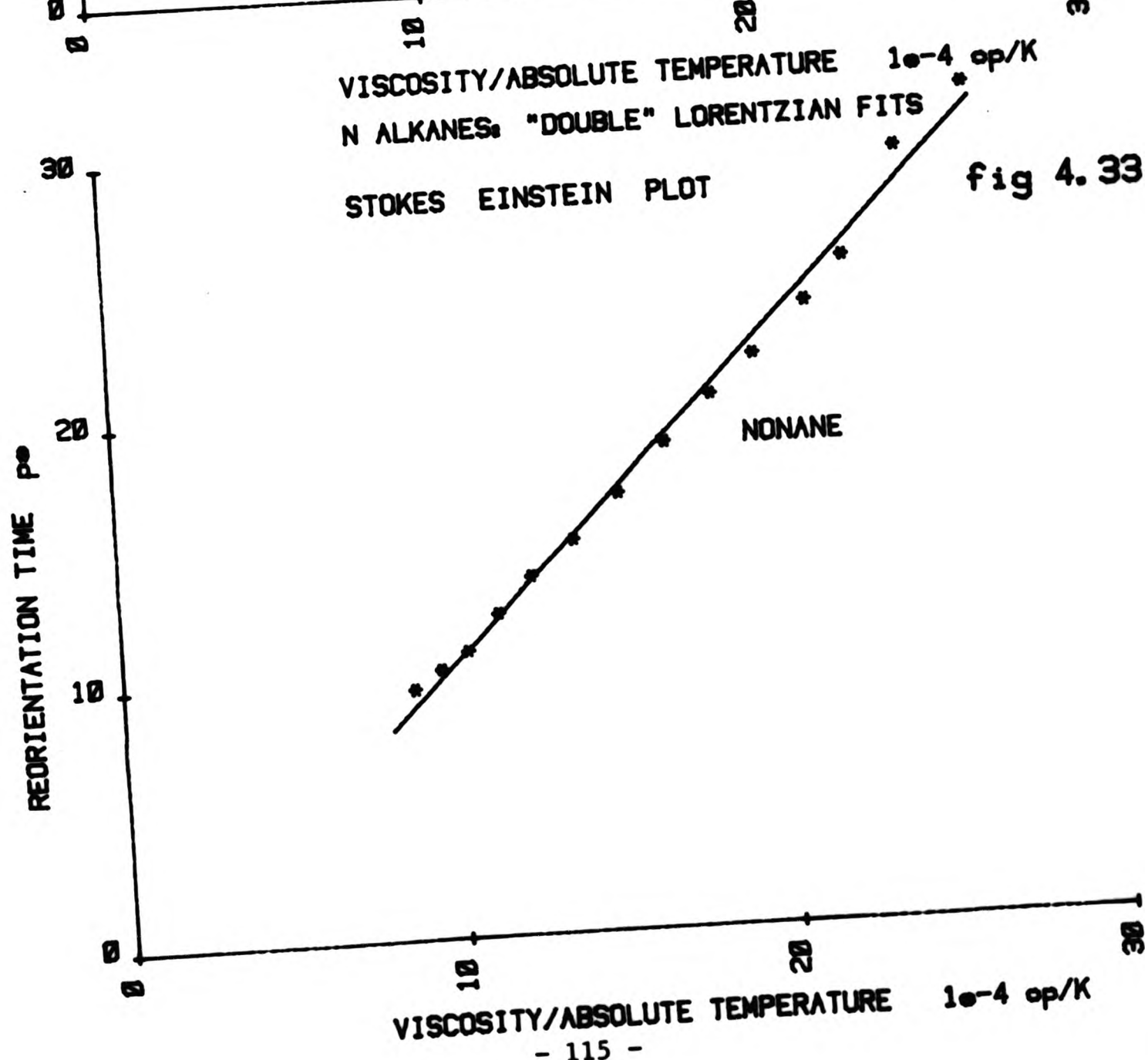
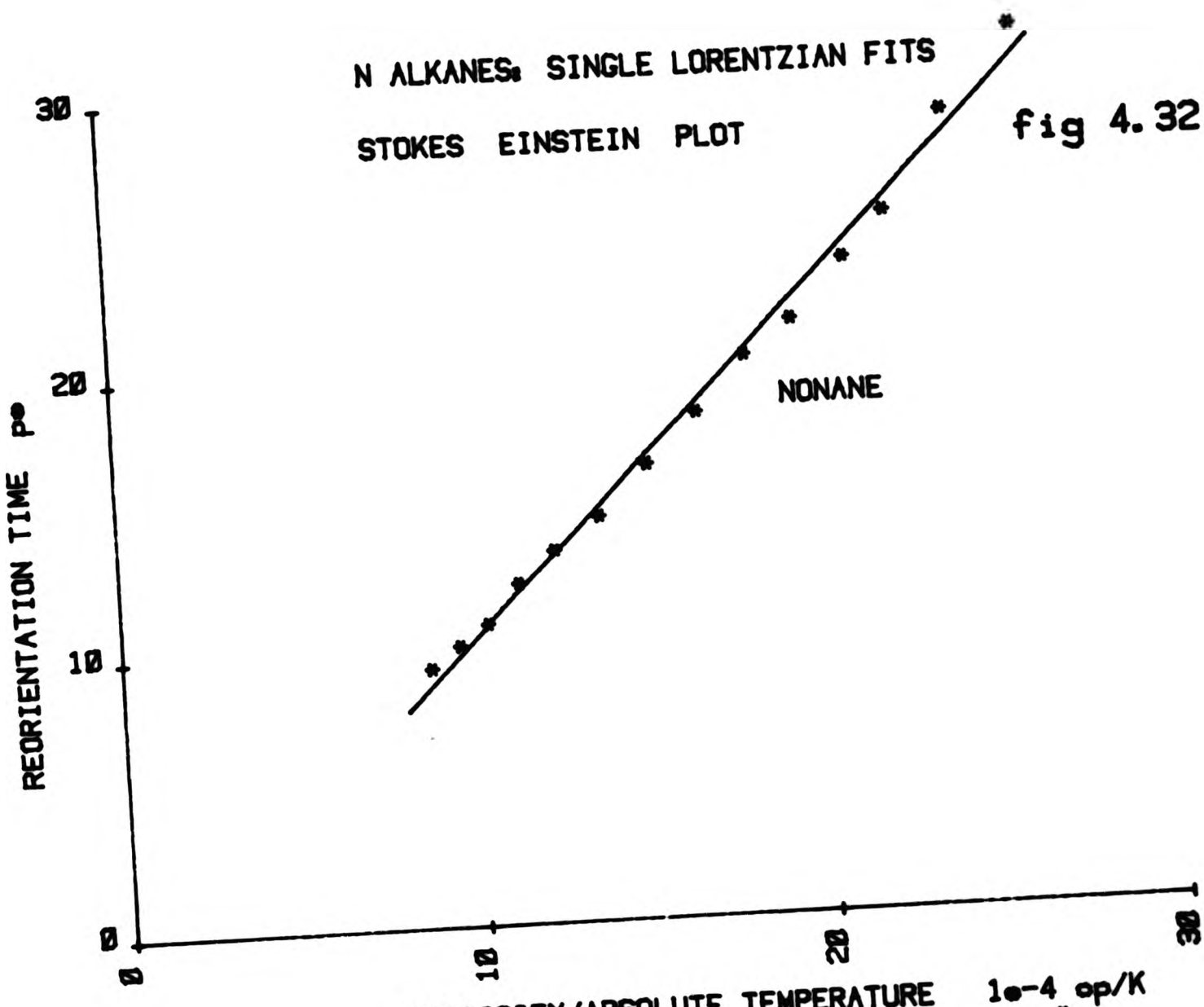
STOKES EINSTEIN PLOT

fig 4.31



VISCOSITY/ABSOLUTE TEMPERATURE 10^{-4} cP/K

- 114 -



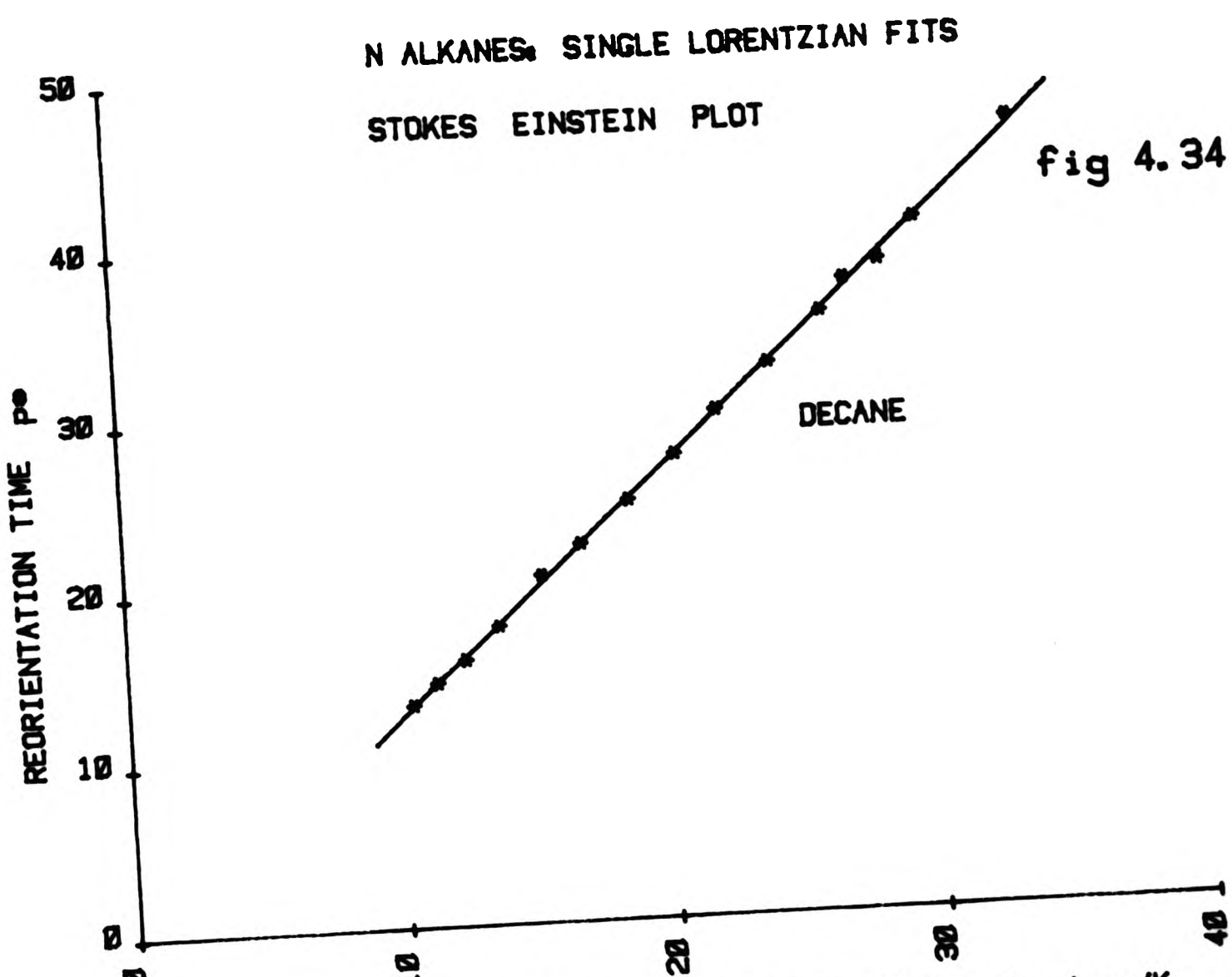


fig 4.34

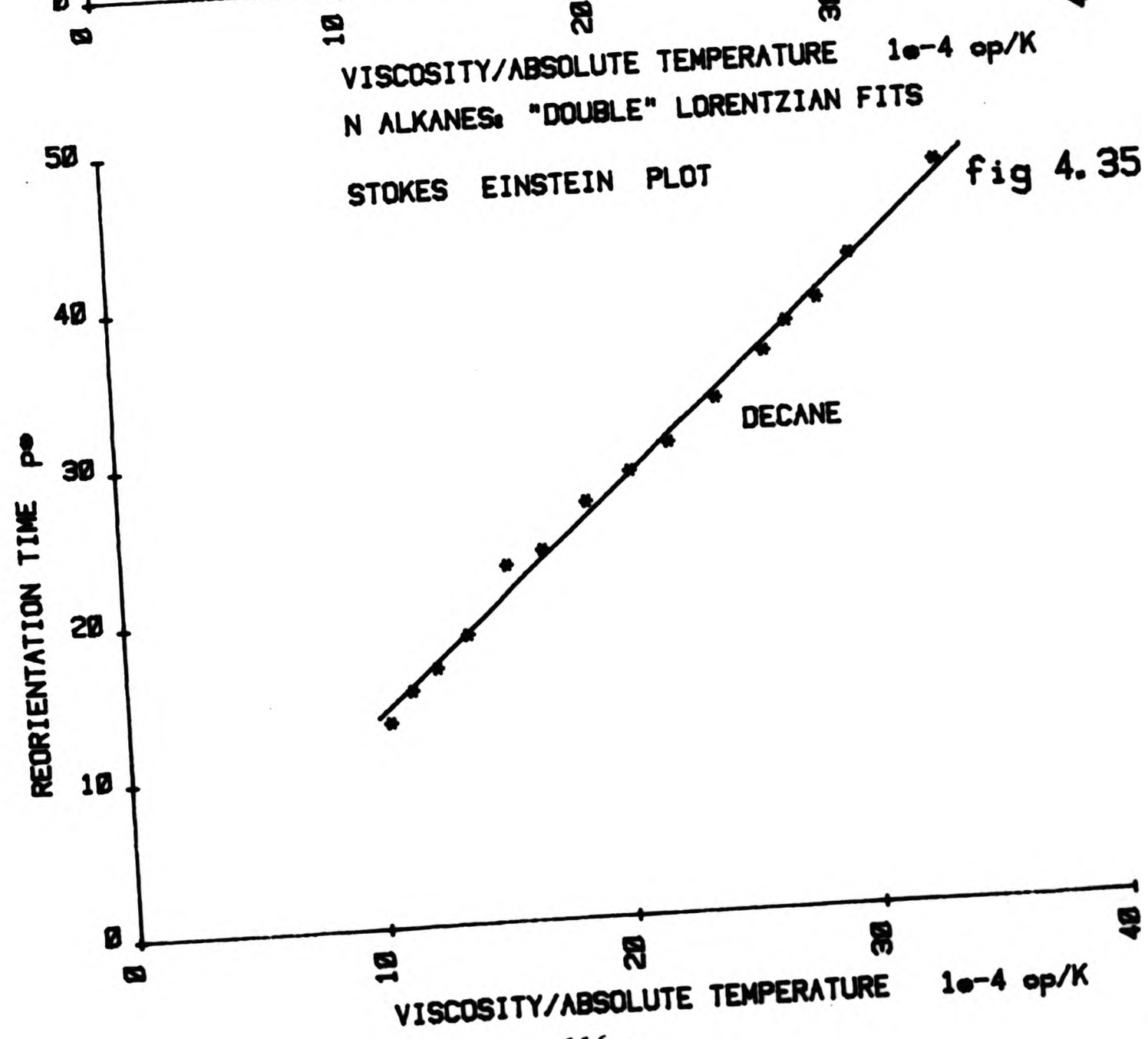
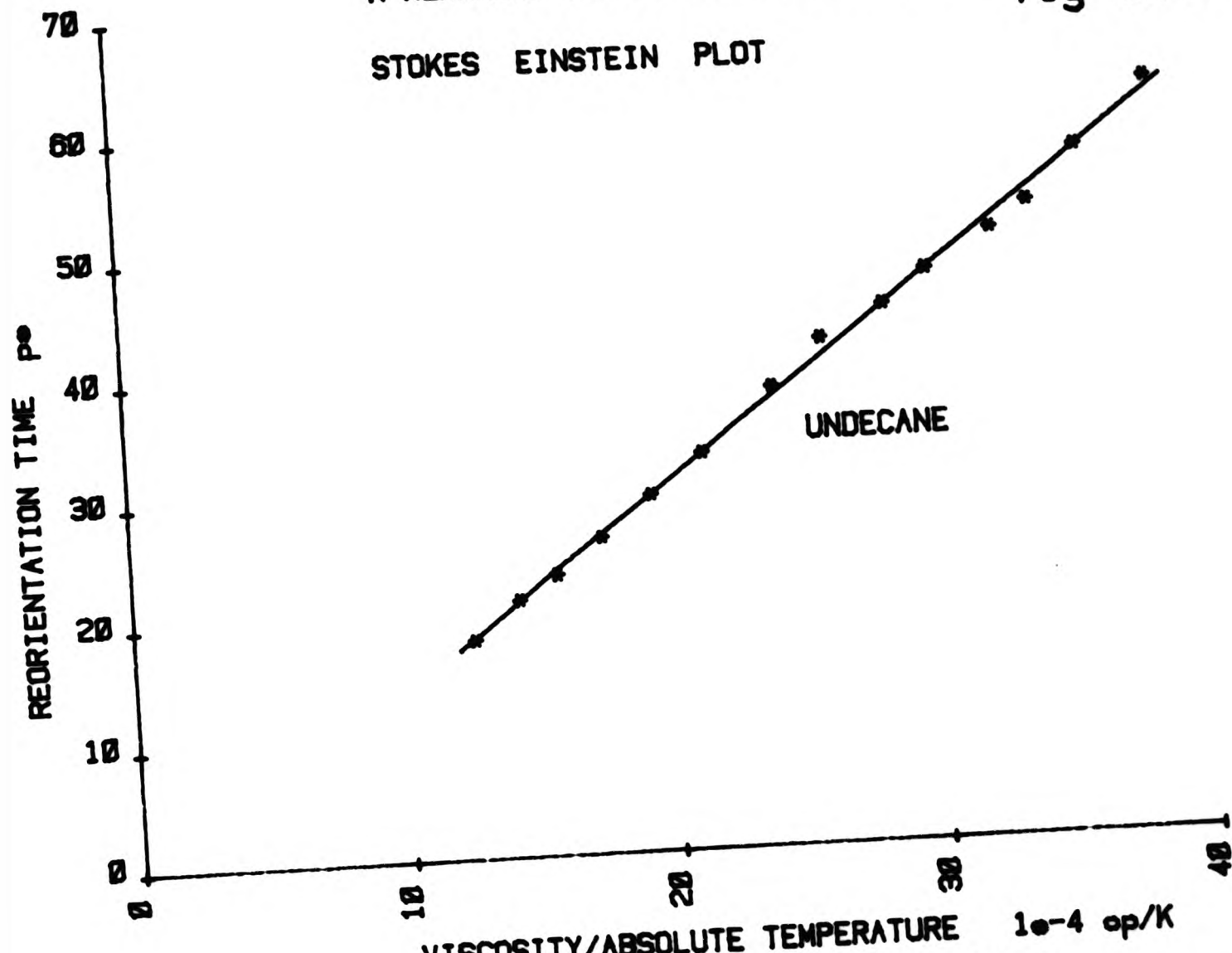
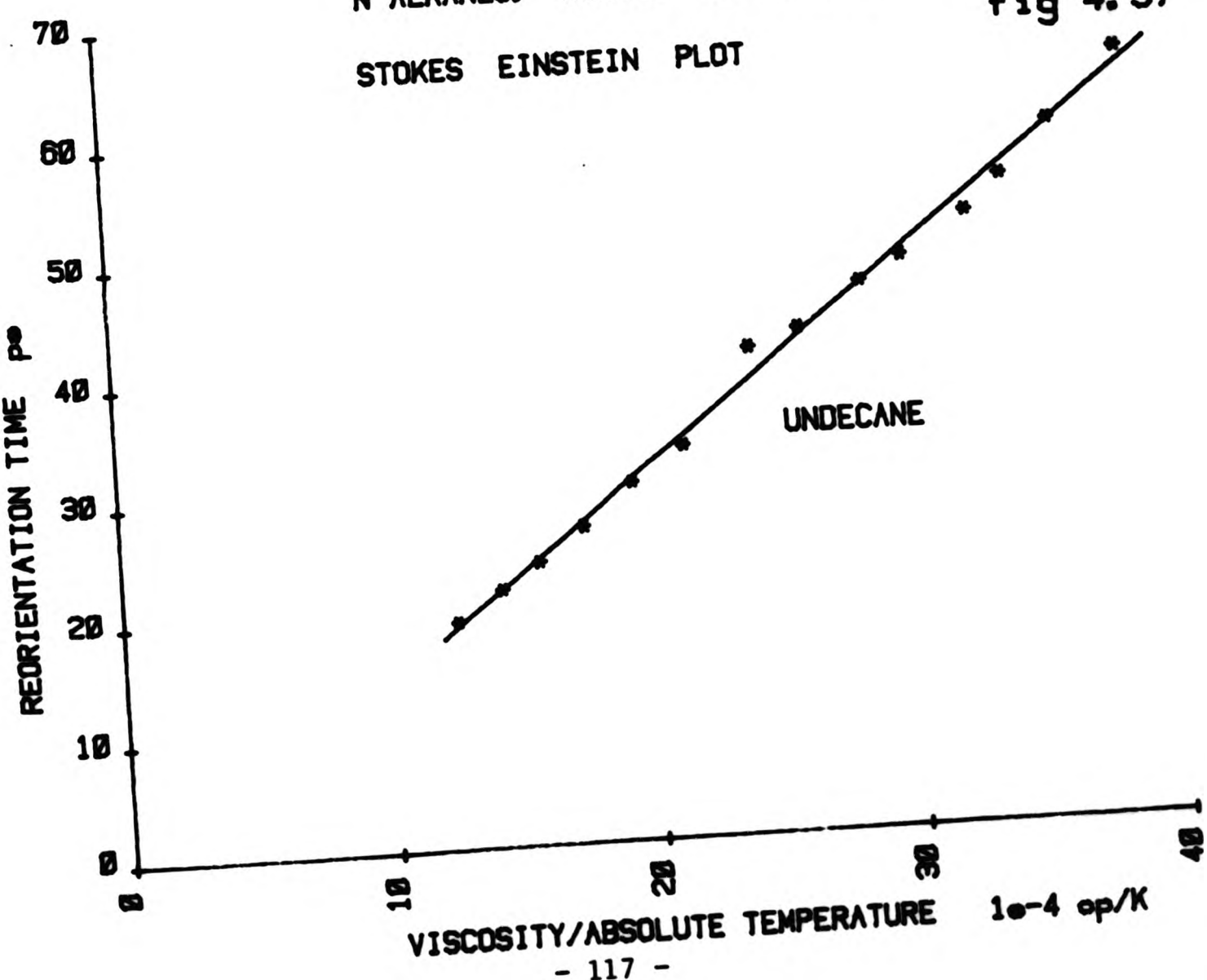


fig 4.35

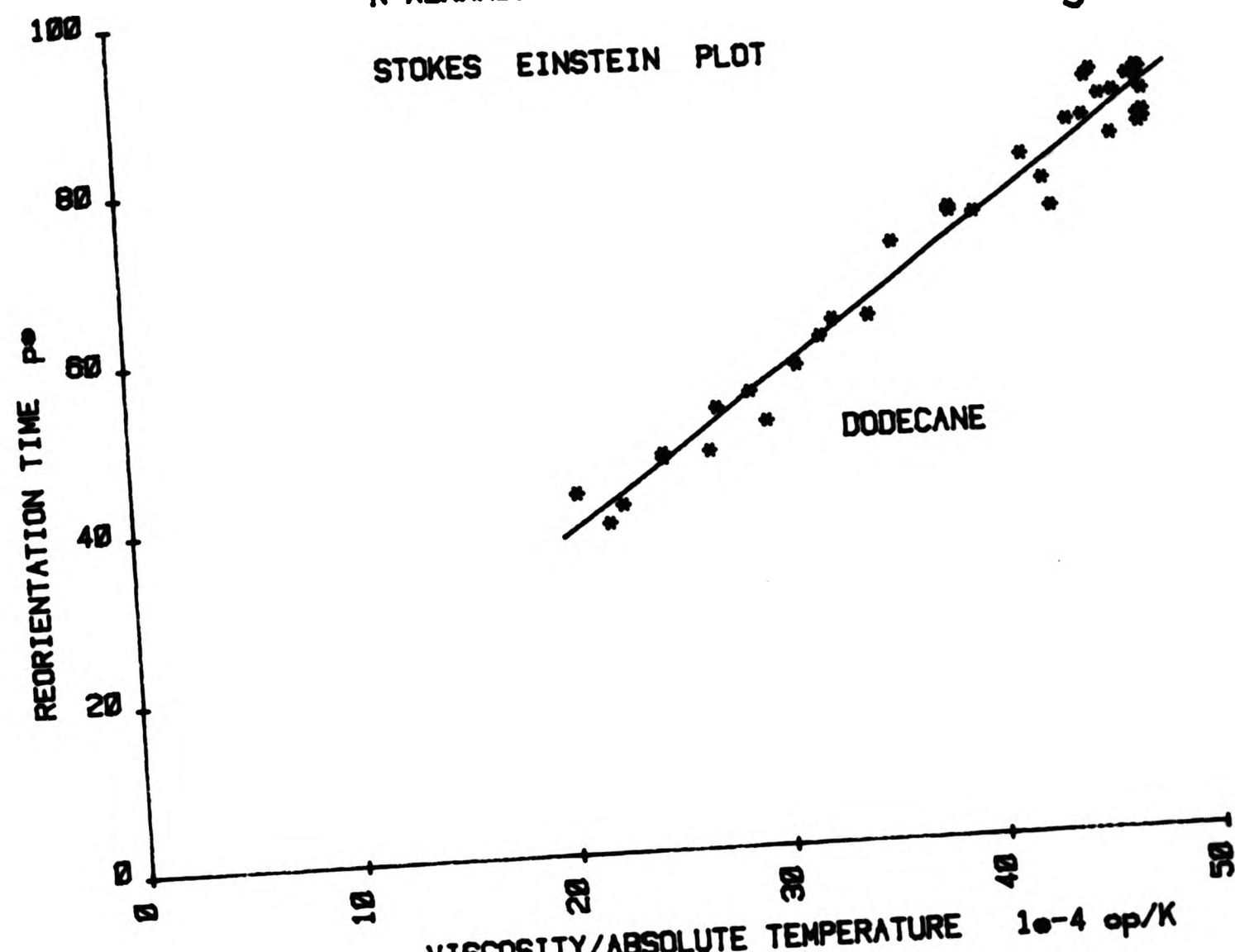
N ALKANES: SINGLE LORENTZIAN FITS fig 4.36



VISCOSITY/ABSOLUTE TEMPERATURE 10^{-4} cP/K
N ALKANES: "DOUBLE" LORENTZIAN FITS
fig 4.37



N ALKANES: SINGLE LORENTZIAN FITS fig 4.38



VISCOSITY/ABSOLUTE TEMPERATURE 10^{-4} op/K
N ALKANES: "DOUBLE" LORENTZIAN FITS

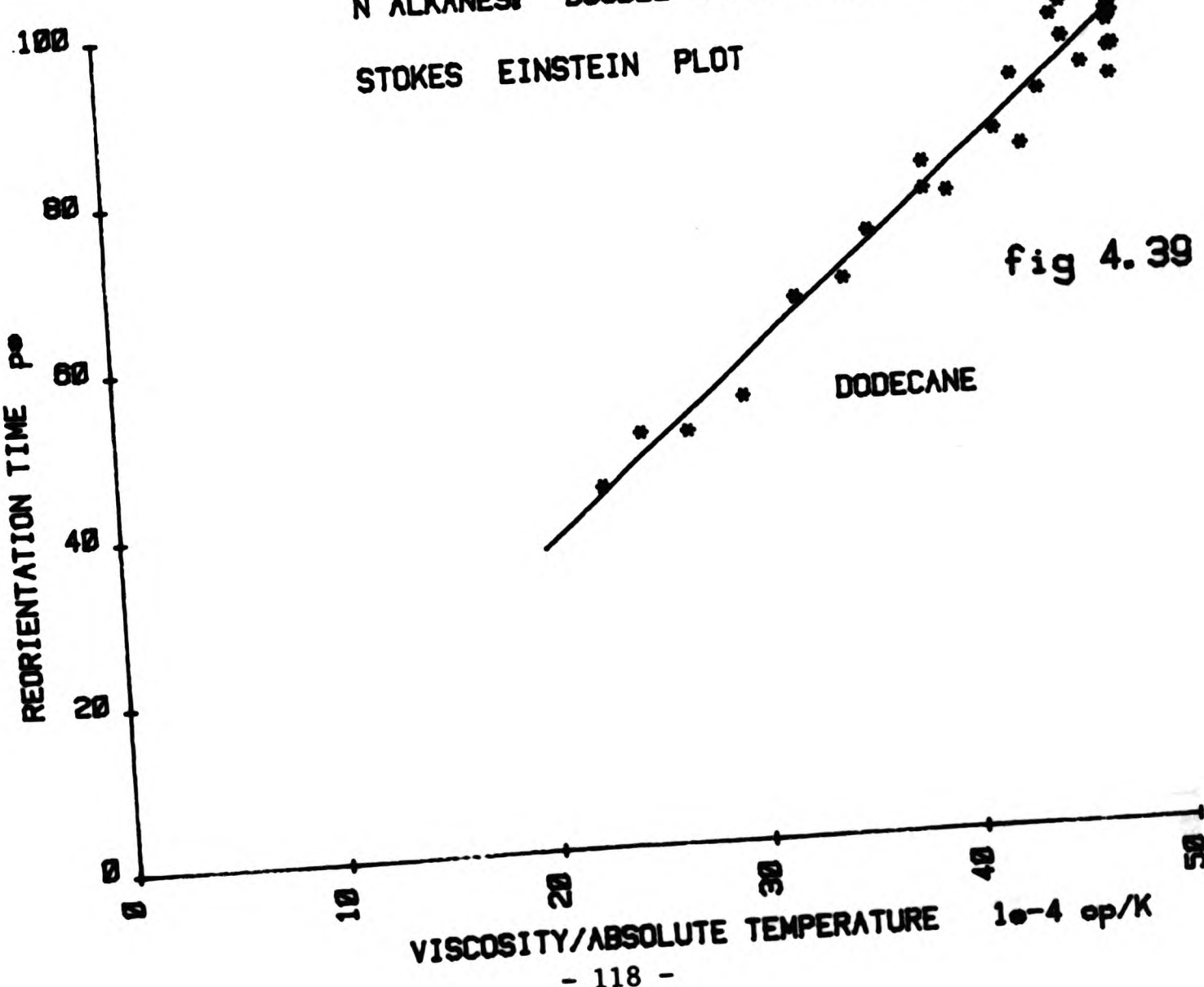
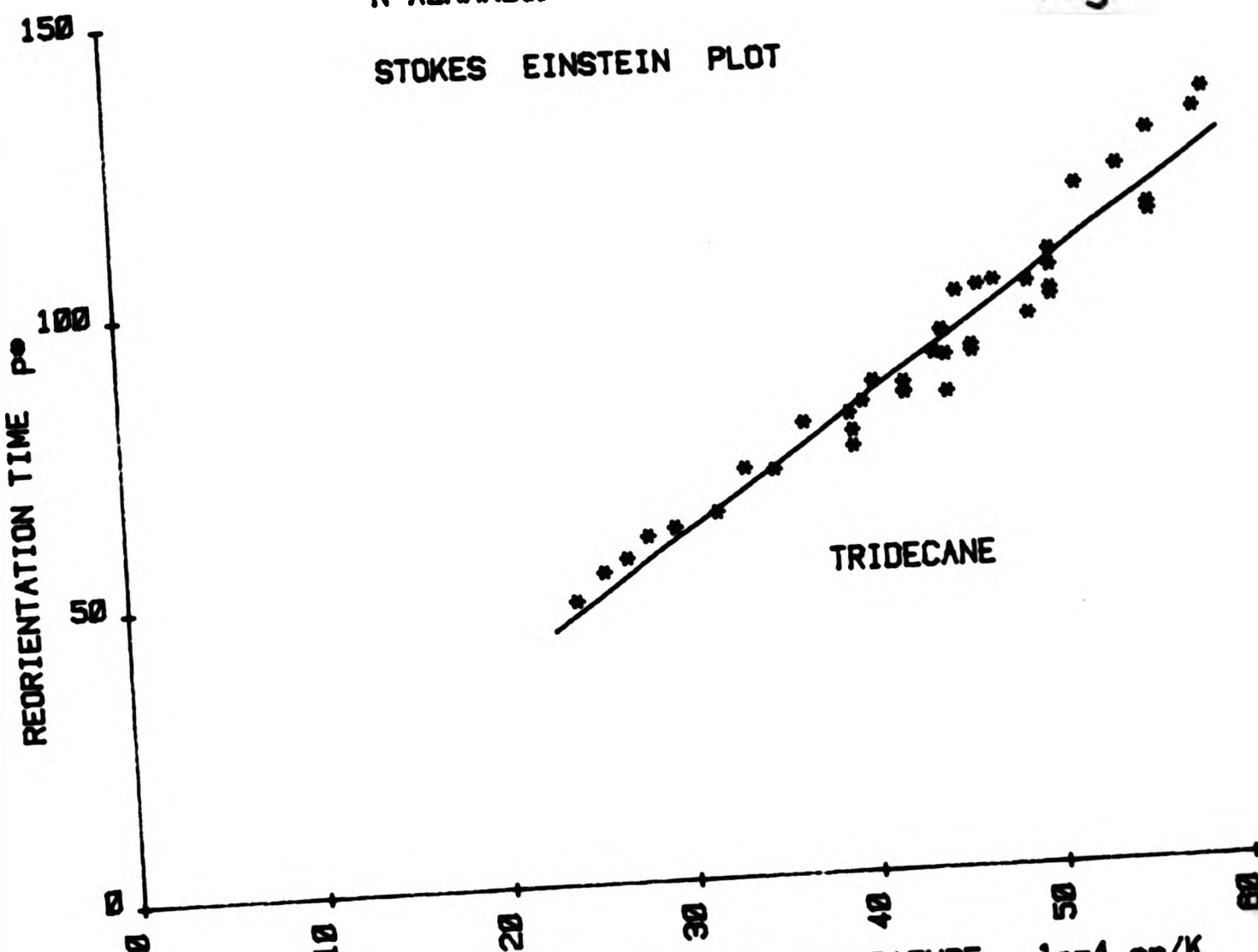


fig 4.39

N ALKANES: SINGLE LORENTZIAN FITS

fig 4.40

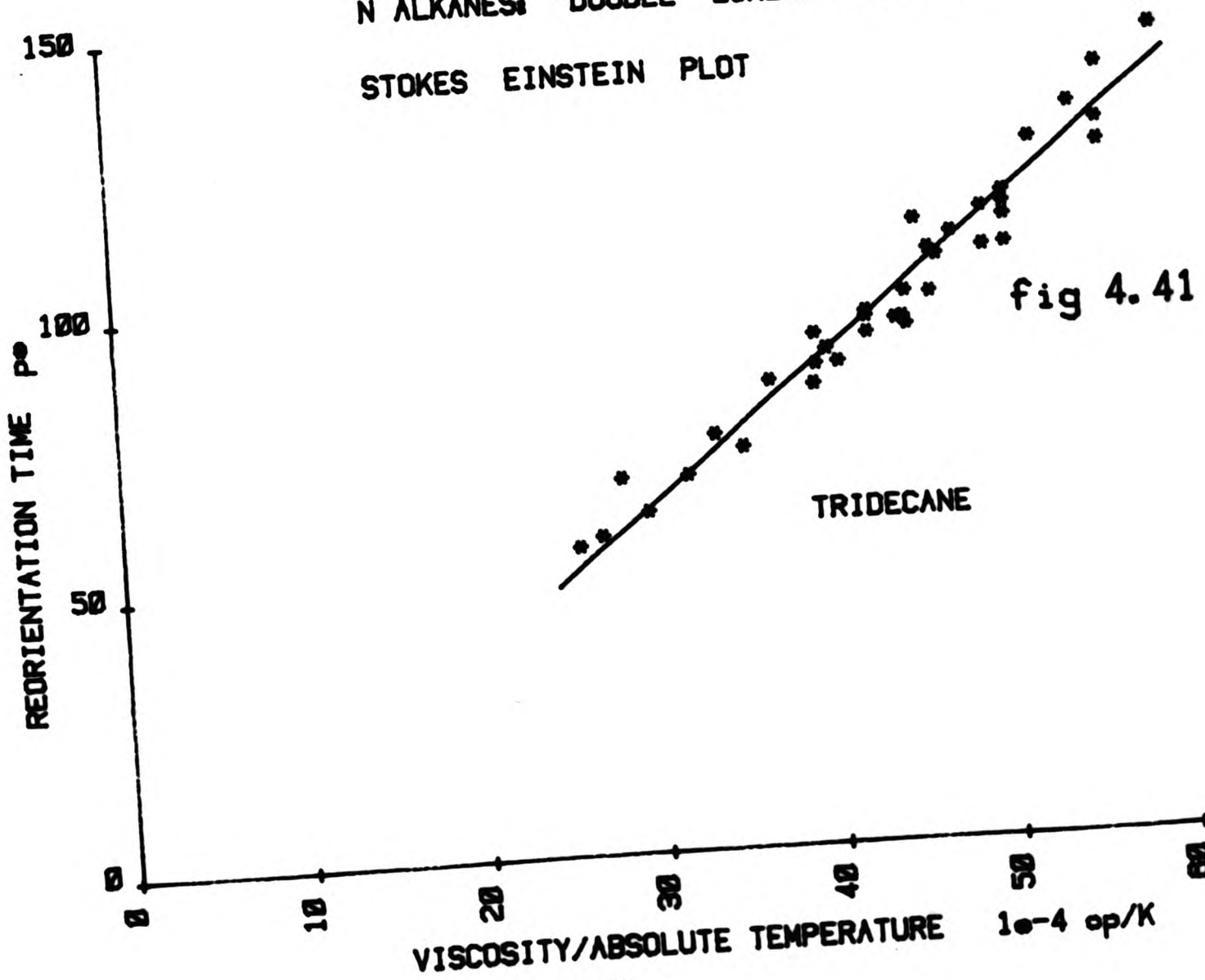
STOKES EINSTEIN PLOT



VISCOSITY/ABSOLUTE TEMPERATURE 10^{-4} cP/K
N ALKANES: "DOUBLE" LORENTZIAN FITS

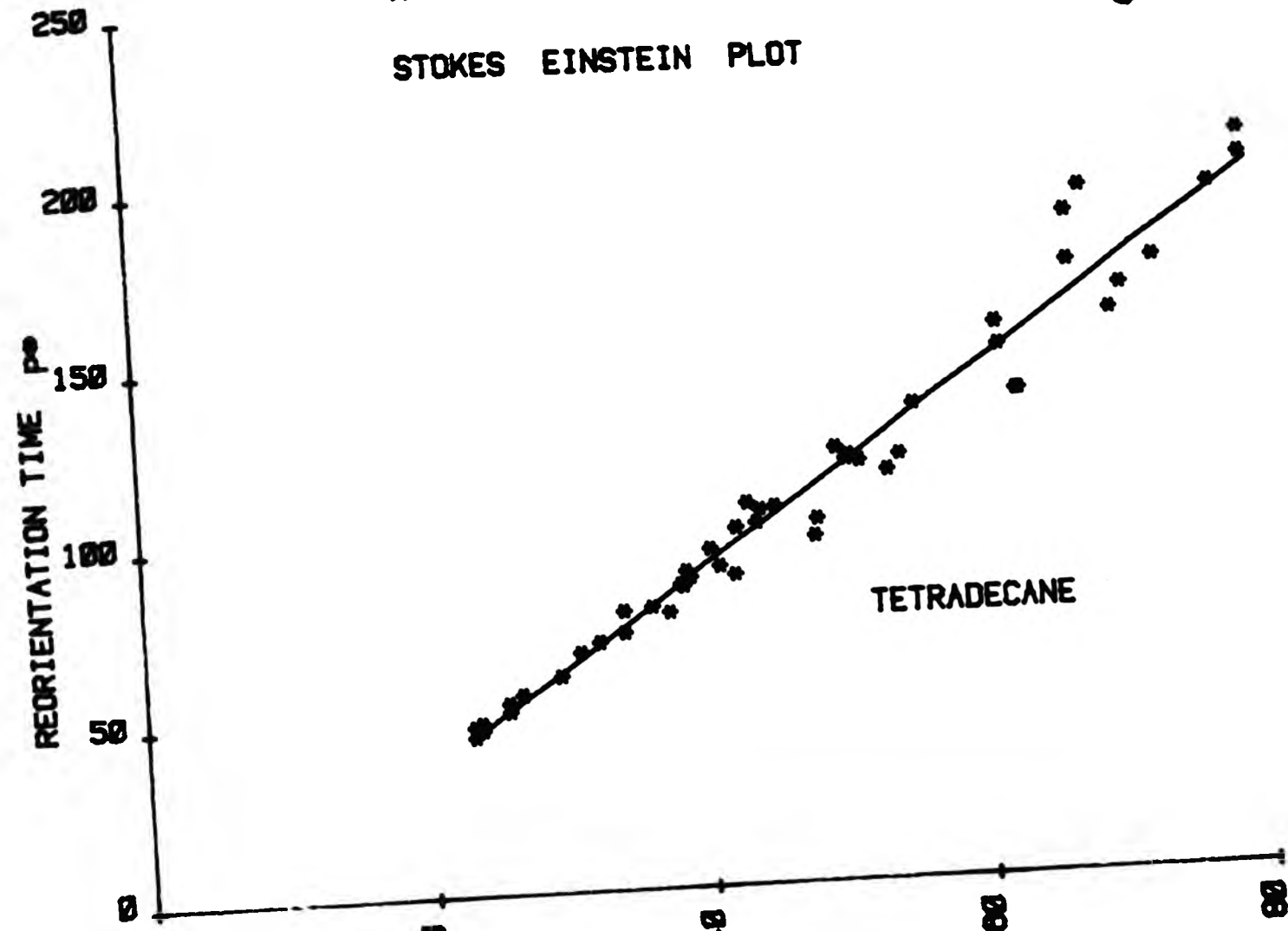
fig 4.41

STOKES EINSTEIN PLOT



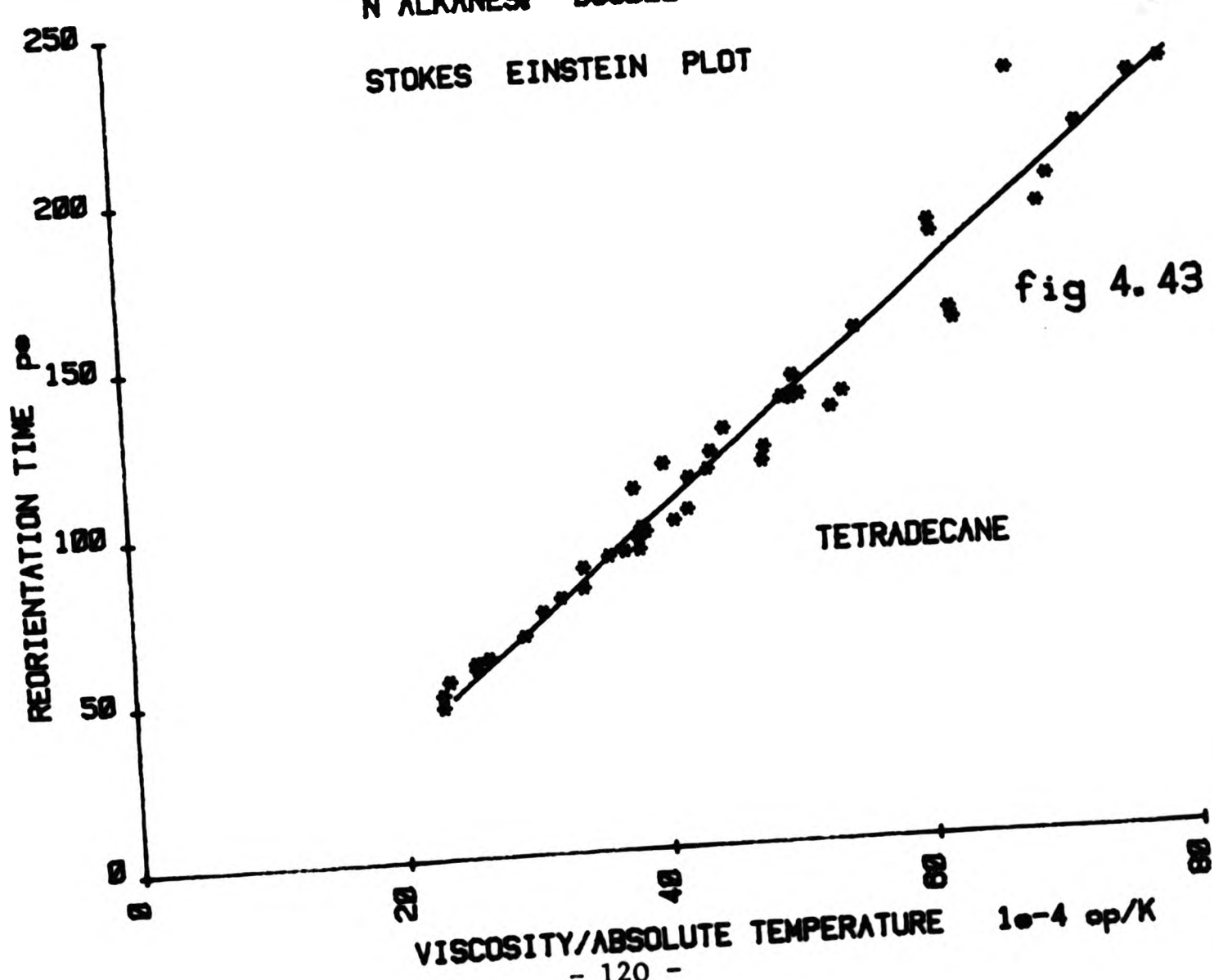
N ALKANES: SINGLE LORENTZIAN FITS fig 4.42

STOKES EINSTEIN PLOT



VISCOSITY/ABSOLUTE TEMPERATURE 10^{-4} cP/K
N ALKANES: "DOUBLE" LORENTZIAN FITS

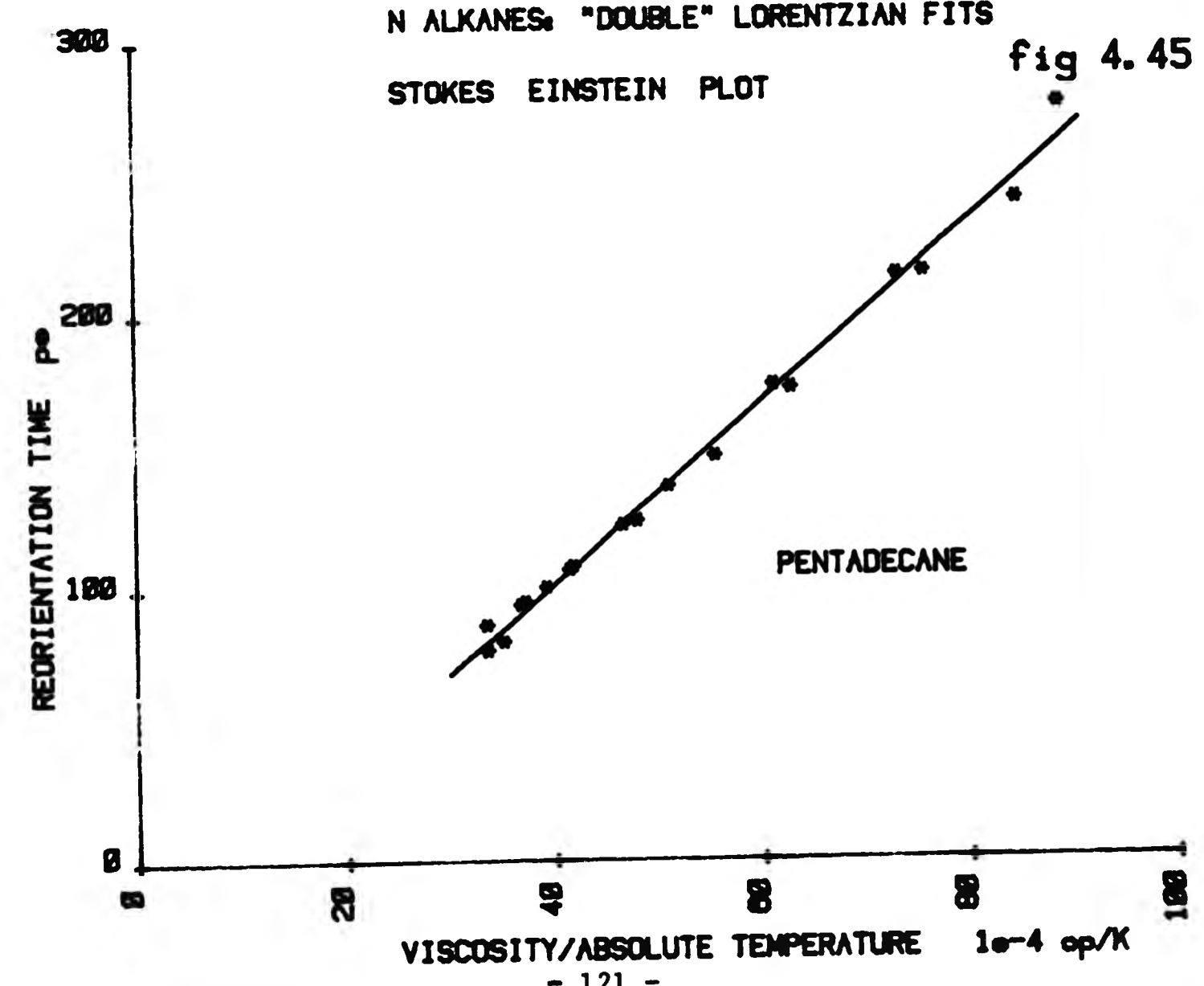
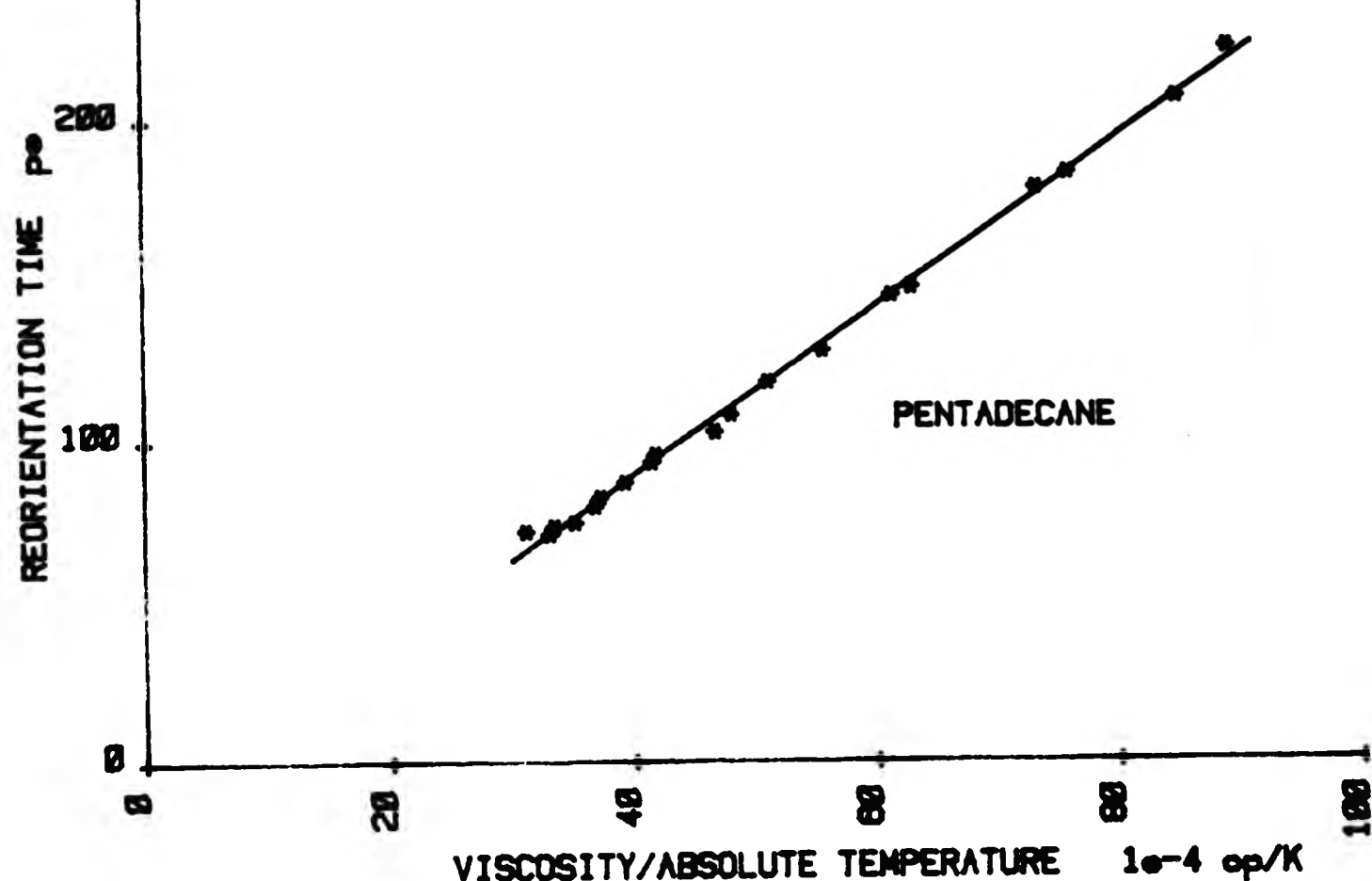
STOKES EINSTEIN PLOT

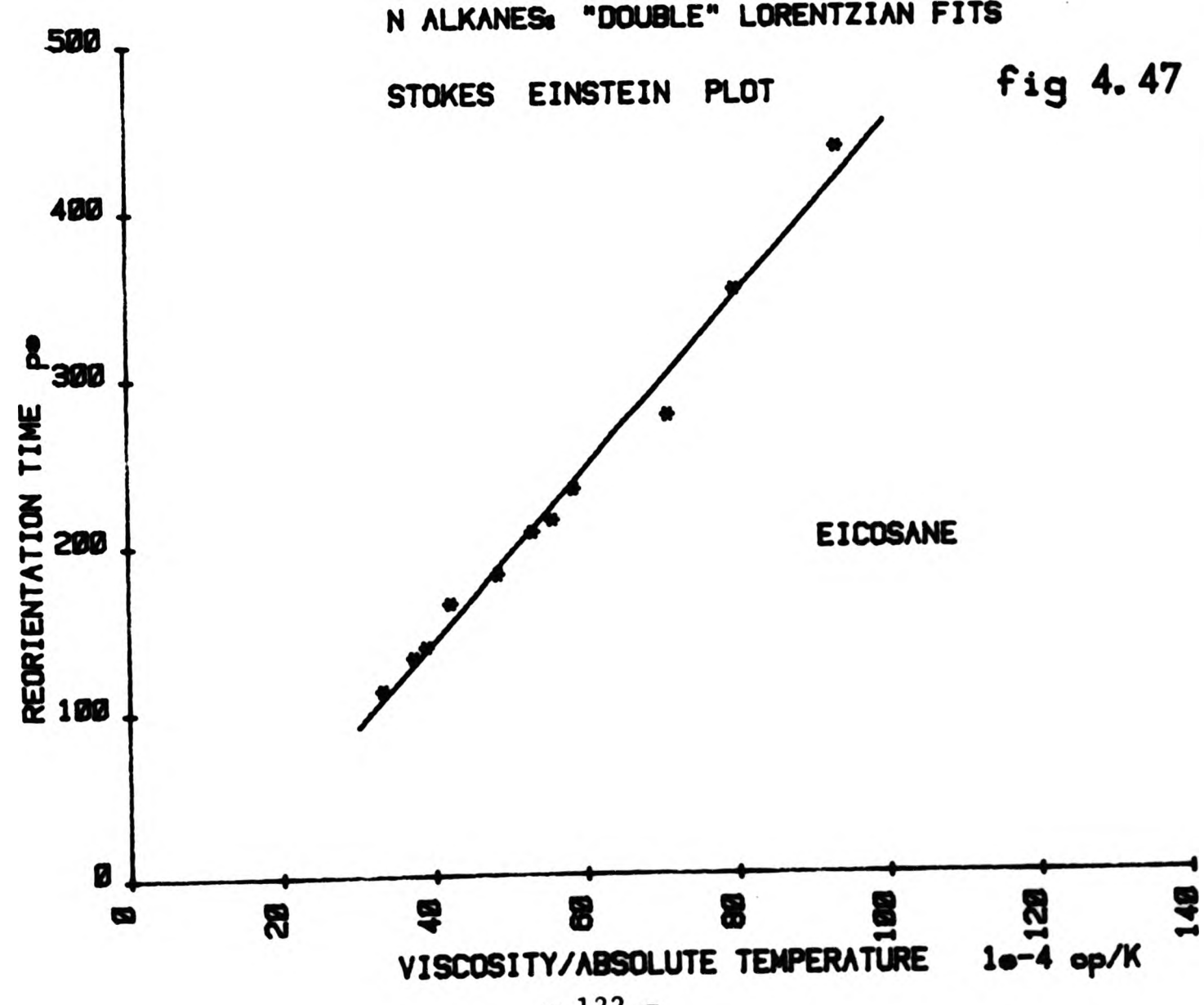
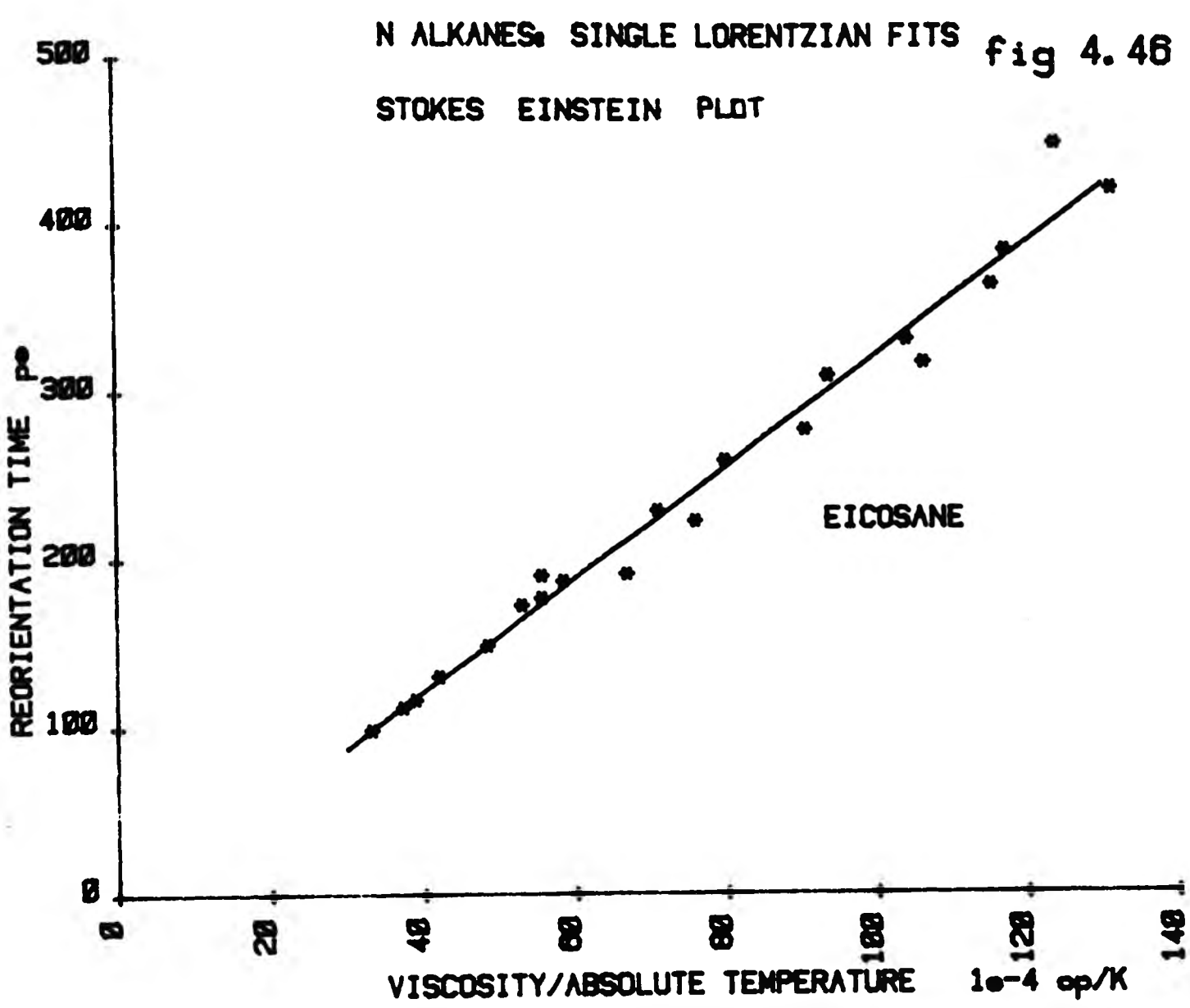


VISCOSITY/ABSOLUTE TEMPERATURE 10^{-4} cP/K

N ALKANES: SINGLE LORENTZIAN FITS
STOKES EINSTEIN PLOT

fig 4.44





(ii) In all cases the value of the intercept observed was negative, the magnitude of this intercept decreasing for the smaller alkanes. For C₅H₁₂, C₆H₁₄ and C₇H₁₆ it is zero within the limits of experimental error.

(iii) For the better quality data (ie that on which the scatter was least) the graphs of τ_{LS} against η/T were observed to curve weakly upward at low τ_{LS} values (Fig 4.45). The curvature was of the same magnitude as the errors on the data points. The significance of this curvature will be discussed later.

The results from the Stokes Einstein fits are presented as follows. The slope of the straight line is multiplied by Boltzmann's constant and is expressed in angstroms³. This is equivalent to an effective molecular volume. The value of the intercept obtained is expressed in picoseconds.

Table 4.5

Results From Stokes Einstein Fits to Data for N-Alkanes

LIQUID	SLOPE $\times K$ - EFFECTIVE VOLUME (\AA^3)		INTERCEPT (ps)	
	SINGLE LORENTZIAN FIT	LORENTZIAN PLUS DIP	SINGLE LORENTZIAN FIT	LORENTZIAN PLUS DIP
$C_{20} H_{42}$	481 ± 14	708 ± 27	-62 ± 3	-13 ± 9
$C_{15} H_{32}$	367 ± 4	456 ± 9	-16 ± 2	-30 ± 4
$C_{15} H_{32}$ (with inputed values of $\frac{K^2 \eta}{\rho}$)		444 ± 7		-29 ± 3
$C_{14} H_{30}$	363 ± 26	441 ± 30		
$C_{13} H_{28}$	322 ± 12	348 ± 17		
$C_{12} H_{26}$	273 ± 7	315 ± 14	-1.9 ± 0.3	-9.9 ± 3.9
$C_{11} H_{24}$	231 ± 3	239 ± 5	-2.5 ± 0.6	-2.9 ± 0.9
$C_{10} H_{22}$	197 ± 1	198 ± 4	-1.7 ± 0.2	-0.5 ± 0.6
$C_9 H_{20}$	174 ± 4	175 ± 3	-2.2 ± 0.5	-2.0 ± 0.5
$C_8 H_{18}$	136 ± 2	134 ± 2	-0.97 ± 0.21	-0.66 ± 0.21
$C_7 H_{16}$	94 ± 3	94 ± 3	-0.14 ± 0.21	-0.14 ± 0.21
$C_6 H_{14}$	66 ± 1.5		0.22 ± 0.1	
$C_5 H_{12}$	49 ± 2		-0.03 ± 0.11	

Referring to the Stokes Einstein equation it is seen that the volumes obtained are given by the quantity $G \alpha p V$. V is the molecular volume, G is the orientational correlation parameter, α is related to the stick slip coefficient and p is the Perrin factor.

When attempting to make a comparison between the molecular volume and the volumes measured in the Stokes Einstein fits to the data it is essential to decide which of the volumes measured is the most

appropriate to use in the comparison. For the lower viscosity liquids ($C_{10}H_{22}$ to C_5H_{12}) the dip is very narrow with respect to the main Lorentzian feature and so the spectra are essentially Lorentzian. The volumes obtained from the single Lorentzian fits are therefore appropriate. For the higher viscosity liquids where the dip is easily observable the volumes obtained from the fits to Lorentzian plus dip are those which are appropriate for analysis.

COMPARISON OF EFFECTIVE VOLUMES OBTAINED WITH STOKES EINSTEIN VOLUMES

In the Stokes Einstein equation the Stokes Einstein volume is given by the quantity $G\alpha pV$.

V is the molecular volume and can be determined simply from the atomic and molecular dimensions. In our case we determined the molecular volume from simple measurements on Courtaulds atomic models.

G , α and p are determined by the molecules' environment in the liquid. G is the angular correlation function and related to the degree of molecular alignment in the liquid. α and p are both related to the hydrodynamics of the molecular reorientation in the liquid. α is related to the efficiency of transfer of momentum across the molecular boundary to the surrounding "fluid". p is determined exclusively by the molecular shape. An oblate, or prolate ellipsoid suspended in a fluid undergoes both reorientational and translational diffusion at a slower rate than a sphere of the same volume. Perrin calculated the effect of shape (for prolate and oblate ellipsoids) on both the rotational, and translational diffusion times. The results are expressed in terms of a Perrin factor p greater than unity. An ellipsoid with a volume V and with a Perrin factor p undergoes diffusion processes such that it acts as a sphere with an equivalent volume pV . The Perrin factor for a prolate ellipsoid is given by equation 2.28.

The molecules examined in these experiments are flexible and have a time varying conformation. In making a comparison between the observed values of the Stokes Einstein volume and the calculated value the question arises for which conformation should pV be calculated. The average molecular conformation lies between completely coiled (and approximating to a sphere) and completely extended (all trans). The quantity pV (the effective molecular volume) should therefore lie between V (the actual molecular volume) and $p_{trans}V$ (where p_{trans} is the Perrin factor for the all trans molecule).

Table 4.6
Comparison of Molecular Volumes

N-Alkane	Axial Ratio b/a	Actual Volume V (\AA^3)	Perrin Factor Volume $p_{trans}V$ (\AA^3)	Stokes Einstein Volume \AA^3
$C_{20}H_{42}$	0.149	327	2334	708 ± 27
$C_{15}H_{32}$	0.188	260	1318	456 ± 9
$C_{14}H_{30}$	0.199	246	1153	441 ± 30
$C_{13}H_{28}$	0.212	231	985	348 ± 17
$C_{12}H_{26}$	0.226	216	841	315 ± 14
$C_{11}H_{24}$	0.243	201	709	239 ± 5
$C_{10}H_{22}$	0.264	185	583	198 ± 4
C_9H_{20}	0.289	168	473	175 ± 3
C_8H_{18}	0.317	154	384	134 ± 2
C_7H_{16}	0.354	138	301	94 ± 3
C_6H_{14}	0.398	123	233	66 ± 1.5
C_5H_{12}	0.452	108	179	49 ± 2

In table 4.6 a comparison is to be made between the Stokes Einstein volume ($GavV$) and the quantity pV which may lie between the

bounds of V and $p_{trans}V$. (Axial ratios and molecular volumes are calculated from Courtaulds scale atomic models.) Because of the large possible range of values which pV may take (for most alkanes, from the information displayed) we can only sensibly deduce qualitative information about the behaviour of the quantity G_a from the above table.

For C_5H_{12} the range of values which pV can take lies between $108 \text{ } \text{\AA}^3$ and $179 \text{ } \text{\AA}^3$. The experimentally observed Stokes Einstein volume for this liquid was $49 \text{ } \text{\AA}^3$. From this we can deduce that for this liquid the value of the quantity G_a lies between 0.45 and 0.27.

For the longer n-alkanes the range of values which pV can take (eg $C_{15}H_{32}$, $260 \text{ } \text{\AA}^3$ to $1318 \text{ } \text{\AA}^3$) are much larger than the equivalent range for the short alkanes. In an analysis of the data molecular conformation plays a much more important part for the longer alkanes than for the short alkanes. Lack of conformational information therefore makes the interpretation of the depolarised light scattering data for the longer alkanes more difficult than for the short chain systems.

The range of possible values of G_a for each liquid can be calculated.

The maximum values of G_a would be appropriate if the n-alkane molecules concerned were completely coiled up in the liquid, the minimum values would be appropriate if the n-alkane molecules were completely extended in the liquid. Neither of the two extremes of G_a is likely, however measurements of infra-red spectra have indicated that for the n-alkanes C_8H_{18} and below in the liquid state, the population of gauche states is less than that of trans states.

The maximum and minimum possible values for G_a for the n-alkanes examined are shown in table 4.7.

Table 4.7

N-Alkane	G _a Maximum Value	G _a Minimum Value
C ₂₀ H ₄₂	2.17	0.303
C ₁₅ H ₃₂	1.75	0.345
C ₁₄ H ₃₀	1.79	0.382
C ₁₃ H ₂₈	1.51	0.353
C ₁₂ H ₂₆	1.46	0.375
C ₁₁ H ₂₄	1.19	0.337
C ₁₀ H ₂₂	1.07	0.340
C ₉ H ₂₀	1.04	0.370
C ₈ H ₁₈	0.88	0.349
C ₇ H ₁₆	0.681	0.313
C ₆ H ₁₄	0.537	0.283
C ₅ H ₁₂	0.454	0.273

For the shorter n-alkanes (C₈ H₁₈ to C₅ H₁₂) G_a is always below 1. The quantity G has been measured for a range of n-alkanes by Clement and Bothorel (6). The study in which these results were obtained involved the measurement of the relative intensities of integrated depolarised light scattering from neat alkanes and their solutions in carbon tetrachloride. Significant corrections were applied to the raw data to account for the internal field effect and the relative refractive indices of the neat liquids and solutions. However these measurements indicate that for the n-alkanes C₈ H₁₈ to C₅ H₁₂ the factor G was approximately equal to 1. For the n-alkanes above C₈ H₁₈ G increases to a value of about 2 for C₁₂ H₂₆. If one assumes that Clement and Bothorel's values of G are correct then for the n-alkanes C₈ H₁₈ to C₅ H₁₂ the data seems to indicate that

the factor α is a function of chain length decreasing with decreasing chain length. A possible reason for this would be that the shorter the n-alkane molecule the more it approximates to a sphere, and a spherical molecule would tend to rotate more within its own volume in the liquid, interacting less with its neighbours than the hydrodynamic model (which is inherent in the Stokes Einstein relation) would indicate. This would lead to the observed decrease in the parameter α .

For $C_{12}H_{26}$ Clement and Bothorel's value of $G \approx 2$ would imply a maximum possible value of α of 0.73 which indicates a perhaps surprising freedom of movement for these n-alkane chains in the neat liquid.

NOTE ON INTERPRETATION OF STOKES EINSTEIN RESULTS FOR NEAT LIQUIDS

The Stokes Einstein volume observed in depolarised light scattering has been shown to be related to the volume of the particle undergoing reorientational diffusion processes in the liquid examined. It is however modified by a number of effects which take place in the liquid. For the n-alkanes one knows from molecular dimensions the value of the molecular volume V . The quantity which is measured in the Stokes Einstein relation for depolarised Rayleigh scattering is $G \alpha V$. $G \alpha V$ is therefore obtained directly. To obtain G , α , V separately is very difficult. G , α and V are all directly or indirectly functions of molecular shape and conformation. To complicate matters further G and α are also likely to be functions of temperature. To adequately separate the three quantities one needs to perform an experiment in which two of the three quantities are held constant and the third is varied as a function of experimental conditions. To design such an experiment for a system such as the n-alkanes, in which these quantities are essentially coupled to each other by the very nature of the

molecule, is very difficult. It may be that the only information which can be reliably obtained from a Stokes Einstein analysis of the data is the quantity Gap.

Table 4.8

N-Alkane	Gap
C ₂₀ H ₄₂	2.17
C ₁₅ H ₃₂	1.75
C ₁₄ H ₃₀	1.79
C ₁₃ H ₂₈	1.51
C ₁₂ H ₂₆	1.46
C ₁₁ H ₂₄	1.19
C ₁₀ H ₂₂	1.07
C ₉ H ₂₀	1.04
C ₈ H ₁₈	0.88
C ₇ H ₁₆	0.681
C ₆ H ₁₄	0.537
C ₅ H ₁₂	0.454

In an attempt to effect the separation of the various factors in the quantity Gap we performed a programme of work on depolarised light scattering from solutions of some n-alkanes in CCl₄. This is detailed in the following section.

4.2.2 N-Alkanes: Solutions in Carbon Tetrachloride

In this section we examine the results from fits to spectra of solutions of the n-alkanes in carbon tetrachloride. The liquids examined were the n-alkanes C₁₅ H₃₂, C₁₀ H₂₂, C₈ H₁₈. The purpose of this piece of work is to attempt a separation of the factors G, a, p

molecule, is very difficult. It may be that the only information which can be reliably obtained from a Stokes Einstein analysis of the data is the quantity Gap.

Table 4.8

N-Alkane	Gap
C ₂₀ H ₄₂	2.17
C ₁₅ H ₃₂	1.75
C ₁₄ H ₃₀	1.79
C ₁₃ H ₂₈	1.51
C ₁₂ H ₂₆	1.46
C ₁₁ H ₂₄	1.19
C ₁₀ H ₂₂	1.07
C ₉ H ₂₀	1.04
C ₈ H ₁₈	0.88
C ₇ H ₁₆	0.681
C ₆ H ₁₄	0.537
C ₅ H ₁₂	0.454

In an attempt to effect the separation of the various factors in the quantity Gap we performed a programme of work on depolarised light scattering from solutions of some n-alkanes in CCl₄. This is detailed in the following section.

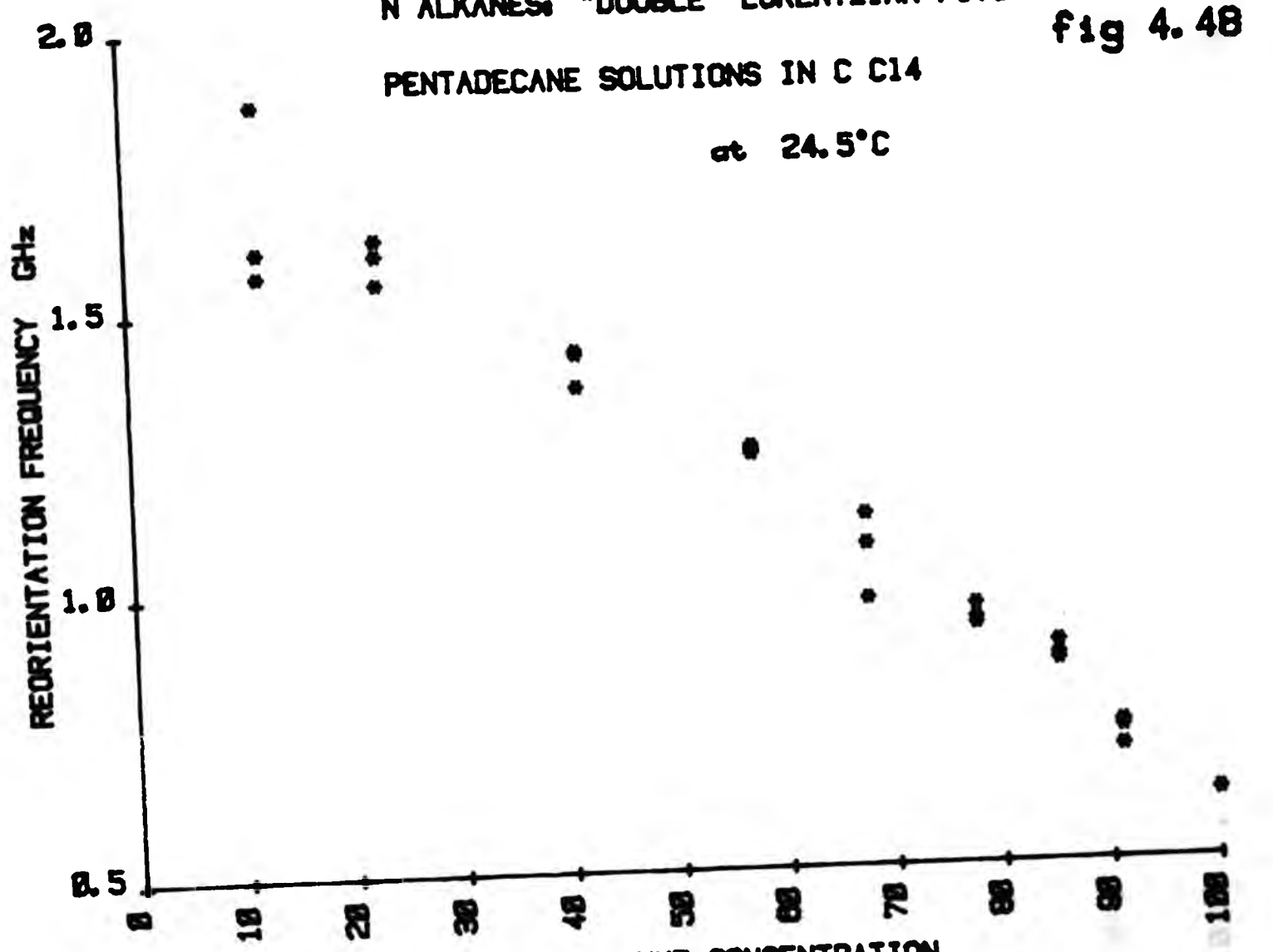
4.2.2 N-Alkanes: Solutions in Carbon Tetrachloride

In this section we examine the results from fits to spectra of solutions of the n-alkanes in carbon tetrachloride. The liquids examined were the n-alkanes C₁₅ H₃₂, C₁₀ H₂₂, C₈ H₁₈. The purpose of this piece of work is to attempt a separation of the factors G, a, p

N ALKANES: "DOUBLE" LORENTZIAN FITS
PENTADECANE SOLUTIONS IN C C₁₄

at 24.5°C

fig 4.48

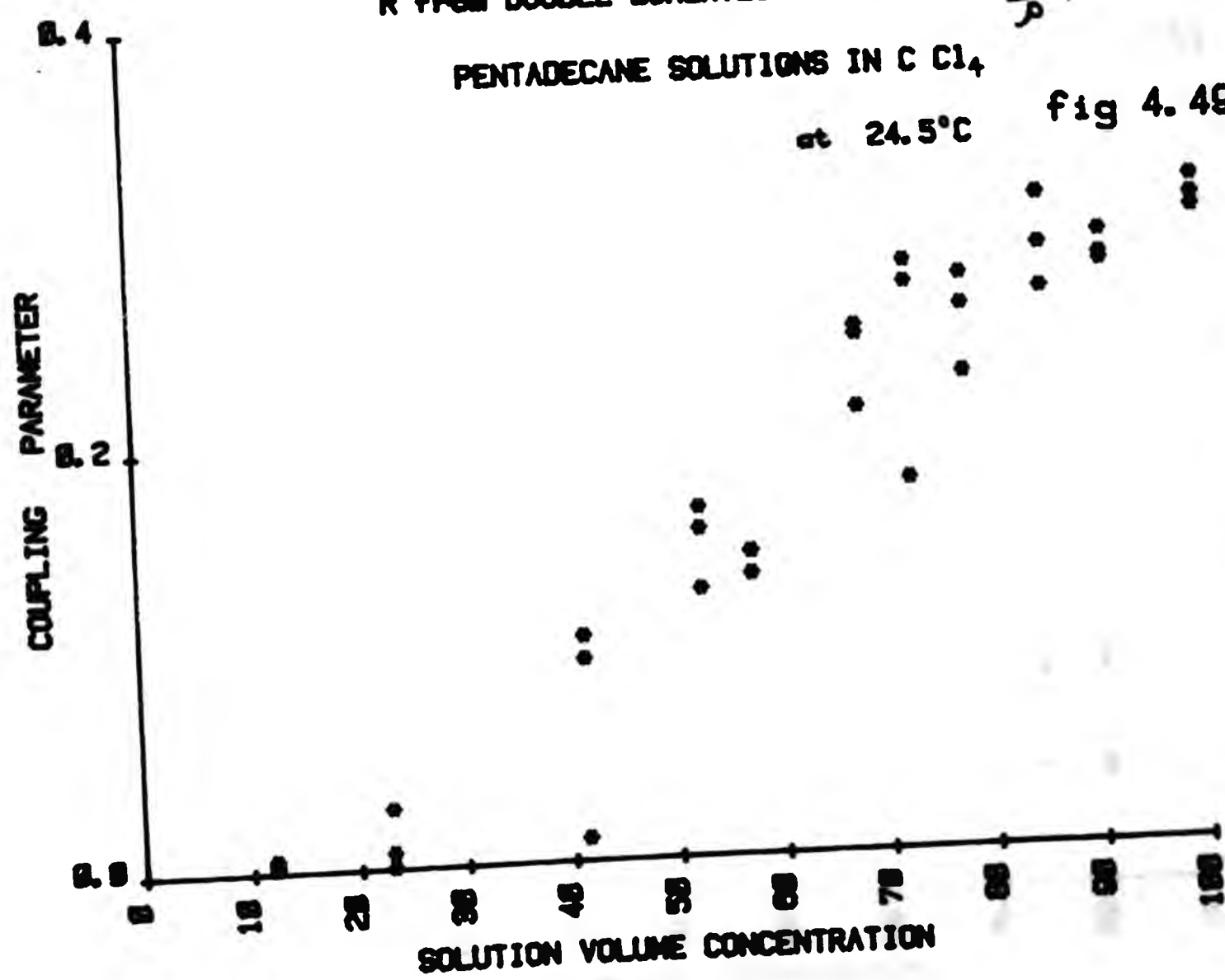


R from "DOUBLE" LORENTZIAN FITS with $K^2\eta / \rho$ floating

PENTADECANE SOLUTIONS IN C C₁₄

at 24.5°C

fig 4.49

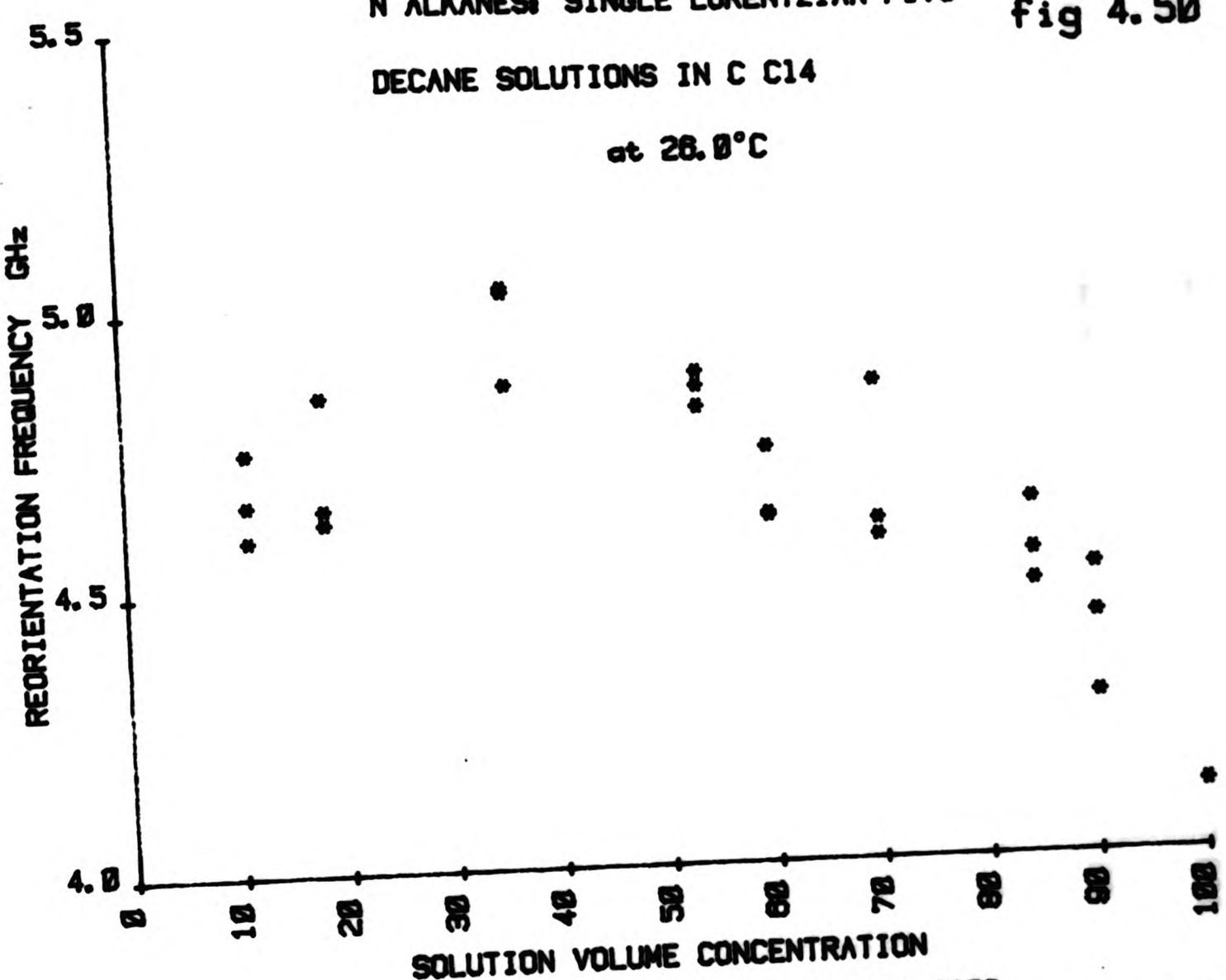


N ALKANES: SINGLE LORENTZIAN FITS

fig 4.50

DECANE SOLUTIONS IN C C14

at 26.0°C



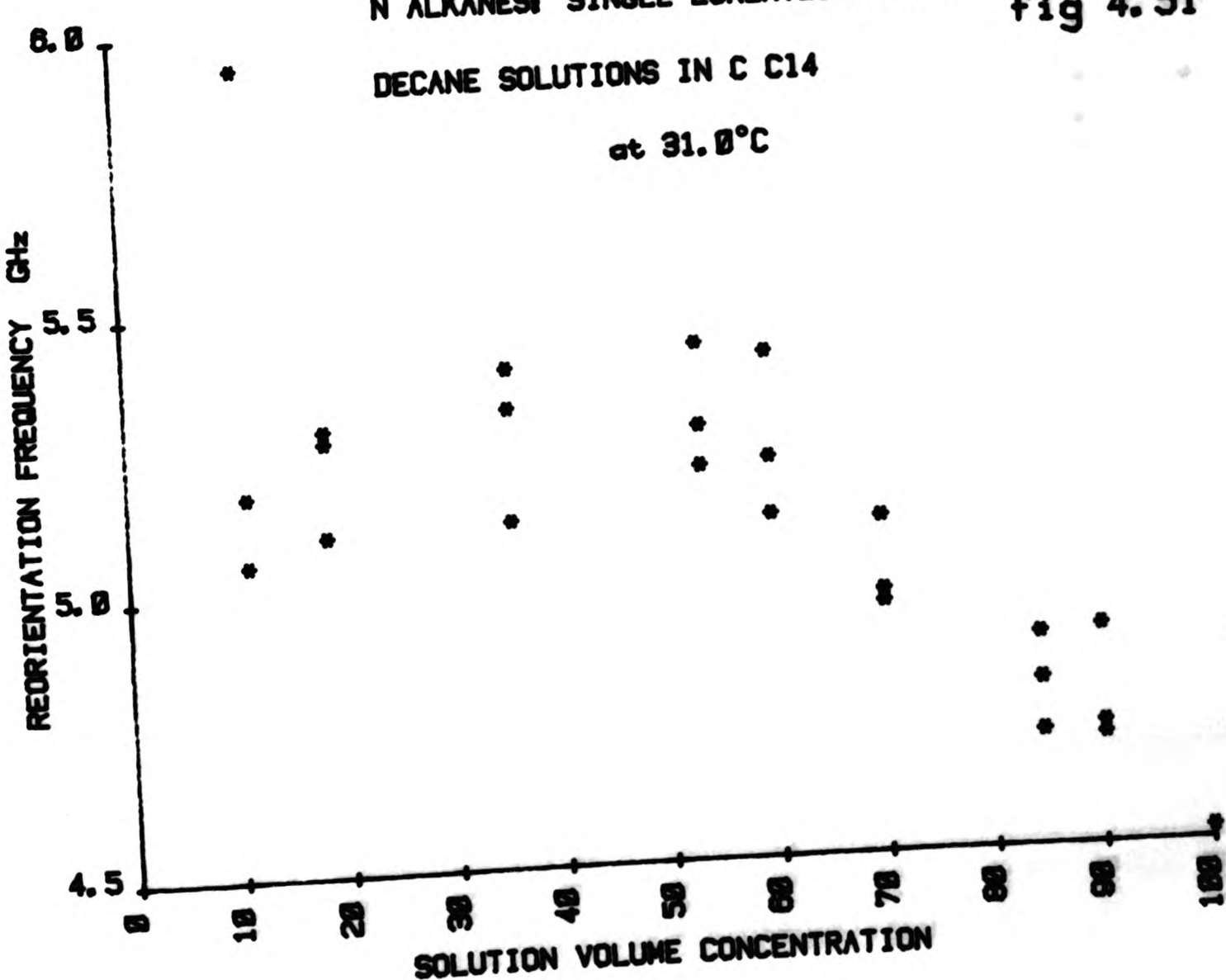
SOLUTION VOLUME CONCENTRATION

N ALKANES: SINGLE LORENTZIAN FITS

fig 4.51

DECANE SOLUTIONS IN C C14

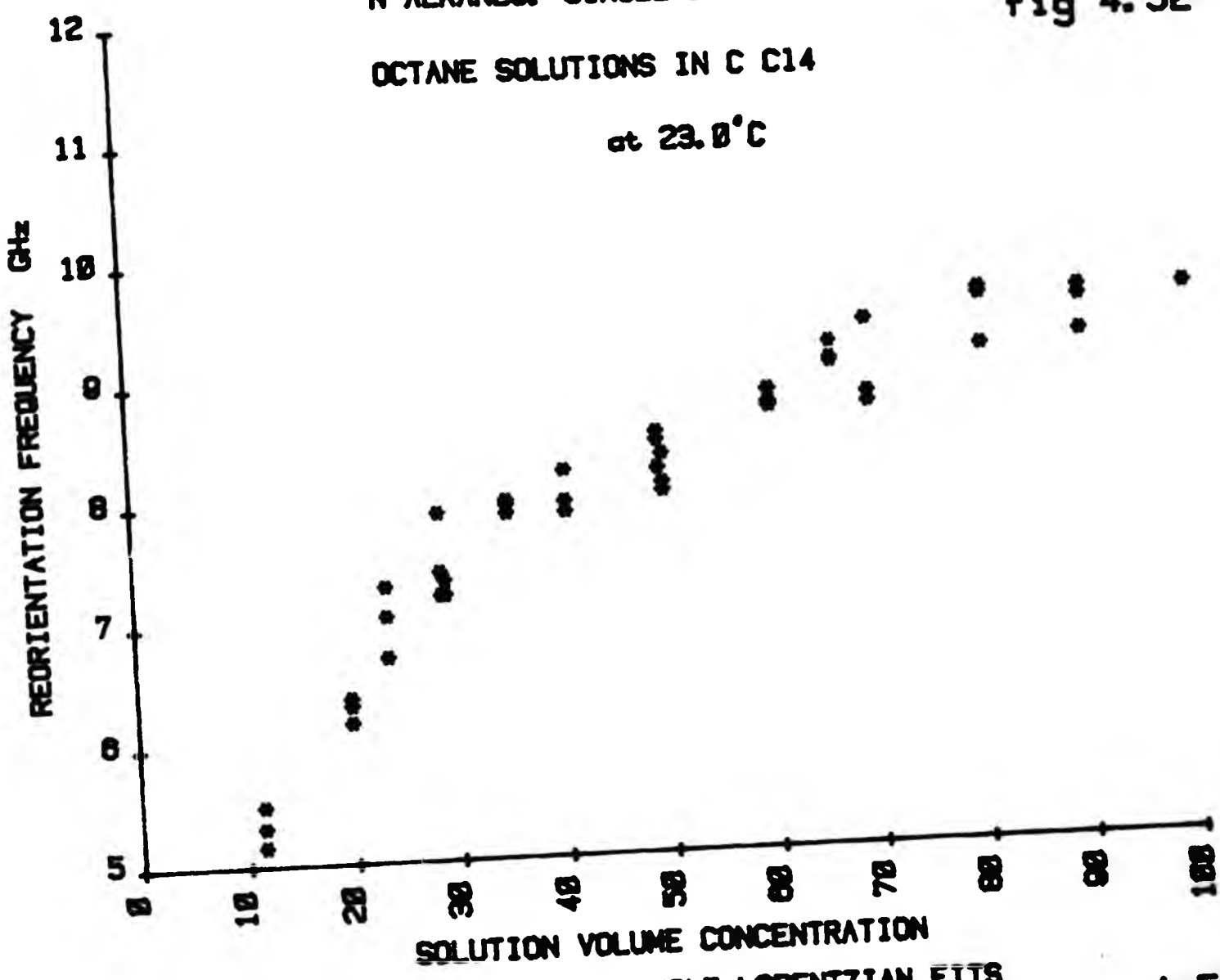
at 31.0°C



SOLUTION VOLUME CONCENTRATION

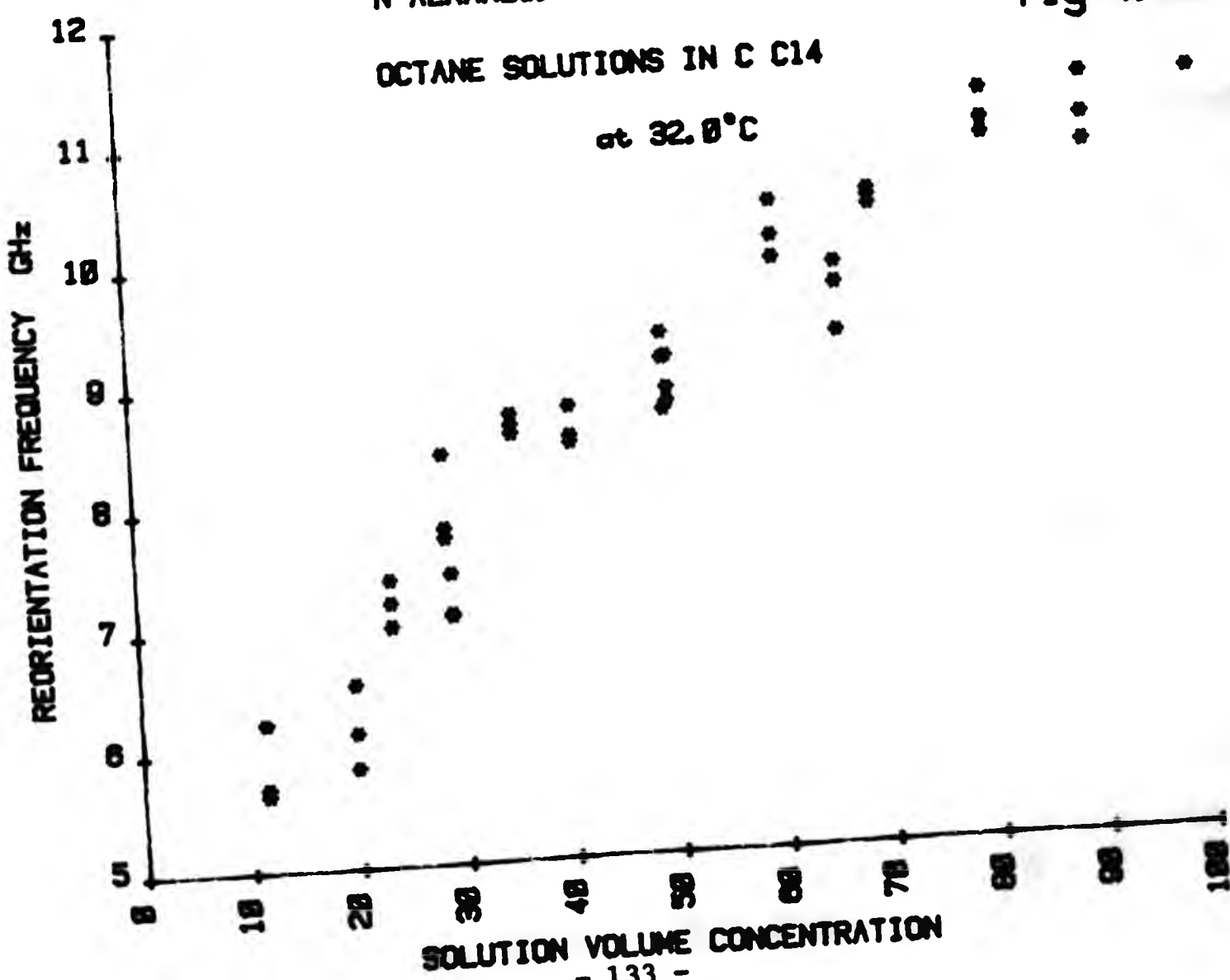
N ALKANES: SINGLE LORENTZIAN FITS
OCTANE SOLUTIONS IN C C14
at 23.0°C

fig 4.52



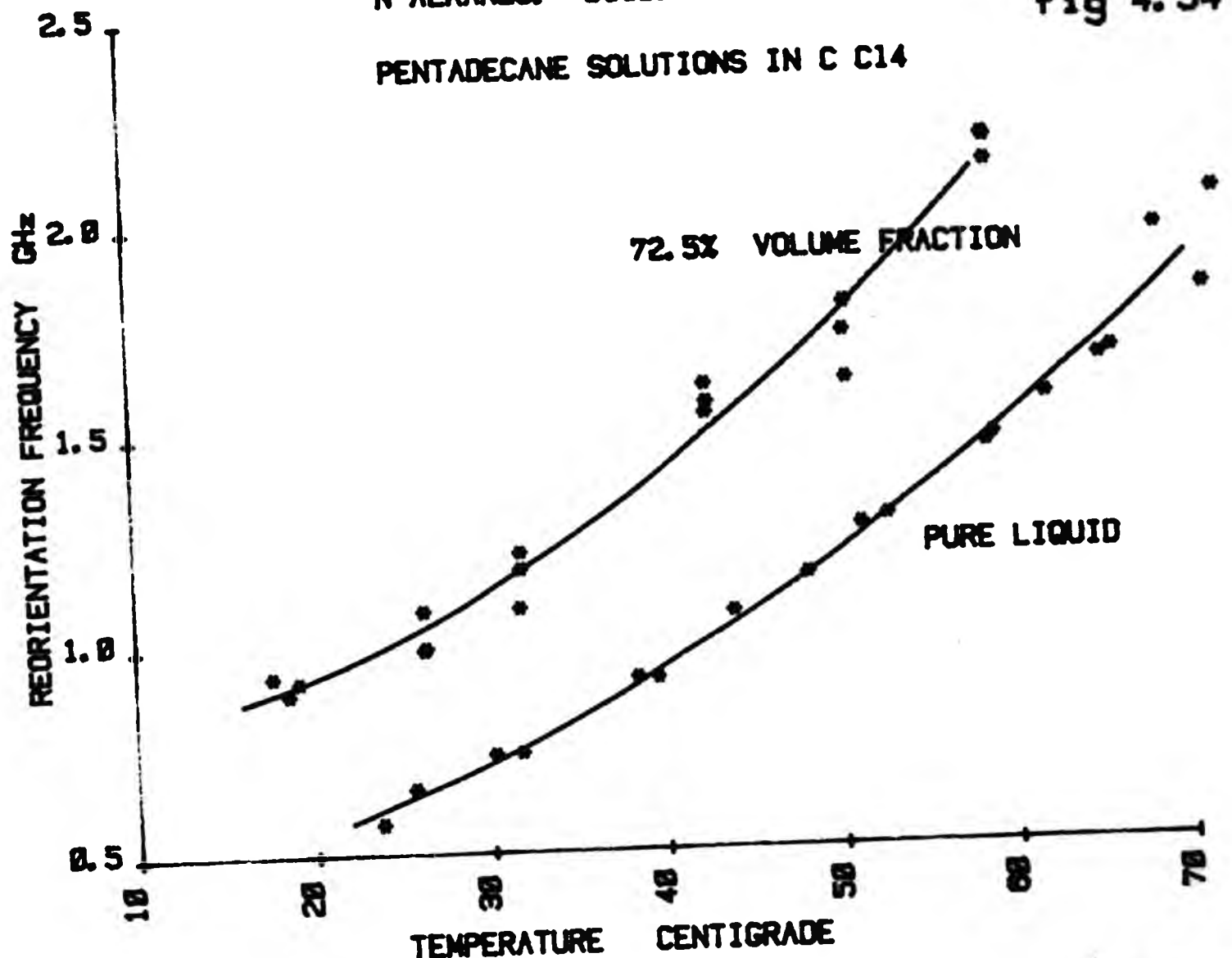
N ALKANES: SINGLE LORENTZIAN FITS
OCTANE SOLUTIONS IN C C14

fig 4.53



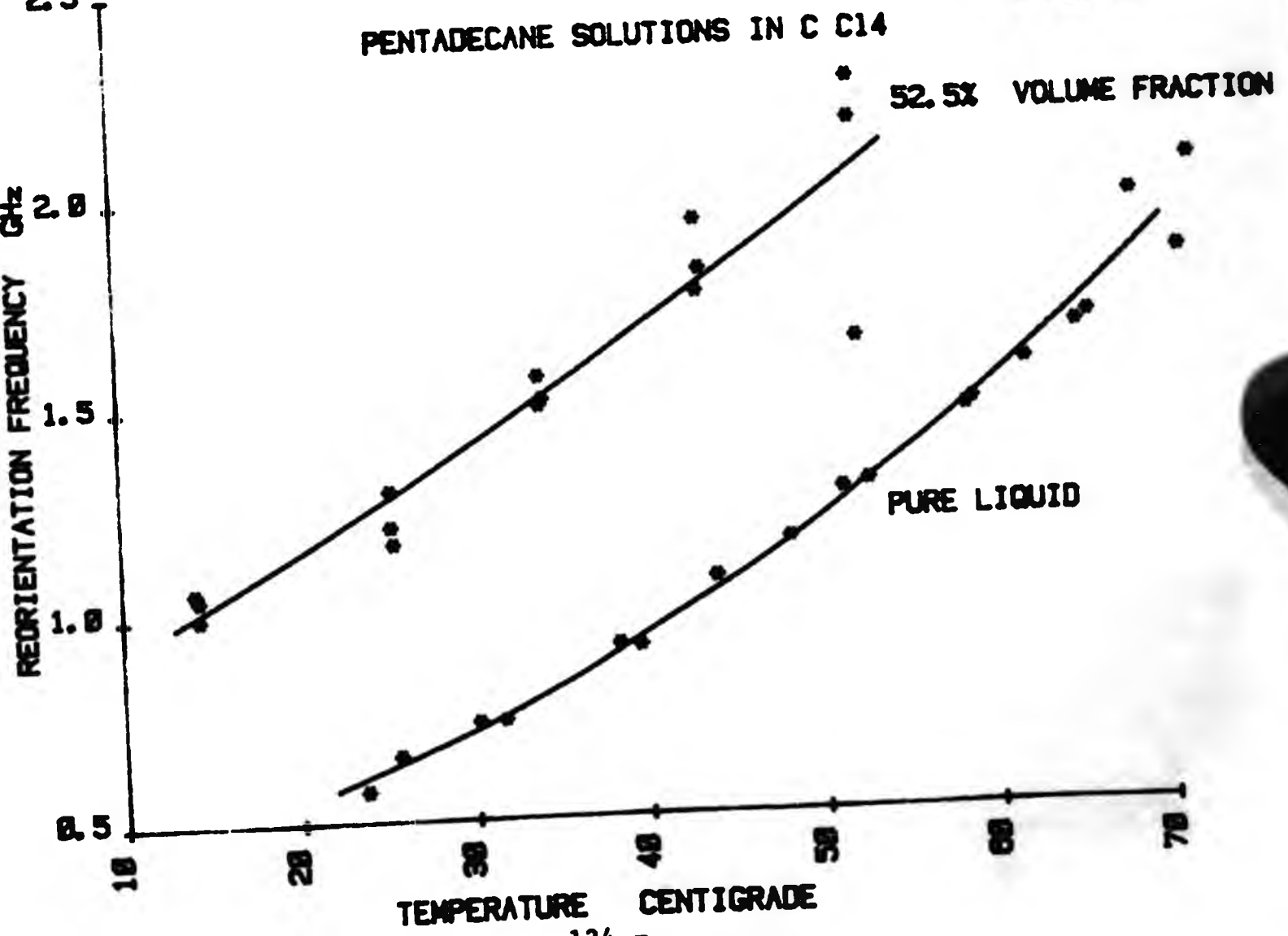
N ALKANES: "DOUBLE" LORENTZIAN FITS
PENTADECANE SOLUTIONS IN C C14

fig 4.54



N ALKANES: "DOUBLE" LORENTZIAN FITS
PENTADECANE SOLUTIONS IN C C14

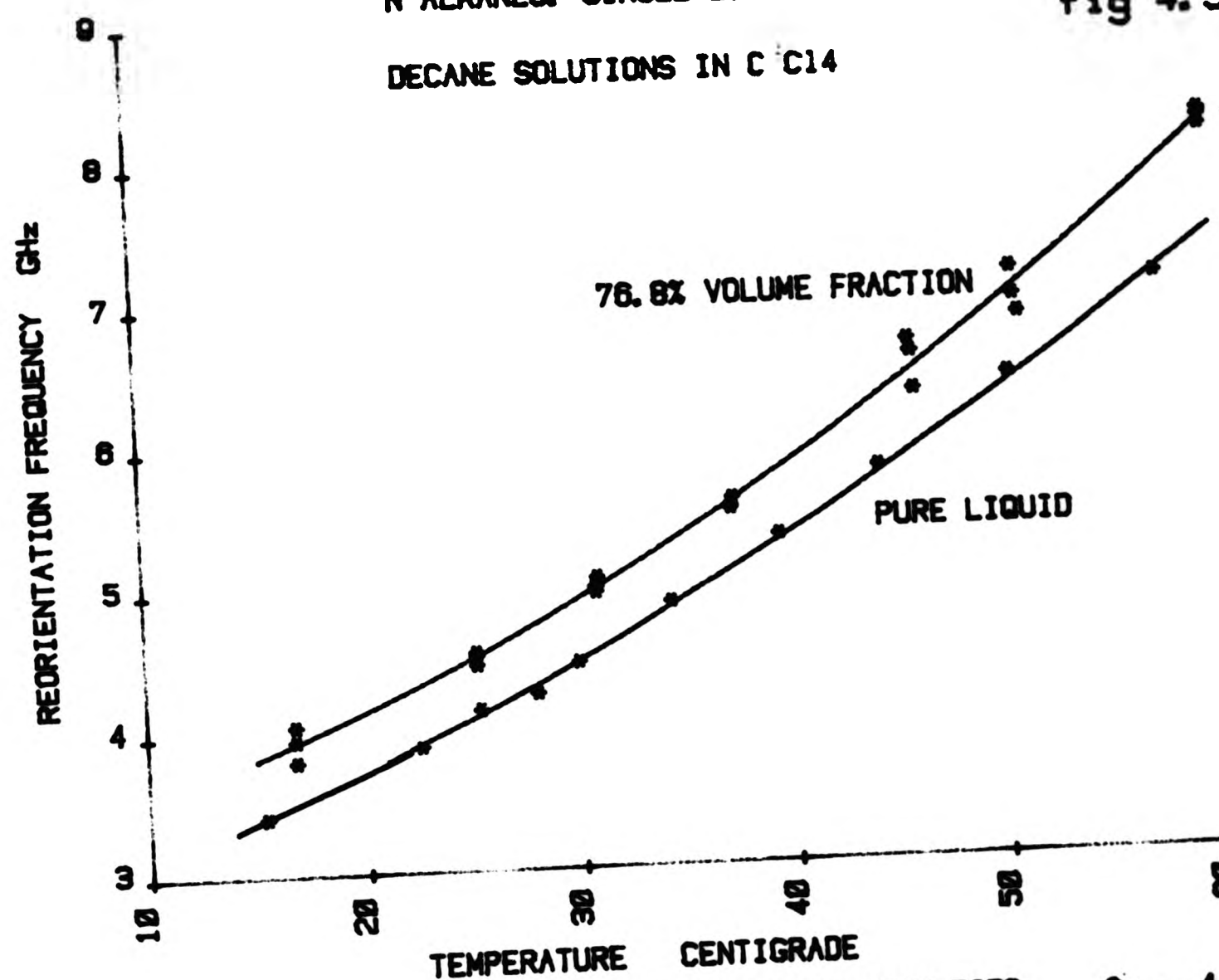
fig 4.55



N ALKANES: SINGLE LORENTZIAN FITS

fig 4.56

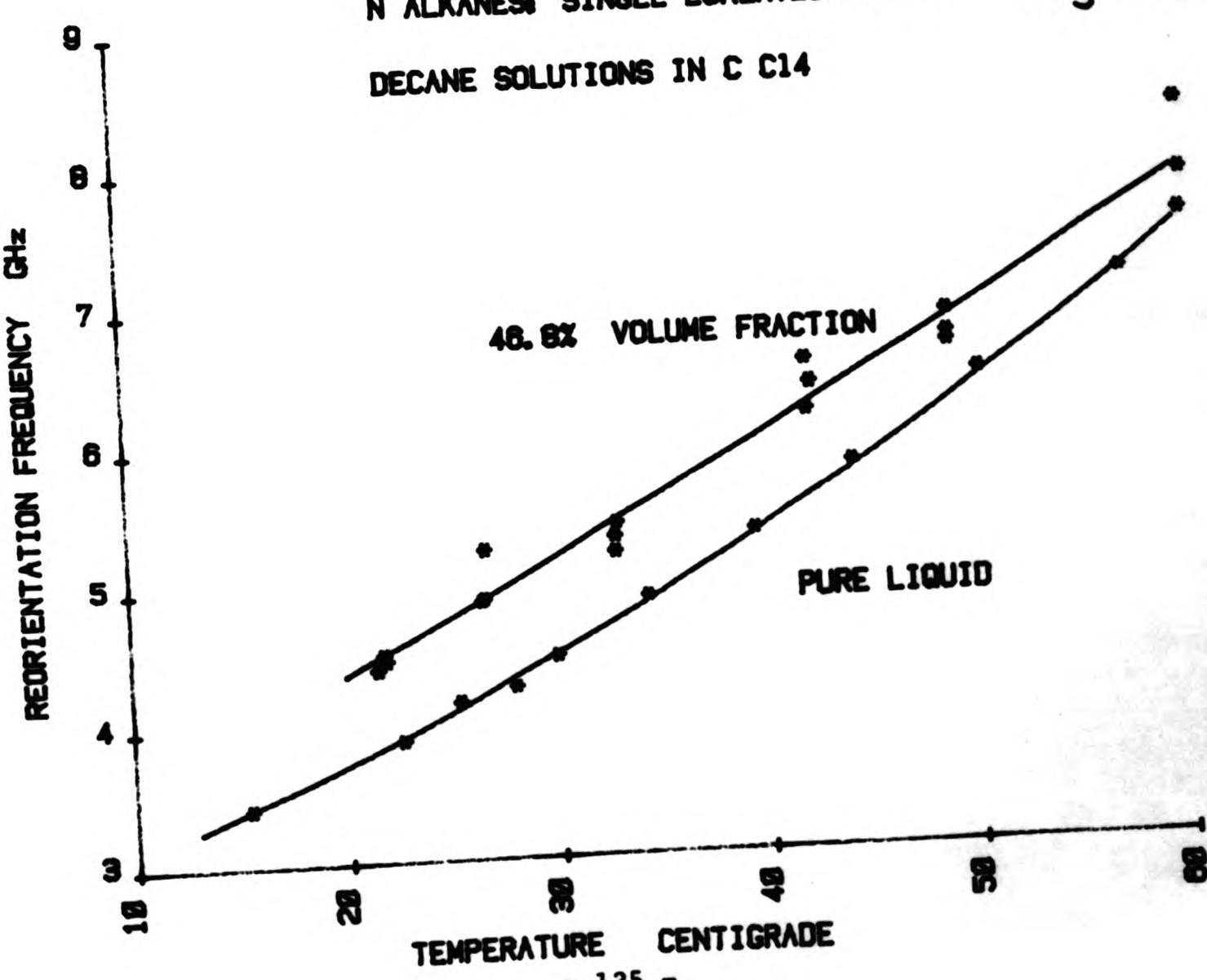
DECANE SOLUTIONS IN C C₁₄



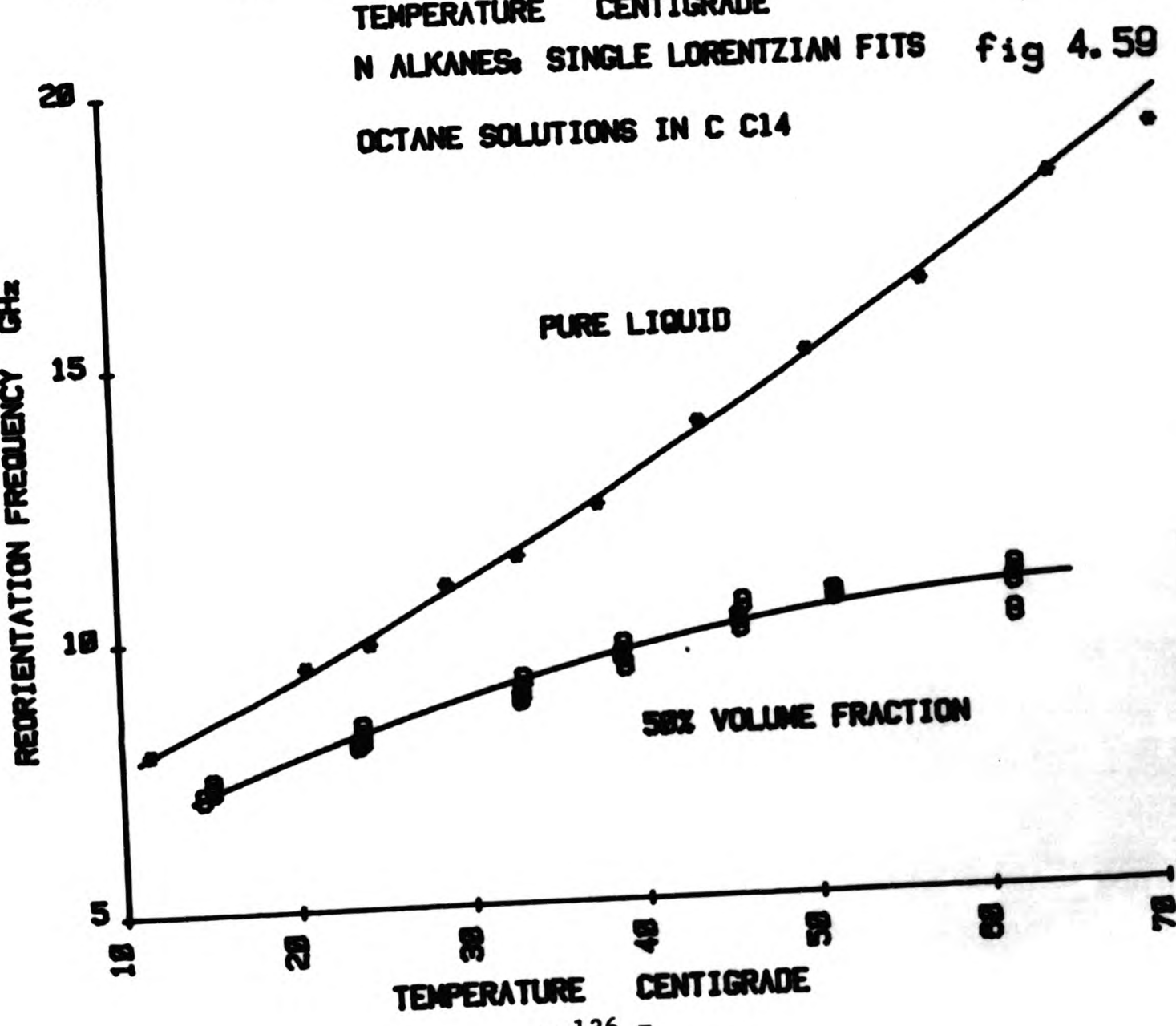
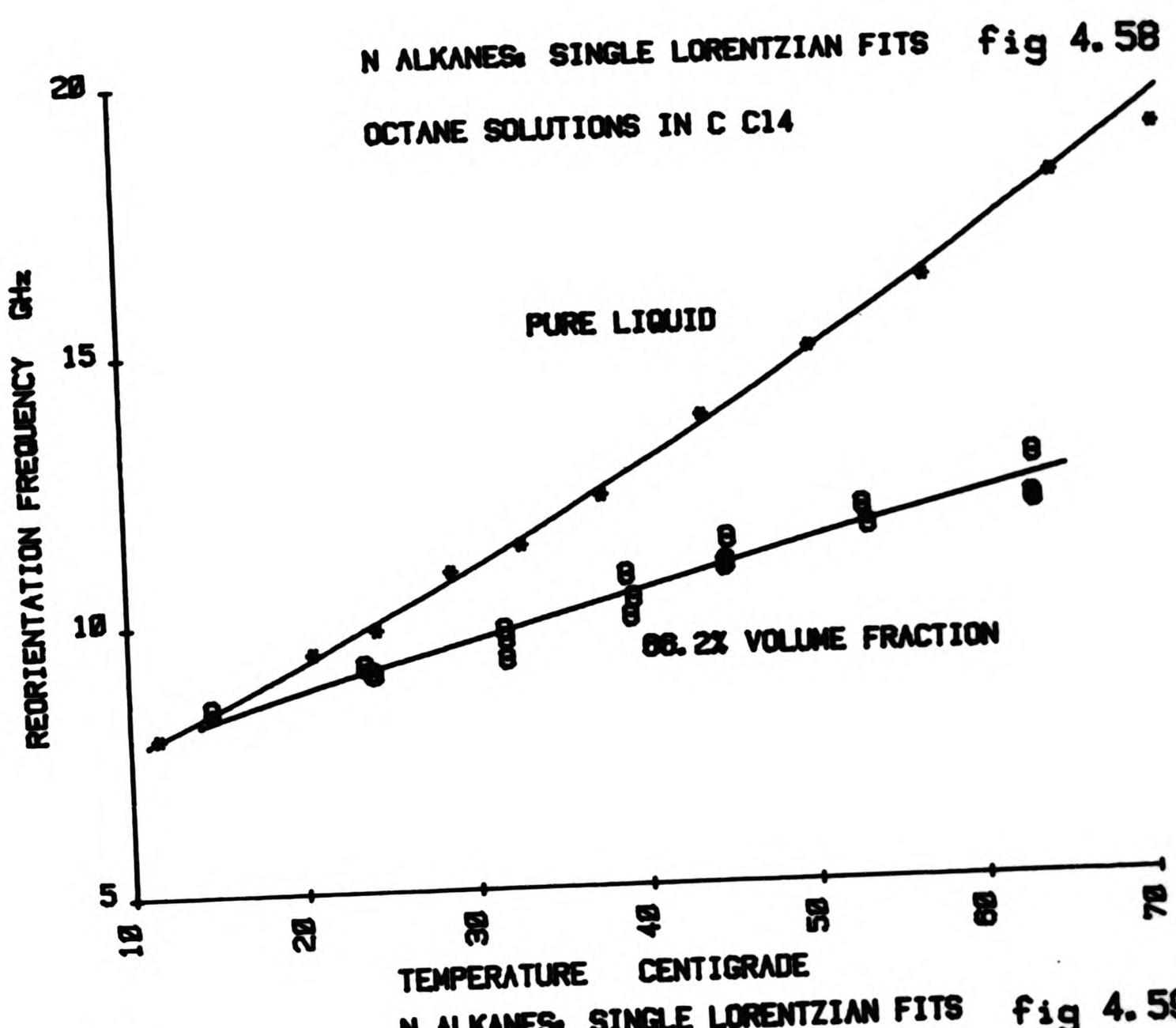
TEMPERATURE CENTIGRADE

N ALKANES: SINGLE LORENTZIAN FITS

fig 4.57



TEMPERATURE CENTIGRADE

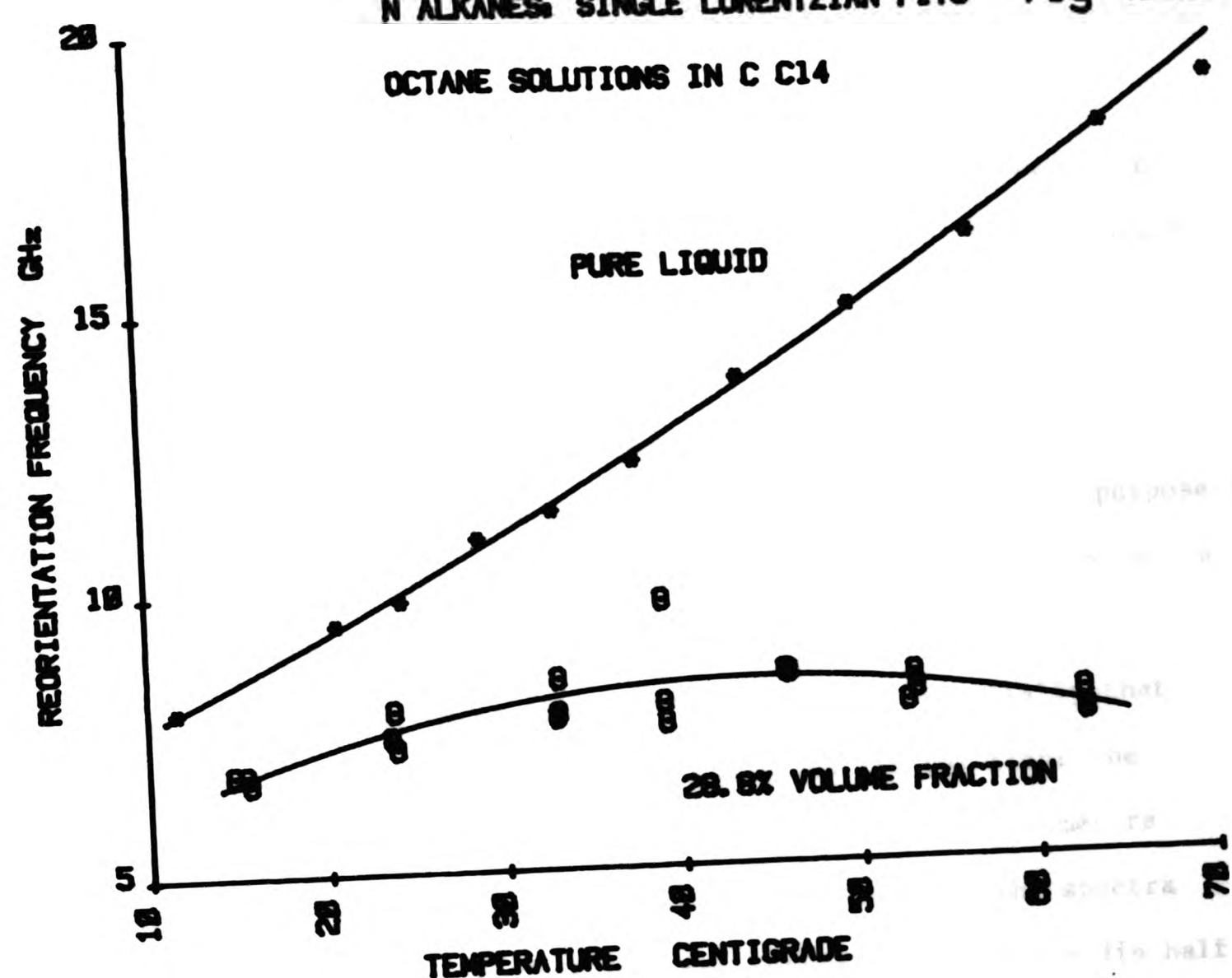


N ALKANES: SINGLE LORENTZIAN FITS fig 4.60

OCTANE SOLUTIONS IN C C14

PURE LIQUID

28.8% VOLUME FRACTION



from the quantity Gap obtained from the Stokes Einstein fits to the data for the neat alkanes.

The work was performed in essentially two parts.

Initially for a fixed temperature each alkane was examined over a range of solution concentrations (Figs 4.48 to 4.53). The intention was to investigate how the quantity Gap varies with solution concentration for a fixed temperature.

Then for a number of solution concentrations samples were examined over a range of temperatures (Figs 4.54 to 4.60). The purpose of this was to investigate how the quantity Gap varies with temperature for a fixed solution concentration.

The method of interpretation of the results is essentially that detailed for the n-alkanes. For pentadecane and its solutions the spectra are analysed in terms of Lorentzian plus dip. R parameters are obtained for these solutions. For decane and octane the spectra are such that the value of $K^2 n / \rho$ (the theoretical value of the dip half width) is much less than the half width of the main feature. The spectra therefore approximate to Lorentzians and are treated as such in the analysis.

RESULTS

R Parameters for Pentadecane

R parameters are obtained for solutions of pentadecane in carbon tetrachloride (see table 4.9). All these were obtained at a temperature of 24.5 °C. For the low concentration solutions (ie below 50% volume concentration) there was an increasing noise level on the spectra which masks the dip, making the values of the R parameter obtained unreliable.

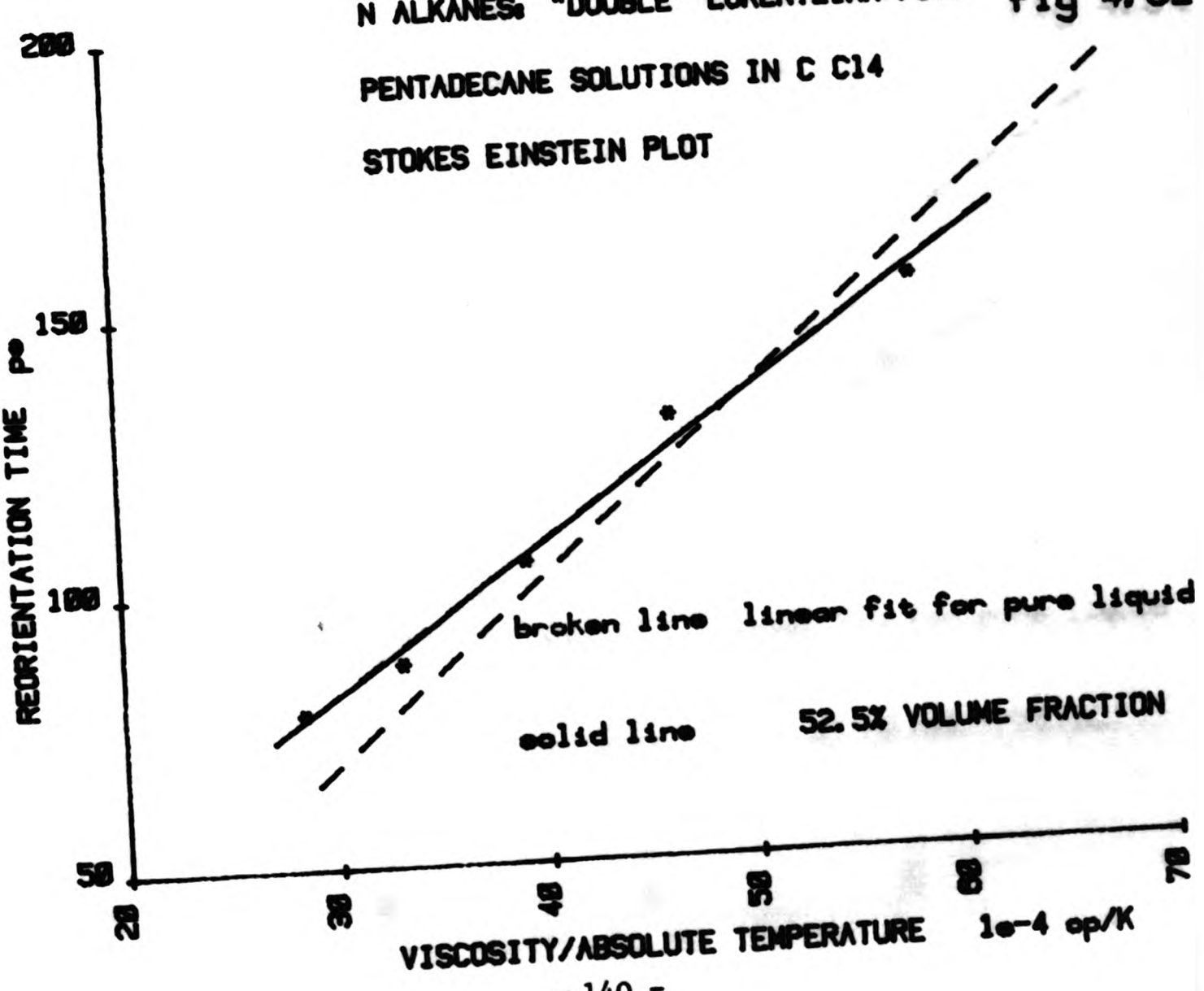
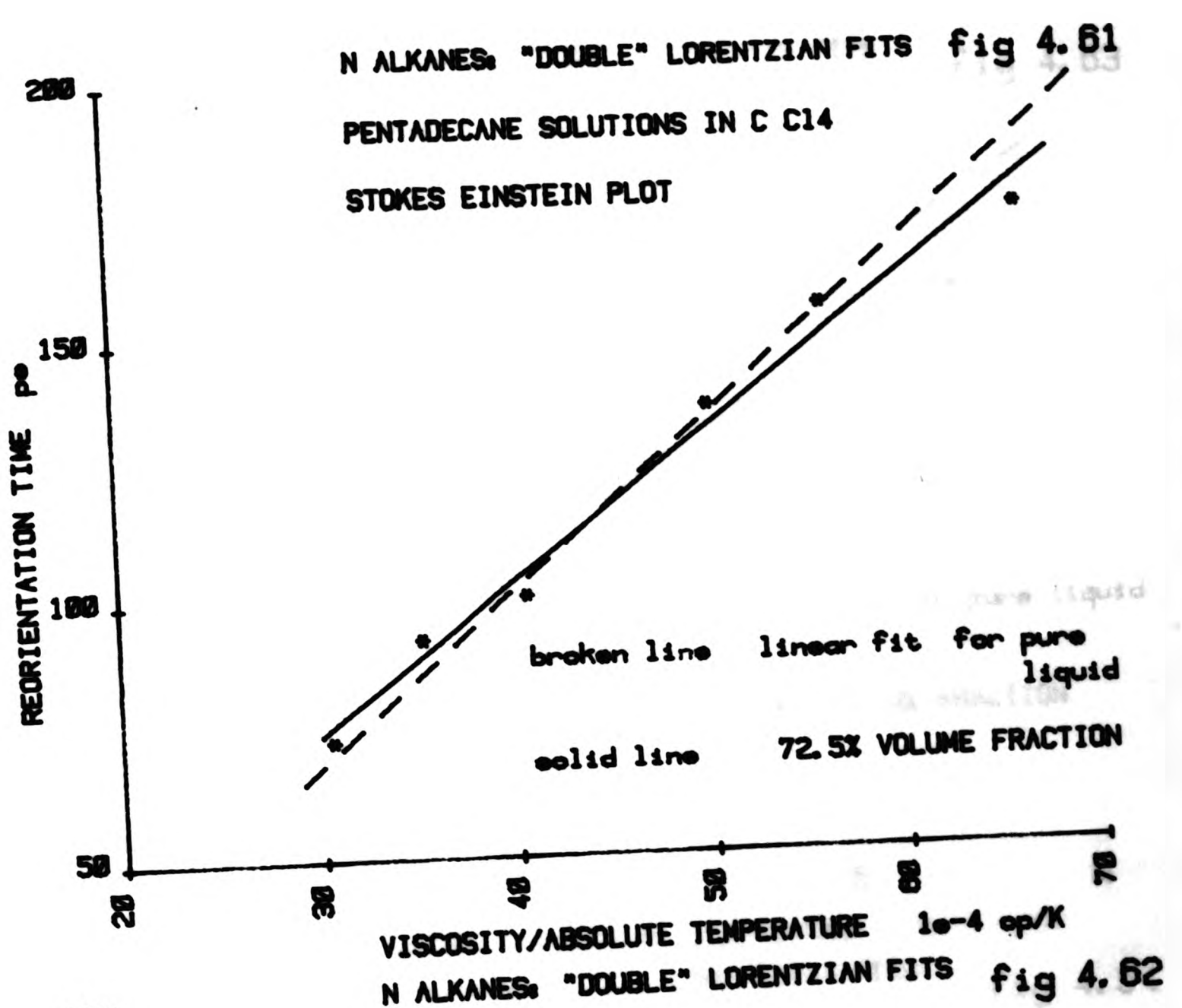
Table 4.9

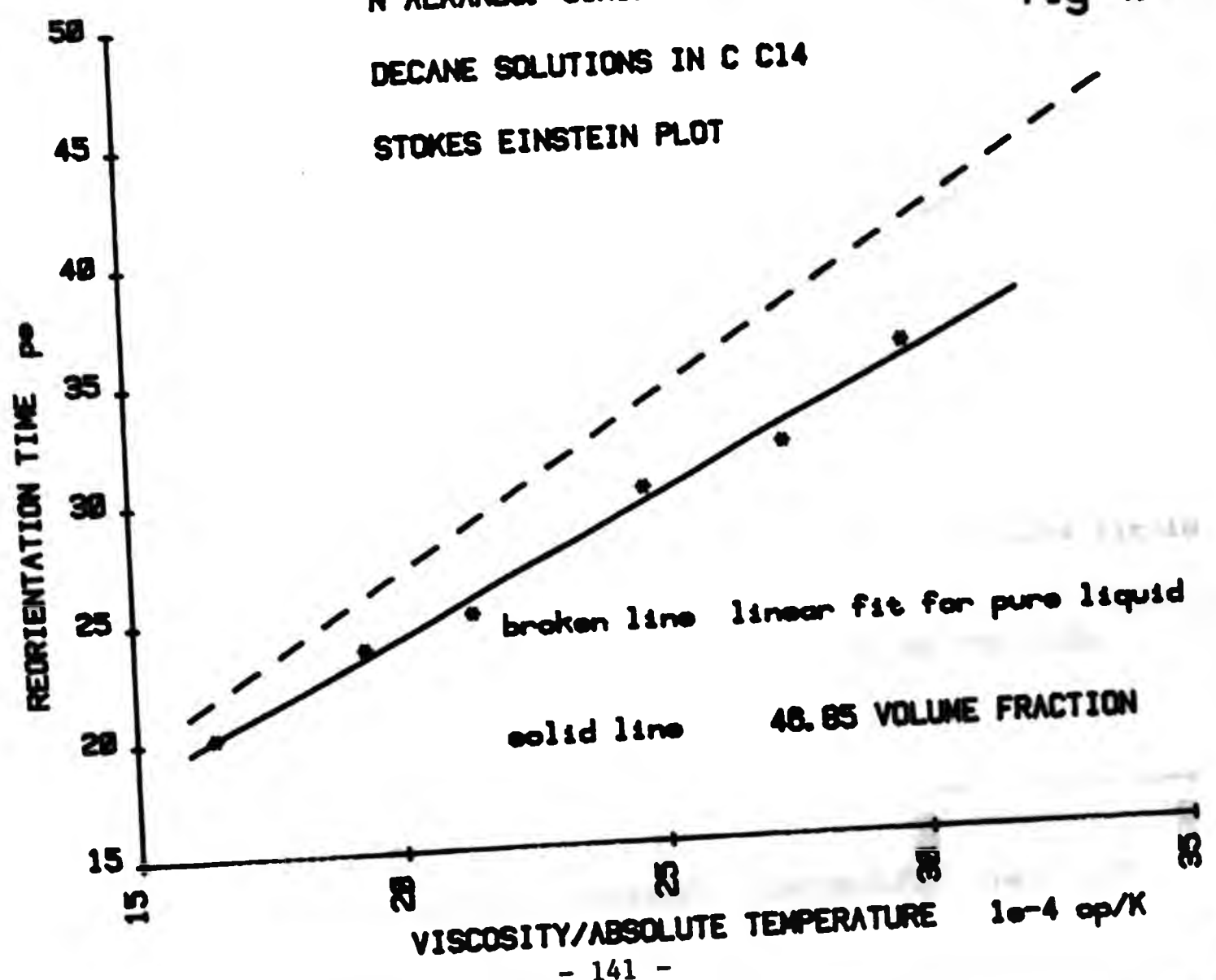
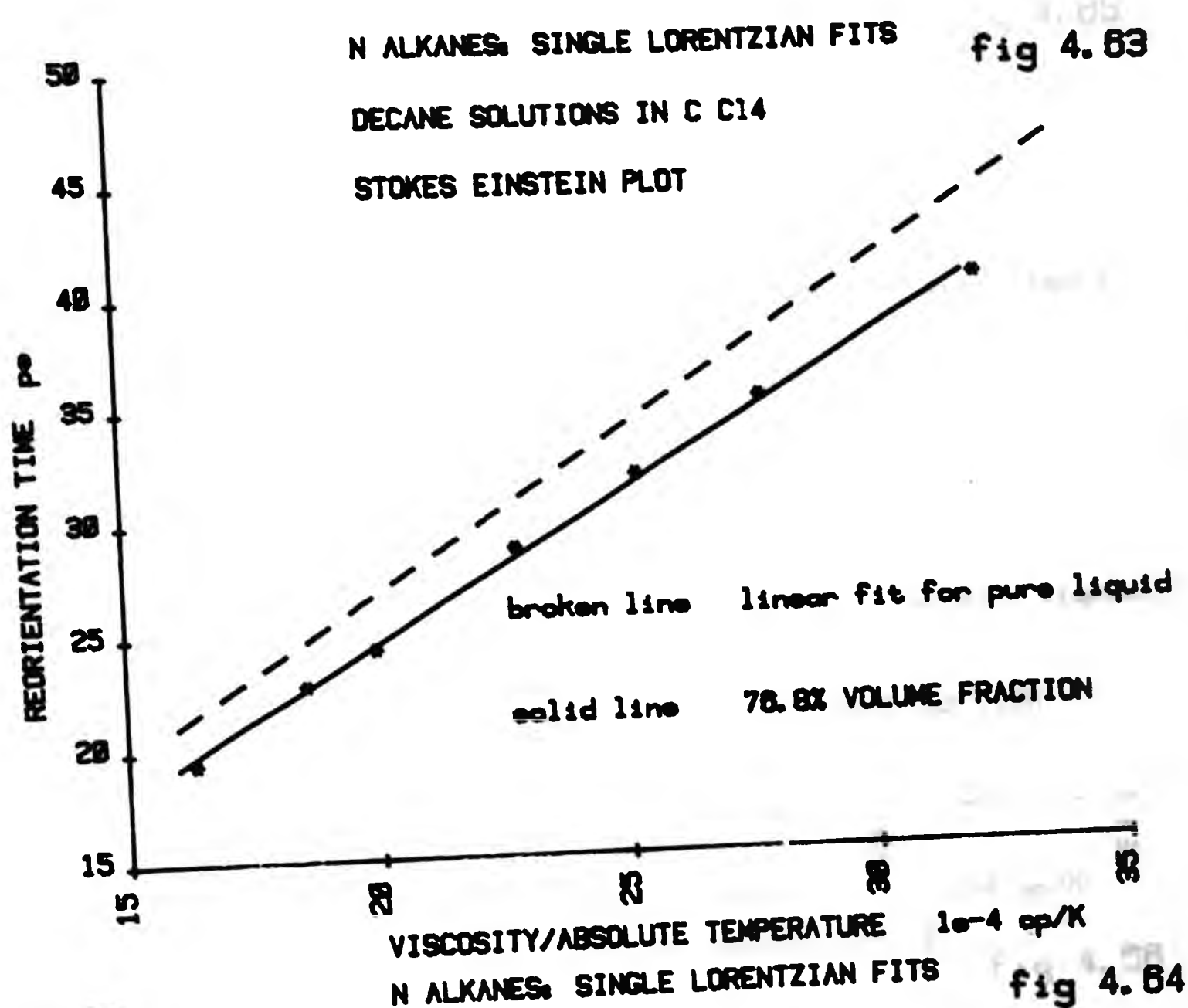
C ₁₅ H ₃₂ Solution Volume Concentration	R Parameter (Average Value)
100.0%	0.310
91.1%	0.285
85.4%	0.289
77.8%	0.254
67.7%	0.237
57.3%	0.142
41.3%	0.072)) large error in) 0.013)) these results) 0.005)
23.1%	
12.1%	

All the data from which the above results are obtained are shown on the graph Fig 4.49. It may be seen that, over the volume concentration regime in which the results for the R parameter are believed to be valid, R is approximately directly proportional to the solution volume concentration. This dependence of R parameter on solution concentration has also been observed (7) for solutions of nitrobenzene in carbon tetrachloride.

STOKES EINSTEIN FITS TO DATA

As stated the solution work supplied two sets of depolarised light scattering data for each n-alkane. The first set has information from light scattering data for each n-alkane over a range of solution concentrations for fixed temperatures. The second set has information for particular solution concentrations over a range of temperatures. It is this second set of data which we first examine.





N ALKANES: SINGLE LORENTZIAN FITS fig 4.65

OCTANE SOLUTIONS IN C C14

STOKES EINSTEIN PLOT

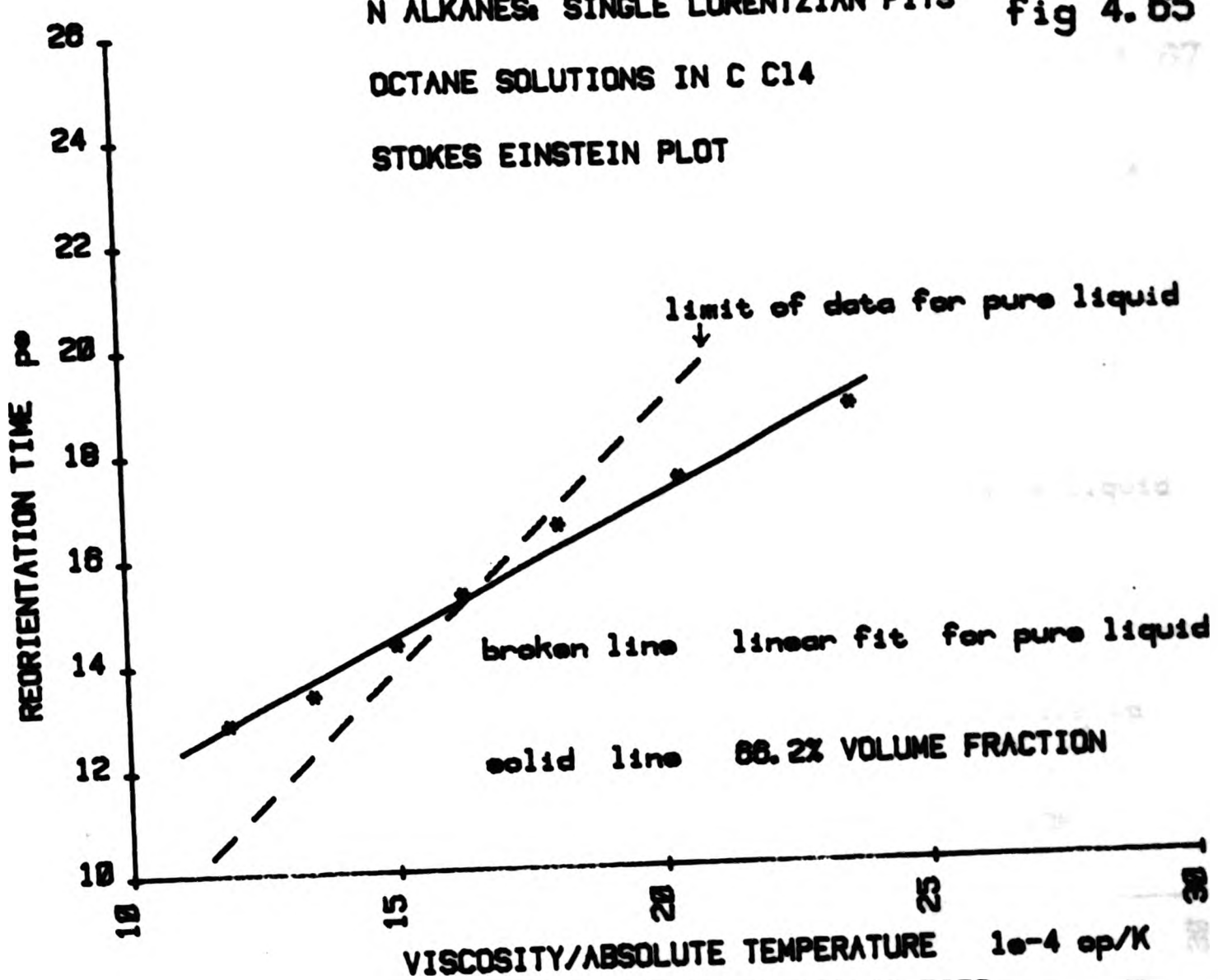
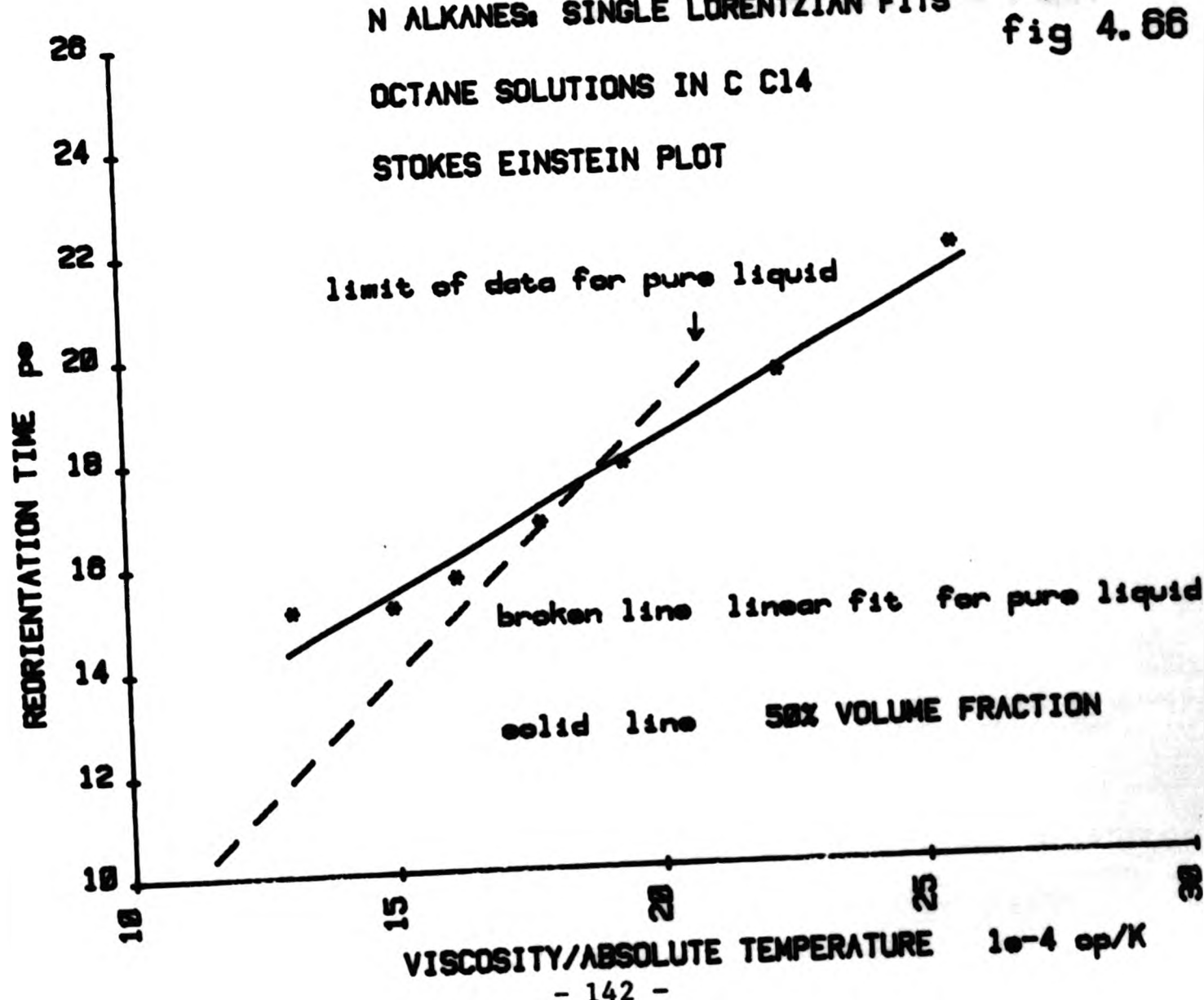


fig 4.65



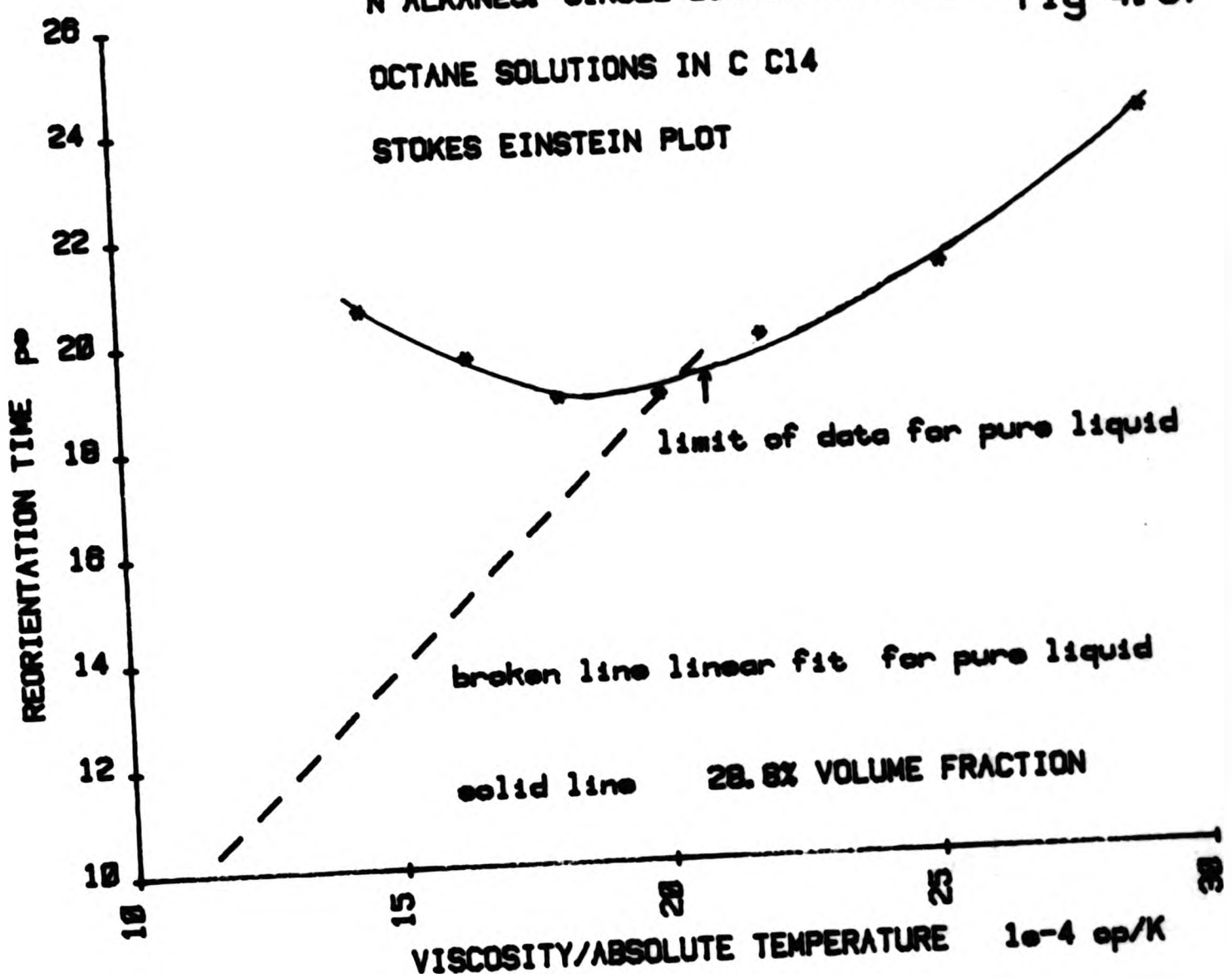
VISCOSITY/ABSOLUTE TEMPERATURE 10^{-4} cP/K

- 142 -

N ALKANES: SINGLE LORENTZIAN FITS fig 4.67

OCTANE SOLUTIONS IN C C14

STOKES EINSTEIN PLOT



The graphs of the results are presented (Figs 4.61 to 4.67). In table 4.10 we present the volumes obtained from the Stokes Einstein fits to spectra taken at different temperatures for the same volume concentration.

Table 4.10

Liquid	% Volume Concentration In CCl_4	Stokes Einstein $\text{Volume } \text{\AA}^3$	Gap
$\text{C}_{15}\text{H}_{32}$	100.0	456	1.75
	72.5	402	1.55
	52.5	367	1.41
$\text{C}_{10}\text{H}_{22}$	100.0	197	1.07
	76.8	183	0.99
	46.8	157	0.85
C_8H_{18}	100.0	136	0.88
	66.2	72.7	0.47
	50.0	77.8	0.51
	28.8	non linear	-

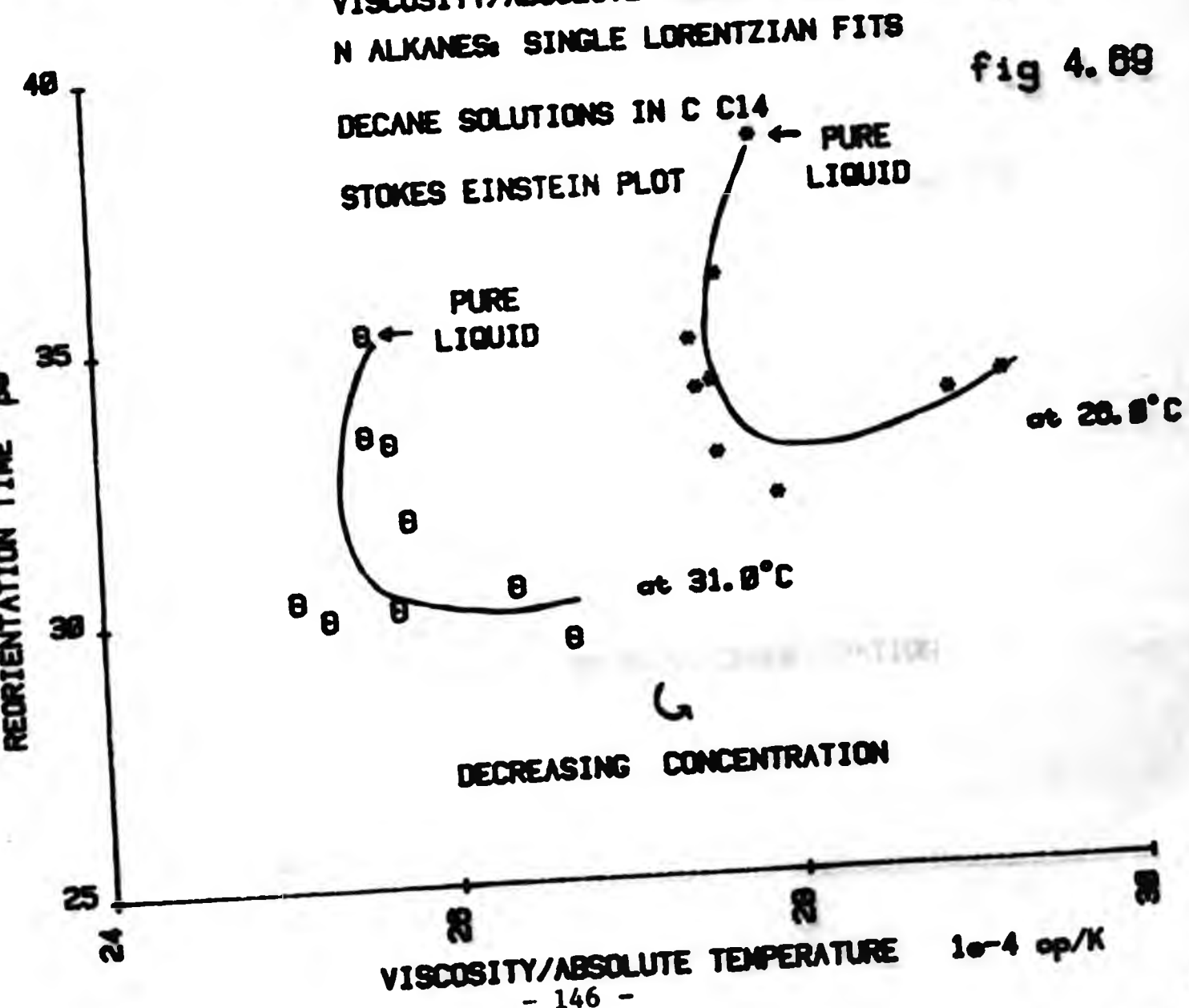
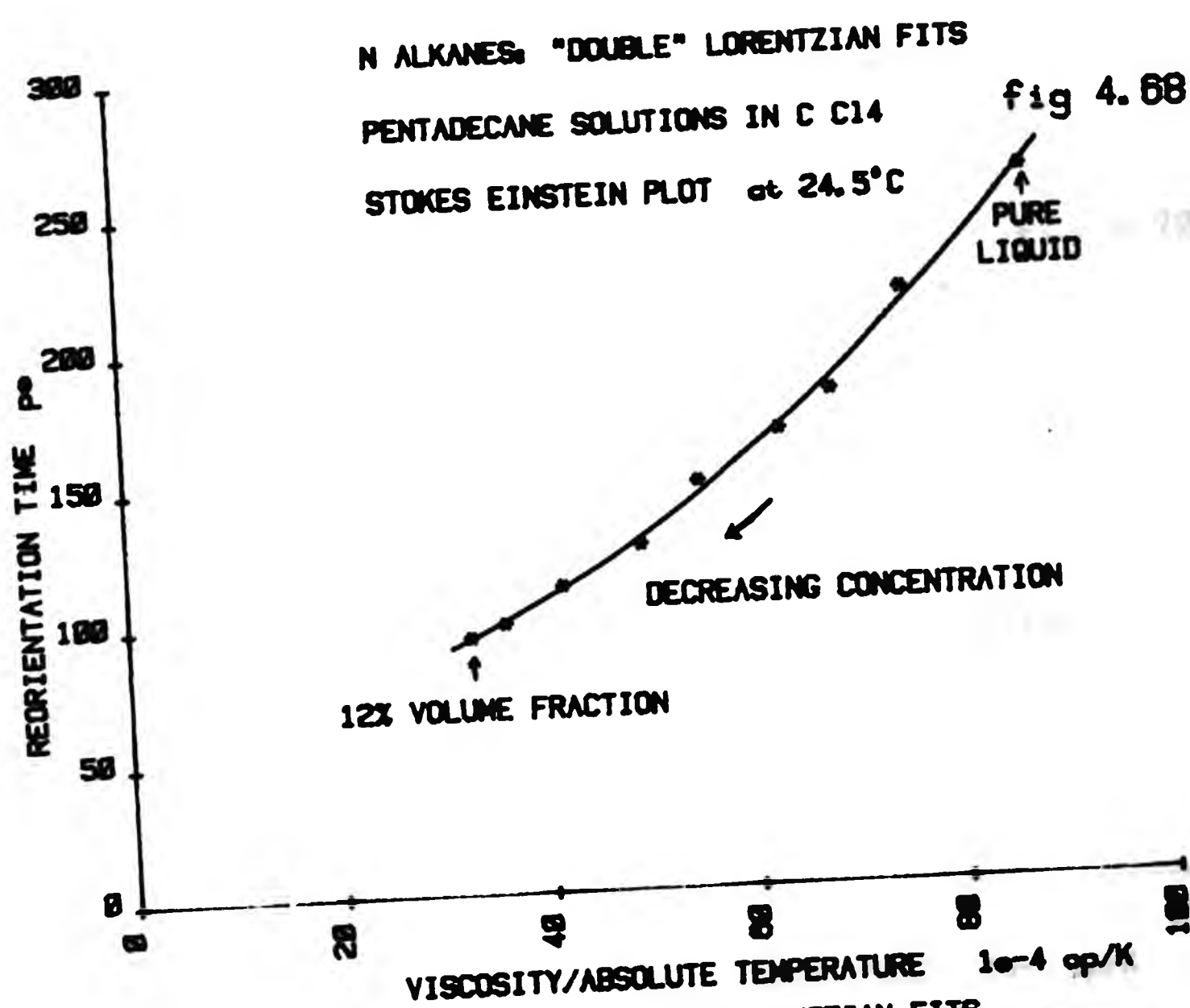
For the $\text{C}_{15}\text{H}_{32}$ and $\text{C}_{10}\text{H}_{22}$ solutions Figs 4.61 to 4.64 show a linear relationship between n/T and τ_{LS} , the relaxation time obtained from the depolarised Rayleigh scattering. The Stokes Einstein volumes obtained decrease with decreasing volume concentration of the solution. For $\text{C}_{10}\text{H}_{22}$ the relative decrease of the Stokes Einstein volume with dilution is slightly less than that for $\text{C}_{15}\text{H}_{32}$. From a simple viewpoint this decrease in the Stokes Einstein volume is due to the changing value of the orientational correlation parameter G with

solution concentration. The fact that the decrease is proportionately less for $C_{10} H_{22}$ is in accord with the accepted behaviour of the G parameter from the depolarised light intensity measurements of Clement and Bothorel.

It should also be noted that for $C_{15} H_{32}$ and $C_{10} H_{22}$ the value of the intercept on the time axis increased with decreasing solution concentration. This may be an indication that inertial effects become more significant in dilute solutions.

For $C_8 H_{18}$ as solution concentration decreases the Stokes Einstein plots become less and less linear, (Figs 4.65 to 4.67). The Stokes Einstein volumes for the lower solution concentrations of $C_8 H_{18}$ are well below those measured for the neat alkane. The accepted value of G for $C_8 H_{18}$ is approximately one which would imply no change in the quantity G upon dilution of the alkane. It is evident however that there is a considerable change in the quantity Gap with decreasing solution concentration from which we would infer that for $C_8 H_{18}$ the quantity αp has a strong concentration dependence. If this also applies to the other n-alkanes it is questionable whether a Stokes Einstein interpretation of the data would furnish a separation of the quantity Gap into its component parts.

Also the parameter G is predicted by De Gennes to be a function of temperature as well as concentration. α and p , which are both functions of molecular shape and hence of conformation are also temperature dependent which results from the fact that the conformation of these flexible molecules is itself temperature dependent. Consequently a range of solution concentrations for a fixed temperature were examined in order to investigate how Gap varies with solution concentration for a fixed temperature and to effect a separation of the various parameters.



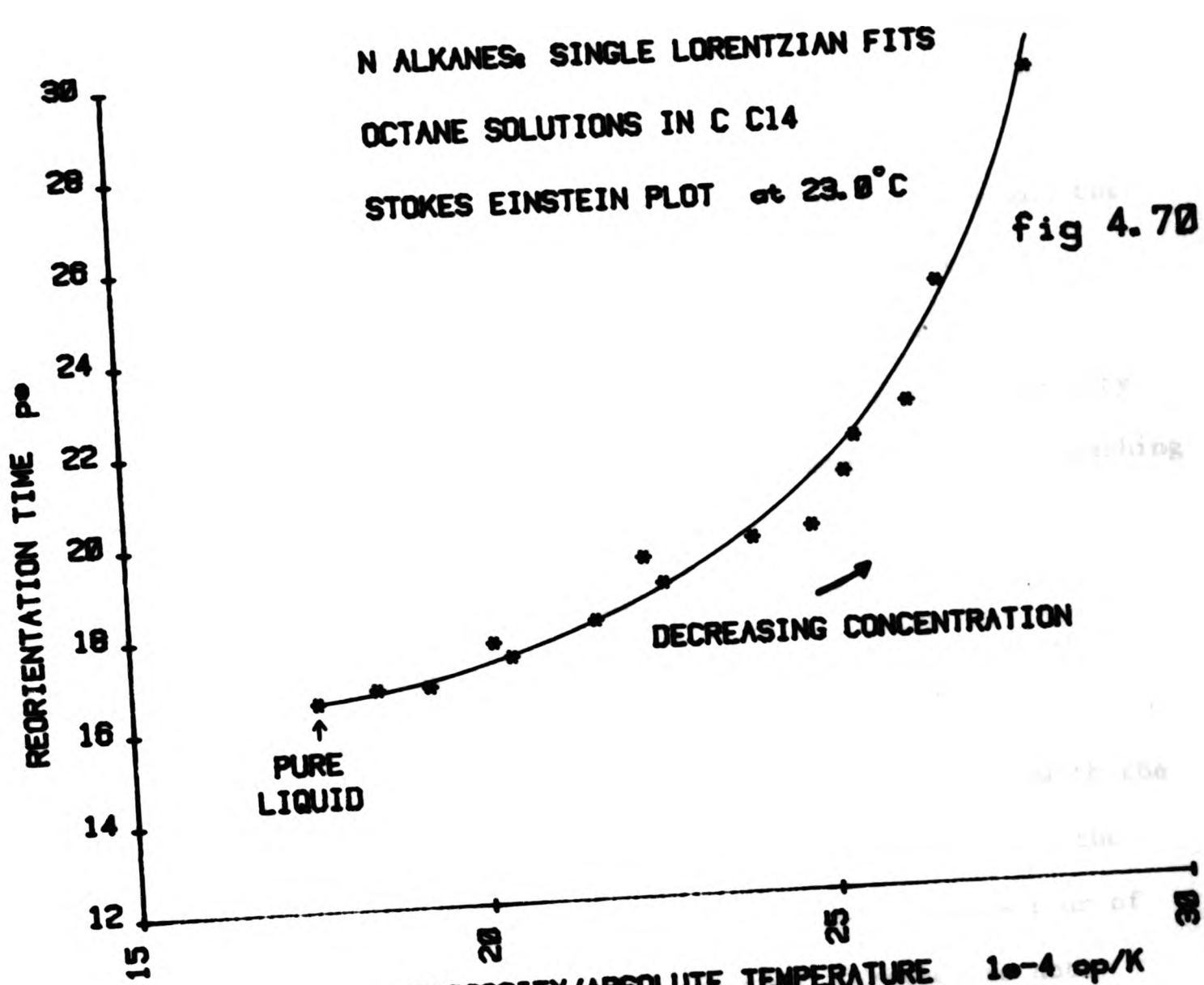


fig 4.70

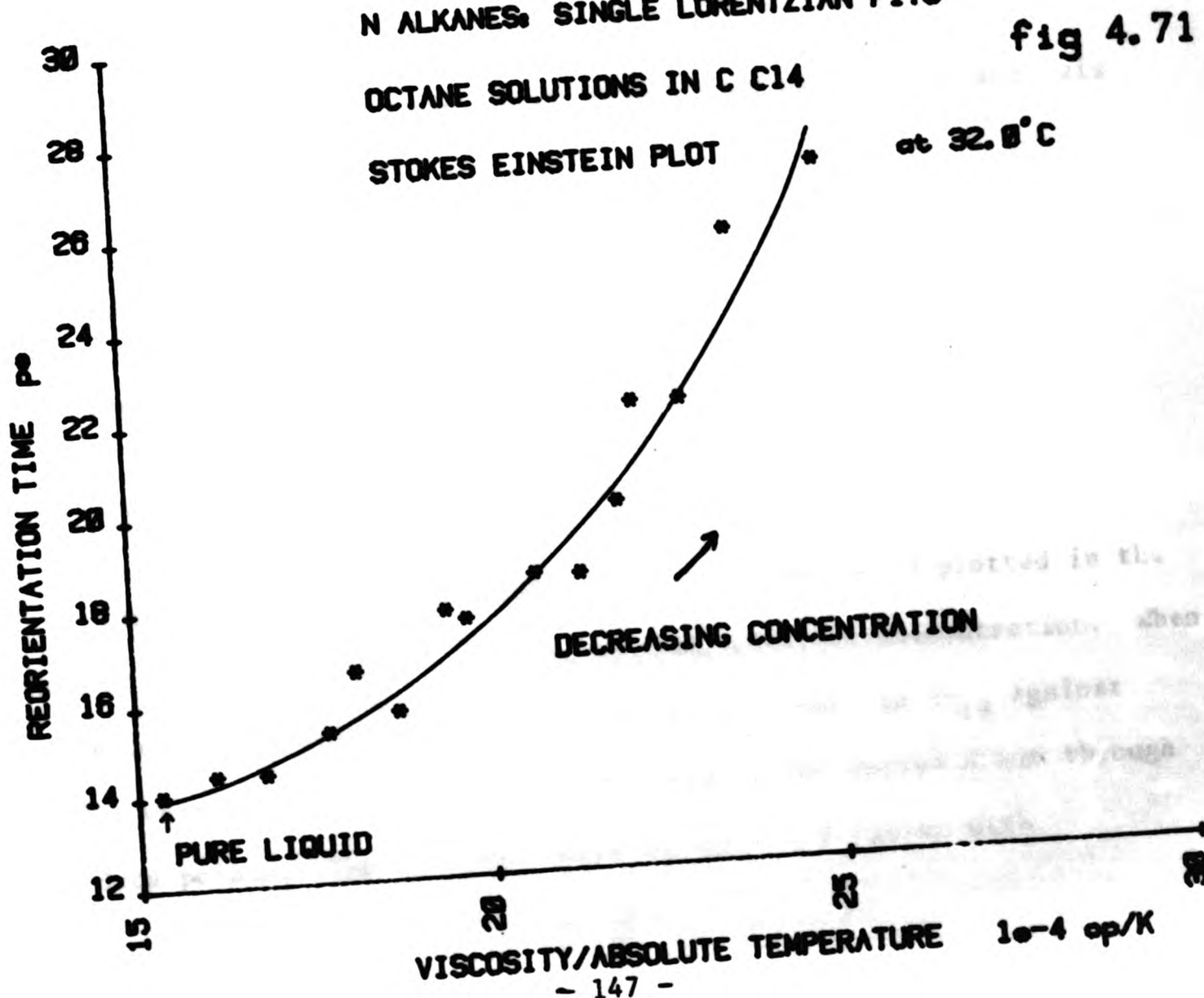


fig 4.71

The data from these experiments on solutions of the n-alkanes $C_{15}H_{32}$, $C_{10}H_{22}$, C_8H_{18} in carbon tetrachloride is presented in Figs 4.68 to 4.71.

$C_{15}H_{32}$ has a higher viscosity than carbon tetrachloride and the viscosity of the resultant solutions is a strong function of concentration, decreasing with decreasing solution concentration.

$C_{10}H_{22}$ at room temperature has approximately the same viscosity as carbon tetrachloride and the viscosity of the mixture varies reaching a minimum at intermediate concentrations.

C_8H_{18} has a lower viscosity than carbon tetrachloride and the viscosity of the resultant solutions is a strong function of concentration, increasing with decreasing solution concentration.

In the case of $C_{15}H_{32}$ and C_8H_{18} the variation of (n/T) with the varying concentration of the solution is much more evident than the changes in τ . Hence a comparison between the molecular behaviour of the different liquids as solution concentration decreases is not directly available.

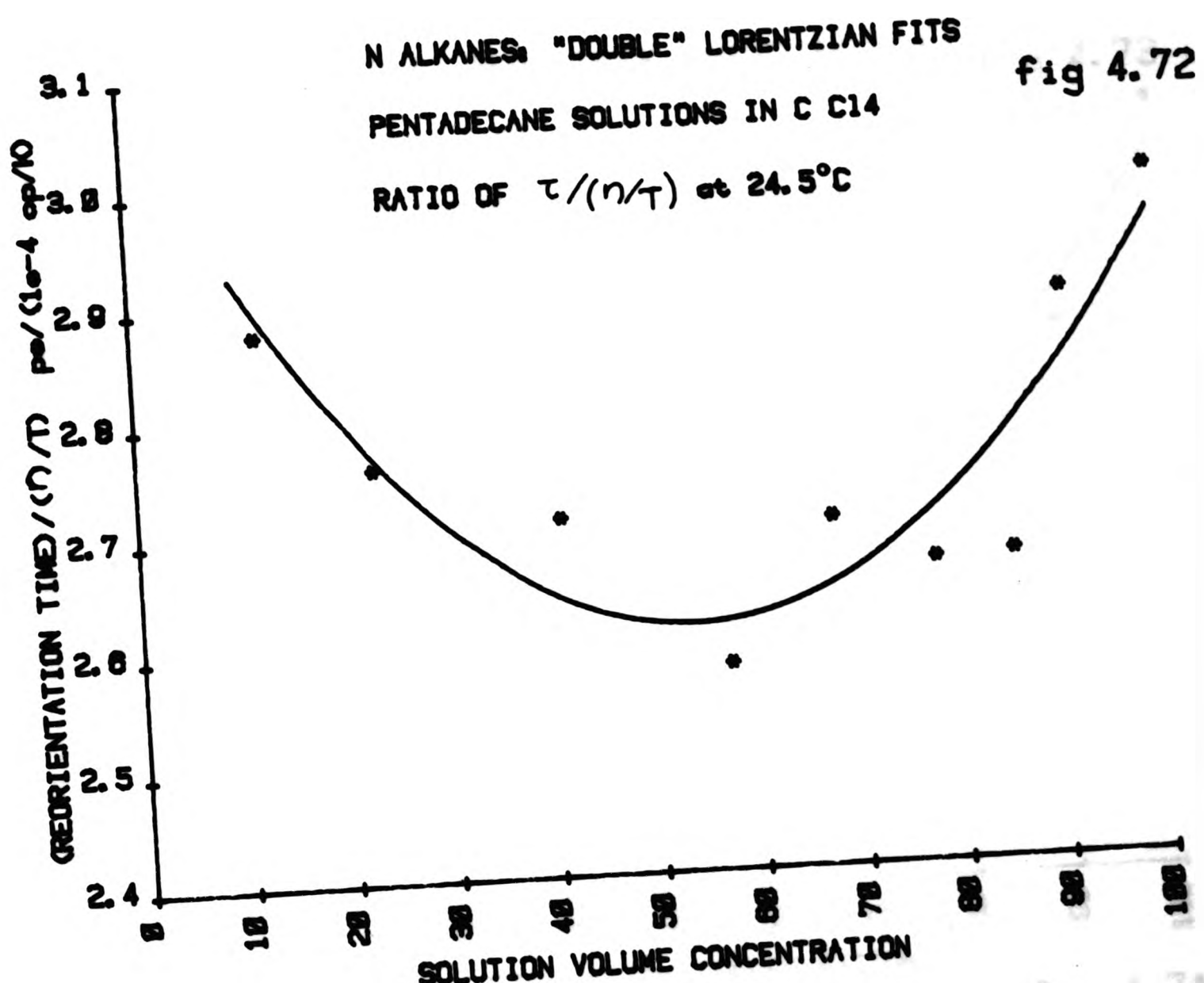
The Stokes Einstein equation which has been used in the analysis of this data is

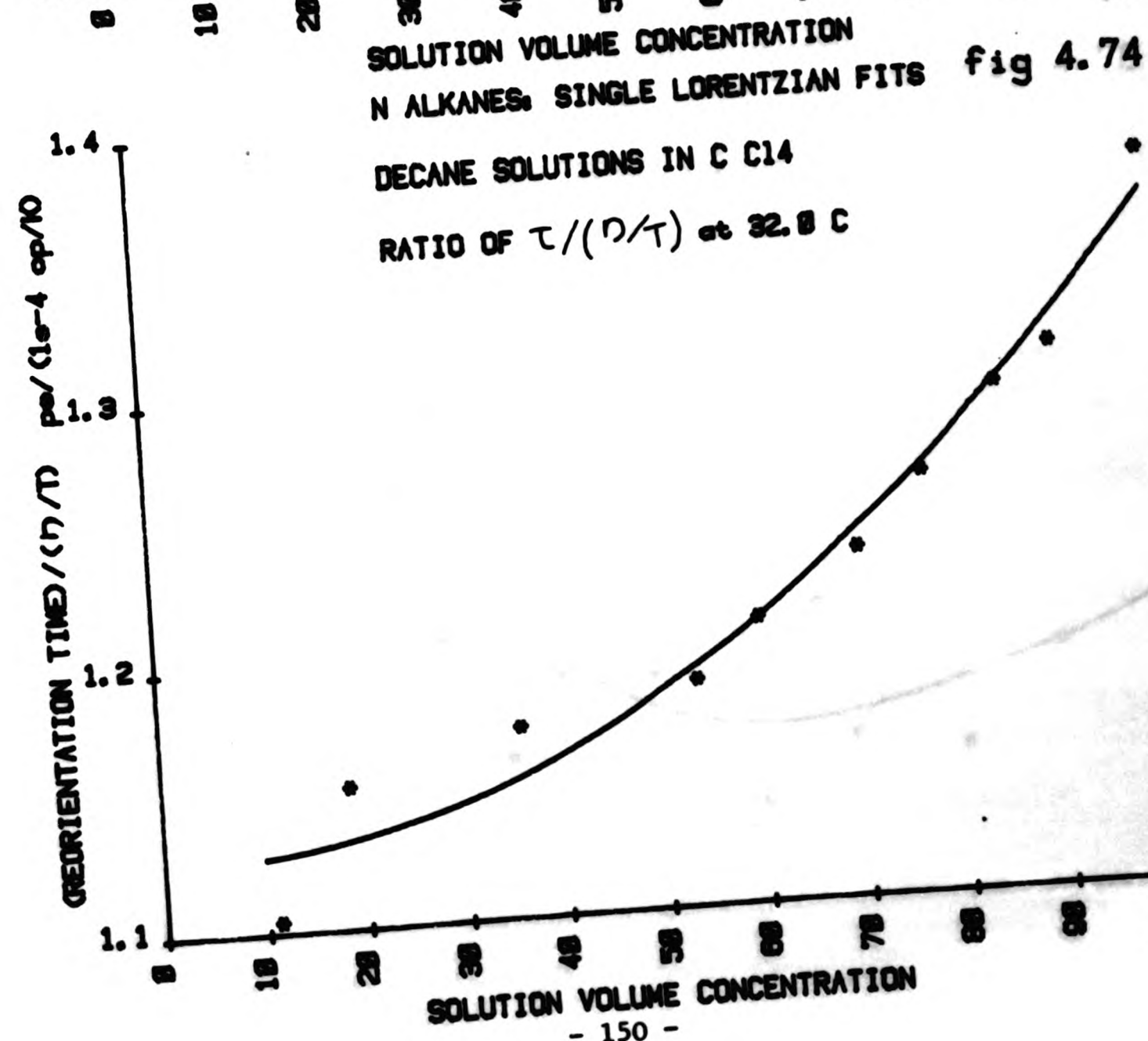
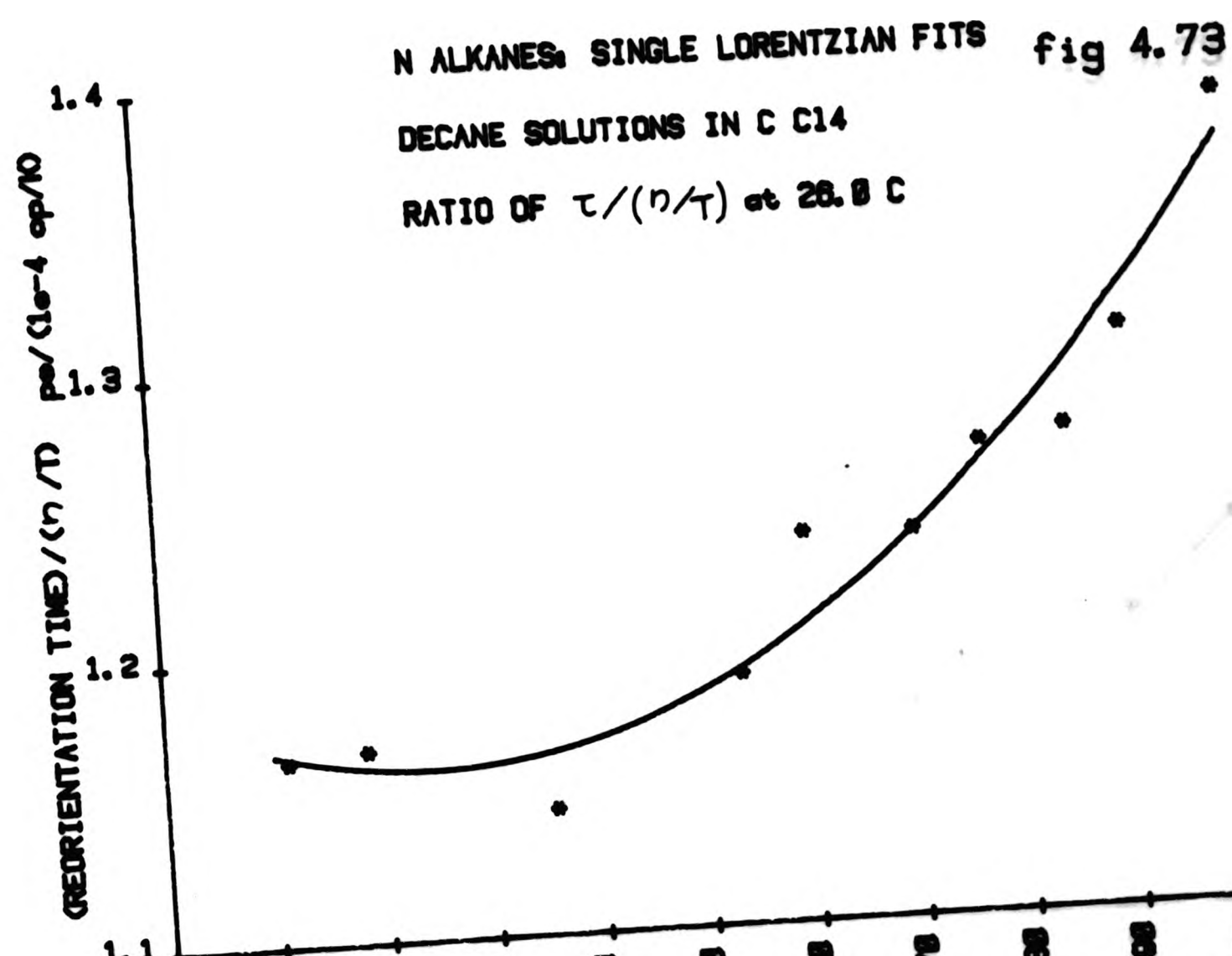
$$\tau_{LS} = G \left[\frac{apV}{K} \frac{n}{T} + \tau_0 \right]$$

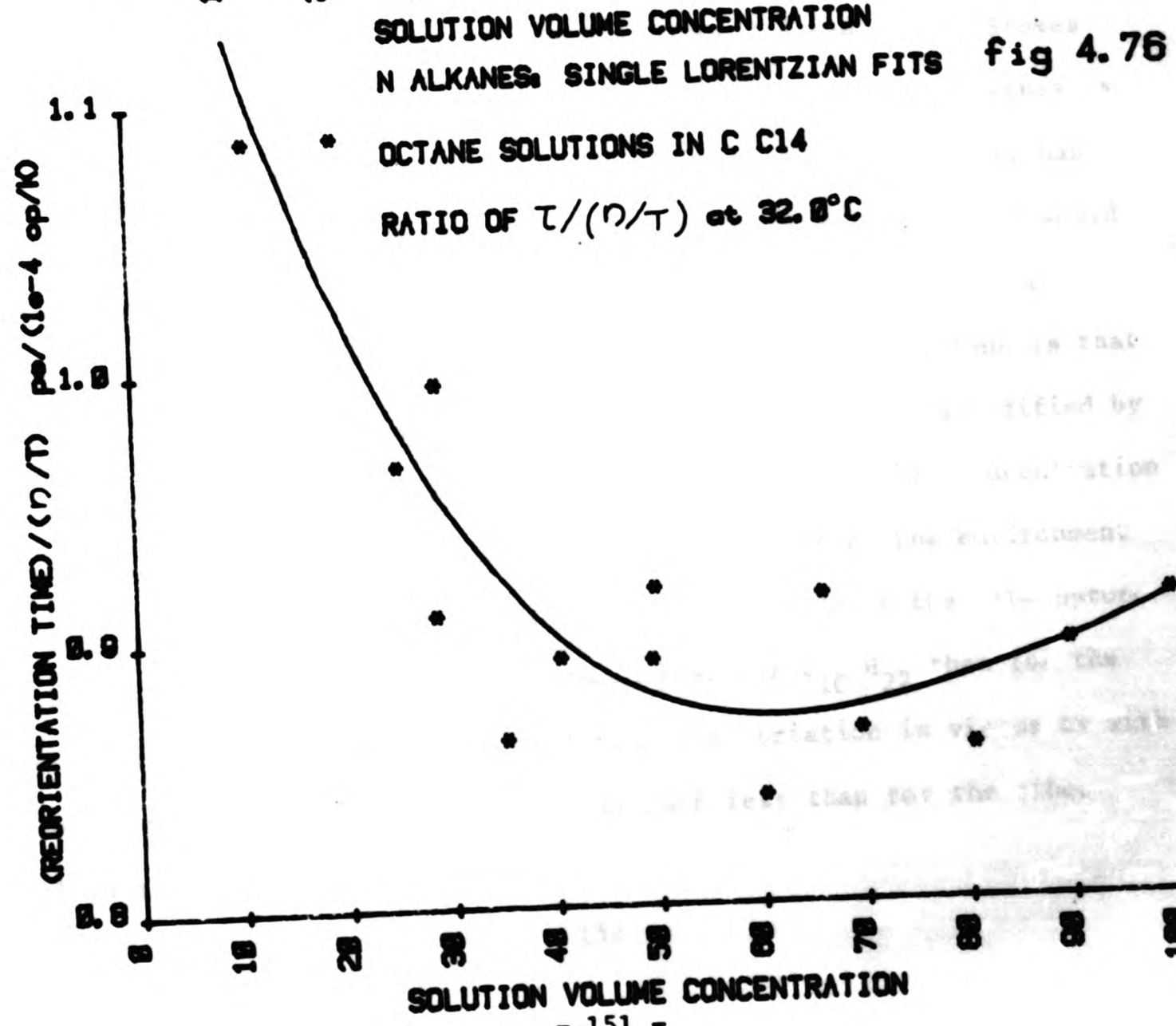
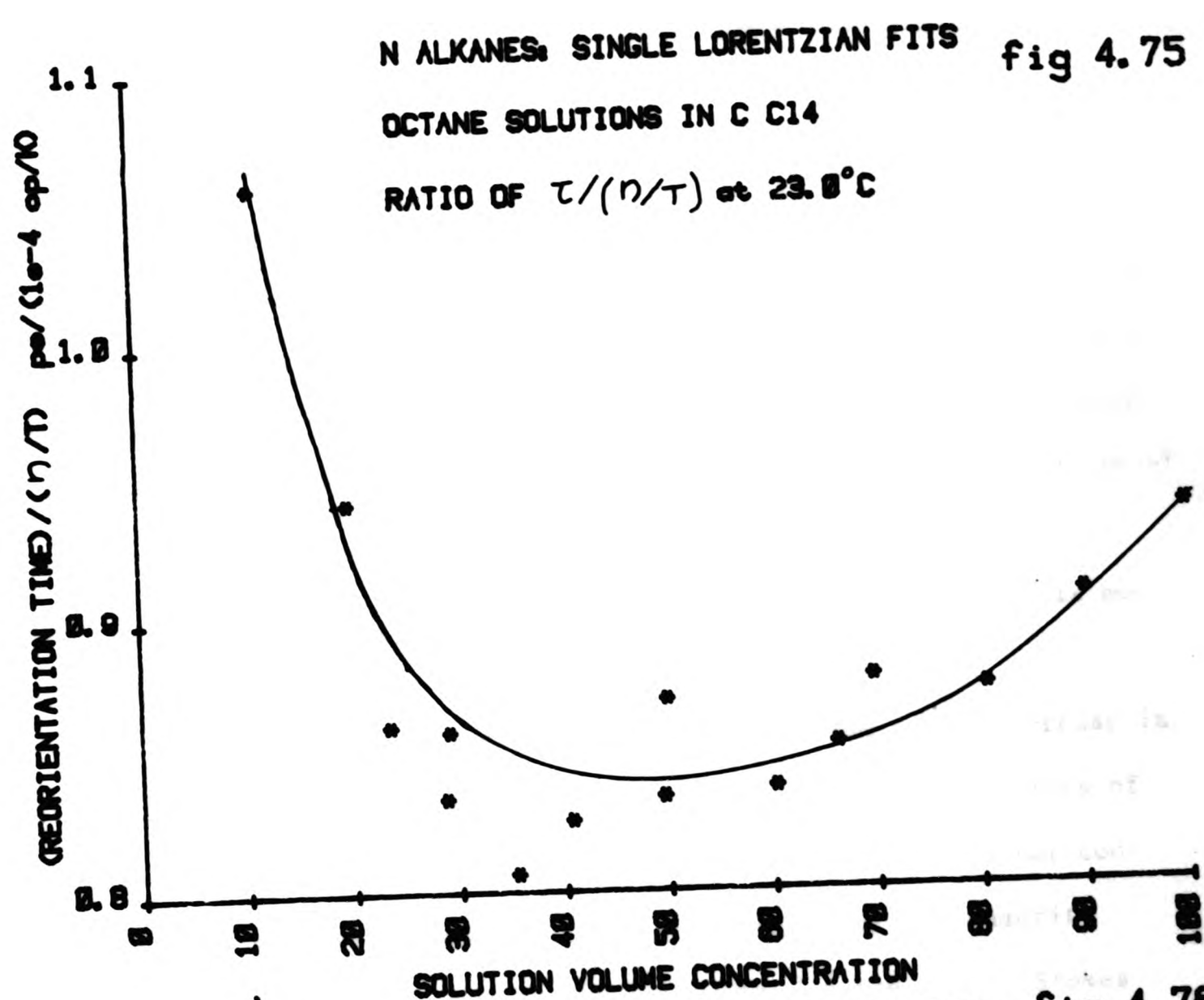
The equation may also be written as

$$\tau_{LS}/(n/T) = G \left[\frac{apV}{K} + \tau_0/n/T \right]$$

The results from these light scattering spectra is plotted in the form of the variation of $\tau_{LS}/(n/T)$ against solution concentration. When the results were plotted in the conventional manner ie (τ_{LS} against (n/T)) very large curvatures were observed on the curves drawn through the data points. The different ways in which n/T varies with







concentration in the three separate liquids made interpretation very difficult.

In the graphs Figs 4.72 to 4.76 of $\tau_{LS}/(n/T)$ against solution concentration for the different n-alkanes a number of similarities are observed. In all cases as solution concentration decreases the value of $\tau_{LS}/(n/T)$ decreased. This is to be perhaps expected from a simple model in which G, the orientation correlation function decreases with solution concentration. However in all cases, below a concentration of about 30% there appears to be an upturn in the value of $\tau_{LS}/(n/T)$. For C₁₅H₃₂ and C₈H₁₈ this is very pronounced, for C₁₀H₂₂ it is much less pronounced.

This upturn could be explained perhaps in terms of an increase in G at low concentrations (which is unlikely) or by changing values of α or p (which may be the case as dilution changes the molecular conformation). Another possibility is the behaviour of the quantity G($\tau_0/(n/T)$) which corresponds to the intercept (in the simple Stokes Einstein approximation) divided by (n/T). τ_0 for the neat alkanes is negative and small compared to the measured values of τ_{LS} . It has been suggested that τ_0 can be related to inertial rotation, and would therefore be a function of temperature only. However a possible explanation of the behaviour observed for the alkane solutions is that τ_0 is also a function of the molecular environment and is modified by the intermolecular torques. Changing the alkane solution concentration changes the macroscopic liquid viscosity and modifies the environment experienced by the molecule. It may be no coincidence that the upturn observed at low concentrations is much less for C₁₀H₂₂ than for the other alkanes, and due to the fact that the variation in viscosity with solution concentration for C₁₀H₂₂ is much less than for the other alkanes.

A simple analysis of reorientational times obtained by depolarised light scattering from both alkane solutions and the neat liquids has indicated that superficially at least the Stokes Einstein model derived from a simple hydrodynamic model describes the reorientational behaviour. However when an attempt is made to analyse the results in greater detail a number of problems have arisen.

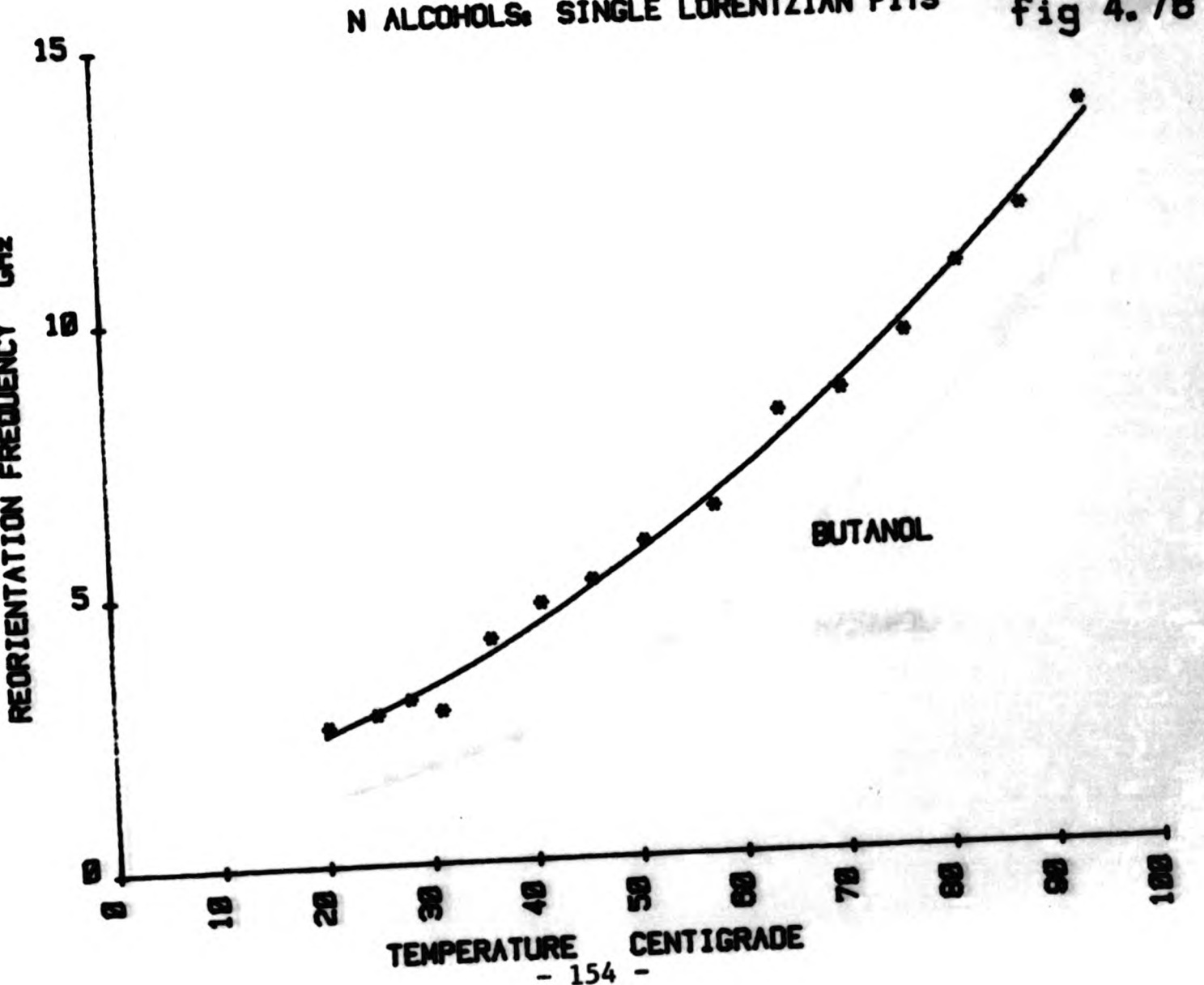
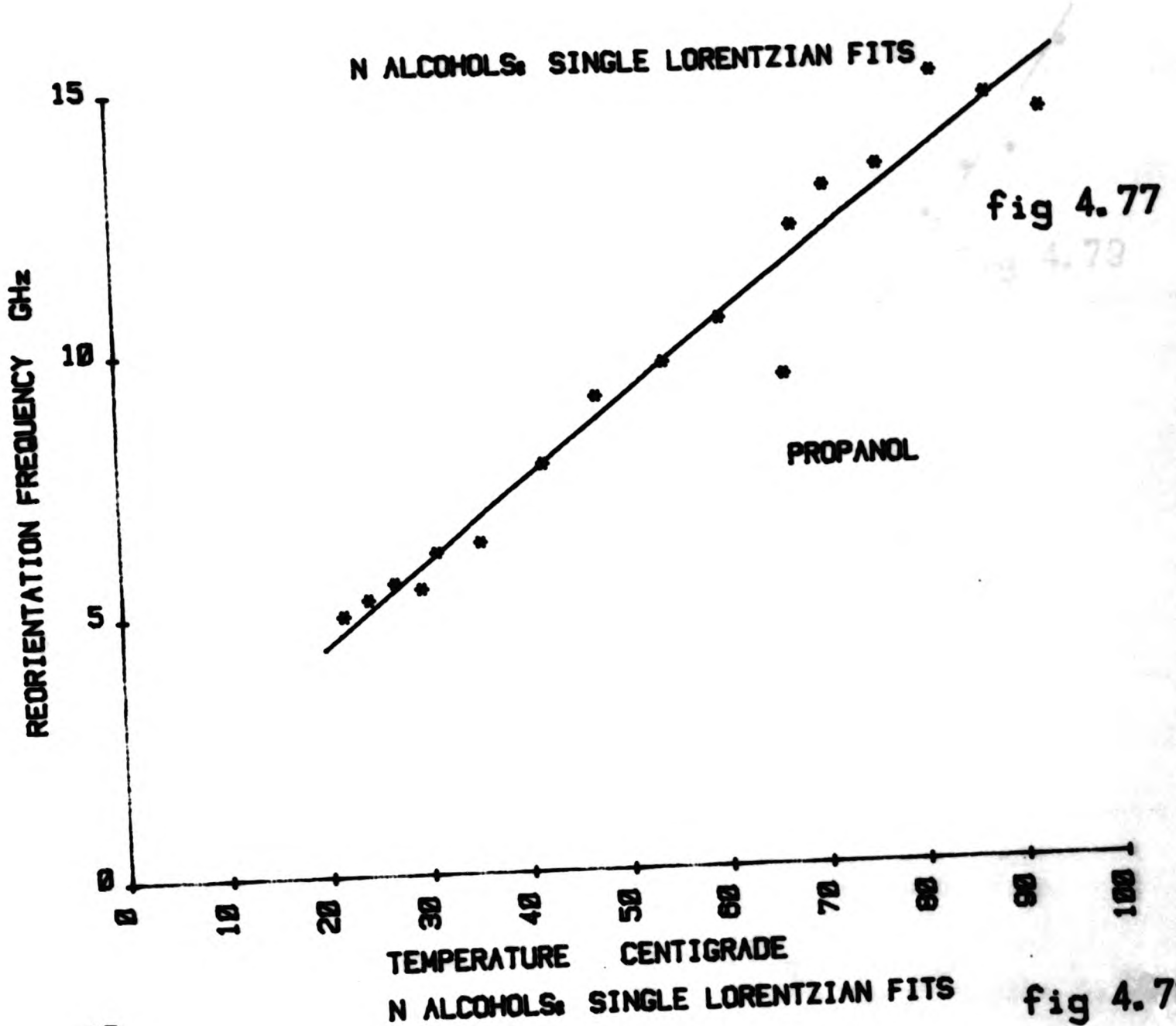
The parameters G , α , and p have been identified. G the orientational correlation parameter, α and p are all functions of solution concentration and of temperature, essentially due to the flexible nature of the molecules examined. $G\alpha p$ are therefore seen to be difficult to separate, indeed at present due to the fact that the standard errors on the individual τ_{LS} measurements are about 6% the problem appears to be intractable.

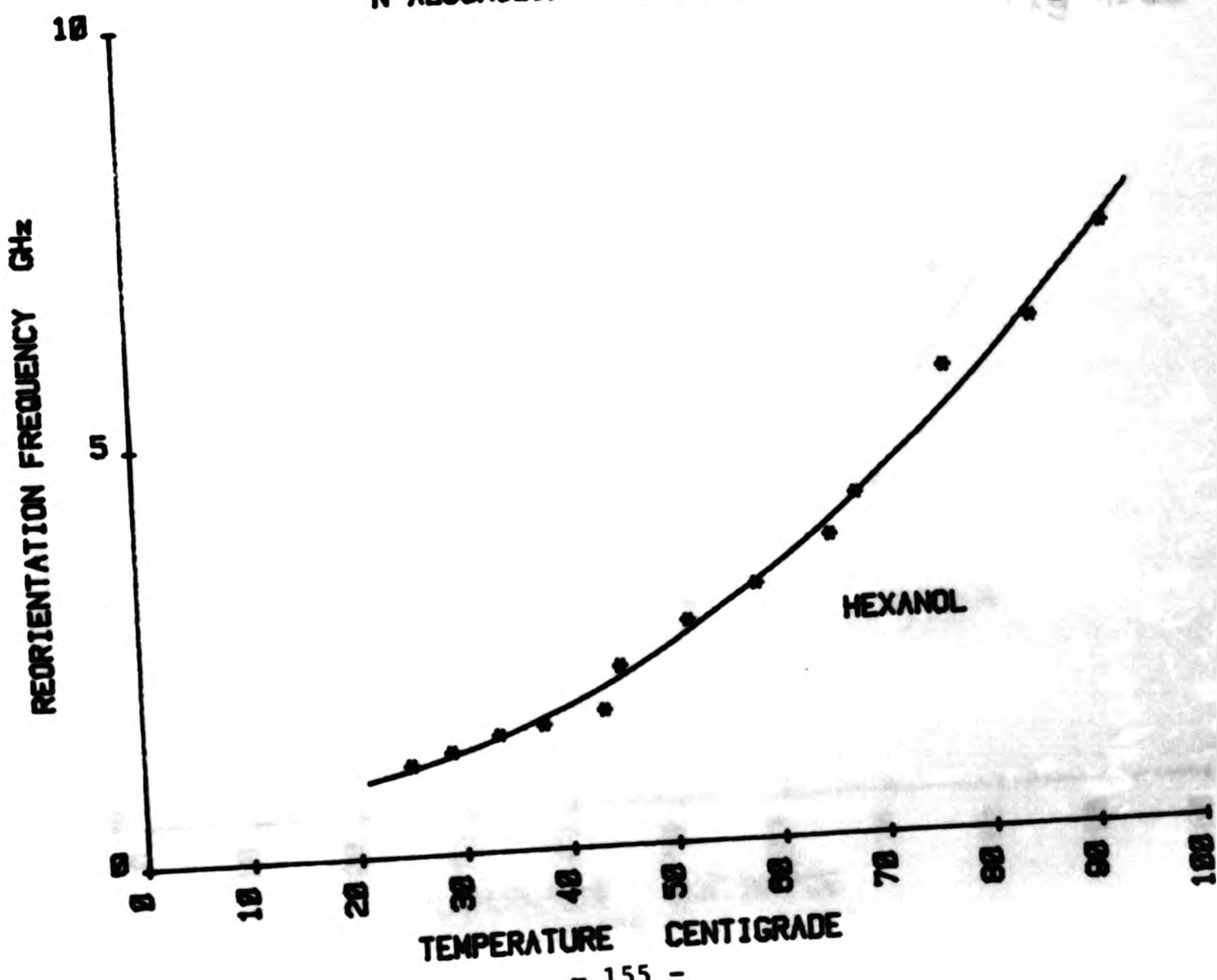
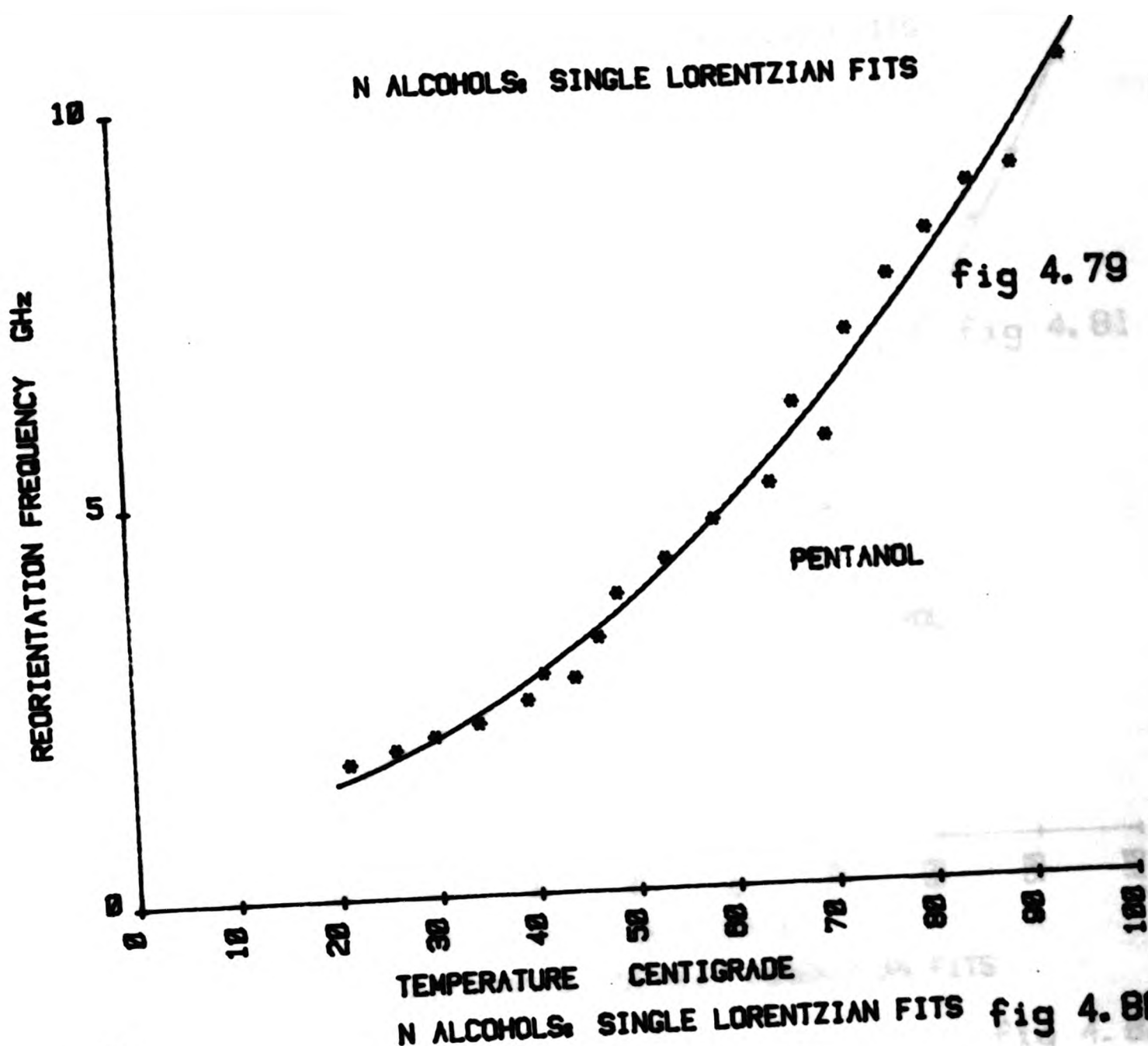
For a flexible molecule it might be more appropriate to develop a theoretical model in which the quantity $G\alpha p$ is a single parameter determined by the molecular flexibility.

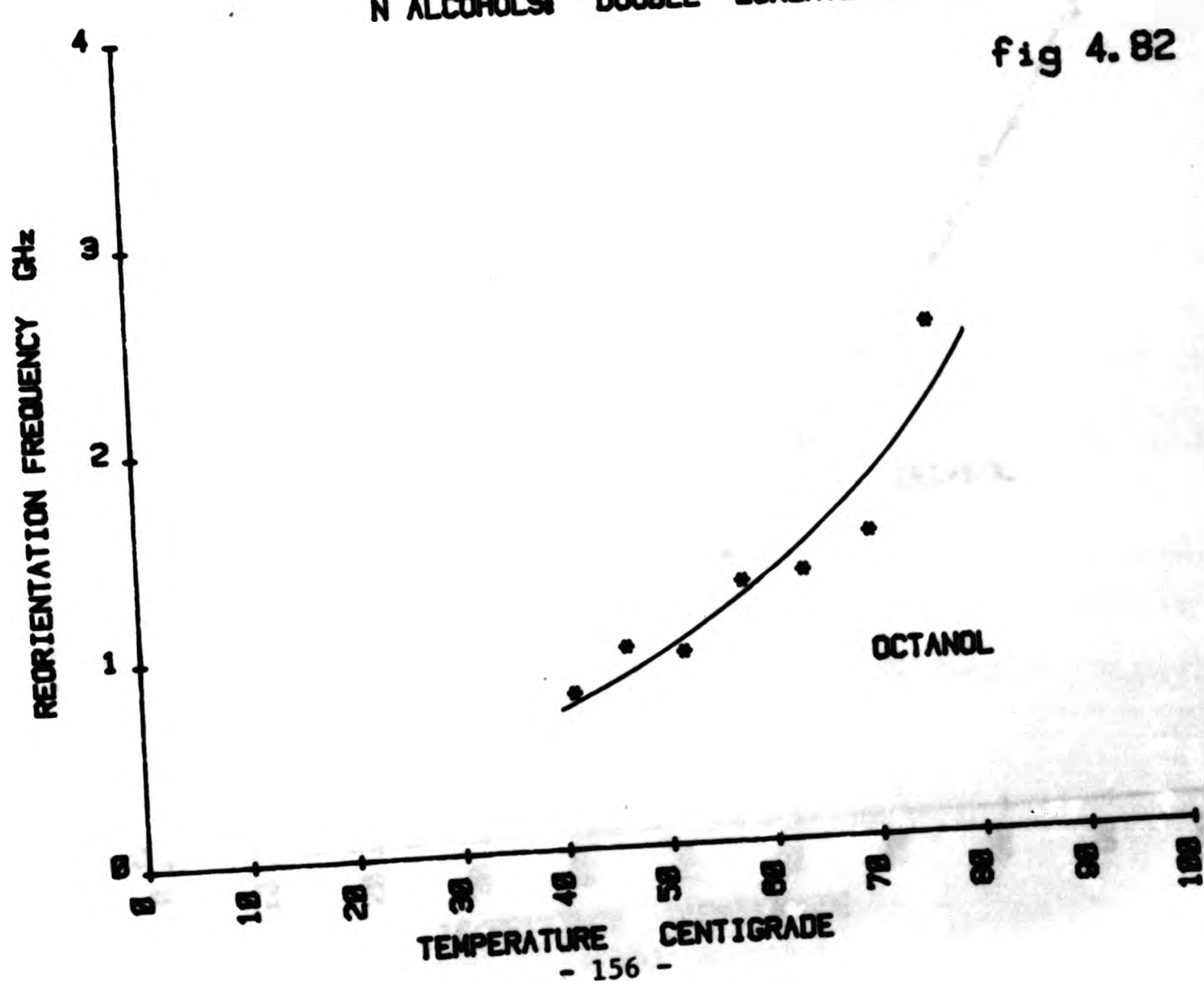
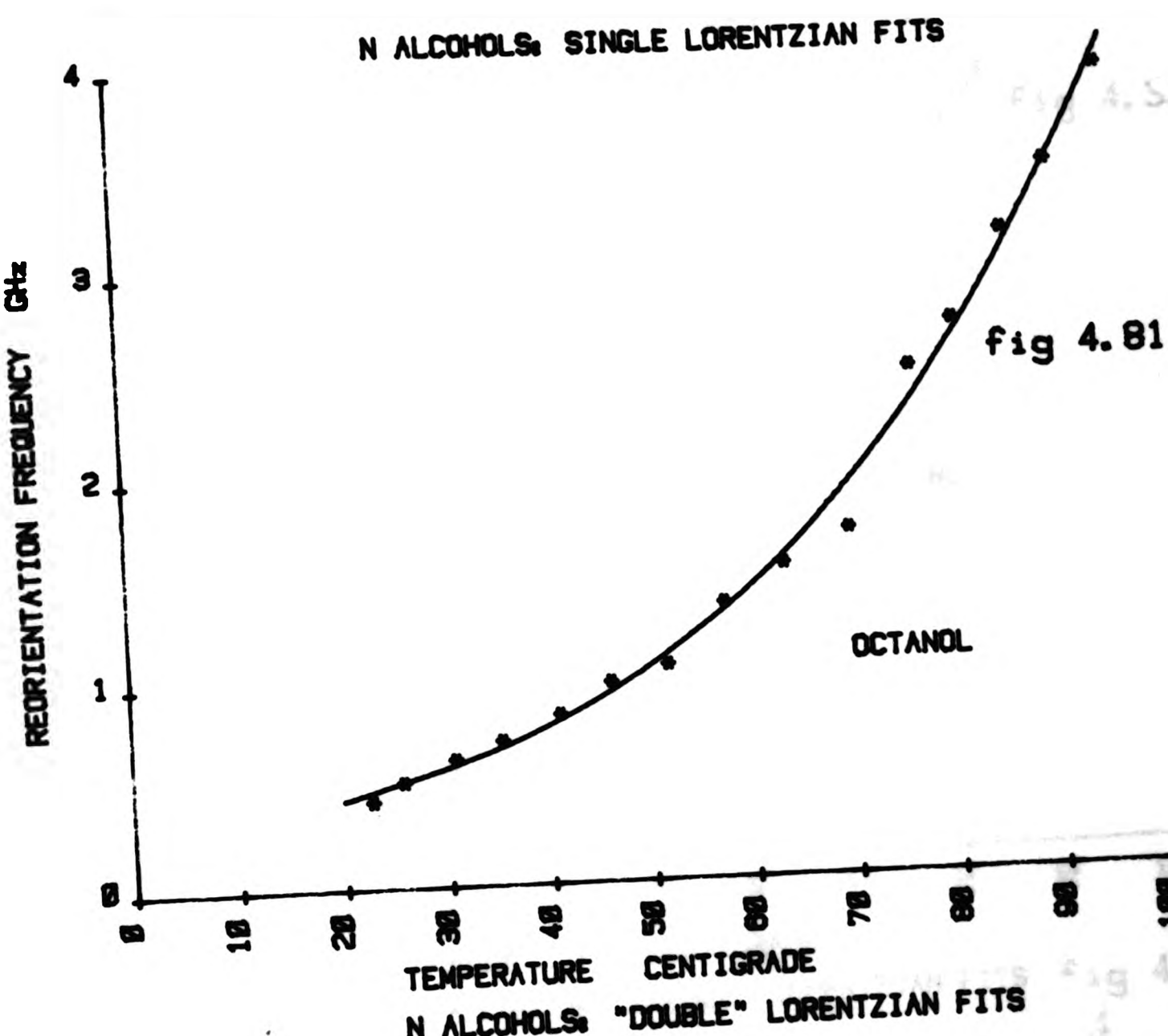
4.2.3 N-Alcohols: Neat Liquids

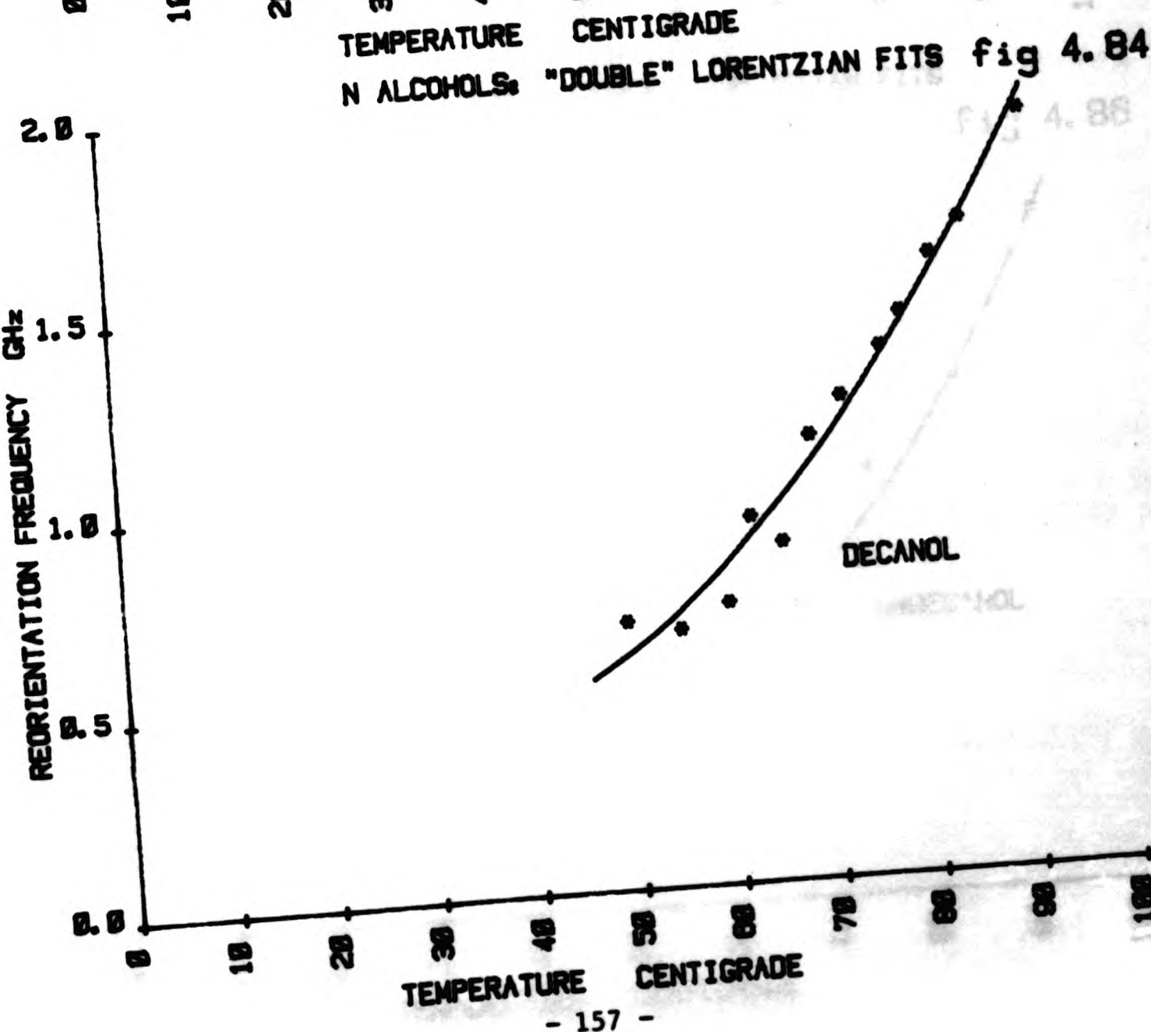
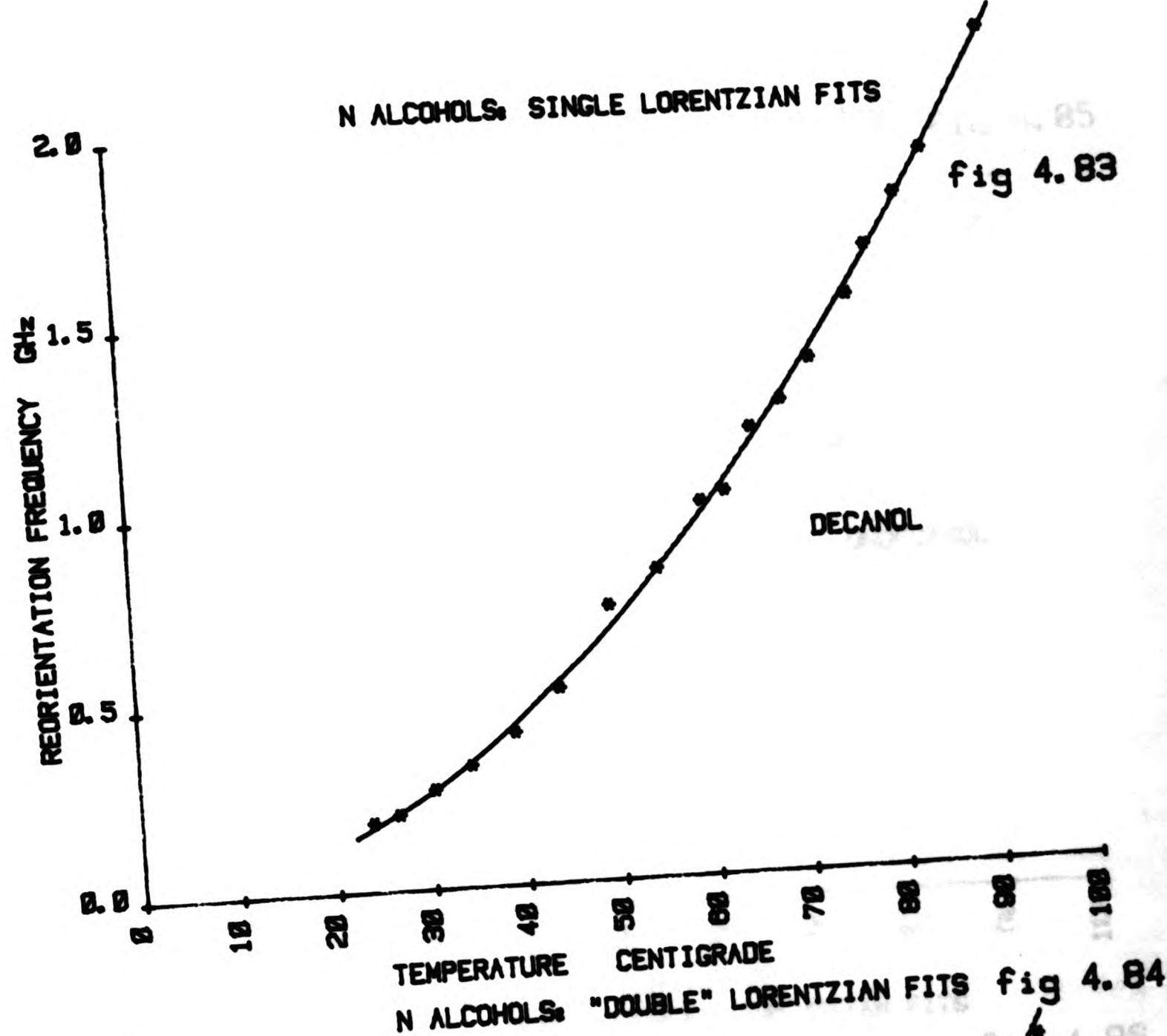
In this section we examine the results from fits to spectra of the n-l-alcohols (Figs 4.77 to 4.88). The liquids investigated were n-undecanol, n-decanol, n-octanol, n-hexanol, n-pentanol, n-butanol and n-propanol. These liquids are much more viscous than the corresponding n-alkanes and therefore proved much more difficult to filter. For one liquid $C_{11}H_{23}OH$ it proved impossible to obtain a dust free sample.

In these liquids over the temperature range examined the change in viscosity is much greater than for the corresponding n-alkane. The information obtained for a Stokes Einstein fit is therefore obtained for a greater range of values of n/T than for the n-alkanes (Figs 4.89 to 4.98). The optical anisotropies of the n-alcohols are comparable to those of the n-alkanes and therefore the intensity of the scattered

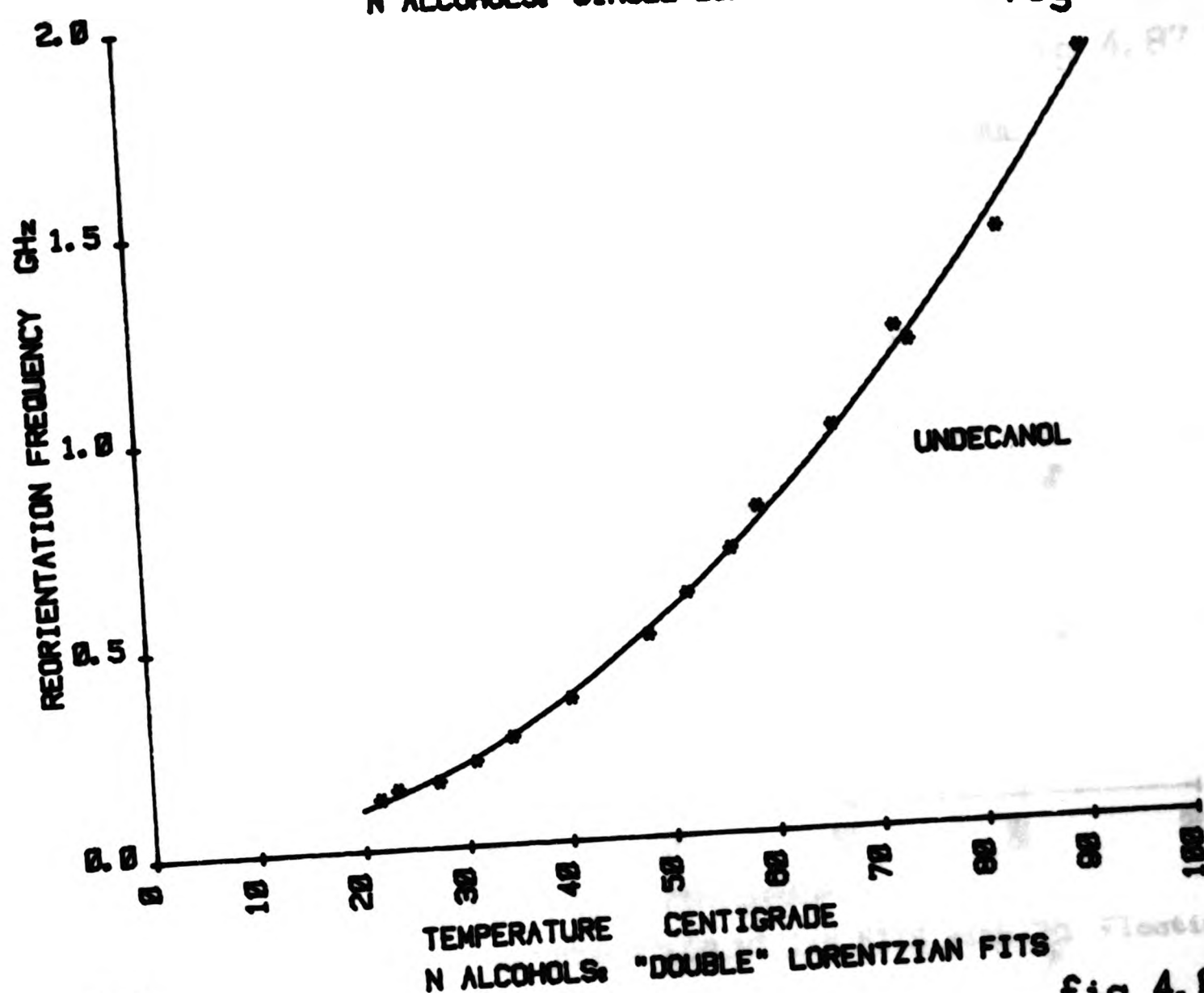




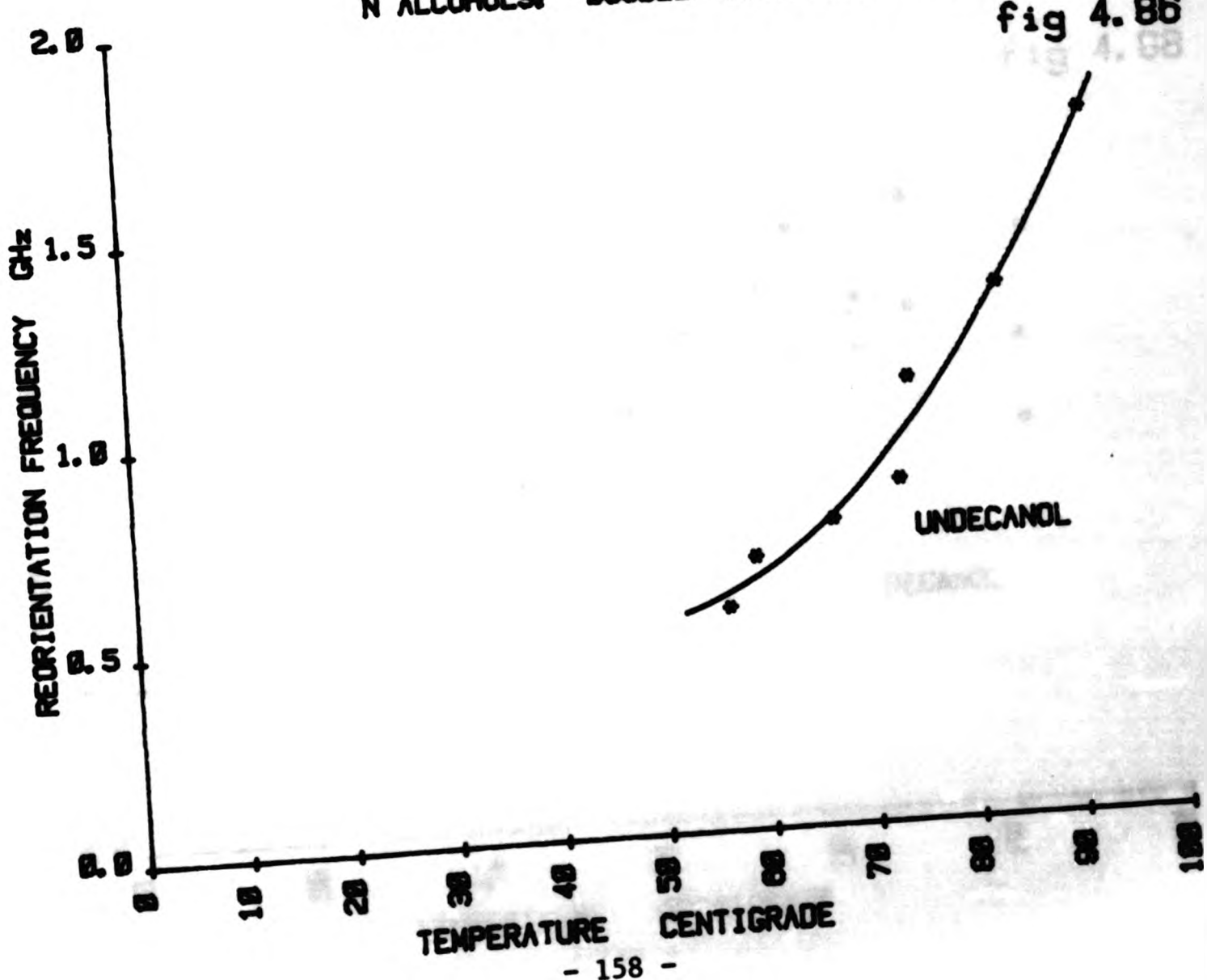




N ALCOHOLS: SINGLE LORENTZIAN FITS fig 4.85

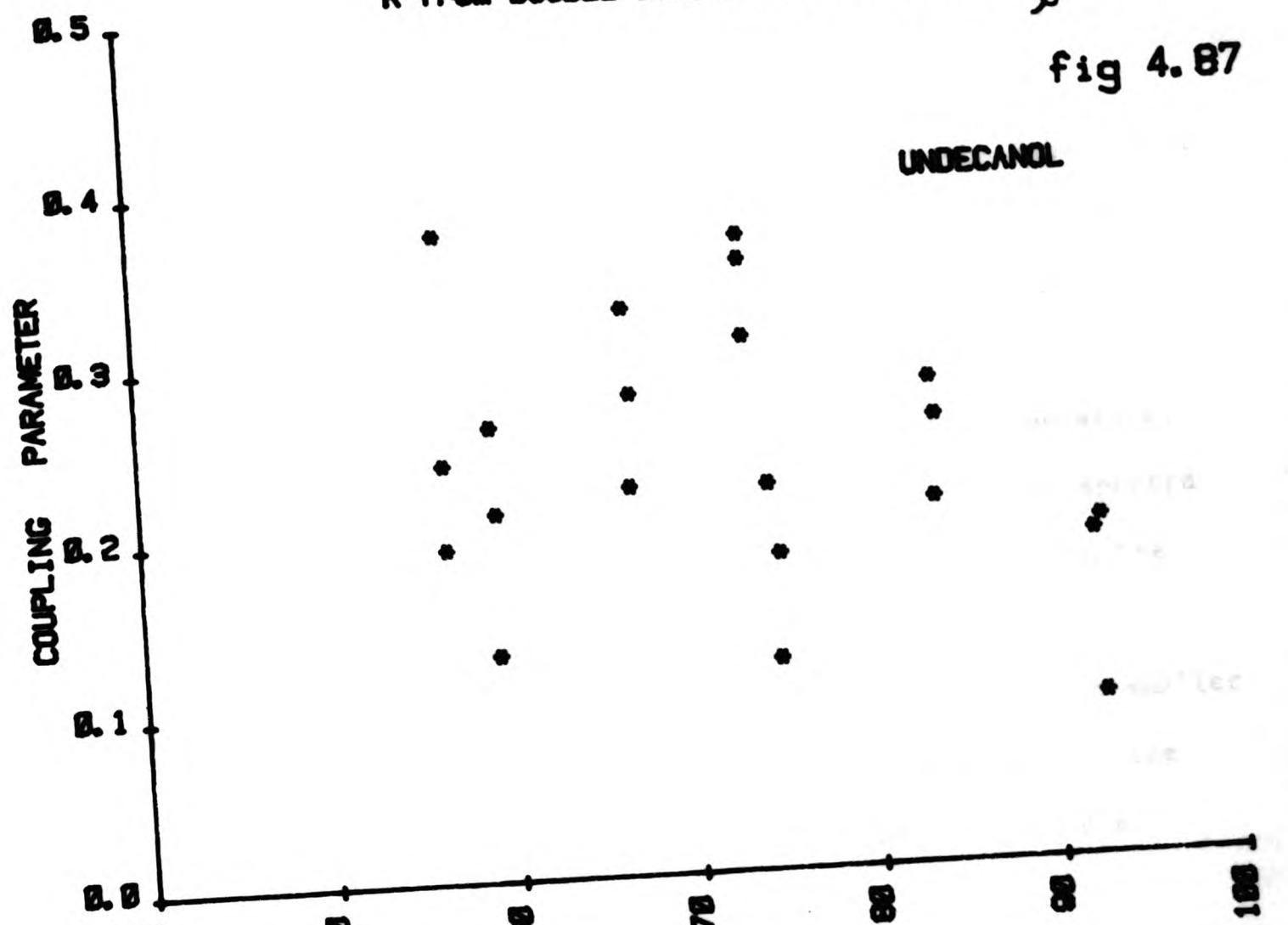


N ALCOHOLS: "DOUBLE" LORENTZIAN FITS



R from "DOUBLE" LORENTZIAN FITS with $\frac{K^2 n}{\rho}$ floating

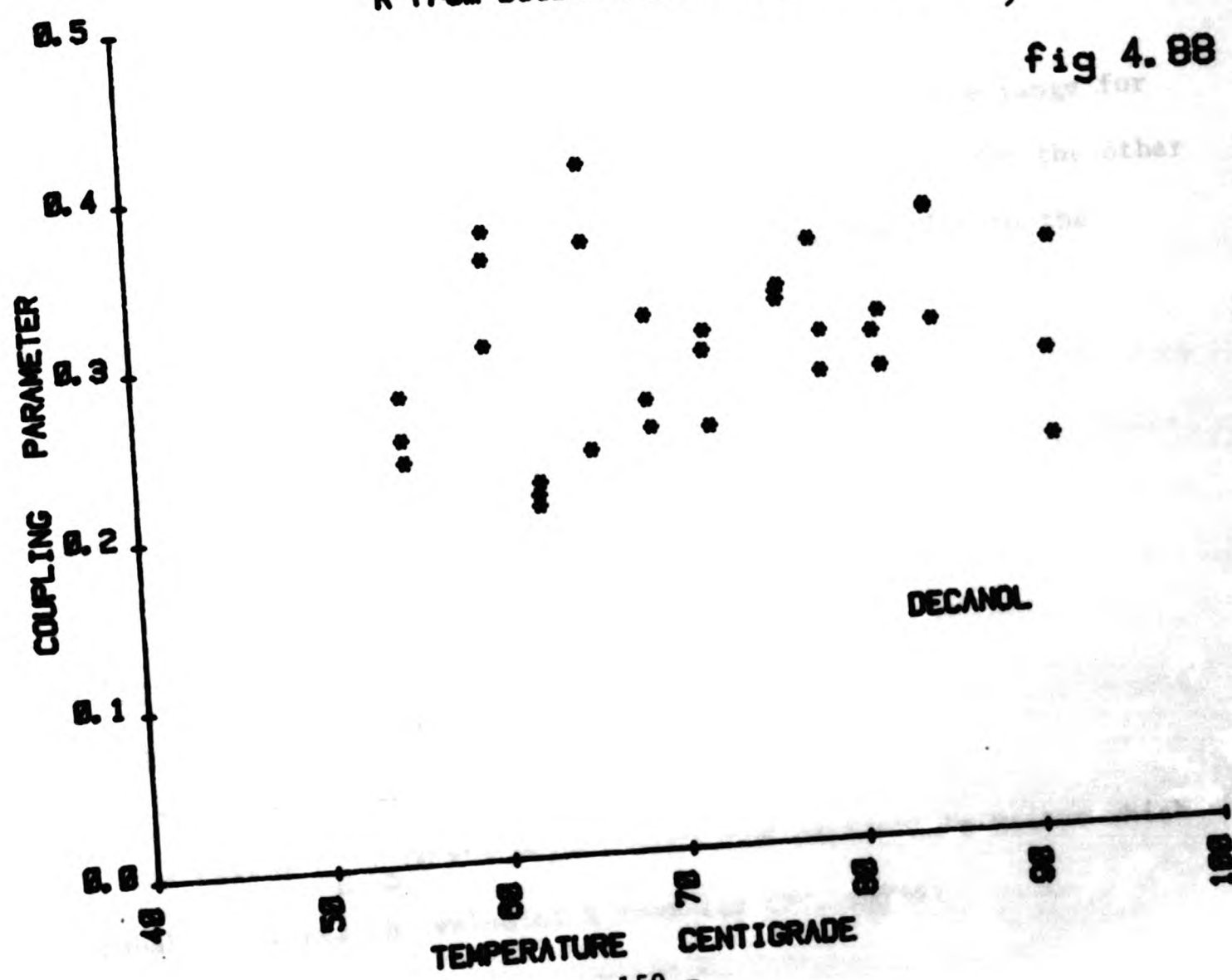
fig 4.87



UNDECANOL

R from "DOUBLE" LORENTZIAN FITS with $\frac{K^2 n}{\rho}$ floating

fig 4.88



DECANOL

light is comparable. The much higher viscosity of the n-alcohols causes the spectra to be much narrower than for the n-alkanes. These two facts taken together with the manner in which the Fabry Perot spectrometer operates means that the signal to noise ratio of the n-alcohol spectra is lower than for spectra from the equivalent n-alkanes.

The viscosity is a much faster varying function of temperature. In the n-alkanes the shear reorientational dip appears in the spectra over a temperature range determined by the relationship between the varying peak half width, and the dip half width ($K^2 n/\rho$). In the n-alcohols due to the behaviour of the viscosity this is a much smaller temperature range. The spectra are also noisier than those for the alkanes which makes the fits to the data for Lorentzian plus dip less reliable than those for the n-alkanes.

RESULTS

R Parameters

These were obtained only over a restricted temperature range for the liquids $C_{11} H_{23} OH$ and $C_{10} H_{21} OH$ (Figs 4.87, 4.88). For the other liquids the spectra were too noisy to obtain adequate fits to the spectral form of Lorentzian plus dip.

Table 4.11

LIQUID	R PARAMETER FITS TO LORENTZIAN PLUS DIP
$C_{11} H_{23} OH$	0.24 ± 0.08
$C_{10} H_{21} OH$	0.30 ± 0.05

* In the case of $C_{11} H_{23} OH$ the sample contained particulate matter which probably lowered the value of R from its true value.

Bearing in mind the above * a comparison of these R parameters with those obtained for the n-alkanes seems to indicate that the R parameter for an n-alcohol is greater than that for the equivalent alkane.

STOKES EINSTEIN RELATION

For $C_{11} H_{23} OH$ and $C_{10} H_{21} OH$ the reorientational times are obtained over an order of magnitude of values of n/T . For the n-alkanes the range for which the data is obtained is approximately half an order of magnitude.

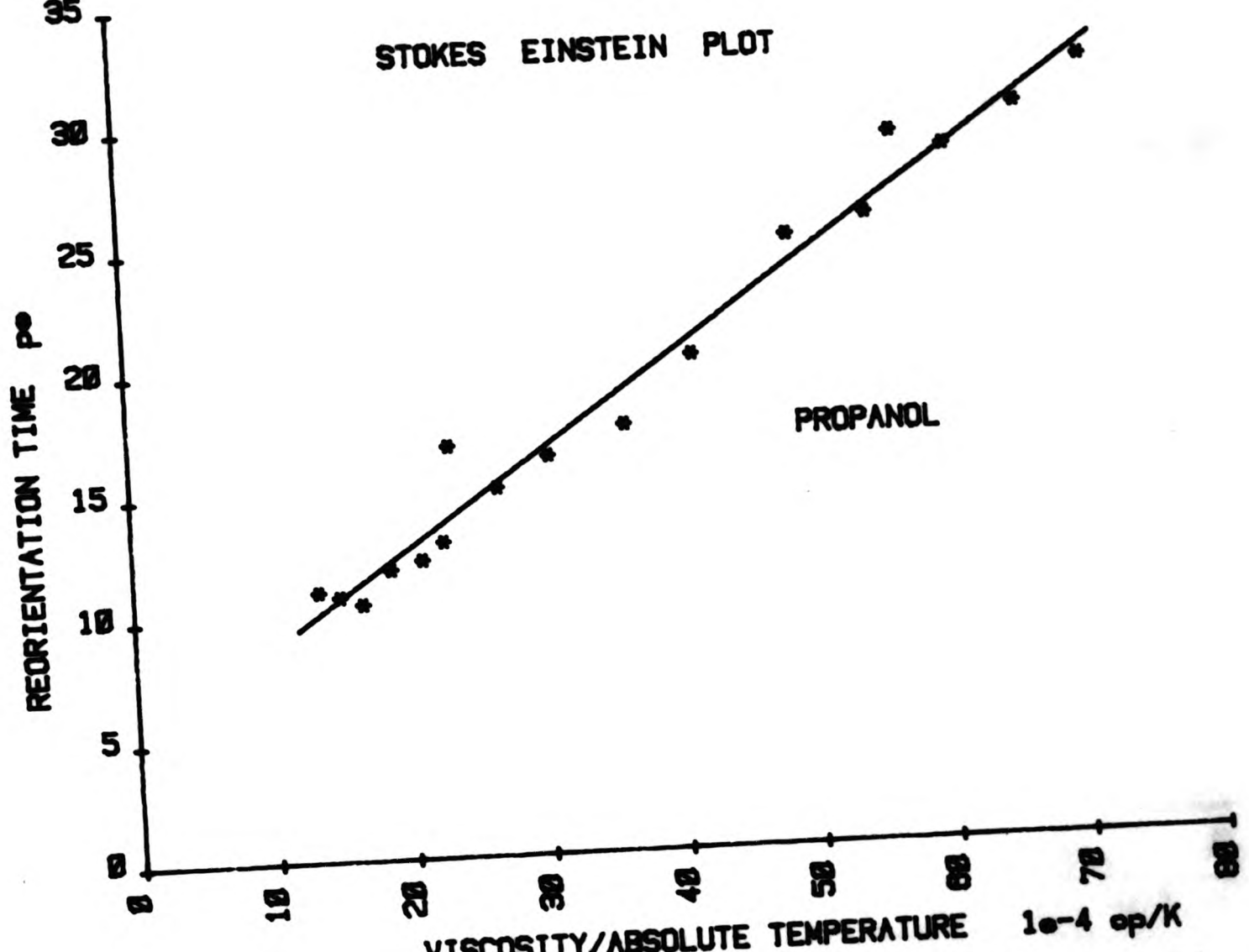
For $C_{11} H_{23} OH$ and $C_{10} H_{21} OH$ fits to the "Lorentzian plus dip" are only achieved over a restricted range of temperatures. This data is fitted to the simple Stokes Einstein model, as is the corresponding data from the single Lorentzian fits to the same spectra. This is for the purpose of comparison.

For $C_{11} H_{23} OH$ and $C_{10} H_{21} OH$ when the single Lorentzian reorientation times obtained are plotted over the full range of n/T values the distribution takes the form of an upward curving line, (Figs 4.95, 4.97).

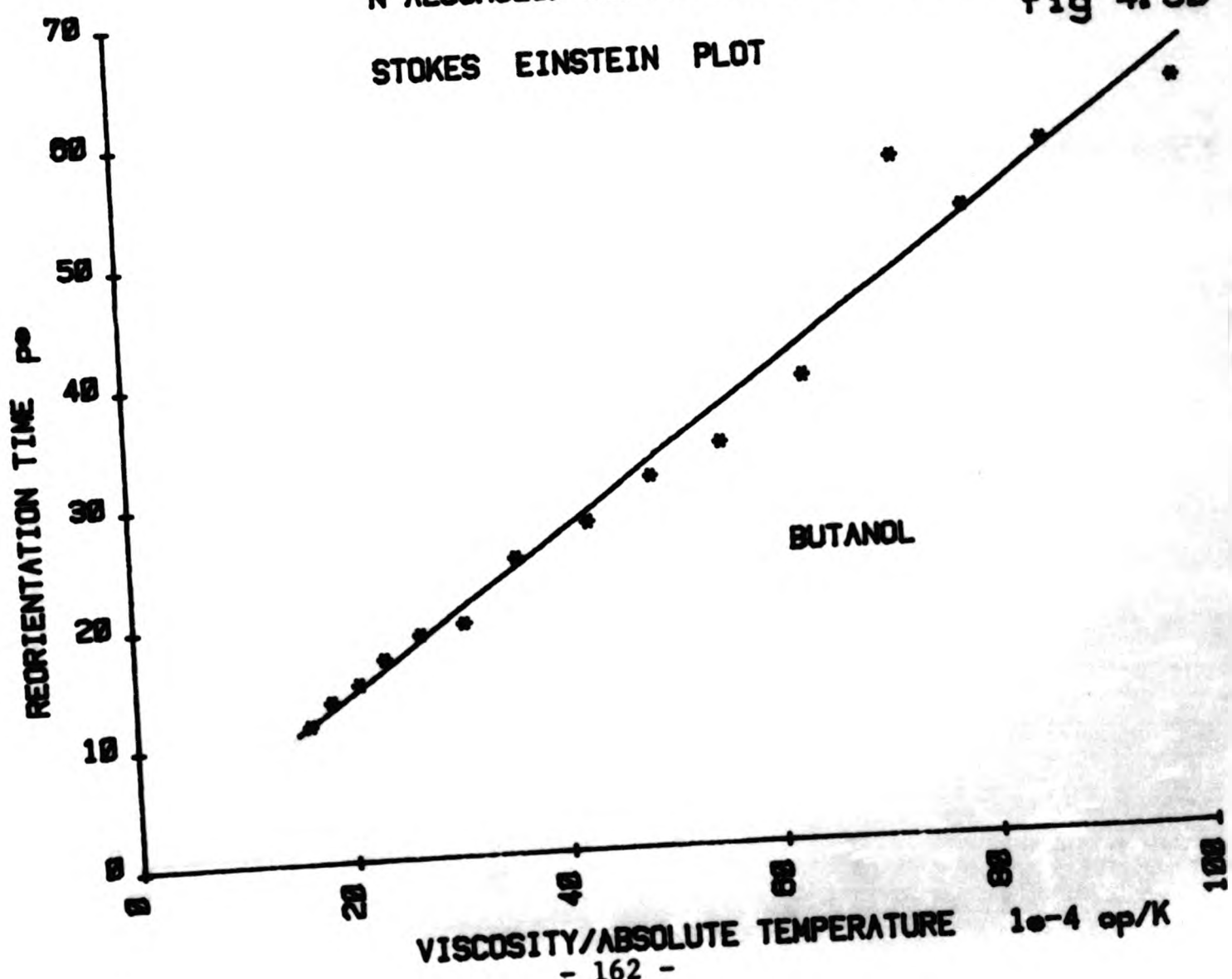
In an analysis of this data it is necessary to point out that the times obtained from the single Lorentzian fits are invalid in the very high viscosity regime observed in these liquids, however the noise level on the spectra prevents a more detailed analysis. The data from the single Lorentzian fits are fitted to the simple linear Stokes Einstein model, however far better agreement is obtained in a fit using a quadratic term, as shown in Figs 4.95, 4.97.

The Stokes Einstein plot for these n-alcohols is curved while for the n-alkanes it appears to be linear, due probably to the much smaller range of values of n/T for the n-alkanes.

N ALCOHOLS: SINGLE LORENTZIAN FITS fig 4.89



N ALCOHOLS: SINGLE LORENTZIAN FITS fig 4.90



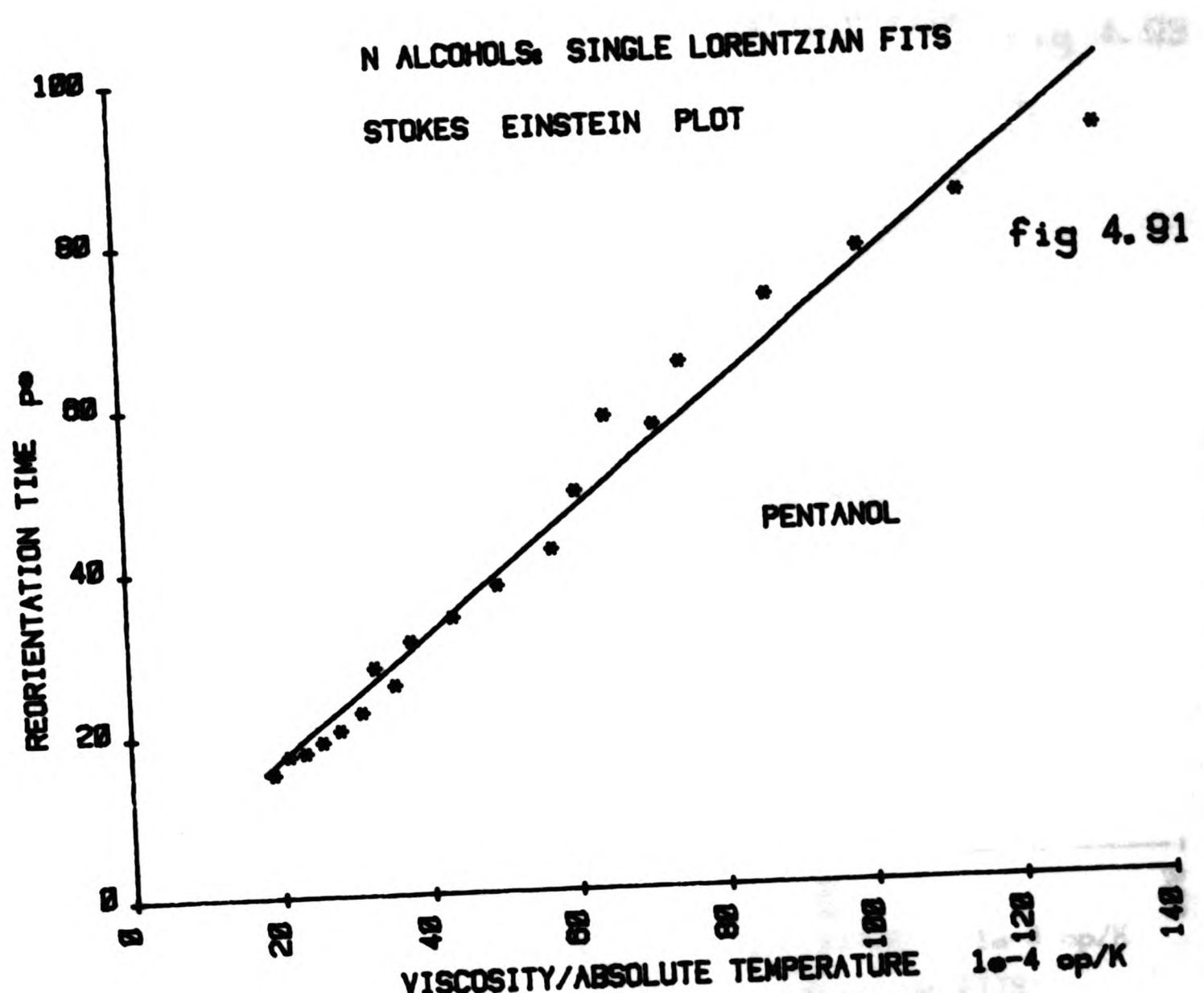


fig 4.91

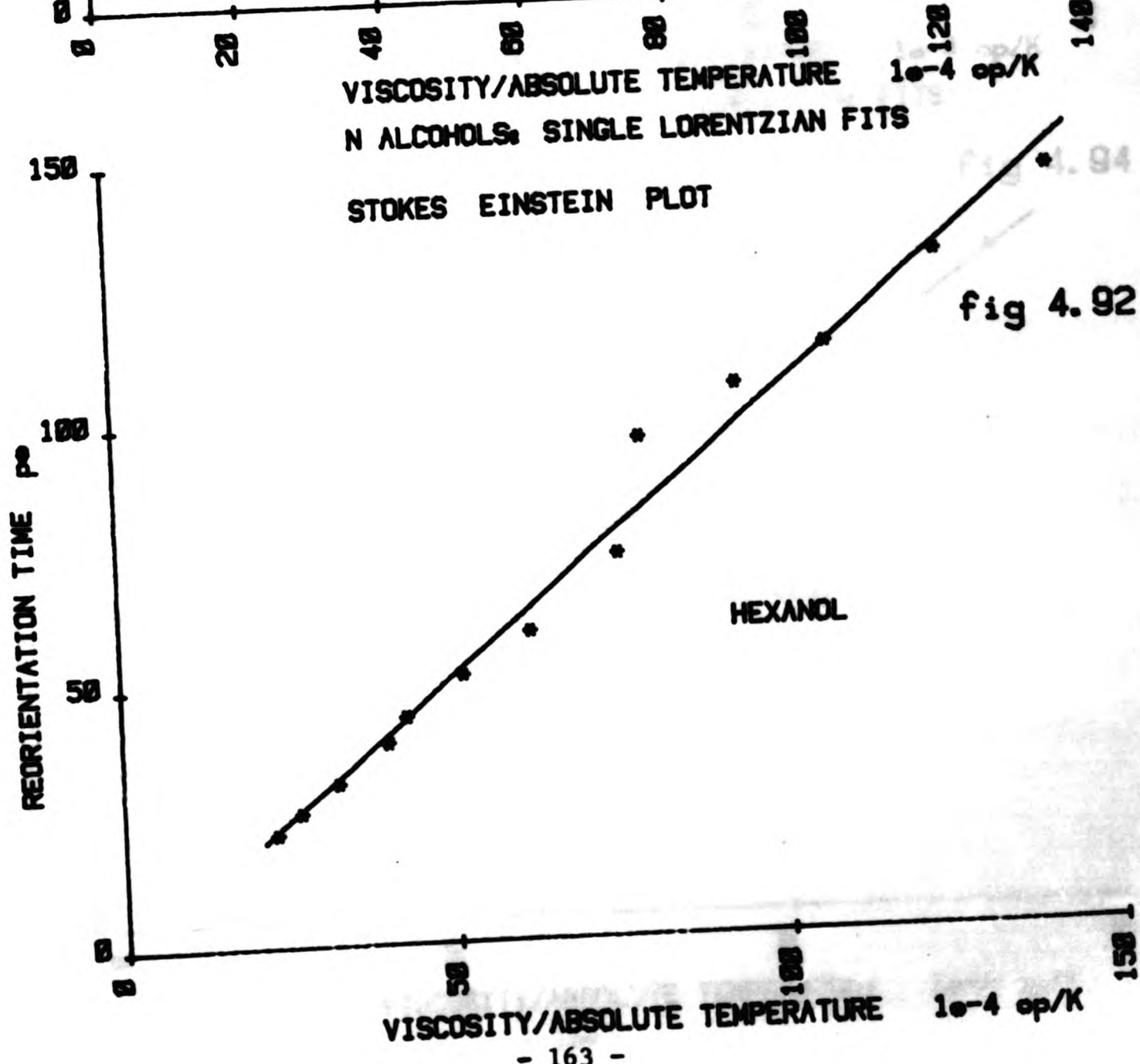
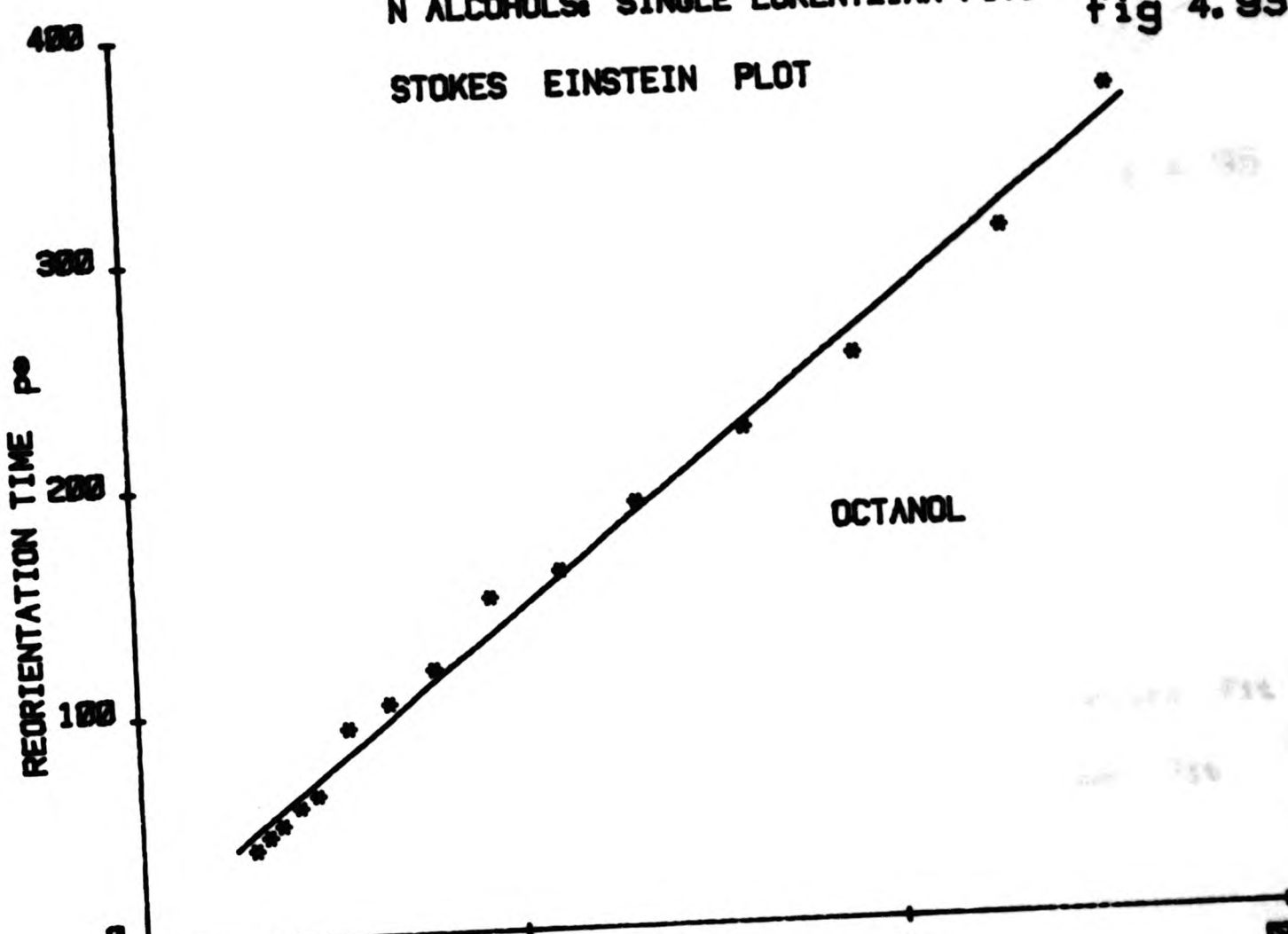


fig 4.92

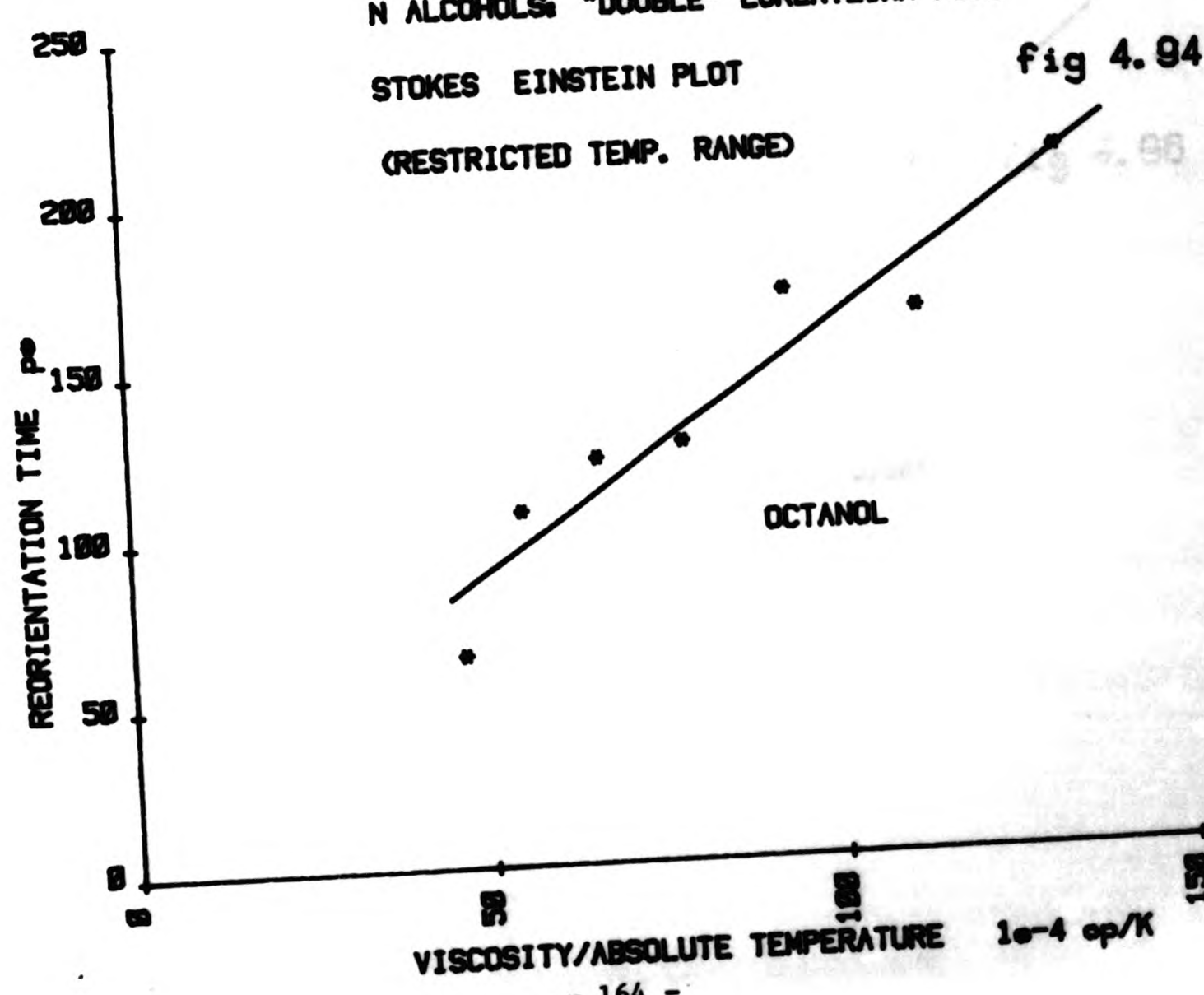
N ALCOHOLS: SINGLE LORENTZIAN FITS
STOKES EINSTEIN PLOT

fig 4.93



VISCOSITY/ABSOLUTE TEMPERATURE 10^{-4} cP/K
N ALCOHOLS: "DOUBLE" LORENTZIAN FITS

fig 4.94



N ALCOHOLS: SINGLE LORENTZIAN FITS
STOKES EINSTEIN PLOT

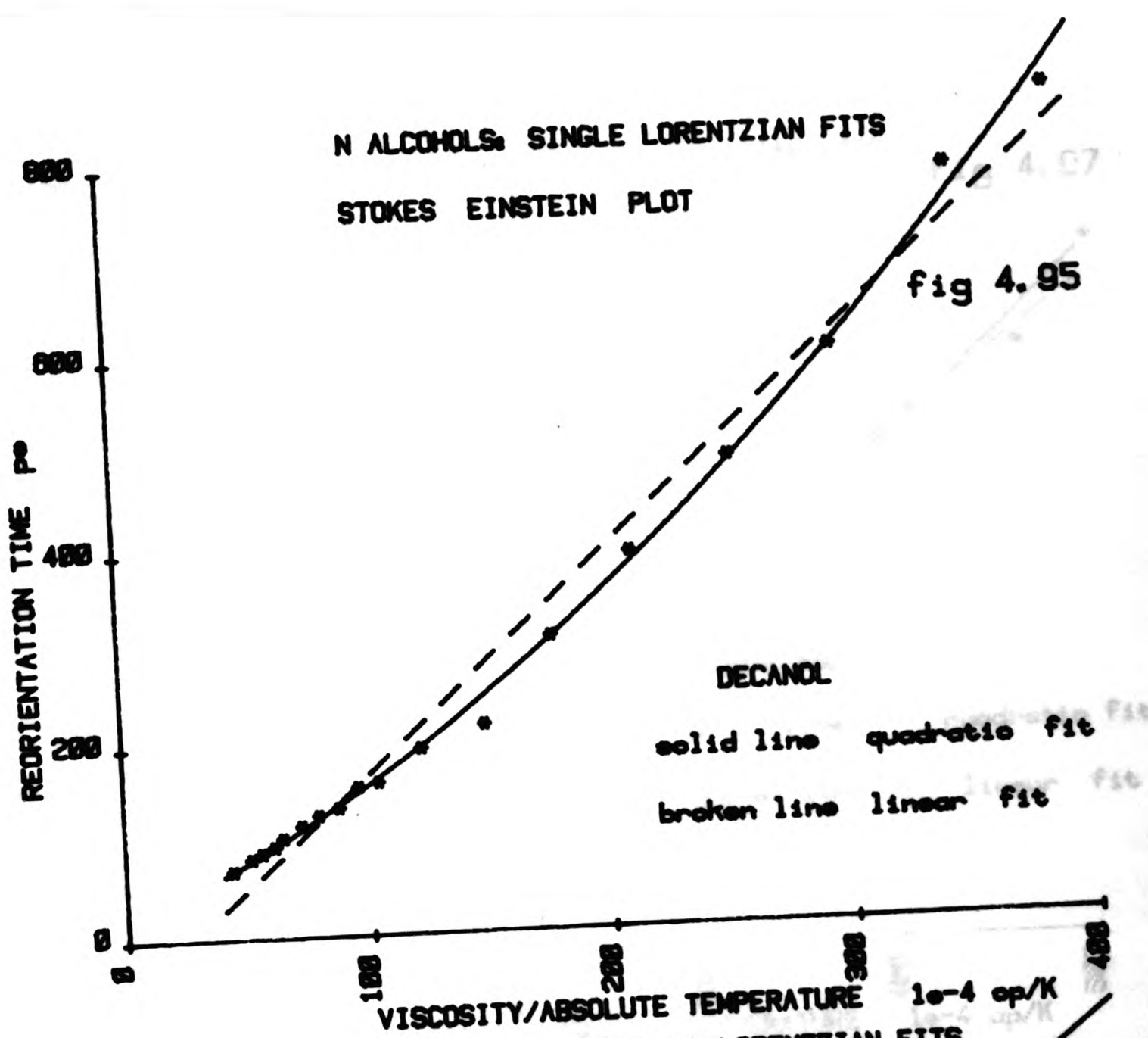


fig 4.95

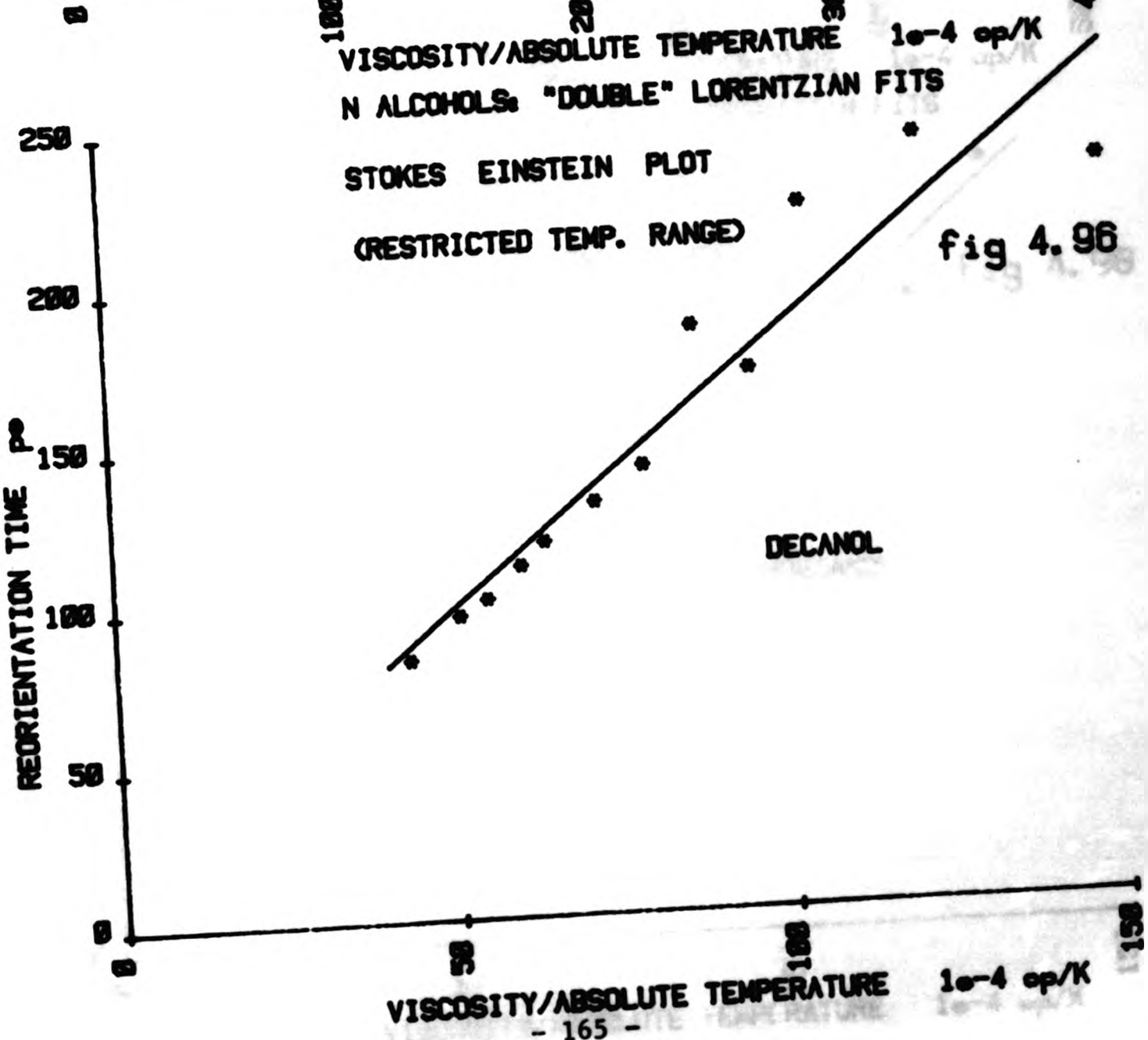
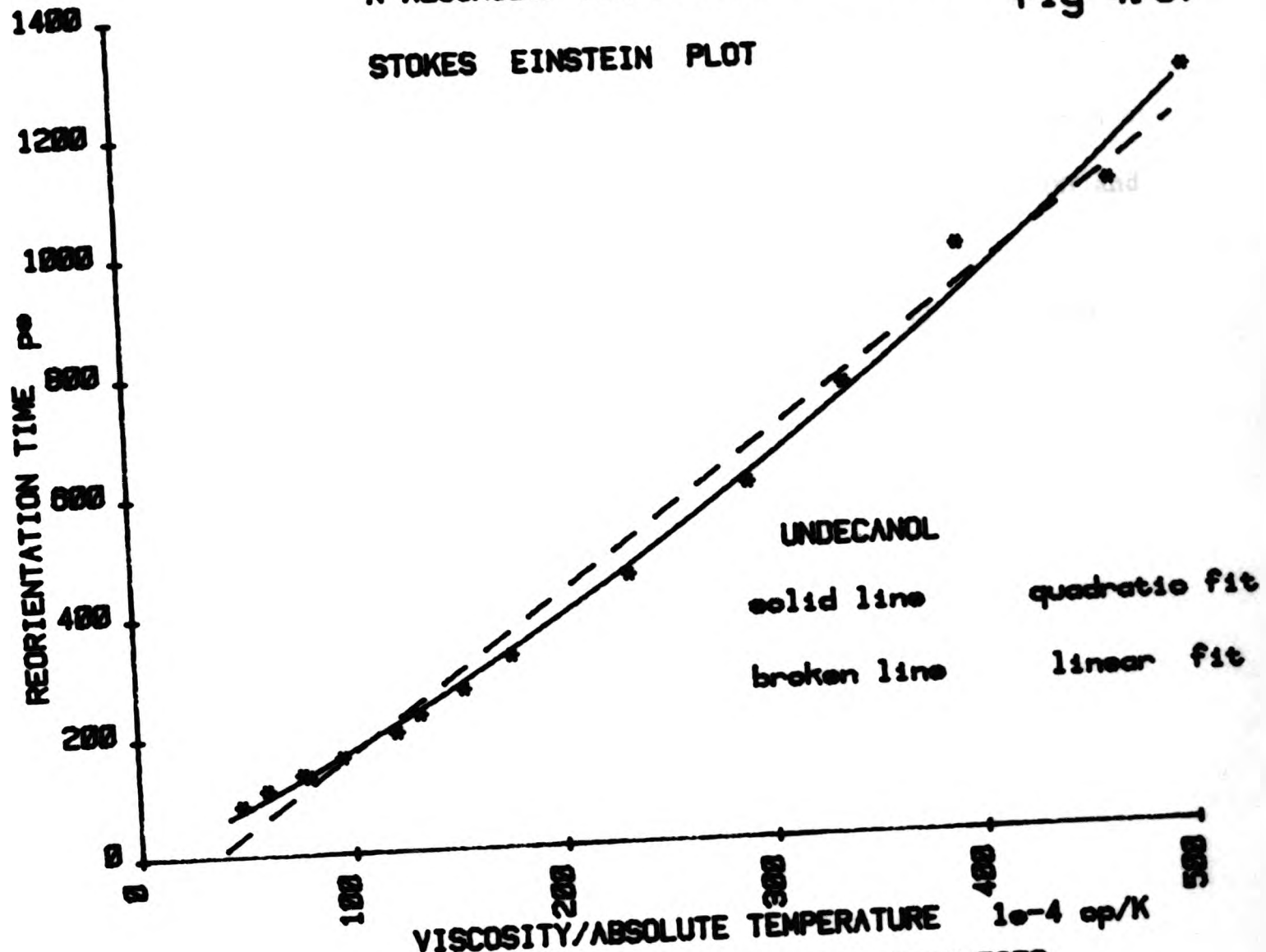


fig 4.96

N ALCOHOLS: SINGLE LORENTZIAN FITS
STOKES EINSTEIN PLOT

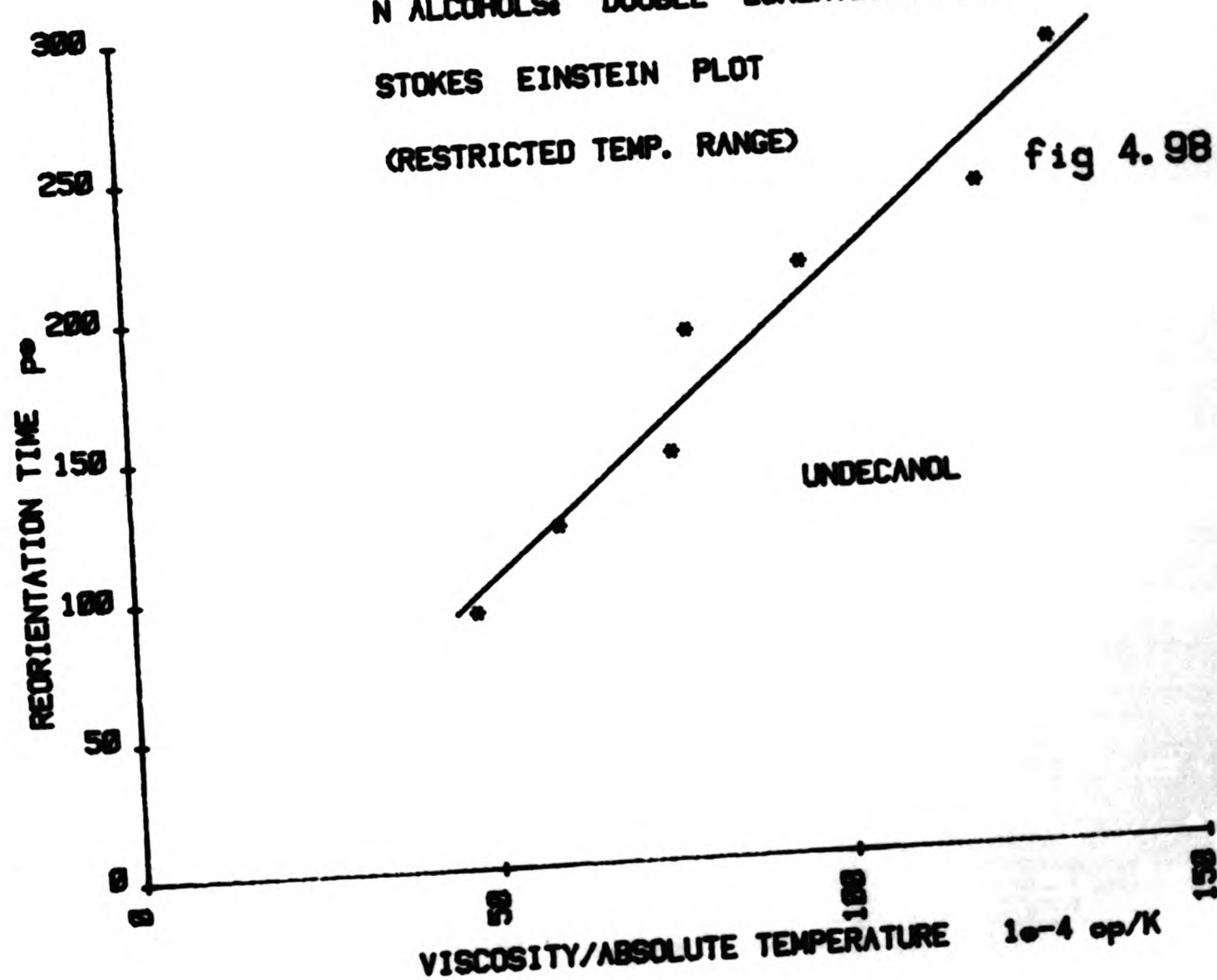
fig 4.97



N ALCOHOLS: "DOUBLE" LORENTZIAN FITS
STOKES EINSTEIN PLOT

(RESTRICTED TEMP. RANGE)

fig 4.98



For the other n-alcohols examined from $C_8 H_{17} OH$ to $C_3 H_7 OH$ the spectra get progressively more noisy and so only single Lorentzian fits to the data are obtained. The Stokes Einstein plots are shown in Figs 4.89 to 4.99 and are much more linear than for $C_{11} H_{23} OH$ and $C_{10} H_{21} OH$.

The results from the Stokes Einstein fits to the data for the n-alcohols are shown in table 4.12.

Table 4.12
RESULTS FROM STOKES EINSTEIN FITS TO DATA FOR N-ALCOHOLS

LIQUID	SINGLE LORENTZIAN FIT VOLUME \AA^3		RESTRICTED TEMPERATURE RANGE LORENTZIAN PLUS DIP \AA^3 INTERCEPT ps		VOLUME \AA^3 INTERCEPT ps	SINGLE LORENTZIAN VOLUME \AA^3 INTERCEPT ps
	VOLUME \AA^3	INTERCEPT ps	VOLUME \AA^3	INTERCEPT ps		
C ₁₁ H ₂₃ OH	353.5 ± 10.7	-90 ± 20	300.7 ± 29.4	6 ± 20	225.1	7
C ₁₀ H ₂₁ OH	315.0 ± 9.8	-60 ± 13	236.2 ± 9.8	13 ± 15	197.0	11
C ₈ H ₁₇ OH	186.0 ± 4.5	6 ± 4				
C ₆ H ₁₃ OH	147.8 ± 5.4	-2.1 ± 3.1				
C ₅ H ₁₁ OH	102.9 ± 3.6	2 ± 1.7				
C ₄ H ₉ OH	89.2 ± 4.1	1.2 ± 1.6				
C ₃ H ₇ OH	53.8 ± 2.1	4.9 ± 0.6				

For $C_{11}H_{23}OH$ and $C_{10}H_{21}OH$ the large negative intercepts from the Stokes Einstein fit to all the data from the single Lorentzian spectral analysis are largely artefacts due to large range of n/T values covered by the data. The Stokes Einstein volumes obtained from this data are however useful for a Stokes Einstein examination of these liquids across the whole temperature range covered. Over the restricted temperatures range over which the fits to "Lorentzian plus dip" are successful the Stokes Einstein volumes obtained from the "Lorentzian plus dip" data are obviously more valid. For the $C_{11}H_{23}OH$ and $C_{10}H_{21}OH$ data (fitted to the restricted temperature range) and for all the data for the rest of the n-alcohols within the experimental error the intercepts are positive (while for the n-alkanes these intercepts are negative). The value of the intercept obtained relative to the τ_{LS} values for each liquid increases with decreasing chain length.

As chain length decreases the noise on the spectra increases, and the scatter on the Stokes Einstein plots of the data also increases. The Stokes Einstein fits appear to become more linear as n-alcohol chain length decreases, however this is possibly purely a reflection of the fact that for a specified temperature range the range of values of n/T decreases with decreasing chain length.

To successfully analyse the light scattering data obtained for the n-alcohols a comparison of this data with that obtained for the n-alkanes is necessary. The n-1-alcohols consist of an n-alkane molecule with a single hydrogen atom on one of the chain ends replaced by a hydroxyl group. The volume of the hydroxyl group is rather large, comparable in size to a chain end. The net result is that the molecular volume of a n-alcohol is comparable to that of the n-alkane which has one extra carbon atom.

Table 4.13

COMPARISON OF VOLUMES/STOKES EINSTEIN VOLUMES N-ALKANES/N-ALCOHOLS

All volumes in A^3

Liquid Alcohols	STOKES EINSTEIN VOLUME		Liquid Alkanes	STOKES EINSTEIN VOLUME	Molecular Volumes
	Single Lorentzian	Restricted * With Dip			
$\text{C}_{11}\text{H}_{23}\text{OH}$	354	301	$\text{C}_{12}\text{H}_{26}$	315	216
$\text{C}_{10}\text{H}_{21}\text{OH}$	315	236	$\text{C}_{11}\text{H}_{24}$	239	201
$\text{C}_8\text{H}_{17}\text{OH}$	186		C_9H_{20}	175	168
$\text{C}_6\text{H}_{13}\text{OH}$	148		C_7H_{16}	94	138
$\text{C}_5\text{H}_{11}\text{OH}$	103		C_6H_{14}	66	123
$\text{C}_4\text{H}_9\text{OH}$	89		C_5H_{12}	49	108
$\text{C}_3\text{H}_7\text{OH}$	54		C_4H_{10}		92.5

* restricted refers to reorientation times obtained from the restricted temperature range over which fits to "Lorentzian plus dip" are successful.

Table 4.13 shows the Stokes Einstein volume decreases with decreasing chain length implying that the quantity Gap, the ratio of the observed Stokes Einstein volume to the molecular volume decreases with decreasing chain length. This is indeed the case as is seen in the following table.

Table 4.14
Gap obtained from Stokes Einstein fits

Liquid Alcohols	Single Lorentzian	Gap Restricted Lorentzian With Dip	Liquid Alkanes	Gap
$C_{11}H_{23}OH$	1.64	1.39	$C_{12}H_{26}$	1.46
$C_{10}H_{21}OH$	1.58	1.17	$C_{11}H_{24}$	1.19
$C_8H_{17}OH$	1.11		$C_{10}H_{22}$	1.07
$C_6H_{13}OH$	1.07		C_9H_{20}	1.04
$C_5H_{11}OH$	0.837		C_8H_{18}	0.88
C_4H_9OH	0.824		C_7H_{16}	0.681
C_3H_7OH	0.584		C_6H_{14}	0.537
			C_5H_{12}	0.454

The values of Gap for the long chains (12 backbone atoms long) are all approximately 1.5 and for the short chains the value falls to approximately 0.5. There is a significant difference however in the rate at which the values of Gap fall with chain length. This can perhaps best be seen by examining the behaviour of the ratio $\text{Gap}(n\text{-alcohol})/\text{Gap}(n\text{-alkane})$ (for we compare the *n*-alcohol with the *n*-alkane).

The results are as follows -

Table 4.15

Liquids Alcohol	Alkane	Gap(alcohol)/Gap(alkane)	
$C_{11}H_{23}OH$	$C_{12}H_{26}$	1.124	0.956 *
$C_{10}H_{21}OH$	$C_{11}H_{24}$	1.318	0.987 *
	$C_{10}H_{22}$		
$C_8H_{17}OH$	C_9H_{20}	1.063	
	C_8H_{18}		
$C_6H_{13}OH$	C_7H_{16}	1.574	
$C_5H_{11}OH$	C_6H_{14}	1.561	
C_4H_9OH	C_5H_{12}	1.816	
C_3H_7OH			

* For these ratios the values for Gap for the n-alcohols are obtained from Stokes Einstein fits to "Lorentzian plus dip" fits to spectra taken over a fixed temperature range.

The scatter on the values of the ratios obtained are large but this arises from the fact that in this ratio the scatter is the combined scatter on the Gap values from both alcohols and alkanes. However a fairly general principle arises. For the long chain lengths the ratio approximates to one, which perhaps implies for alkanes and alcohols, despite the enormously differing viscosities of the liquids there is an equivalence in the reorientational behaviour.

For the shorter chain lengths the value of the ratio rises sharply perhaps implying that the short chain alcohol molecules are locked far more into the hydrodynamic structure of the liquid than the corresponding n-alkane molecule.

Reasons why this should be so, are not difficult to envisage.

For the short chain alcohol molecules there is the possibility of the formation of end-to-end dimers by hydrogen bonding. In the longer chain liquids the hydroxyl groups are separated by a far greater distance on average and so the probability of dimerisation in the long chain liquids is much less than for the short chain liquids.

Another possible reason hinges on the flexibility of the alcohol-alkane chain molecules. In a flexible molecule it is possible that the motion probed by depolarised light scattering is not a whole molecular reorientation but a reorientation of a portion of the molecule. The reorientation of the molecular portion is still controlled by the macroscopic viscosity of the liquid, however as it is only a portion of the molecule, the chain ends (and hence for the n-l-alcohols the -OH group) play little part in the motion probed. For a shorter molecule the flexibility inherent in the molecular structure is much reduced and reorientation becomes progressively more that of the whole molecule. The -OH group therefore plays a greater part in molecular reorientation for the short chain molecules than for the long chain molecules.

These are two possible explanations of the facts. The behaviour observed is likely to be due to a combination of these plus others not discussed here. At present there is no comprehensive theoretical description of depolarised light scattering from flexible molecules. All the data so far presented has been discussed in terms of the parameters G, α and p. In a full description as G, α and p are all to a greater or lesser extent, functions of molecular conformation, it may prove that G, α and p are not simply separable.

4.2.4 Iso Octane: 224 Trimethyl Pentane

Because molecular conformation plays an important part in molecular reorientation, it is very difficult to obtain a completely satisfactory interpretation of the reorientation times determined from depolarised light scattering for flexible molecules. The isomers of the alkanes should be far less flexible than the n-alkanes and so information from light scattering on the isomers should aid interpretation of the light scattering data from the n-alkanes.

Only one liquid was examined in this short study. A sample of the iso octane, 224 trimethyl pentane was prepared by standard filtering techniques.

The optical anisotropy of 224 trimethyl pentane is much lower than that of n-octane, and therefore the depolarised light scattering intensity is lower and the spectral noise is much greater than for n-octane.

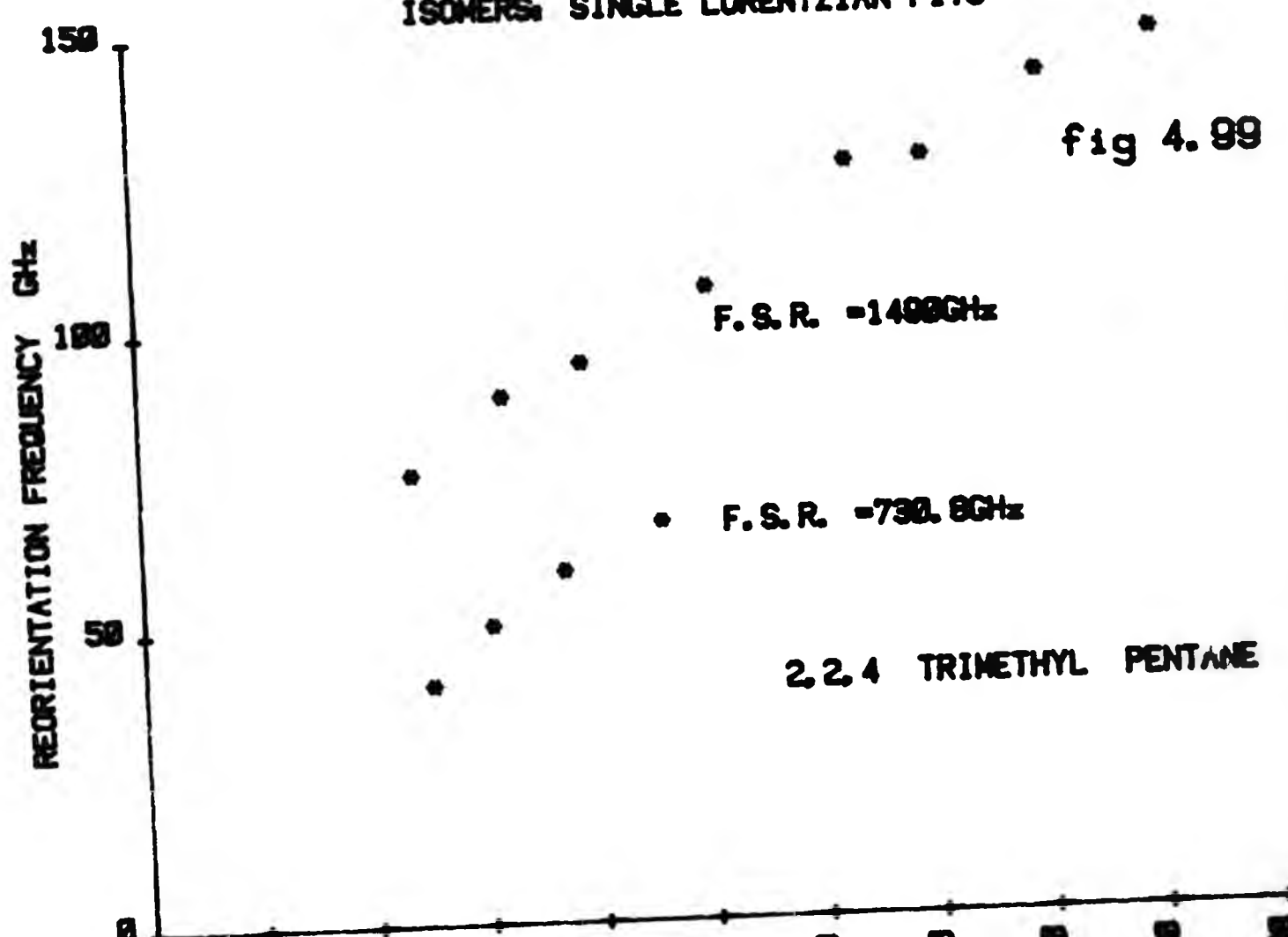
An initial analysis indicated that the spectra were very broad. In the analysis of the data from this liquid, very large free spectral ranges of approximately 730 GHz and 1500 GHz were used which correspond to etalon spacings of approximately 0.02 cm and 0.01 cm respectively. These free spectral ranges were measured by projection of the etalon diffraction pattern onto a screen while shining a laser through the etalon and measurement and calculation from that pattern.

The reorientational frequencies observed ranged from 150 GHz at 91 °C to 40 GHz at 25 °C (Fig 4.99).

In the data for the low temperatures the spectral fits for approximately the same temperature, obtained using different free spectral ranges give quite different reorientation frequencies. This was not encountered with the other liquids and the implication is that the spectra were not single Lorentzians. This will be discussed in more detail.

ISOMERS: SINGLE LORENTZIAN FITS

fig 4.99

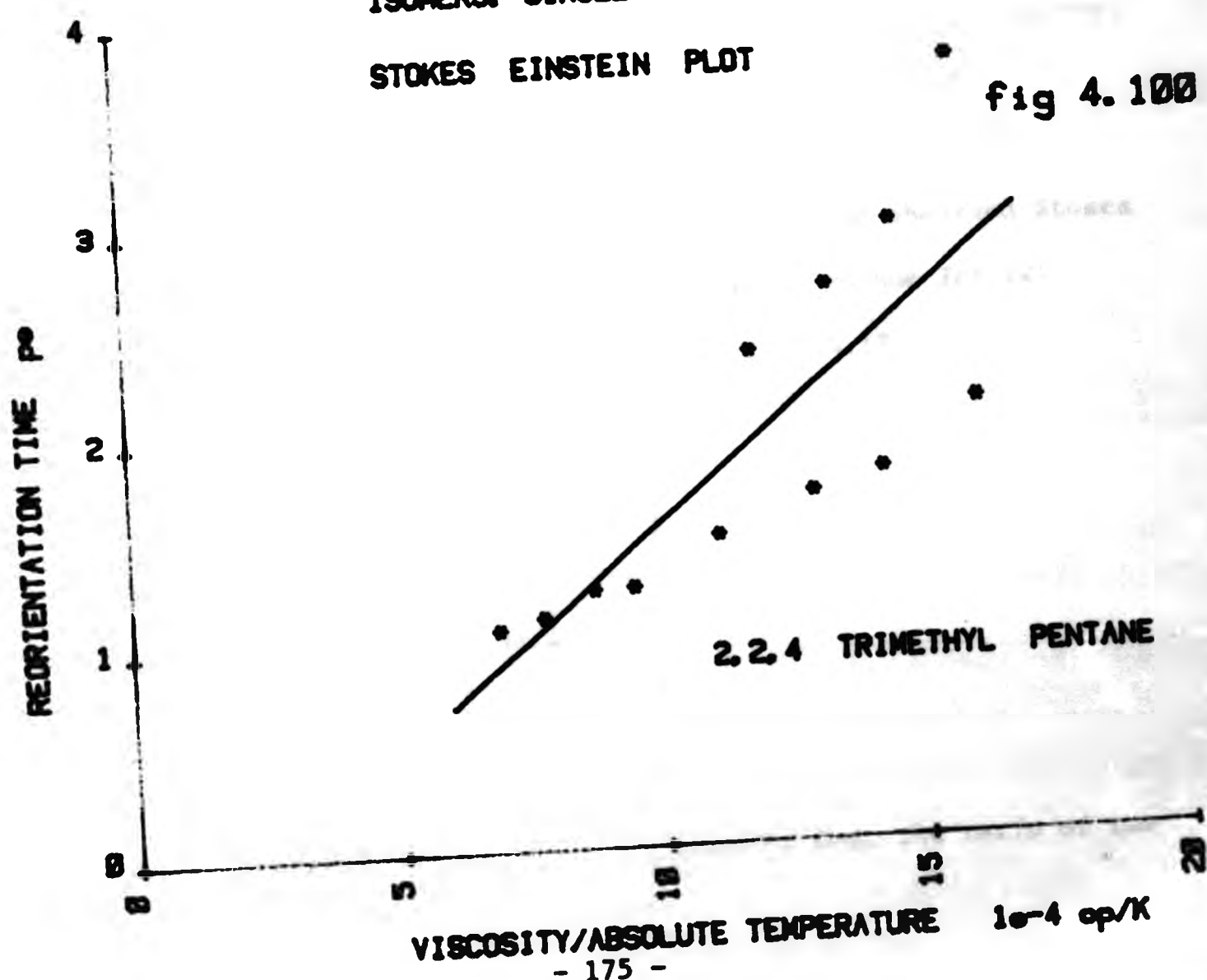


2,2,4 TRIMETHYL PENTANE

TEMPERATURE CENTIGRADE
ISOMERS: SINGLE LORENTZIAN FITS

STOKES EINSTEIN PLOT

fig 4.100



2,2,4 TRIMETHYL PENTANE

VISCOSITY/ABSOLUTE TEMPERATURE 10^{-4} op/K

RESULTS

Stokes Einstein Relation

A Stokes Einstein plot is shown in Fig 4.100. Owing to the large scatter on the data the error on the Stokes Einstein volumes obtained is very large. The values of the intercept obtained have such a large error that they are of little significance. The data is expressed in table 4.16.

Table 4.16

Results From Data Fits At	Stokes Einstein Volume A^3	Intercept (ps)
1490 GHz FSR	15.07	+0.27
731 GHz FSR	46.34	-1.74
All Results	29.18	-0.57

An average value of the Stokes Einstein volume for 224 trimethyl pentane is $30 \text{ A}^3 \pm 16 \text{ A}^3$ and for the intercept $-0.9 \pm 0.8 \text{ ps}$.

Compared to the molecular volume of the n-octane molecule (calculated from Courtaulds atomic molecules) and the observed Stokes Einstein volume for n-octane, the Stokes Einstein volume for 224 trimethyl pentane is very small as shown in table 4.17.

Table 4.17

Stokes Einstein Volumes		Molecular Volume Octane
224 Trimethyl Pentane	N-Octane	
$30 \pm 16 \text{ A}^3$	$134 \pm 2 \text{ A}^3$	154 A^3

and may be interpreted in terms of the quantity Gap, the ratio of the

observed Stokes Einstein volume to the molecular volume.

Table 4.18

Gap	
224 Trimethyl Pentane	N-Octane
0.195 ± .104	0.87 ± .013

The differences between Gap for n-octane and the isomer can only be successfully explained in terms of the behaviour of the parameter α . The isomer molecule is very much more globular in shape than the n-alkane molecule, and would tend to rotate within its own volume in the medium, interacting less with the surrounding molecules than the macroscopic viscosity would suggest. The differences are very striking, indicating there is a fundamental difference between the reorientation of flexible molecules and that of small rigid, or quasi rigid molecules.

However the fact that using different free spectral ranges gives spectra which after analysis give different half widths implies that the spectra are not single Lorentzians. The half widths measured for this liquid were typically 100 GHz. This value is not too different from the values measured for pentane, whilst for pentane, the spectral analysis is straightforward.

Now for small anisotropic molecules the depolarised Rayleigh spectrum can be conveniently separated into two parts. I_{ROT} is Lorentzian in shape and is associated with the inherent molecular anisotropy while I_{COLL} , the collisional wing is exponential in shape, and is associated with collisional motion. The separation depends on a separation of the time scales associated with collisional motion and

reorientational motion. Without the time scale separation the simple analysis breaks down and there is a contribution to the spectrum resulting from coupled reorientational/collisional motion.

For pentane $f_r \sim$ the reorientational frequency is ~ 60 GHz and $\omega_0 \sim$ the time scale of the collisional motion is $30 \text{ cm}^{-1} \sim 900$ GHz. Using the expression due to Levine and Birnbaum a value for the mass of the colliding entities can be calculated for the n-alkanes and is shown to be approximately 19 amu, the mass of a chain end.

For the isomer examined, the molecule is much more globular in shape and could be described as being quasi rigid. The colliding entities in this liquid are therefore likely to be much larger than in the case of the n-alkane liquid, and may be the whole molecule.

This would give for the isomer (224 TMP)

$$\omega_0 \sim 13 \text{ cm}^{-1} \sim 390 \text{ GHz}$$

and as f_r the reorientational frequency ~ 100 GHz the time scale separation for the isomer would be approximately a factor of 3.9, while for n-pentane the same separation is 15.

It is likely that the reorientational Lorentzian spectrum is sitting on top of a collisional spectrum which has a time scale such that single Lorentzian fits to the spectra are no longer appropriate. The different results obtained for different free spectral ranges are what would be expected if this is the case. However, the noise level on the spectra prevented an adequate fitting of spectra to Lorentzian plus exponential.

Also if the simple analysis of time scales for 224 trimethyl pentane is correct, then this implies that a spectral analysis which depends on a separation of reorientational and collisional motion is not appropriate.

Therefore an examination of the depolarised Rayleigh spectra for the various isomers of the alkane molecules and a comparison with the n-alkanes should give a large amount of information about how molecular flexibility affects molecular reorientation. This effect is apparently very significant.

We would suggest that a future programme of work on light scattering from the alkanes should include a study of the isomers. To obtain an adequate spectral analysis for these liquids it may prove necessary to use a monochromator to accurately separate the time scales of collisional and reorientational motion and to investigate the contribution to the spectra from collisional/reorientational coupling.

4.3 References for Chapter 4

- (1) A Dandridge, 1978, "An Experimental Investigation of the Conformational Behaviour of Short Chain Polymers", PhD Thesis, CNAA.
- (2) J A Bucaro and T A Litovitz, 1971, J Chem Phys 54, 9, 3846.
- (3) H B Levine and G Birnbaum, 1968, Phys Rev Lett 20, 439.
- (4) J P Ryckaert and A Bellemans, 1978, Faraday Disc 66/5.
- (5) E E Nikitin, 1959, Optics and Spectroscopy 6, 93.
- (6) P Bothorel, Such, C Clement, 1972, J Chimie Phys 10, 1453.
- (7) W Lempert and C H Wang, 1980, J Chem Phys 72, 6, 3490.

CHAPTER 5 SUMMARY OF CONCLUSIONS AND SUGGESTIONS FOR FURTHER WORK

5.1 Results From Spectral Fits - A Summary

From the results of sections 4.2.1 (n-alkanes: neat liquids), 4.2.2 (n-alkanes: solutions in carbon tetrachloride) and 4.2.3 (n-alcohols: neat liquids) a number of points are evident about a Stokes Einstein analysis of the data.

The Stokes Einstein equation provides a useful approach to an analysis of the data, giving a quantity, the Stokes Einstein volume, which can be interpreted in terms of the dynamic behaviour of the molecule in the liquid. The quantity obtained, $G_0 p V$ may be interpreted with some success for rigid molecules because G , α , and p are separable in solution measurements, as G is a function of concentration and α and p are essentially functions of the molecular geometry which remains fixed. For flexible molecules, i.e. those considered here, G , α and p are not simply separable in the solution measurements. This is because α and p are, for flexible molecules, also a function of concentration as the molecular shape is directly related to the molecular conformation which changes with solution concentration.

For flexible molecules it might be more appropriate to develop a theoretical model in which the quantity $G_0 p$ is a single parameter determined by the molecular flexibility, and is related to the molecular environment.

A further problem arises from the different spectral analyses used. For the low viscosity liquids the correlation times used in the Stokes Einstein fits are obtained from single Lorentzian (one variable) fits to the spectra. For the higher viscosity liquids the correlation times are obtained from Lorentzian plus dip (two variable)

fits to the spectra. In the case of the higher viscosity n-alcohols it is evident that the two variable fits are inadequate in the very high viscosity regime in which the dip is not observed. For liquids for which spectra are observable over a large viscosity range, (1) it has been found necessary to fit the spectra to a form resulting from a "three variable" theory. The liquids examined in this study were of a high optical anisotropy (and hence scattered a large amount of light) and the spectra were "double" fitted to a three variable model i.e. two spectra were taken with the liquid in identical thermodynamic states, but with the Fabry-Perot spectrometer at different free spectral ranges. The three variable model describes spectra over a far larger viscosity regime than the corresponding two variable model, however there are deficiencies in the three variable model when it is used in an attempt to explain the temperature variation of the stress optical coefficient (obtained from flow birefringence measurements).

In this thesis all the R parameters obtained are from fits to the spectra appropriate to a two variable model of depolarised Rayleigh spectra. In common with all other two variable fits to depolarised Rayleigh spectra R is found to be either constant with temperature or to have a weak temperature dependence. In the three variable approach used by Chappell et al (1) R is found to be a strong function of absolute temperature, decreasing with temperature.

The R values obtained have been found to be a strong function of chain length, decreasing with decreasing chain length, except perhaps in the case of the n-alcohols for which the R parameters were obtained only for n-undecanol, and n-decanol. However the results for n-undecanol were somewhat inconclusive due to the poor quality of the liquid sample investigated experimentally.

Section 4.1 provides an examination of results obtained from an analysis of depolarised Rayleigh spectra recorded using a double grating monochromator. The results for the half width of the central Lorentzian obtained with this instrument agree well with the half widths obtained using the Fabry Perot interferometer. The results for the collisional portion of the spectrum indicate that the optical anisotropy and time scale of this portion of the spectrum are such that interaction induced phenomena in the n-alkanes are associated with motion of the chain ends.

In our examination of the spectra of flexible molecules we have therefore arrived at a separation of the spectra into two components. One an intrinsic component is associated with molecular reorientation, i.e. reorientation of the whole molecule, the other interaction induced component is associated with collisional processes which for the n-alkanes appear to be due to the motion of the chain ends. The collisional motion may be interpreted as a translational diffusion process of the chain ends.

In section 4.2.4 the octane isomer, 224 trimethyl pentane was examined. This molecule has a very small optical anisotropy, also it is almost globular in shape. The molecule therefore reorientates much faster than its isomer n-octane, and with the small optical anisotropy this gives a broad noisy Lorentzian due to the intrinsic component in the depolarised Rayleigh spectrum. A problem arises for this liquid in the interpretation of the data. For the n-alkanes the evidence is that the collisional motion is associated with the chain ends. For the isomer 224 trimethyl pentane it is likely that the entity involved in collisional motion would be the whole molecule. This would result in a much narrower interaction induced component.

Because the intrinsic component is much broader than for the corresponding n-alkane the time scale separation between the reorientational and collisional motion which exists for the n-alkane does not exist for the isomer. This implies that for the isomer extra features may appear in the spectra due to coupled reorientational collisional motion. However the noise on the spectra obtained prevented an examination of this possibility.

Patterson and Carroll (2) examined depolarised Rayleigh spectra from a number of n-alkanes and alkane isomers. They reasoned that for small alkanes, that as the intrinsic molecular anisotropy decreases with decreasing molecular size, and increasing branching the Lorentzian component of the spectra may be due to interaction induced effects. Madden (3) calculated the depolarised Rayleigh spectrum for isotropic molecules, in a model in which scattering is by pairs of density fluctuations and the central region of the spectrum is Lorentzian with a line width given by

$$f_{\frac{1}{2}} \propto 2D K_0^2$$

5.1

D is the translational self diffusion coefficient.

K_0 is the magnitude of the scattering vector at the maximum in the centre of the mass structure factor.

This translational diffusion central Lorentzian is present in spectra for all liquids, however for most liquids it is masked by the reorientational diffusion component due to the intrinsic molecular anisotropy.

Patterson and Carroll use this approach in their analysis of the light scattering times obtained for the n-alkanes and branched alkanes. The translational self diffusion coefficients were determined by the NMR spin echo method and K_0 was determined by X-ray scattering.

Patterson and Carroll's results indicate that for the n-alkanes the spectra are due to rotational diffusion (essentially equivalent to our analysis of the n-alkanes: neat liquid data). For the highly branched alkanes the results indicate that the molecular re-orientational rate is much more rapid than for the equivalent n-alkane (which is an observation in agreement with our results for 224 trimethyl pentane). Patterson and Carroll interpret this as indicating that for the highly branched alkanes, the central Lorentzian component of the spectra is an interaction induced phenomenon characterised by translational diffusion.

Our approach to the results for the single isomer examined in this thesis is to identify a molecular rotational friction constant α which is a strong function of molecular shape and modifies rotational diffusion. The more globular a molecule (the more highly branched an alkane chain) the closer α is to zero.

Both our approach, and that of Patterson and Carroll do not take account of contributions to the spectra due to coupled re-orientational/collisional motion.

In the analysis of the n-alkane solution data R is found to be approximately proportional to the solution volume concentration in agreement with the predictions of theory (6). The solution data has also provided us with an indication of the true complexity of Stokes Einstein behaviour for flexible molecules, particularly of the non-separability of the parameter $G\alpha p$ in solution measurements, of depolarised light scattering. To be able to effect such a separation one needs information about the variation of molecular conformation with solution concentration. Such information may be provided by Raman scattering (7). Raman scattering is particularly useful in that information can be obtained down to very low solution concentrations,

(< 1%), while for depolarised light scattering spectral noise and parasitic scattering appear to limit measurements to concentrations above about 10%.

It is perhaps important to note that low concentration solution work is of great relevance to computer simulation, for most of the simulations so far are not for chain molecules in a fluid of themselves but for chain molecules dissolved in rather simpler model fluids.

5.2 The Stokes Einstein Relation

A Comparison of Results from Spectral Fits with Theoretical Modelling.

Evans and Knauss (as discussed in chapter 2) simulated n-alkane chains using a variety of techniques. Results were obtained from a Brownian dynamics simulation, (4) using a model for the torsional characteristics of the chain which is an extension of the rotational isomeric model of Flory. The n-alkanes examined were liquids from n-butane to n-undecane and the results obtained were orientational correlation times for first and second rank harmonics for the different possible modes of molecular motion. The results were expressed in terms of reduced units which are related to the Stokes Einstein friction constant for a single backbone atom. The results may be converted into time units by multiplying by $(3\pi b^3 n/KT)$ where $b (= 1.54 \text{ \AA}^0)$ is the diameter of a single backbone bead. The results may be converted to volume units by the multiplier $3\pi b^3$.

A significant point about these theoretical results is that in changing from one model of torsional motion to another, the values of the correlation times obtained change significantly. Also changing the values of the torsional potentials significantly changes the

correlation times. When the results obtained are so sensitive to the form and detail of so many of the parameters involved in the simulations, one has to be confident that the input data selected for the simulation is correct.

Evans and Knauss identify the $Q = 1$ mode, first harmonic correlation time as that closest to the overall molecular orientation time. The calculation of this was performed for a number of potentials for a number of molecules. They choose the $\beta u = 5$ potential ($\beta = 1/kt$) as being the most appropriate and obtained results for this potential by interpolation between results obtained for $\beta u = 0$, 4, 8 and ∞ (rigid body) and compared correlation times calculated with those obtained experimentally for the 1 bromoalkanes and find reasonable agreement.

We have calculated, from Evans and Knauss's data, Stokes Einstein volumes for the n-alkanes examined for the $\beta u = 5$ and $\beta u = \infty$ (rigid chain case) potentials, shown in table 5.1.

Table 5.1

Stokes Einstein Volume (simulation)

No of Bonds	Liquid	$\beta u = 5$	$\beta u = \infty$
4	C ₅ H ₁₂	36.8 Å ³	55.8 Å ³
5	C ₆ H ₁₄	43.7 Å ³	82.3 Å ³
6	C ₇ H ₁₆	65.1 Å ³	115.0 Å ³
8	C ₉ H ₂₀	78.1 Å ³	198.0 Å ³
10	C ₁₁ H ₂₄	103.0 Å ³	

No of Bonds	Liquid	$\beta u = 5$	$\beta u = \infty$
4	C ₅ H ₁₂	36.8 Å ³	55.8 Å ³
5	C ₆ H ₁₄	43.7 Å ³	82.3 Å ³
6	C ₇ H ₁₆	65.1 Å ³	115.0 Å ³
8	C ₉ H ₂₀	78.1 Å ³	198.0 Å ³
10	C ₁₁ H ₂₄	103.0 Å ³	

These results may be compared with our results obtained by light scattering from the n-alkanes, shown in table 5.2.

Table 5.2

Liquid Stokes Einstein Volume (light scattering)

Liquid	Stokes Einstein Volume (light scattering)
C ₅ H ₁₂	49 ± 2 Å ³
C ₆ H ₁₄	66 ± 1.5 Å ³
C ₇ H ₁₆	94 ± 3 Å ³
C ₉ H ₂₀	175 ± 3 Å ³
C ₁₁ H ₂₄	239 ± 5 Å ³

The difference between the Stokes Einstein volumes obtained from the simulation, and those obtained by light scattering is that the simulation results give the purely dynamic quantity, while for light scattering using a coherent probe one measures the dynamic quantity modified by the orientational correlation.

Simply the simulation results represent the quantity αpV , and the light scattering results represent the quantity $G\alpha pV$. For the alkanes from C₅ H₁₂ to C₈ H₁₈, G has been measured to be approximately equal to one (5) and for the higher alkanes it gradually increases, being approximately two for C₁₂ H₂₆.

For the alkanes C₅ H₁₂, C₆ H₁₄ and C₇ H₁₆ (for which G ≈ 1) comparison of the results from the simulations with those from the light scattering reveals that the values of Stokes Einstein volumes from light scattering lie approximately midway between the results from simulations for $\beta_u = 5$ and $\beta_u = \infty$ indicating perhaps that a torsional potential of $\beta = 5$ which Evans and Knauss choose as being the most appropriate, is too weak to explain the observed light scattering results.

For $C_9 H_{20}$ the light scattering Stokes Einstein volume lies closer to the volume from the simulation for $\beta u = \infty$, perhaps an indication of the increasing value of the G parameter for the n-alkanes above $C_8 H_{18}$.

Therefore there is fair agreement between the results from simulations and results from our light scattering experiments. We will not pursue a deeper analysis of this point as there is a strictly limited amount of data for comparison. Also there is the fact that the torsional potential which Evans and Knauss use in their simulations is very simple, having equal potential wells and equal potential peaks. Despite this, Evans and Knauss's theoretical modelling provides the only data which can be compared to experimental results and we find their contribution extremely useful.

5.3 Suggestions for Future Work

In our analysis of the light scattering correlation times from the n-alkane solutions and pure liquids we have arrived at a combination of parameters Gap which we are at present unable to separate, at least partially due to the problem of molecular flexibility. The problem of separability may be overcome by investigating molecular liquids which are related to the n-alkanes but consist of less flexible molecules. Obvious candidate molecules are the alkenes, which are given an extra degree of rigidity given by a double bond. The molecular shape would be less of a function of temperature and of solution concentration than for the alkanes and correspondingly the data obtained from such a study should be easier to interpret than that for the n-alkanes.

A further point is of note. It is likely that a n-alkene molecule will be less coiled up in the neat liquid than the equivalent n-alkane molecule due to the extra degree of rigidity. On average therefore the

n-alkene molecule should be more extended than the n-alkane molecule. This should increase the quantities α , the frictional constant and p the Perrin factor. It is likely therefore that the observed Stokes Einstein volume for a n-alkene molecule will be greater than that of the equivalent n-alkane.

From our analysis of the light scattering data for the octane isomer 224 trimethyl pentane we have concluded that there is a very large difference between the value of the frictional constant α for the isomer and that for the n-alkane. Therefore a study of the correlation times for the isomers of small alkanes should provide information which may enable a separation of the quantities G , α and p to be made. For the alkanes above octane interpretation of the data may be quite complicated due to the fact that for these liquids $G > 1$ and G is likely to be dependent on the particular isomer. For those below octane G is likely to be one.

For the more globular isomers there is also the possibility that there may be contributions to the spectra due to coupled reorientational collisional motion. The possibility of this needs to be examined by inspection of the spectral wings using a double grating spectrometer. It is also likely that for the isomers the entities involved in collisional motion are quite different from the chain ends which we believe are responsible for collisional motion in the n-alkanes.

The R parameters obtained using a "two variable" spectra fit are almost independent of temperature. Values of R are obtained only over relatively small temperature ranges. "Three variable" fits have been obtained (1) over a large viscosity range, and for these fits R is found to be a strong function of absolute temperature. It would therefore be appropriate to develop a three variable fitting procedure and

to re-examine the spectra from the n-alkanes for which R parameters have been obtained. Also if the problem of spectral noise could be solved it would be useful to re-examine the spectra of the n-alcohols. The large viscosity variation with temperature of these liquids would provide both a useful test of a three variable fitting procedure and would give values of R parameters over a large range of possible spectral shapes.

Therefore there are a large number of ways in which this work could develop in the future. All of these are potentially fruitful, all of these should help to develop a better understanding of the motions of flexible molecules in the liquid state.

5.4 References for Chapter 5

- (1) P J Chappell, M P Allen, R I Hallem and D Kivelson, 1981, J Chem Phys 74, 11 5929.
- (2) G D Patterson and P J Carroll, 1982, J Chem Phys 76, 9, 4356.
- (3) P A Madden, 1978, Mol Phys 36, 365.
- (4) G T Evans and D C Knauss, 1980, J Chem Phys 72, 2, 1504.
- (5) P Bothorel, Such, Clement, 1972, J Chimie Phys 10, 1453.
- (6) D Kivelson and R Hallem, 1979, Mol Phys 38, 5, 1411.
- (7) S L Wunder and S D Merajver, 1981, J Chem Phys 74, 10, 5341.

194

D48198/84

BAGSHAW J.M.

194

Attention is drawn to the fact that the copyright of this thesis rests with its author.

This copy of the thesis has been supplied on condition that anyone who consults it is understood to recognise that its copyright rests with its author and that no quotation from the thesis and no information derived from it may be published without the author's prior written consent.

D48198 / 84

END